AWARD NUMBER: W81XWH-15-1-0716

TITLE: Enhancing the prevention and treatment of orthopaedic infections associated with traumatic injury

PRINCIPAL INVESTIGATOR: Mark S. Smeltzer, PhD

CONTRACTING ORGANIZATION: University of Arkansas for Medical Sciences

REPORT DATE: December-2019

TYPE OF REPORT: Final

PREPARED FOR: U.S. Army Medical Research and Development Command
                        Fort Detrick, Maryland 21702-5012

DISTRIBUTION STATEMENT: Approved for Public Release;
                        Distribution Unlimited

REPORT DOCUMENTATION PAGE

1. REPORT DATE	2. REPORT TYPE	3. DATES COVERED
December-2019	Final	**09/30/2015 - 09/29/2019**

4. TITLE AND SUBTITLE	5a. CONTRACT NUMBER
Enhancing the prevention and treatment of orthopaedic infections following traumatic injury	
	5b. GRANT NUMBER
	W81XWH-15-1-0716
	5c. PROGRAM ELEMENT NUMBER

6. AUTHOR(S)	5d. PROJECT NUMBER
Mark S. Smeltzer	
	5e. TASK NUMBER
	5f. WORK UNIT NUMBER
E-Mail: smeltzermarks@uams.edu	

7. PERFORMING ORGANIZATION NAME(S) AND ADDRESS(ES)	8. PERFORMING ORGANIZATION REPORT NUMBER
University of Arkansas for Medical Sciences 4301 W. Markham Little Rock, AR 72205	

9. SPONSORING / MONITORING AGENCY NAME(S) AND ADDRESS(ES)	10. SPONSOR/MONITOR'S ACRONYM(S)
U.S. Army Medical Research and Development Command Fort Detrick, Maryland 21702-5012	
	11. SPONSOR/MONITOR'S REPORT NUMBER(S)

12. DISTRIBUTION / AVAILABILITY STATEMENT

Approved for Public Release; Distribution Unlimited

13. SUPPLEMENTARY NOTES

14. ABSTRACT

Injuries to the bone resulting from traumatic injury are highly susceptible to infection, and the resulting infections are therapeutically recalcitrant to antibiotic therapy. The overall goal of this project was to develop improved treatment methods that could be used to overcome this therapeutic recalcitrance. To this end, we evaluated existing antibiotics based on their efficacy in the specific context of a biofilm, took advantage of our knowledge regarding the pathogenesis of *Staphylococcus aureus* as a cause of bone infection to identify small molecule inhibitors of the staphylococcal accessory regulator (*sarA*), and explored methods to enhance the systemic delivery of the most efficacious antibiotics and effective *sarA* inhibitors directly to the bone. The ultimate goal was to then evaluate the efficacy of these novel approaches, alone and in combination with each other, in a relevant animal model of post-traumatic osteomyelitis. The first of these objectives was accomplished, and the second and third were extensively explored at an antimicrobial, anti-biofilm, and pharmacological basis.

15. SUBJECT TERMS

16. SECURITY CLASSIFICATION OF:			17. LIMITATION OF ABSTRACT	18. NUMBER OF PAGES	19a. NAME OF RESPONSIBLE PERSON USAMRMC
a. REPORT	b. ABSTRACT	c. THIS PAGE			19b. TELEPHONE NUMBER *(include area code)*
Unclassified	Unclassified	Unclassified	Unclassified		

TABLE OF CONTENTS

INTRODUCTION

The overall focus of this grant was to develop improved methods that could be used to overcome the therapeutic recalcitrance of bone infections arising after traumatic injury. Part of the effort would be applicable to diverse bacterial pathogens, specifically the conjugation of conventional antibiotics to the bone-targeting agent BT2-minipeg-2 (BT2-peg2), thus potentially providing a means of enhancing the accumulation of diverse antibiotics in the bone (Albayati et al., 2015). However, our specific focus was on infections caused by *Staphylococcus aureus* because *S. aureus* is the leading cause of such infections and because the ability to treat all forms of *S. aureus* infection is increasingly compromised by the persistent emergence of antibiotic-resistant strains, most notably methicillin-resistant *S. aureus* (MRSA). Additionally, many forms of *S. aureus* infection, including those involving bone, are characterized by formation of a bacterial biofilm, the presence of which provides a clinically-relevant degree of intrinsic resistance to both conventional antibiotics and host defenses. Thus, the first three tasks were to 1) identify and prioritize antibiotics that are active against MRSA based on their relative activity in the context of a biofilm, 2) determine whether the most promising of these antibiotics could be conjugated to BT2-peg2 without diminishing their antibacterial activity, and 3) assess the pharmacological properties of these antibiotics and their BT2-peg2 conjugates in the context of effective targeting to the bone.

In addition, a primary focus in the Smeltzer laboratory is on defining the attributes of *S. aureus* that make it the predominant cause of bone infection. This work led us to focus on the staphylococcal accessory regulator (*sarA*) based on the following observations: 1) mutation of *sarA* limits biofilm formation to a greater degree than mutation of any other *S. aureus* regulatory locus we have examined (Atwood et al., 2015), 2) the limited capacity of *sarA* mutants to form a biofilm can be correlated with increased antibiotic susceptibility (Atwood et al., 2016), and 3) mutation of *sarA* limits the ability to cause bone infection (osteomyelitis) in diverse clinical isolates of *S. aureus* including MRSA (Loughran et al., 2016, Rom et al, 2020). Additionally, we confirmed that mutation of *sarA* limits the virulence of *S. aureus* in other forms of infection including sepsis (Rom et al., 2017), which is relevant in that osteomyelitis is often a secondary consequence of blood-borne infection. These observations led us to conclude that *sarA* is a valid therapeutic target that could be exploited to help overcome the problem of diverse forms of *S. aureus* infection, including osteomyelitis and other biofilm-associated infections.

To this end, we worked with the laboratory of Dr. Peter Crooks, Chair, UAMS Department of Pharmaceutical Sciences, in an attempt to identify small molecule inhibitors of *sarA*-mediated regulation. This was done by screening a chemical library available in the Crooks' laboratory (Task 4) and based on evaluating previously identified molecules of potential interest including compounds reported in the literature to limit *S. aureus* biofilm formation (Task 5)(Abraham et al., 2016, Arya et al., 2015, Balmurugan et al., 2015, Balmurugan et al., 2016, Basak et al., 2016, Bottcher et al., 2013, Goswami et al., 2013, Goswami et al., 2014, Joseph et al., 2016, Kolodkin-Gal et al., 2010, Minivielle et al., 2013, Romero et al., 2013, Sambanthamoorthy et al., 2011, Williams et al., 2012). Tasks 6-8 were then directed toward assessing whether the most promising compounds were active against diverse strains of *S. aureus*, determining whether these compounds could also be conjugated to BT2-peg2 without a loss of efficacy, and assessing whether the conjugates effectively enhanced delivery of the inhibitor to the bone. Thus, Tasks 6-8 precisely parallel Tasks 1-3, the only difference being that Tasks 1-3 focus on existing antibiotics while Tasks 6-8 focus on small molecule inhibiters of *sarA*-mediated regulation. Once these studies were completed, the goal was to evaluate the efficacy of these novel therapeutic compounds both alone and in combination with each other (Task 9).

KEYWORDS

Osteomyelitis, BT2-minipeg-2, BT2-peg2, daptomycin, ceftaroline, oxacillin, ciprofloxacin *Staphylococcus aureus*, staphylococcal accessory regulator (*sarA*), biofilm, protease.

ACCOMPLISHMENTS

Major goals of the project.

The overall goals of this project were to 1) explore the use of a novel bone targeting agent (BT2-peg2) as a means of enhancing antibiotic therapy in the specific context of bone infections caused by methicillin-resistant *Staphylococcus aureus*, 2) identify small molecule inhibitors of *sarA*-mediated regulation in *S. aureus* that can also be conjugated to BT2-peg2 without compromising their biological activity, and 3) evaluate BT2-peg2 conjugates to antibiotics and *sarA* inhibitors both alone and in combination with each other with respect to the prevention and treatment of *S. aureus* bone infections. To accomplish these goals, the tasks to be undertaken as stated in the original SOW are detailed below. This includes a statement of the original timelines of the proposed experiments and an estimation of the extent to which each of these tasks were accomplished:

Task 1: Compare antibiotics active against MRSA in the context of a biofilm. We will use our established *in vitro* model of catheter-associated biofilm formation to directly compare the therapeutic efficacy of telavancin, oritavancin, dalbavancin, ceftaroline, vancomycin, and daptomycin. Timeframe: Months 1-6. Status: Completed.

Task 2: Determine whether the most promising antibiotic can be conjugated to BT-2-minipeg-2 without compromising its efficacy in the context of a biofilm. Time frame: Months 7-12. Status: Completed. All of the most promising antibiotics were successfully conjugated to BT2-peg2, but the antibacterial activity of some was compromised to an unacceptable degree. The conjugate of greatest interest, BT2-peg2-daptomycin, was found to be unstable *in vivo* (see Task 3).

Task 3: Evaluate *in vivo* pharmacological properties of antibiotics and antibiotic conjugates in the context of bone targeting. Timeframe: Months 13-15. Status: Completed.

Task 4: Optimize previously identified compounds based on inhibition of *sarA*-mediated regulation. Timeframe: Months 1-3. Status: 75% complete.

Task 5: Screen additional compounds to identify small molecule inhibitors of *sarA*-mediated regulation. Timeframe: Months 1-6. Status: Completed.

Task 6. Expand the screen of small molecule inhibitors to include additional staphylococcal strains and species. Timeframe: Months 4-6. Status: Completed.

Task 7: Evaluate conjugation of most promising *sarA* inhibitor to BT2-peg2. Timeframe: Months 19-21. Status: 0% complete.

Task 8: Evaluate *in vivo* pharmacological properties of the most promising *sarA* inhibitor and its BT2-peg2 conjugate. Timeframe: Months 22-24. Status: 0% complete.

Task 9: Evaluate the efficacy of the most promising small molecule inhibitor and the most promising antibiotic *in vivo* with and without conjugation to BT2-peg2. Timeframe: Months 19-36. Status: 0% complete.

Summary statement: As detailed below, a great deal was accomplished during the funding period, but significant difficulties were also encountered, specifically with respect to the early tasks focused on developing effective BT2-peg2 conjugates to conventional antibiotics and identifying effective *sarA* inhibitors. With respect to the first of these goals, this was unexpected given the existing literature regarding the efficacy of BT2-peg2 as a bone targeting agent (see below). With respect to the second, identifying effective inhibitors of any bacterial process is a challenging task that comes with no guarantees, and while we did not identify a *sarA* inhibitor that warranted comprehensive *in vivo* analysis, we did define promising chemical scaffolds that we can be exploited moving forward. Nevertheless, Tasks 7-9 were all dependent on overcoming these problems. Every effort was made to do so, and using funds from other sources these efforts are continuing. Nevertheless, this precluded addressing these tasks aimed at determining whether *sarA* inhibitors could be conjugated to BT2-peg2 (Task 7) and assessing *in vivo* pharmacological properties (Task 8) and overall therapeutic efficacy (Task 9).

Major accomplishments toward these goals.

Task 1. Compare antibiotics active against MRSA in the context of a biofilm. We compared the relative activity of vancomycin, daptomycin, ceftaroline, tigecycline, telavancin, oritavancin, and dalbavancin in the specific context of an established *S. aureus* biofilm (Meeker et al., 2016). These antibiotics were chosen because they are all active against methicillin-resistant *S. aureus* (MRSA). In keeping with the intent of Task 6, these studies were done using two divergent strains of *S. aureus*, specifically the CC8, USA300 MRSA strain LAC and the CC30, USA200, MSSA strain UAMS-1. Because we included UAMS-1, we also evaluated oxacillin. With the exception of LAC and oxacillin, both strains were clinically defined as sensitive to all of the test antibiotics (Table 1, Meeker et al., 2016):

TABLE 1 Relationship between breakpoint MIC and MIC for each test strain

		LAC		UAMS-1	
Antibiotic	BkPt[a] (µg/ml)	MIC (µg/ml)	Ratio (MIC/BkPt)	MIC (µg/ml)	Ratio (MIC/BkPt)
Vancomycin	2.0	2.0	1.0	1.5	0.75
Daptomycin	1.0	0.5	0.5	0.5	0.5
Ceftaroline	1.0	0.5	0.5	0.5	0.5
Tigecycline	0.5	0.125	0.25	0.19	0.38
Telavancin	0.12	0.047	0.39	0.047	0.39
Oxacillin	2.0	128	64	1.5	0.75

[a] BkPt, breakpoint MIC. The breakpoint MICs cited are those defined by the United States Food and Drug Administration (FDA) for a susceptible strain of *S. aureus*.

The relative efficacy of each of these antibiotics in the context of an established biofilm was first tested under in vitro conditions using our catheter-based assay. Daptomycin and ceftaroline were found to exhibit significantly greater activity than any of the other antibiotics tested, and to do so against both LAC and UAMS-1 (Fig. 2 and 3, Meeker et al., 2016):
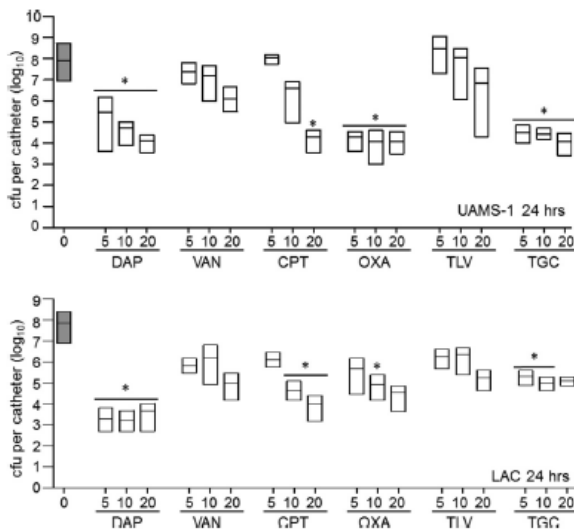

FIG 2 Relative activity of different antibiotics against LAC and UAMS-1 at 24 h in the context of a biofilm *in vitro*. Activity was evaluated using daptomycin (DAP), vancomycin (VAN), ceftaroline (CPT), oxacillin (OXA), telavancin (TLV), and tigecycline (TGC) at concentrations corresponding to 5×, 10×, and 20× the breakpoint MIC for each antibiotic. Results are shown as the number of CFU per catheter, with each box illustrating the maximum and minimum values observed within each experimental group and the horizontal line indicating the mean for that group. Gray bars, results observed with catheters that were not exposed to any antibiotic; white bars, results observed after exposure of UAMS-1 (top) or LAC (bottom) biofilms to the indicated antibiotics; *, significant reduction in the number of viable bacteria (*P* ≤ 0.05) relative to that achieved with vancomycin at the equivalent concentration.

FIG 3 Relative activity of different antibiotics against LAC and UAMS-1 at 72 h in the context of a biofilm *in vitro*. Activity was evaluated using daptomycin (DAP), vancomycin (VAN), ceftaroline (CPT), oxacillin (OXA), telavancin (TLV), and tigecycline (TGC) at concentrations corresponding to 5×, 10×, and 20× the breakpoint MIC for each antibiotic. Results are shown as the number of CFU per catheter, with each box illustrating the maximum and minimum values observed within each experimental group and the horizontal line indicating the mean for that group. Gray bars, results observed with catheters that were not exposed to any antibiotic; white bars, results observed after exposure of UAMS-1 (top) or LAC (bottom) biofilms to the indicated antibiotics. *, significant reduction in the number of viable bacteria (*P* ≤ 0.05) relative to that achieved with vancomycin at the equivalent concentration; **, significant reduction relative to that achieved with daptomycin at the equivalent concentration.
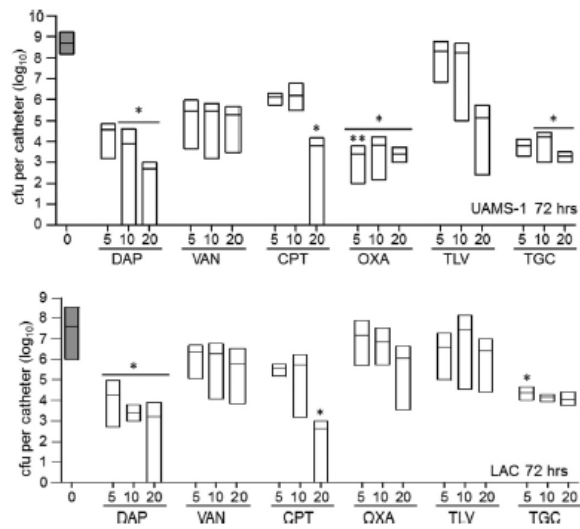
We next assessed the efficacy of these antibiotics under *in vivo* conditions. In this case, ceftaroline was found to exhibit greater activity even by comparison to daptomycin (Fig. 7, Meeker et al., 2016).
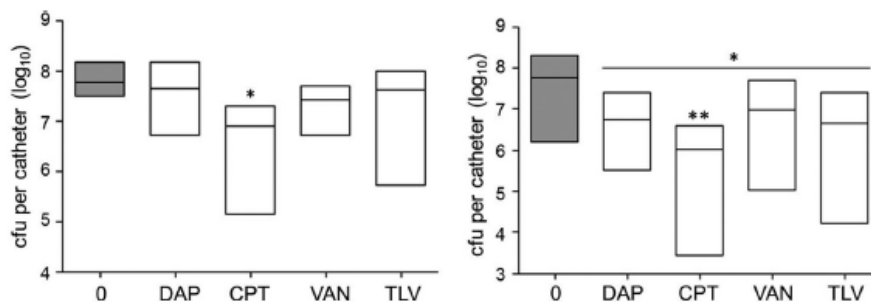

FIG 7 Relative activity of different antibiotics assessed *in vivo*. Catheters colonized with LAC were evaluated after 5 days of exposure to daptomycin (DAP), ceftaroline (CPT), vancomycin (VAN), and telavancin (TLV) at a concentration corresponding to 20× (left) or 40× (right) the breakpoint MIC for each antibiotic. Gray bars, results observed with catheters that were not exposed to any antibiotic; white bars, results observed after exposure to the indicated antibiotics. *, significant reduction in the number of viable bacteria ($P \leq 0.05$) relative to the number of untreated control bacteria; **, statistical significance by comparison to the results obtained with vancomycin.

Based on these results, much of our emphasis in Task 2 was placed on these two antibiotics. In addition, based on studies done in collaboration with Dr. En Huang in the UAMS College of Public Health, we also explored the efficacy of a group of novel linear lipopeptide paenipeptin antibiotics against diverse bacterial pathogens. One of these (analogue 17) was found to have significant activity against *S. aureus*, and based on this we evaluated the efficacy of analogue 17 in the context of a biofilm. Importantly, analogue 17 was found to exhibit activity comparable to that observed with daptomycin and ceftaroline (Moon et al., 2017).
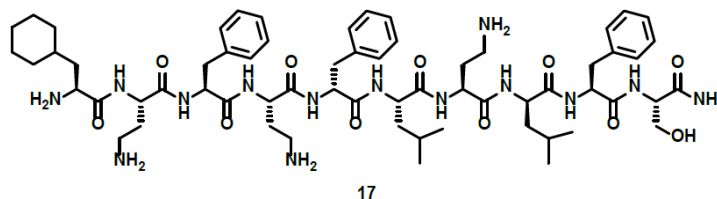
Chemical structure of paenipeptin analogue **17**
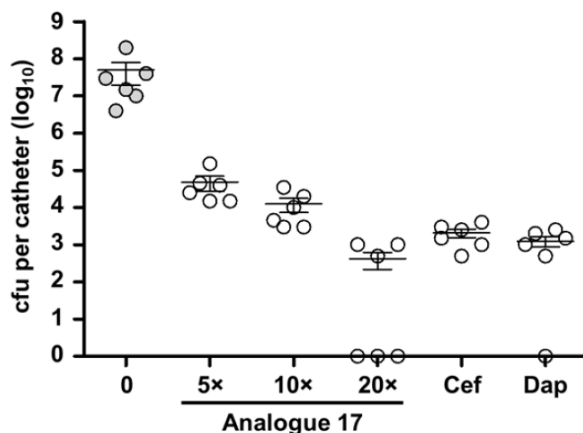
Activity of paenipeptin C' analogue **17** in an established *S. aureus* biofilm. Relative activity was assessed using our established catheter assay (Meeker et al. 2016). Results are shown as colony-forming units (cfu) per catheter remaining after 3 days in the absence of antibiotic exposure (0) or after exposure to the indicated antibiotics at the indicated concentrations. Analogue **17** was assessed at concentrations of 5, 10 and 20x the MIC for the *S. aureus* strain under study. Based on our previous experiments (Meeker et al., 2016), ceftaroline (Cef) and daptomycin (Dap) were tested at 20x the MIC for each antibiotic as defined using the same test strain.

Although this compound has not been approved for clinical use, we assessed the ability to conjugate analogue 17 to BT2-peg2. However, to date we have been unable to confirm the structure of this conjugate, although our efforts also continue in this regard.

Task 2. Determine whether the most promising antibiotics can be conjugated to BT2-peg2 without compromising efficacy in the context of a biofilm. Tetracycline binds hydroxyapatite and is known to be efficiently taken up by bone. This has been attributed to the tricarbonylmethane group of the A ring of tetracycline (Myers et al., 1983). A derivative of the A ring (3-amino-2,6-dihydroxybenzamide, upper right) was synthesized and shown to bind hydroxyapatite at a level ~50% of that observed with tetracycline itself (Neale et al., 2009). It was also demonstrated that this compound could be conjugated to estradiol (BTE$_2$-A1) to enhance its delivery to the bone, thus potentially providing an improved method for the treatment of osteoporosis.
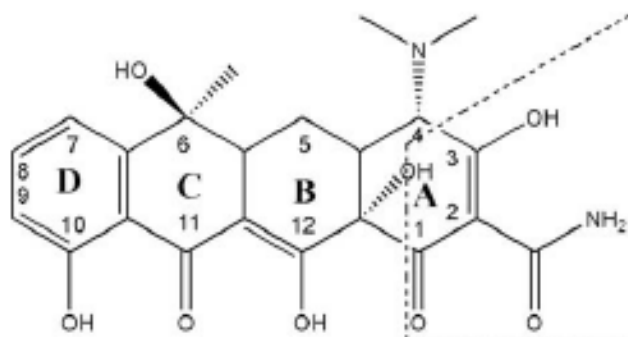
Based on this work, Pradama Inc. developed a derivative of this compound (BT2-peg2) as a "bone targeting" agent and showed that this derivative could be conjugated to vancomycin (Karau et al., 2013). The BT2-peg2-vancomycin conjugate was also shown to bind hydroxyapatite and to exhibit antibacterial activity comparable to vancomycin itself. The relative accumulation of vancomycin in the bone observed with the BT2-peg2-vancomycin conjugate by comparison to vancomycin alone was not directly assessed in this study, but it was demonstrated that intraperitoneal (IP) injection of 63.85 mg/kg of BT2-peg2-vancomycin conjugate twice daily in rats resulted in lower bacterial burdens in the femur than any other treatment regimen examined, including IP injection of the molar equivalent of vancomycin itself. However, the mean difference was only 1.0 log even by comparison to untreated animals, and none of the femurs in the treated group were cleared of viable bacteria (Karau et al., 2013).
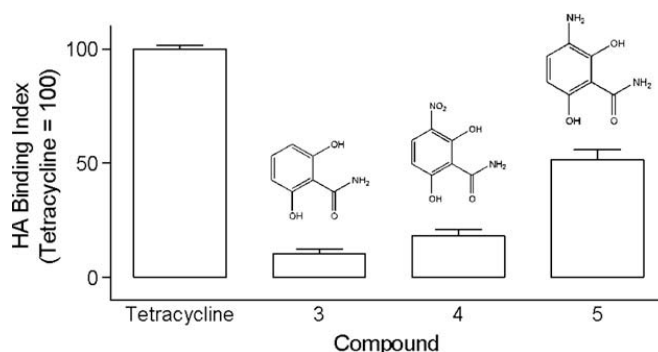
Additionally, plasma levels in the BT2-peg2-vancomycin treated group were dramatically higher (74.56-207.90 µg/ml) by comparison to animals treated with vancomycin alone (0.24-2.00 µg/ml). Moreover, kidney weight, creatinine levels, and blood urea nitrogen (BUN) levels were all elevated in the BT2-peg2-vancomycin treated group, and all animals in this group exhibited tubulointerstitial nephritis. Thus, while bone targeting was enhanced using the BT2-peg2-vancomycin conjugate, it had the adverse consequence of causing renal dysfunction, presumably owing to increased plasma levels of vancomycin.
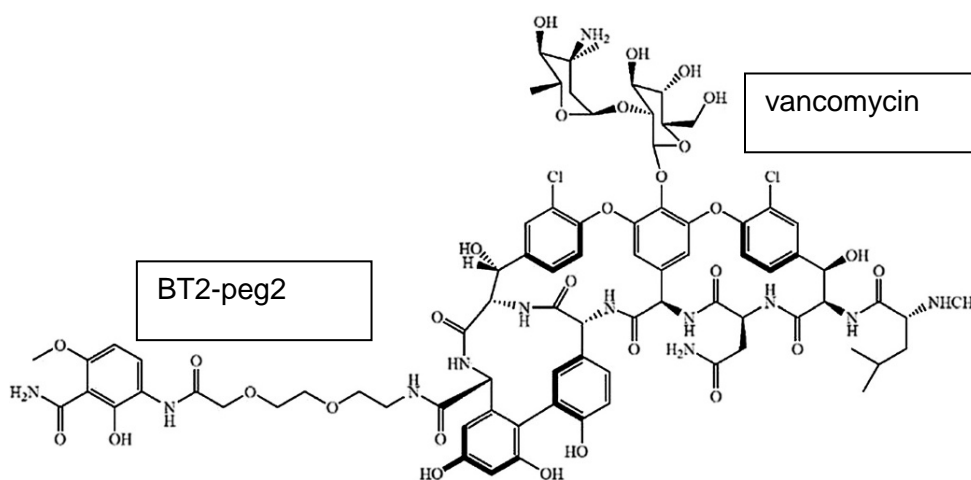
To evaluate the accumulation of vancomycin in the bone directly, we synthesized BT2-peg2-vancomycin and administered the molar equivalent of this conjugate and vancomycin itself to rats by both IP and

intravenous (IV) injection. These studies confirmed increased uptake of vancomycin in the bone with the BT2-peg-2-vancomycin conjugate, but they also confirmed elevated plasma levels in these animals (Fig. 2-3, Albayati et al., 2016).
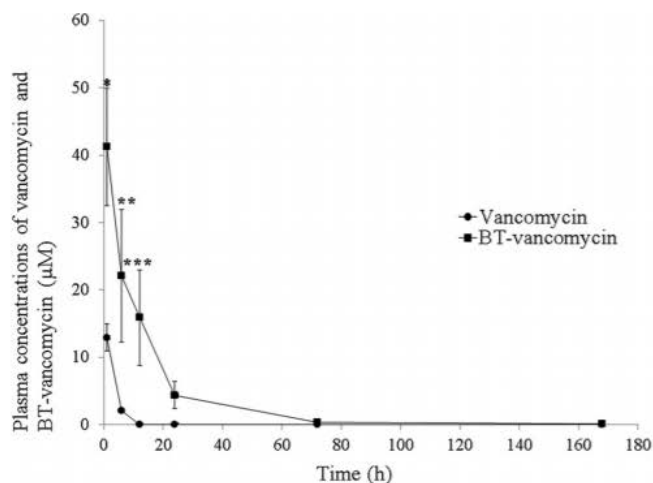

FIG 2 Plasma concentration-time profile of vancomycin (circles) and BT-vancomycin (squares) after i.v. administration of 50 mg/kg vancomycin or 63.85 mg/kg BT-vancomycin (molar equivalent to 50 mg/kg vancomycin). Results are the mean $\pm$ SEM ($n = 5$ rats). *, significantly higher than results for vancomycin, $P < 0.05$; **, significantly higher than results for vancomycin, $P < 0.01$; ***, significantly higher than results for vancomycin, $P < 0.0001$.
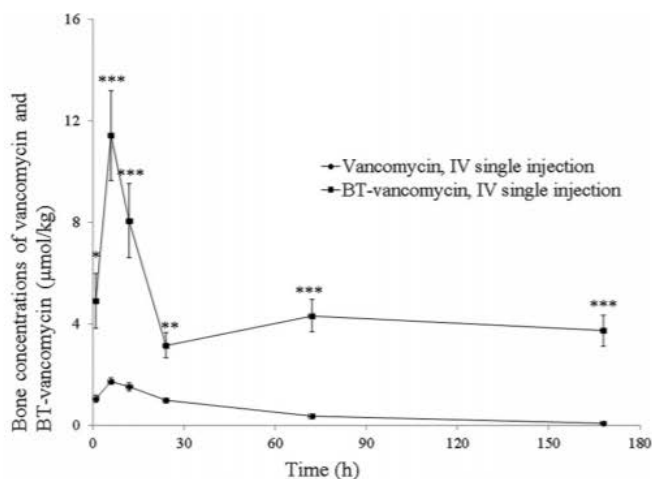

FIG 3 Concentration-time profile in bone of vancomycin (circles) and BT-vancomycin (squares) after i.v. administration of vancomycin (50 mg/kg) or BT-vancomycin (63.85 mg/kg). Results are the mean $\pm$ SEM ($n = 5$ rats per group). *, significantly higher than results for vancomycin, $P < 0.05$; **, significantly higher than results for vancomycin, $P < 0.01$; ***, significantly higher than results for vancomycin, $P < 0.001$.

With respect to the bone, the difference appeared to be clinically relevant as defined by the breakpoint minimum inhibitory concentration (MIC) that defines a vancomycin-sensitive strain of *S. aureus* ($\leq$ 2.0 µg/ml). Specifically, with IV administration of unconjugated vancomycin, levels in the bone fell below this value within one day, while with the BT2-peg2-vancomycin conjugate they remained well above this value for at least 7 days (Table 1, Albayati et al., 2016):

TABLE 1 Comparative concentrations of vancomycin and BT-vancomycin in bone after i.v. administration of 50 mg/kg vancomycin or 63.85 mg/kg BT-vancomycin[a]

Time (h)	Concn (µM) (mean $\pm$ SEM)[a]		BT-vancomycin/ vancomycin ratio
	Vancomycin	BT-vancomycin	
1	1.04 $\pm$ 0.14	4.89 $\pm$ 1.08[b]	4.7
6	1.73 $\pm$ 0.13	11.41 $\pm$ 1.79[c]	6.6
12	1.51 $\pm$ 0.15	8.06 $\pm$ 1.46[c]	5.3
24	0.97 $\pm$ 0.09	3.15 $\pm$ 0.49[b]	3.3
72	0.35 $\pm$ 0.10	4.31 $\pm$ 0.63[c]	12.3
168	0.08 $\pm$ 0.05	3.73 $\pm$ 0.61[c]	46.6

[a] $n = 5$ rats per group.
[b] Significantly higher than results for vancomycin ($P < 0.01$).
[c] Significantly higher than results for vancomycin ($P < 0.001$).

Similar results were observed after IP administration of vancomycin or the BT2-peg2-vancomycin conjugate (Table 2, Albayati et al., 2016), thus further confirming that vancomycin levels can be significantly increased in the bone by conjugating the antibiotic to BT2-peg2. However, these studies also confirmed a dramatic increase in plasma levels of the BT2-peg2-vancomycin conjugate.

TABLE 2 Comparative concentrations of vancomycin and BT-vancomycin in plasma and bone after i.p. administration of 50 mg/kg vancomycin or 63.85 mg/kg BT-vancomycin

Time (h)	Concn (µM) (mean $\pm$ SEM)[a] in plasma		Concn (µM) (mean $\pm$ SEM)[a] in bone		BT-vancomycin/ vancomycin ratio in bone
	Vancomycin	BT-vancomycin	Vancomycin	BT-vancomycin	
1	15.6 $\pm$ 2.0	21.1 $\pm$ 2.1[b]	7.3 $\pm$ 0.4	56.6 $\pm$ 8.4[c]	7.8
6	1.6 $\pm$ 0.2	37.7 $\pm$ 5.1[c]	7.9 $\pm$ 1.5	58.4 $\pm$ 9.2[d]	7.4
12	0.4 $\pm$ 0.04	27.4 $\pm$ 3.1[c]	0.9 $\pm$ 0.1	42.9 $\pm$ 11.1[c]	47.7

[a] $n = 5$ rats per group.
[b] Not significantly different from results for vancomycin.
[c] Significantly higher than results for vancomycin ($P < 0.0001$).
[d] Significantly higher than results for vancomycin ($P < 0.01$).

6

Pharmacokinetic (PK) analysis further confirmed that a decrease in total clearance (CL_{tot}) of 13.5-fold was observed for BT2-peg2-vancomycin compared to vancomycin itself, with a 14.7-fold increase in half-life ($t_{1/2}$) allowing for a 10.8-fold enhancement in the area under the concentration-time curve (AUC). The significant changes in the AUC indicate a higher degree of *in vivo* exposure to BT2-peg2-vancomycin, facilitating the accumulation of drug in bone due to an enhanced permeation and retention effect. Consequently, BT-vancomycin shows a longer systemic mean residence time (MRT) than vancomycin ($P \leq 0.001$). The higher MRT value of BT2-peg2-vancomycin could be due in part to a more

TABLE 3 PK parameters in rats following i.v. administration of a single bolus of 50 mg/kg vancomycin or 63.85 mg/kg BT-vancomycin

Parameter[a]	Result (mean ± SEM) for:	
	Vancomycin	BT-vancomycin
$t_{1/2}$ (h)	1.44 ± 0.09	21.14 ± 4.86[d]
T_{max} (h)	1.00 ± 0.00	1.00 ± 0.00
C_{max} (μM)	12.63 ± 2.38	43.82 ± 9.45[b]
AUC (h · μM)	58.71 ± 10.33	631.39 ± 95.13[c]
V_z (liters/kg)	1.10 ± 0.18	1.13 ± 0.21
CL (liters/h/kg)	0.65 ± 0.12	0.048 ± 0.01[c]
AUMC (h · h · μM)	162.63 ± 25.67	14,225.62 ± 3,012.66[e]
MRT (h)	1.93 ± 0.17	12.45 ± 1.63[d]
V_{ss} (liters/kg)	1.32 ± 0.35	0.80 ± 0.25

[a] T_{max}, time to maximum concentration of drug in serum; V_z, volume of distribution; CL, clearance; AUMC, area under the first moment of the concentration-time curve; V_{ss}, volume of distribution at steady state.
[b] Significantly higher than results for vancomycin ($P < 0.05$).
[c] Significantly higher than results for vancomycin ($P < 0.01$).
[d] Significantly higher than results for vancomycin ($P < 0.001$).
[e] Significantly higher than results for vancomycin ($P < 0.0001$).

protracted steady state *in vivo*, resulting in improved delivery, dramatically increased access into bones, and prolonged exposure in bone tissue (Table 3, Albayati et al., 2016).

Thus, two independent reports confirmed that conjugation of vancomycin to BT2-peg2 was an effective way to increase the accumulation of vancomycin in the bone, but that this was associated with a corresponding increase in the accumulation and retention of vancomycin in the plasma, thus suggesting a cause-and-effect relationship between retention of the conjugate in the plasma and nephrotoxicity. To further explore this possibility, and to determine whether the bone-targeting agent itself contributed to nephrotoxicity, we carried out an experiment in which rats were given IP injections of 11 mg/kg of BP2-peg2 itself, which is the molar equivalent of the BT2-peg2 present in the BT2-peg2-vancomycin conjugate. To ensure that we were able to detect any toxicity, injections were given twice daily for 21 days. BT2-peg2 was detected in the right tibia at concentrations of 235 ± 96.8 ng/gm of bone but was undetectable in plasma. We also did not observe any

Group	Untreated	BT2-peg2-treated
Kidney weight (g)	2.5 ± 0.22	2.4 ± 0.35
BUN (mg/dl)	22.1 ± 2.5	23.0 ± 0.9
Albumin (gm/dl)	3.4 ± 0.02	3.5 ± 0.01
Creatinine (mg/dl)	0.5 ± 0.01	0.6 ± 0.01
Plasma (ng/mL)	-	< 1
Bone (ng/g)	-	235.0 ± 96.8

differences between treated and untreated rats with respect to kidney weight or BUN, creatinine, and albumin levels, nor did we observe any gross histopathological changes in the kidney (Albayati et al., manuscript submitted). We also did not observe any gross histopathological changes in the bone itself. These are key observations because they confirm that the nephrotoxicity observed with the BT2-peg2-vancomycin conjugate is likely due to the vancomycin and not the BT2-peg2 itself, thus suggesting that this agent can be safely used as a means of enhancing the delivery of therapeutic agents to the bone assuming we can identify appropriate therapeutic agents, including conventional antibiotics and small molecule inhibitors of *sarA*-mediated regulation. Accomplishing this task was a principle goal of the work carried out in this grant.
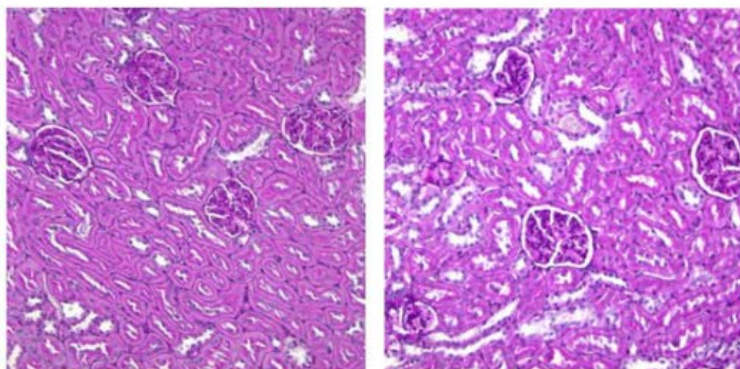
Histological analysis of Albino Wister rat kidneys as a function of BT2-peg2 treatment (11mg ip 2 x daily x 21 days). Periodic acid–Schiff (PAS) stained histopathologic sections from untreated (left) and BT2-peg2-treated kidneys (right) showing no discernible evidence of microscopic glomerular or renal tubular damage.

Fig. 4. Bone histology as a function of BT2-peg2 treatment. Representative H&E stained sections of the right tibia are shown from untreated (left) and BT2-peg2 treated rats.

Based on this, we took the information gained in Task 1 and evaluated the ability to conjugate the most promising antibiotics to BT2-peg2. The primary focus was on daptomycin, ceftaroline, and the paenipeptin analogue 17, but we also explored the ability to generate conjugates with other antibiotics including oxacillin, ciprofloxacin, moxifloxacin, and sparfloxacin. Given the results of our Task 1 studies, we first conjugated BT2 and BT2-peg2 to daptomycin. The resulting conjugates were designated PNR-1-17 and PNR-10-15/2 (PNR-10-15) respectively, with the structures of each shown below.
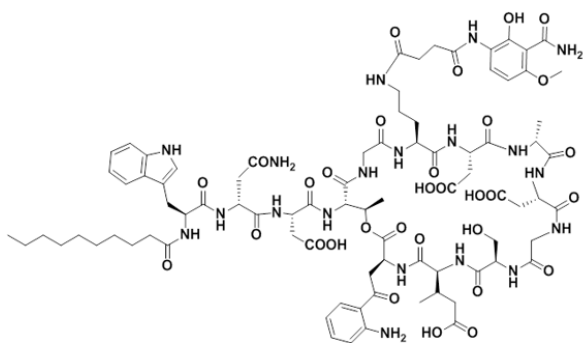
PNR-10-17; Daptomycin BT2-succinic acid conjugate
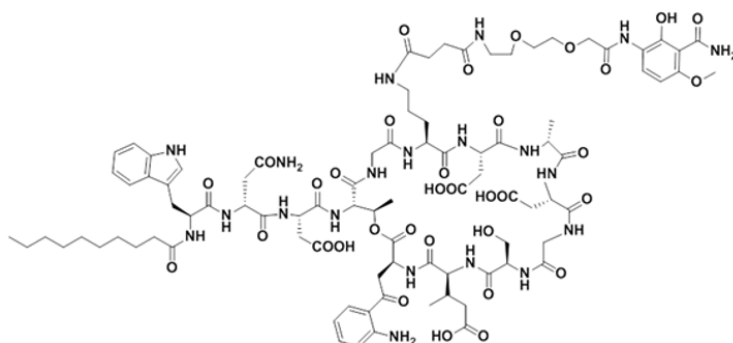
PNR-10-15/2; Daptomycin BT2- minipeg conjugate

The antibacterial activity of each of these was evaluated using a standard broth microdilution assays with daptomycin itself included as a positive control. The results confirmed that in both LAC and UAMS-1, conjugation to BT2-peg2 did result in a decrease in activity and that this decrease was greater with the BT2 conjugate by comparison to the BT2-peg2 conjugate. Importantly, the decrease observed with the BT2-peg2 conjugate was only 2-fold, which we did not consider unacceptable given the degree to which BT2-peg2 was shown to increase the accumulation of vancomycin in the bone (Albayati et al., 2016).
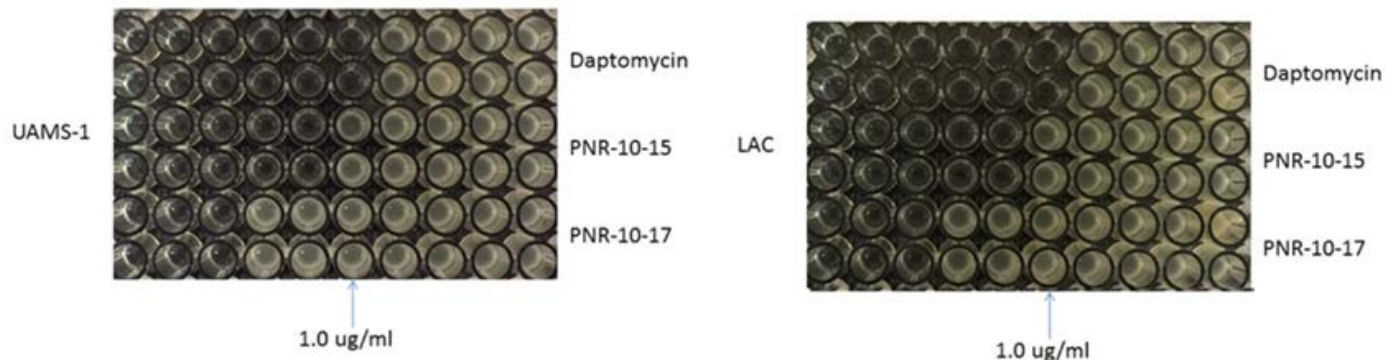
The arrow indicates the CLSI-defined breakpoint MIC for a daptomycin-sensitive strain of *S. aureus*. The BT2 and BT2-peg2-daptomycin conjugates were tested at the molar equivalent of daptomycin itself.

PNR-10-15 was synthesized with a succinic acid linker, and while this did not limit its antibacterial activity to an extent that we felt precluded further study in Task 3, as detailed below we found that bone targeting was compromised with this conjugate. Taken together, these results demonstrate the potential of the approach we explored, but they also emphasize the complexity of doing so. More directly, these results demonstrate that we can successfully conjugate alternative antibiotics to BT2-peg2 but that doing so has the potential to limit the activity of antibiotic and/or the bone targeting properties of the BT2-peg2. In an attempt to address this, we synthesized two alternative BT2-peg2-daptomycin conjugates, one of which incorporated a propanamide linker (**PNR-11-25**) while the other used an ethanamide linker (**PNR-11-26**):

Daptomycin BT2-peg2 propanamide (PNR-11-25)   Daptomycin BT2-peg2 ethanamide (PNR-11-26)
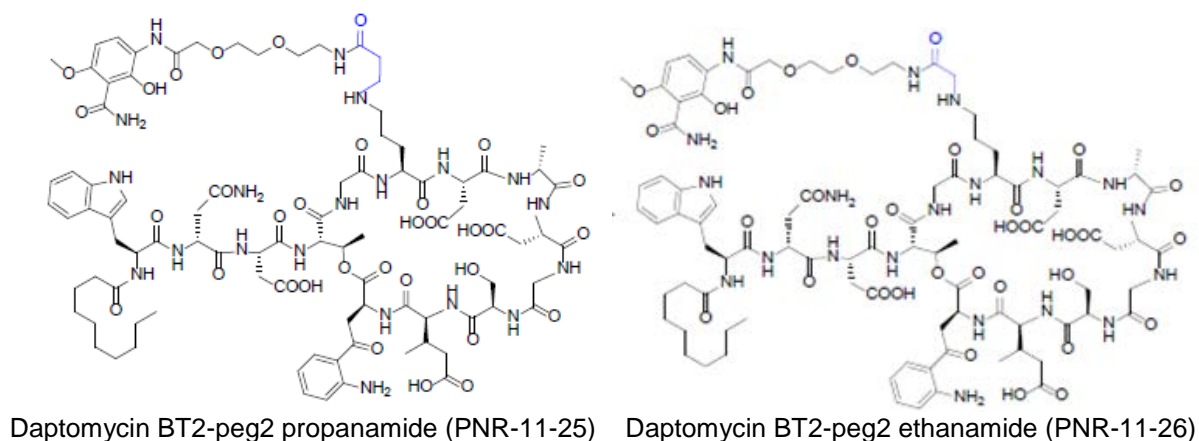
Synthesis of PNR-11-25 has proven problematic, but we have successfully synthesized PNR-11-26. However, to date the yield of PNR-11-26 has been low as illustrated below. Continued efforts to synthesize PNR-11-15, and attempts to enhance the synthesis and purification of PNR-11-26 to a degree sufficient to generate an appropriate BT2-peg2 conjugate, are ongoing. If successful, these will be then be evaluated *in vivo* as described for Task 3.

Daptomycin BT2-peg2 ethanamide conjugate (PNR-11-26)

Daptomycin BT2-peg2 ethanamide conjugate HPLC

Daptomycin HPLC
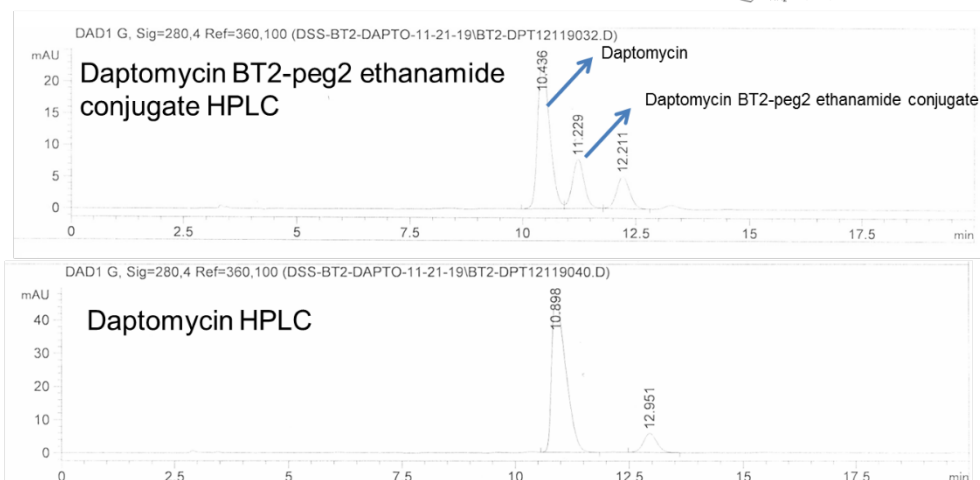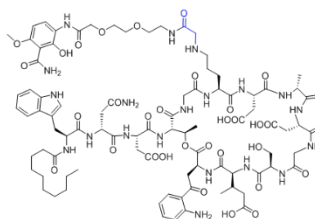
For the reasons oulined above, we also placed a particular emphasis on generating a BT2-peg2 conjugate to ceftaroline. Ceftaroline is commercially available as a prodrug (ceftaroline fosamil), and we initially encountered significant difficulties in generating the desired conjugate using this prodrug. To overcome this, we synthesized a ceftaroline analogue **(BS-7-54)**, and we were successful in conjugating this analogue to BT2-peg-2 (**BS-5-02**). In a previous progress report (April, 2019), it was stated that "additional testing has confirmed that the antibacterial activity of **BS-5-02** is reduced ~2-4 fold by comparison to ceftaroline itself", but that "this activity was not further reduced by conjugation to BT2-minipeg-2" (BT2-minipeg-2 and BT2-peg2 are the same compound, but we have chosen to refer to this compound in this report at BT2-peg2 in the interest of being consistent with the existing literature). However, when we synthesized more of this compound, we were unable to reproduce this result, suggesting that the original analogue conjugate was either in error or was not purified sufficiently. Thus, we were unable to move forward with a BT2-peg2-ceftaroline conjugate even with this analogue. Similarly, in the 2017 annual progress report we stated that we also synthesized a BT2-peg2 conjugate to ceftaroline fosamil itself. This statement was made based on the structure below and information provided to the PI by the Crooks' laboratory, the members of which had the primary responsibility for chemical synthesis and verification.

BT2-peg2   ceftaroline fosamil

BS-6-71
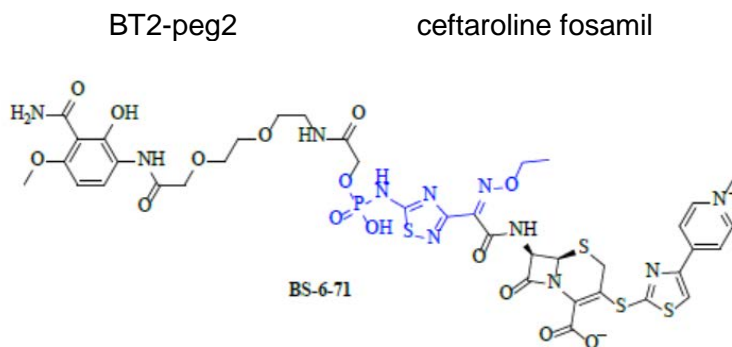
However, we were unable to confirm this upon further characterization of this molecule. Using funds from other sources, efforts are continuing to overcome this issue based on the increased efficacy of ceftaroline in the context of an established *S. aureus* biofilm as demonstrated in our earlier studies (Meeker et al., 2016) and taking advantage of the chemical scaffold defined by this structure.

As detailed above, our primary emphasis in Task 2 was on daptomycin and ceftaroline and assessing the ability to conjugate these antibiotics to BT2-peg2. This was based on our extensive studies confirming that the overall objective of enhancing the accumulation of an antibiotic that is active against MRSA in the bone is not a viable option with vancomycin owing to systemic toxicity associated with prolonged retention of vancomycin in plasma. Despite our efforts to develop BT2-peg2 conjugates to daptomycin and ceftaroline, we encountered unanticipated issues with both of these antibiotics. We made extensive efforts to overcome these issues, but to date we have been unable to do so. That said, we remain committed to the goal and are continuing our efforts in this regard. Because the funding period has ended, we are pursuing these studies using discretionary funds available to the PI (Dr. Smeltzer).

Although our primary emphasis in Task 2 was on daptomycin and ceftaroline, we also explored the ability to conjugate BT2-peg2 to other antibiotics, most notably oxacillin and a group of fluoroquinolones including moxifloxacin, sparfloxacin, and ciprofloxacin. With moxifloxacin and sparfloxacin, the MIC was increased to an unacceptable degree, but this was not the case with BT2-peg2-ciprofloxacin. If these results can be verified, this opens up the possibility that this compound warrants *in vivo* consideration.

BS-6-68
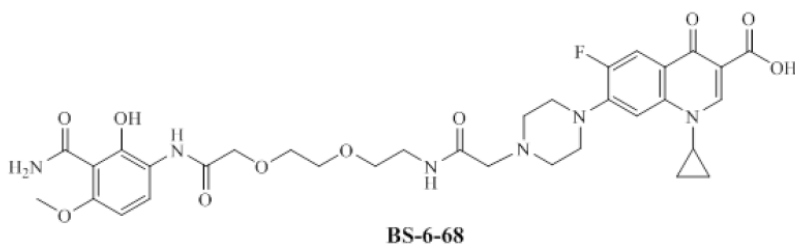
Chemical structure of BT2-minipeg-2 ciprofloxacin.

This was not the case with oxacillin. Specifically, we generated several BT2-peg2 conjugates to oxacillin that differed with respect to the length of the polyethylene glycol linker, but when these were tested none were found to exhibit significant antibacterial activity:

Oxacillin

11

Task 3: Evaluate *in vivo* pharmacological properties of antibiotics and antibiotic conjugates in the context of bone targeting. To summarize the results discussed above, the only BT2-peg2-antibiotic conjugates we were able to successfully and reproducibly generate were to daptomycin (**PNR-10-15**) and ciprofloxacin (**BS-6-68**). Because ciprofloxacin is active against some but not all MRSA strains, and because we demonstrated that daptomycin has greater efficacy than most other antibiotics in the context of an established biofilm (Meeker et al., 2016), we focused first on addressing this task in the context of PNR-10-15. Specifically, to examine the *in vivo* pharmacological properties of our BT2-peg2-daptomycin conjugate and assess its accumulation in bone relative to unconjugated daptomycin itself, female C57BL/6 mice (20-25 g, n = 2-5) were injected with a single IP dose of 40 mg/kg of daptomycin or 50 mg/kg of BT2-peg2-daptomycin (the molar equivalent of 40 mg/kg of daptomycin) or with an intravenous dose of 2 mg/kg of daptomycin or 2.5 mg/kg of BT2-peg2-daptomycin (the molar equivalent of 2 mg/kg of daptomycin). Mice were euthanized and blood and bone tissues collected at 6 time points (30 min and 1, 2, 4, 7 and 24 h). Tissues were stored at -80ºC for subsequent LC/MS/MS analysis. Significant amounts of daptomycin and BT2-peg2-daptomycin were detected in the bone after both IV and IP administration. However, the results were surprising in that, after IV administration of daptomycin and BT2-peg2-daptomycin, the area under the curve (AUC) values were 19,193 µg/hr/L and 10,463 µg/hr/L, respectively. This indicates that, following IV administration, the accumulation of daptomycin in the bone was actually 1.4-fold greater than that observed with BT2-peg2-daptomycin. Unfortunately, similar results were observed after IP administration. Specifically, IP injection showed AUC values of 159,201 and 12,955 µg/hr/L, demonstrating a 12.3-fold greater bone exposure of daptomycin compared to BT2-peg2-daptomycin. Estimates of bone bioavailability values indicated 41.5% and 6.2% for daptomycin and BT2-peg2 daptomycin, respectively, when administered via the IP route. Similar results were observed when daptomycin and BT2-peg2-vancomycin were administered by the IV route.
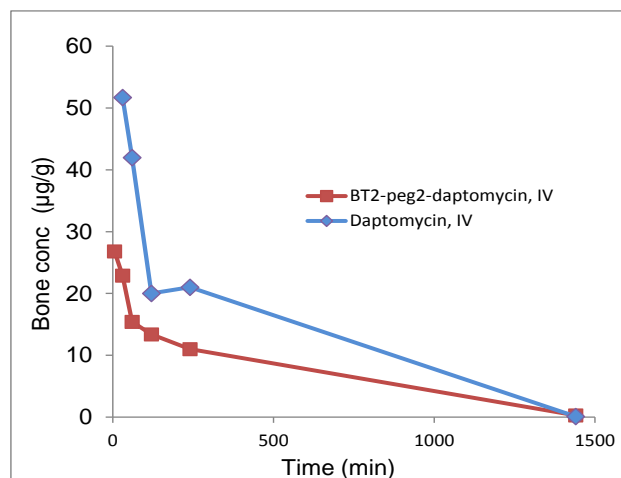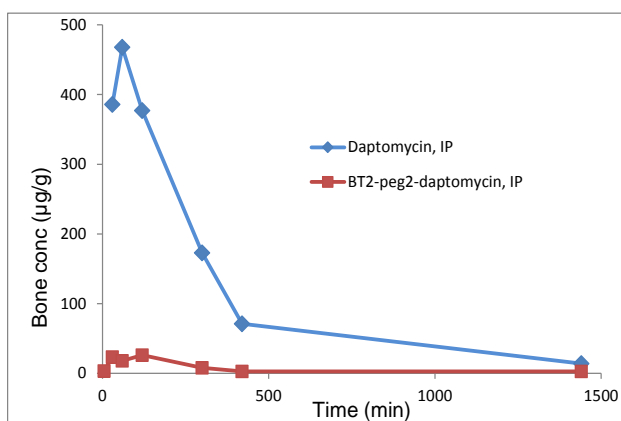
We also carried out *in vivo* studies with our BT2-peg2-ciprofloxacin conjugate. As a prerequisite to these studies, we developed an LC/MS/MS analytical method to quantify ciprofloxacin and its conjugate BT2-minipeg-2 ciprofloxacin in plasma and bone. The chromatograms shown below illustrate the specificity of this method and the fact that we can readily distinguish between the BT2-peg2-ciprofloxacin conjugate next page, top panel) and unconjugated ciprofloxacin itself (next page, bottom panel).
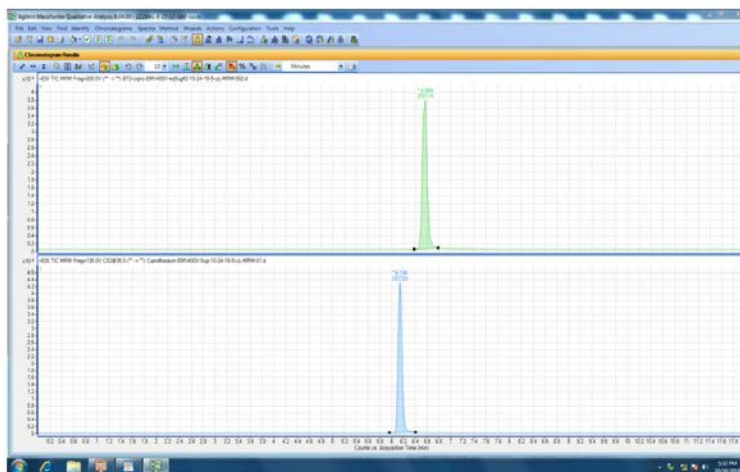
To assess our analytical ability to accomplish this task with samples obtained *in vivo*, a single female C57BL/6 mouse weighing 20-25 gms was treated IP with a single dose of BT2-peg2-ciprofloxacin at 22.2 mg/kg (the molar eq. to 10 mg/kg ciprofloxacin, a simulated human dose as defined by Jimenez-Valera et al. (Jimenez-Valera M, Sampedro A, Moreno E, Ruiz-Bravo A. 1995. Modification of immune response in mice by ciprofloxacin. Antimicrob Agents Chemother. 39:150-154). Plasma and bone tissues were collected at 5, 10, 20, 45 and 120 min. Plasma was analyzed for BT2-peg2-ciprofloxacin. The results indicate absorption of BT2-peg2-ciprofloxacin into plasma was fast and peaked at 5 min and reached maximum at 45 min and then started to decrease after 120 min. The next step was to apply the LC/MS/MS method of analysis to bone tissues. Based on the results from plasma, a sample of bone tissue was taken 1 h after treatment and analyzed to determine the level of BT2-minipeg-2 ciprofloxacin. The results showed a broad chromatogram for BT2-minipeg-2 ciprofloxacin in bone, suggesting interference from endogenous substances from bone tissue.
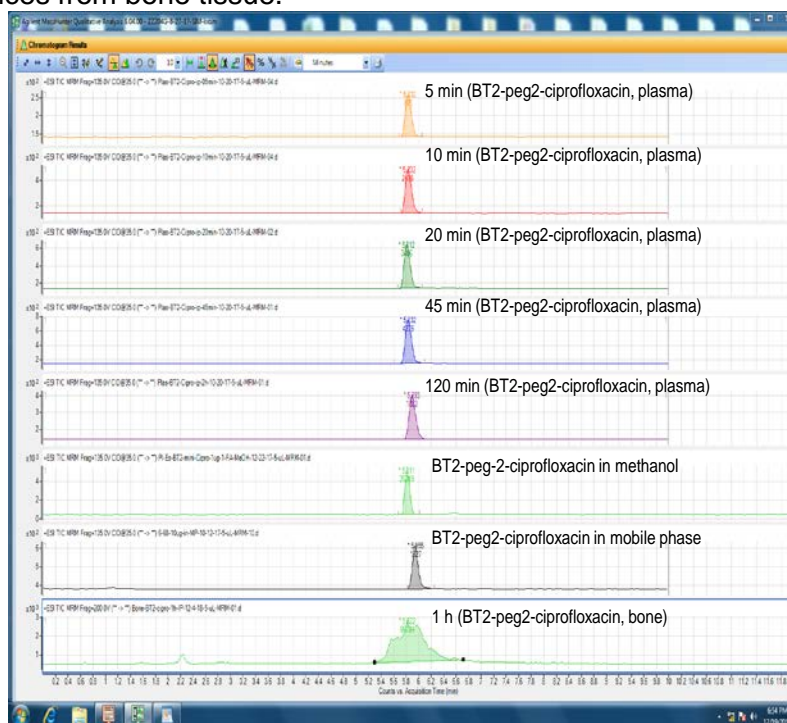
After refining and optimizing the analysis method to interference from matrix in bone tissue, and IP dose of 10 mg/kg and 22.2 mg/kg for ciprofloxacin and BT2-peg2-ciprofloxacin, respectively. This resolved the issue of interference and allowed us to quantify ciprofloxacin and BT2-minipeg ciprofloxacin in plasma and bone tissues. Using these doses, we determined the levels of ciprofloxacin and BT2-minipeg ciprofloxacin in plasma and bone tissues 5, 10, 20, 45 min and 1, 3, 5, 7 and 24h after administration. A parallel experiment was carried out to compare levels observed at the same time points after IV administration. As illustrated below, irrespective of the method of administration the BT2-peg-ciprofloxacin conjugate was found to be unstable *in vivo* as reflected by the ability to detect ciprofloxacin itself in both the plasma and bone of rats administered the BT2-peg2-ciprofloxacin conjugate (see next page). Efforts are currently underway to determine why this is the case and ultimately overcome this issue of instability, with the ultimate goal being to characterize the pharmacokinetic profile and bioavailability of BT2-minipeg ciprofloxacin and compare it to that of ciprofloxacin.
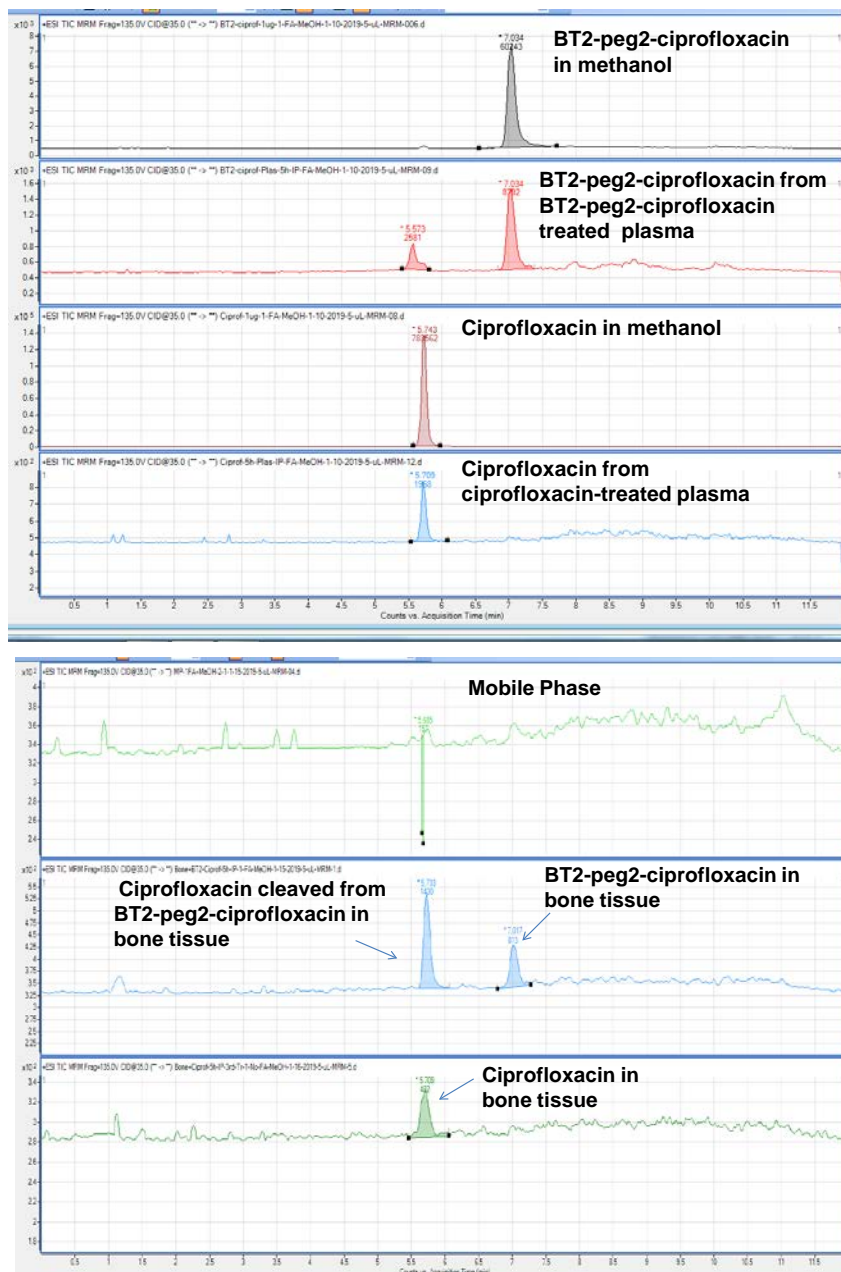
Chromatograms illustrating that unconjugated ciprofloxacin was detected in both the plasma and bone after administration of BT2-peg2-ciprofloxacin.

14

Task 4: Identify small molecule inhibitors of *sarA*-mediated regulation. Conventional antibiotic therapy does not work effectively in biofilm-associated infections including those involving bone. This is why surgical debridement, often accompanied by some form of local antibiotic therapy directly at the wound site, is often necessary to resolve the infection, and even then the failure rate remains unacceptably high. One way to potentially help overcome this is to enhance systemic delivery of antibiotics to the bone while avoiding unwanted side effects. As detailed above, based on previous studies, one way to do this is to take advantage of BT2-peg2 as a bone targeting agent. We and others have confirmed the increased accumulation of vancomycin in the bone using a BT2-peg2-vancomycin conjugate, but we do not believe it is possible to take therapeutic advantage owing to the fact that it also resulted in increased kidney toxicity owing to increased and more persistent levels of vancomyin in the blood. This accounts for our focus on BT2-peg2 conjugated to alternative antibiotics, but as noted above we have thus far been unsuccessful in generating an alternative that retained both its antibacterial and bone targeting properties. As was also noted above, we are continuing to work toward this goal to the best of our ability despite the fact that the funding period for this grant has ended.

At the same time, we also expended a great deal of effort on the alternative and potentially complimentary approach of identifying effective inhibitors of *sarA*-mediated regulation. This effort was based on our extensive studies demonstrating that mutation of *sarA* in S. aureus limits biofilm formation to a degree that can be correlated with increased antibiotic susceptibility (Weiss et al., 2009, Atwood et al., 2016). It also limits cytotoxicity for both osteoblasts and osteoclasts (Loughran et al., 2016) and virulence in animal models of both bacteremia (Rom et al., 2017) and osteomyelitis (Loughran et al., 2016). It is this observation that led us to efforts to identify effective small molecule inhibitors of *sarA*-mediated regulation. We also demonstrated that the primary mechanistic factor that defines all of these *sarA*-associated phenotypes is the increased production of extracellular proteases in *sarA* mutants and the resulting decrease in the accumulation of multiple surface-associated and extracellular virulence factors (Beenken et al., 2014, Loughran et al., 2014, Tsang et al., 2008, Zielinska et al., 2012). Specifically, *S. aureus* encodes 10 known extracellular proteases encoded by individual genes (aureolysin; *aur*) or organized into each of 3 operons (*scpAB*, *splA-F*, and *sspABC*). Thus, we generated reporter constructs consisting of the promoters from these genes/operons fused to superfolder green fluorescent protein (*gfp*). Subsequent studies confirmed that, relative to levels observed in the isogenic parent strains, fluorescence was significantly increased with all four reporters when they were present in *sarA* mutants generated in both the methicillin-sensitive strain UAMS-1 (U1) and the methicillin-resistant strain LAC.
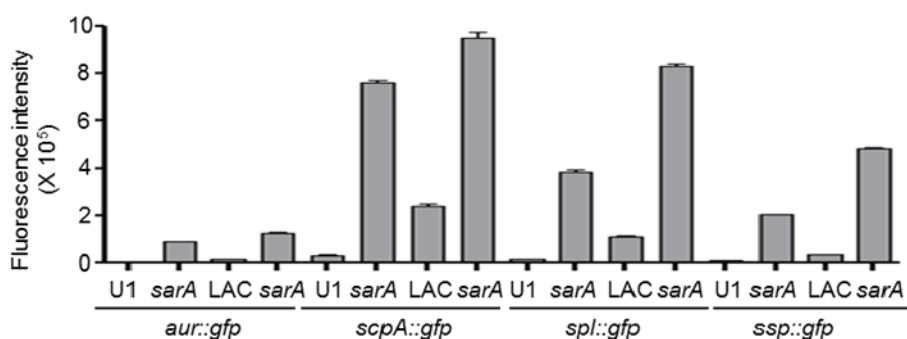
Fluorescence intensity is shown in each of two *S. aureus* strains (LAC and UAMS-1, designated here as U1) and their isogenic *sarA* mutants. The specific protease gene/operon promoter fused to the gfp reporter is shown below the graph. While expression from all 4 promoters was increased in the *sarA* mutant generated in both strains, we chose to use the *scpA::gfp* reporter in our primary screen based on the fact that fluorescence was highest in both strain with this reporter, thus providing us with an extended dynamic range.

Using the scp::grp reporter, we screened ~3,000 compounds available in the Crooks' laboratory that has been "pre-screened" based on chemical characteristics similar to those observed with drugs in current clinical use. The screen was initially done with LAC and its *sarA* mutant with the objective of identifying and prioritizing compounds that did not inhibit the growth of *S. aureus* but did result in increased

fluorescence levels in the parent strain, thus suggesting possible inhibition of *sarA* activity. To ensure that we did not fail to identify a promising compound, we set a standard of a fluorescence level in the parent strain in the presence of the test compound that was at least 25% of the level observed in the *sarA* mutant in the absence of the same compound after accounting for any intrinsic fluorescence of the test compound itself. Compounds that met these criteria were designated as primary "hits" that potentially warranted further investigation and development.

Upon completion of screening our small molecule library, we had identified 15 compounds that registered as hits during the screening process. We then compared each hit using each of the other three protease reporters. In this respect it is important to note that a recent report described a highly complex regulatory network that impacts the production of *S. aureus* proteases, but none were found to do so to the extent associated with *sarA*, and most did not impact the production of all 10 proteases (Gimza et al., 2019). Thus, identifying compounds in which fluorescence is increased in the parent strain using all four reporters would further enhance our chances of identifying an inhibitor of *sarA*-mediated regulation.

16

spl Reporter Assay
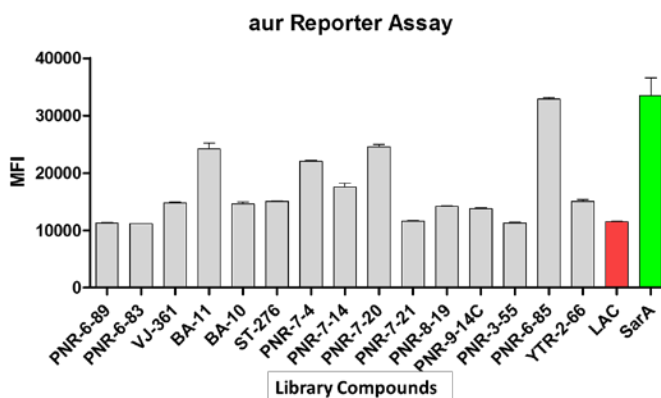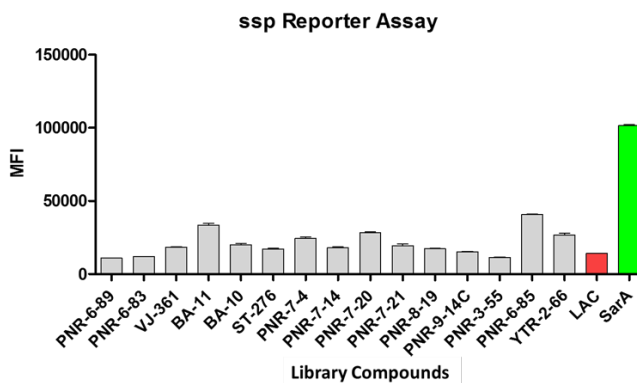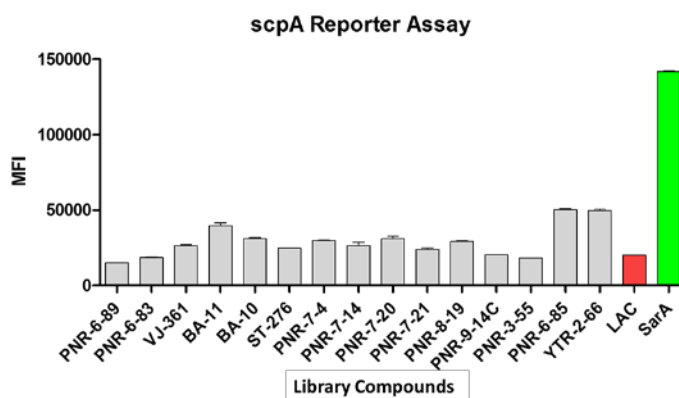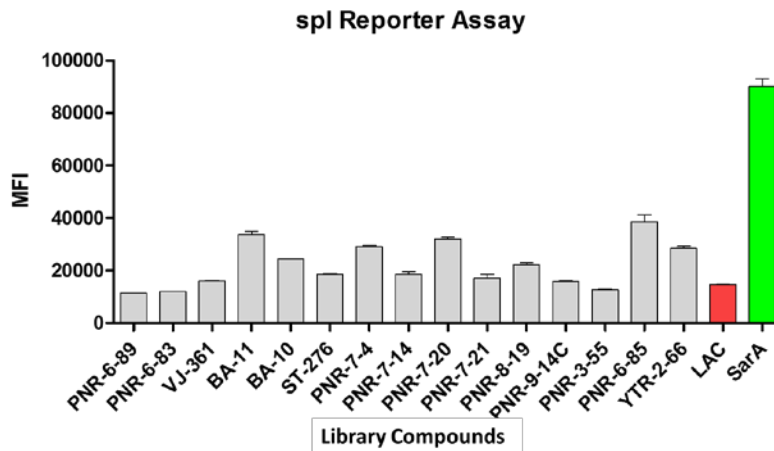
The two compounds that were found to have the greatest impact with all four reporters were PNR-6-85 and YTR-2-66. Of these, YTR-2-66 was found to have the greatest impact on biofilm formation itself:

Biofilm Assay: Relative to LAC over two biological replicates
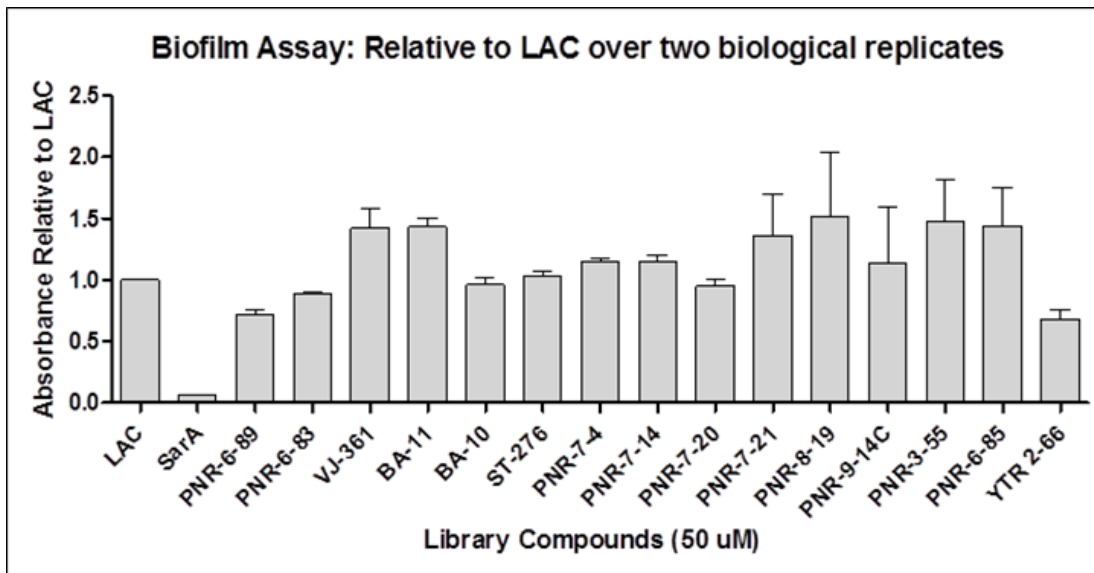
YTR-2-66 was found to limit biofilm formation to a level ~50% of that observed in a LAC *sarA* mutant, and this effect was shown to be concentration dependent.

Biofilm Assay: Relative to LAC
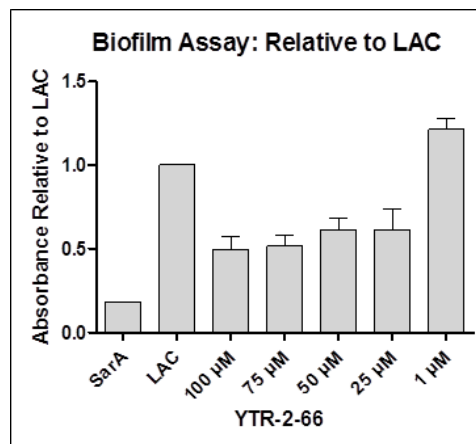
To optimize the biofilm inhibition observed, we focused on generating analogs of YTR-2-66. Due to working with a smaller number of test compounds, this allowed us to focus on identifying compounds that inhibited biofilm formation irrespective of whether they function through *sarA* as suggested by our reporter assay. For this reason, newly synthesized compounds were evaluated using our biofilm assay instead of our reporter assay. We then compared the most promising of these to YTR-2-66 in the context of biofilm formation by both LAC and UAMS-1. None of these were found to inhibit bacterial growth, and when assessed using both LAC and UAMS-1 the compounds BS-6-123c and BS-7-61b were found to be the most promising biofilm inhibitors.
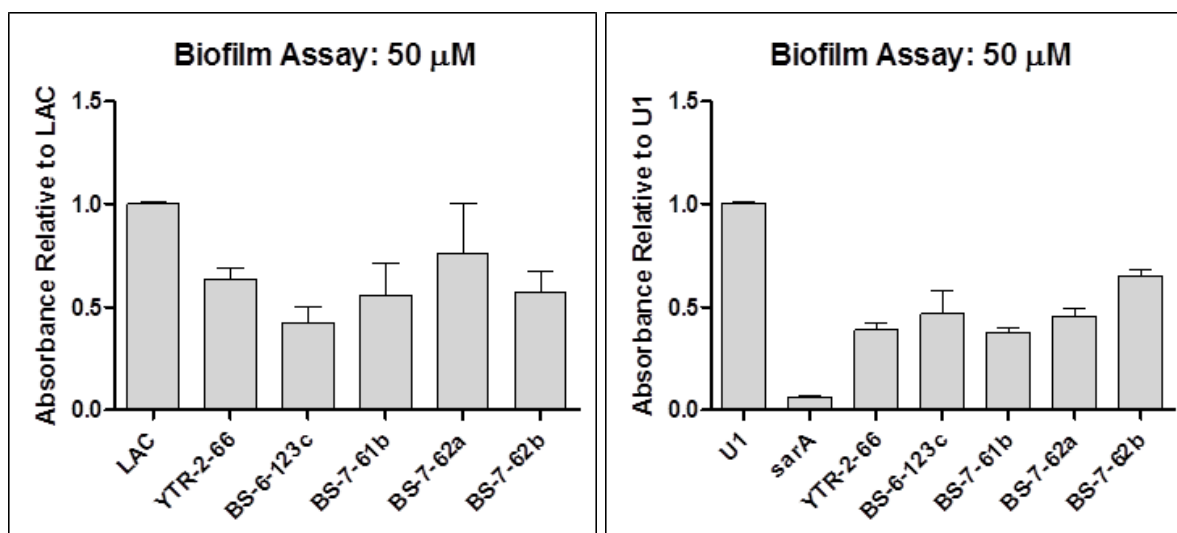
Compound	Biofilm Reduction (compared to LAC)	Biofilm Reduction (compared to U1)
YTR-2-66	36%	61%
BS-6-123c	57%	53%
BS-7-61b	44%	62%
BS-7-62a	24%	55%
BS-7-62b	43%	35%

These studies were done using a microtiter plate biofilm assay and do not take relative antibiotic susceptibility into account. We addressed this by determining whether the degree of biofilm inhibition we observed can be correlated with increased antibiotic susceptibility. Using our *in vitro* catheter model, we have tested both BS-6-123c and BS-7-61b, using the methicillin-resistant strain LAC with daptomycin as the test antibiotic. Below, we show the data representing BS-6-123c after 24 and 72 hours, respectively. The same results were observed with BS-7-61b, indicating that neither compound significantly enhanced daptomycin susceptibility in the context of an established *S. aureus* biofilm.
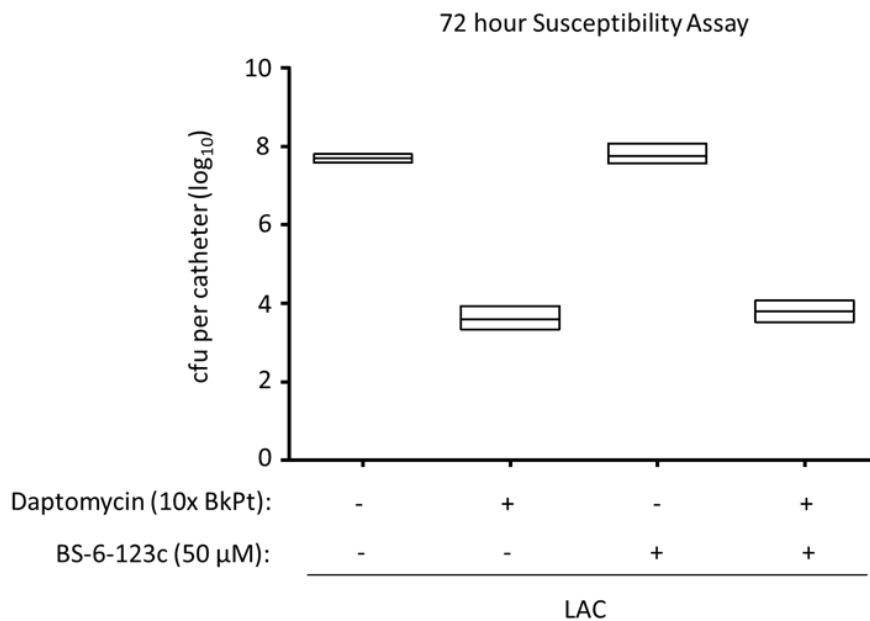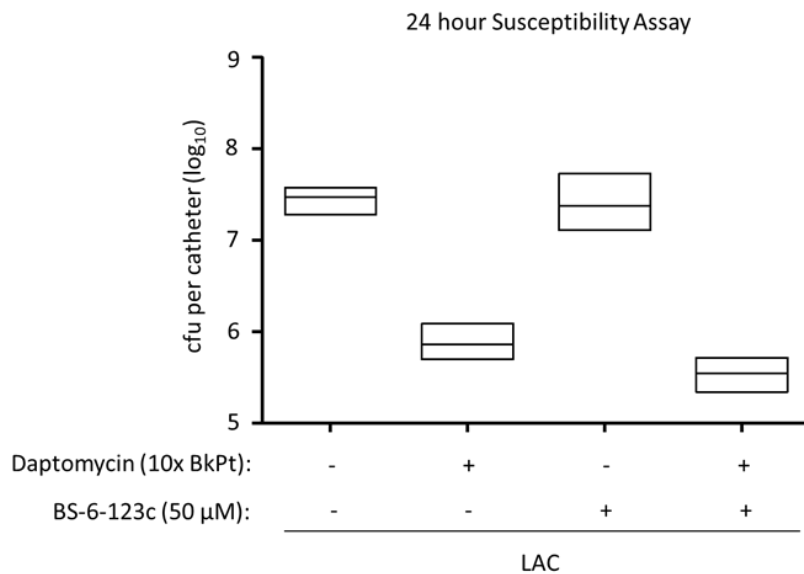
24 hour Susceptibility Assay

cfu per catheter (log_{10})

| Daptomycin (10x BkPt): | - | + | - | + |
| BS-6-123c (50 µM): | - | - | + | + |

LAC

72 hour Susceptibility Assay

cfu per catheter (log_{10})

| Daptomycin (10x BkPt): | - | + | - | + |
| BS-6-123c (50 µM): | - | - | + | + |

LAC

Task 5: Screen additional compounds to identify small molecule inhibitors of *sarA*-mediated regulation. During the course of our work focusing on Task 4, we identified a number of reports in the literature describing small molecule inhibitors of biofilm formation in *S. aureus*, some of which were reported to function via a *sarA*-dependent mechanism. To address these reports, the Crooks' laboratory began synthesizing these compounds as well as analogues of each compound. Below is a table of the compounds that we evaluated using our protease reporter assay as detailed in Task 4. By way of explanation, the column labeled "Identical/analogue" indicates whether the compound tested was identical to that reported in the literature or an analogue of the same compound. The column labeled "hit" indicates whether the compound was considered promising with the caveat that we also noted compounds that came "close" to the standard we set for a legitimate hit but technically failed to reach this standard. This was based on the presumption that additional analogues of such compounds may warrant further consideration. The relevant literature citation is also included in the far right column.

	Compound	Identical / Analogue	Hit	Literature
1.	PNR-10-143A	Analogue	No	Bottcher et al. 2013. *J Am Chem Soc.* 135: 2927-2930. PMID:23406351
2.	PNR-10-143B	Analogue	No	
3.	PNR-10-143C	Identical	No	
4.	PNR-10-150C	Identical	No	Basak et al. 2016. *Chemistry.* 22:9181-9189. PMID:27245927.
5.	PNR-10-150F	Identical	No	
6.	PNR-10-147C	Analogue	No	
7.	PNR-10-147F	Analogue	No	
8.	BSK-3-03	Analogue	No	
9.	BSK-3-14	Analogue	No	
10.	BSK-3-15	Analogue	No	
11.	BSK-3-16	Analogue	No	
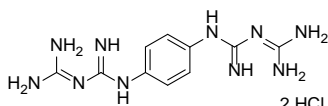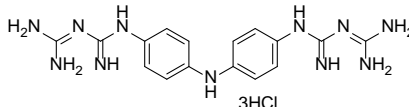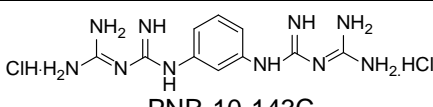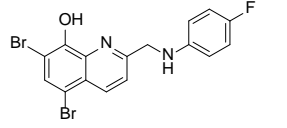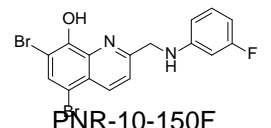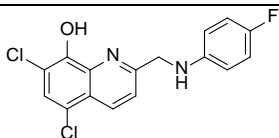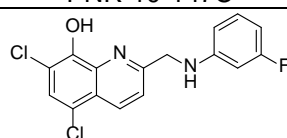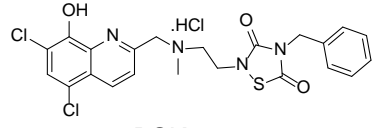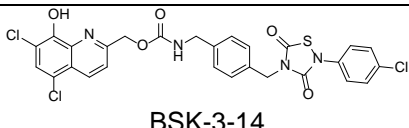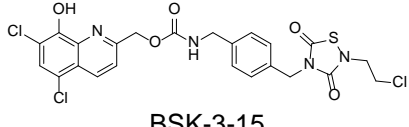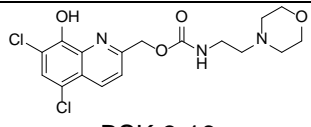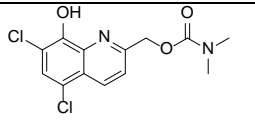
12.	BSK-3-17	Analogue	No	
13.	BSK-3-18	Analogue	No	
14.	BSK-3-19	Analogue	**Yes**	
15.	BSK-3-20	Analogue	No	
16.	BSK-3-21	Analogue	No	
17.	BSK-3-22	Analogue	No	
18.	BSK-3-24	Analogue	**Yes**	
19.	BSK-3-25	Analogue	Close	
20.	BSK-3-26	Analogue	No	
21.	BSK-3-33	Analogue	No	
22.	BSK-3-49	Analogue	**Yes**	
23.	BSK-3-50	Analogue	No	
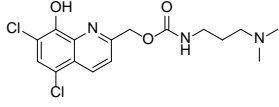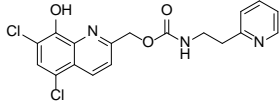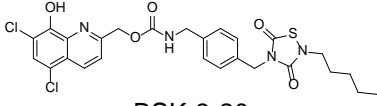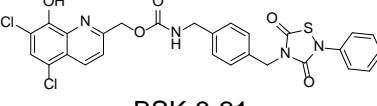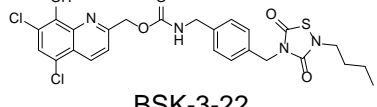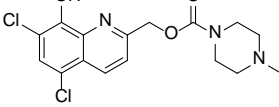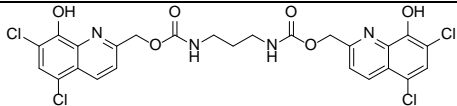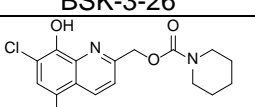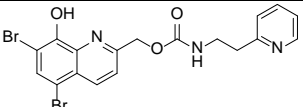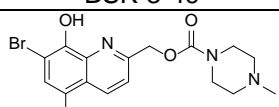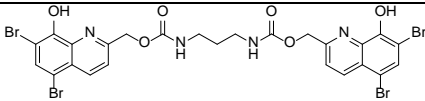
24.	BSK-3-51	Analogue	No	
25.	BSK-3-53	Analogue	No	
26.	BSK-3-56	Analogue	No	
27.	BSK-3-57	Analogue	No	
28.	BSK-3-58	Analogue	No	
29.	BSK-3-60	Analogue	Close	
30.	BSK-3-61	Analogue	Close	
31.	BSK-3-62	Analogue	No	
32.	BSK-3-63	Analogue	No	
33.	BSK-3-64	Analogue	No	
34.	BSK-3-66	Analogue	No	
35.	BSK-3-67	Analogue	No	
36.	BSK-3-68	Analogue	**Yes**	
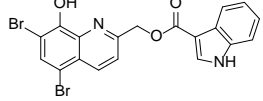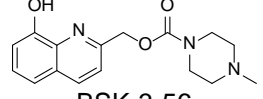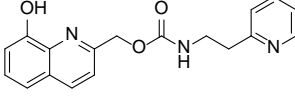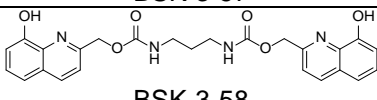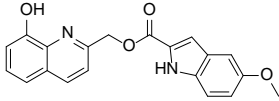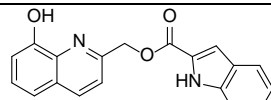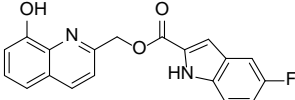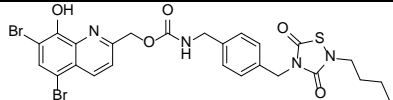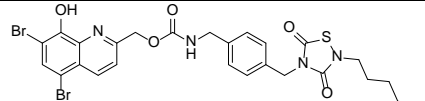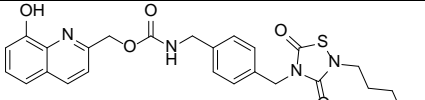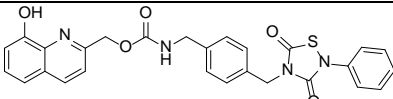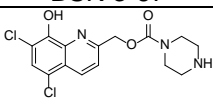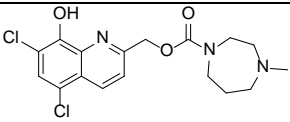
37.	BSK-3-70	Analogue	No	
38.	BSK-3-72	Analogue	No	
39.	BS-6-163	Analogue	Close	
40.	BS-6-157	Identical	Close	
41.	PNR-9-92	Analogue	No	Arya et al., 2015. *Front Microbiol.* 6:416. PMID:26074884
42.	PNR-10-01	Identical	No	
43.	PNR-10-109A	Identical	No	Balamurugan et al. 2015, *Front Microbiol.* 6:832. PMID: 26322037
44.	PNR-10-117	Identical	No	Balamurugan et al. 2017. *Front Microbiol.* 8:1290. PMID: 28744275
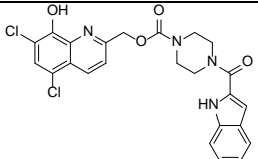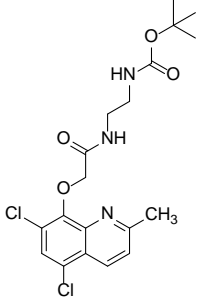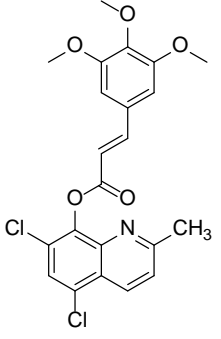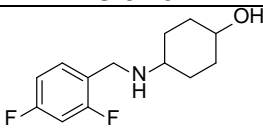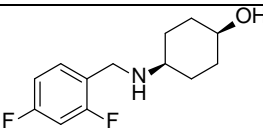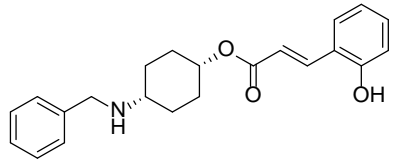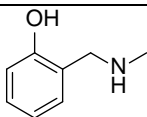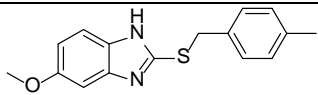
#	Structure			Reference
45.	PNR-10-126A	Identical	No	Sambanthamoorthy et al. 2011. *Antimicrob Agents Chemother*, 55:4369-78. PMID: 21709104
46.	PNR-10-126B	Identical	No	
47.	PNR-10-84	Identical	No	Minvielle et al., 2013. *Medchemcomm.* 4:916-919. PMID: 23930199
48.	BS-5-98	Analogue	No	Abraham et al., 2016. *J Med Chem.* 59: 2126-2138. PMID: 26765953
49.	BS-5-91	Analogue	No	
50.	BS-7-16a	Analogue	Close	
51.	BS-7-17b	Analogue	**Yes**	
52.	BS-7-17a	Analogue	Close	
53.	BS-7-39a	Analogue	No	
54.	BS-7-39b	Analogue	No	
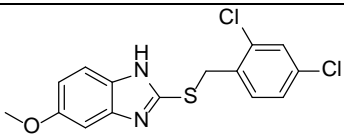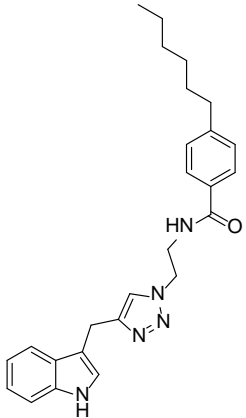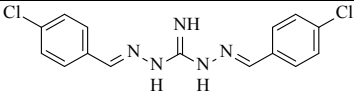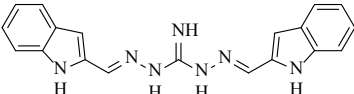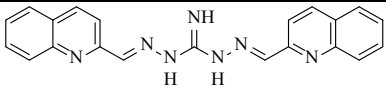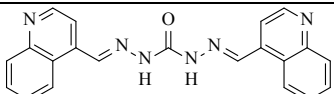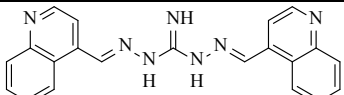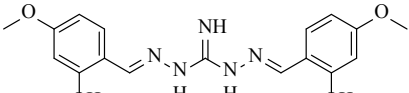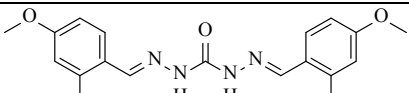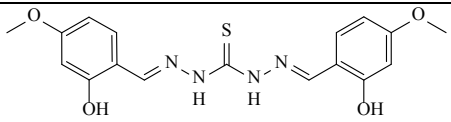
55.	BS-7-39c	Analogue	No
56.	BS-7-41a	Analogue	No
57.	BS-7-41b	Analogue	No
58.	BS-7-41c	Analogue	No
59.	BS-7-42a	Analogue	No
60.	BS-7-42b	Analogue	No
61.	BS-7-42c	Analogue	No
62.	BS-7-43a	Analogue	No
63.	BS-7-43b	Analogue	No
64.	BS-7-43c	Analogue	No
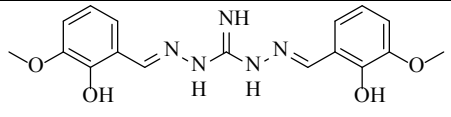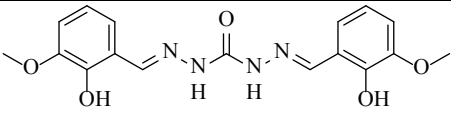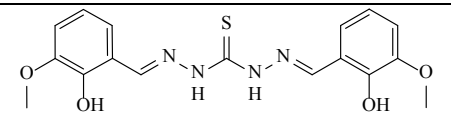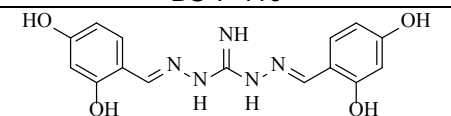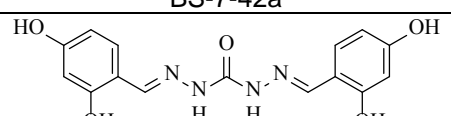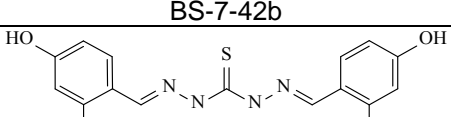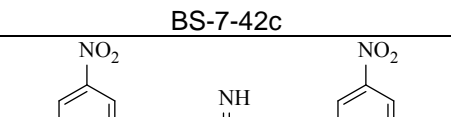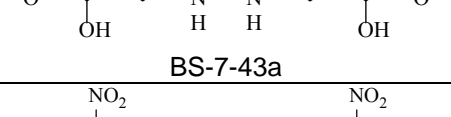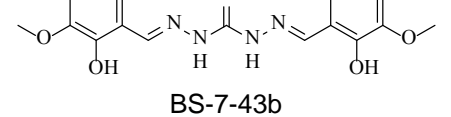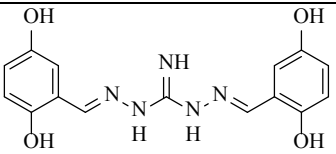
#	Structure		Relationship	Marker	Reference
65.	BS-7-44a		Analogue	No	
66.	BS-7-44b		Analogue	No	
67.	BS-7-44c		Identical	No	
68.	PTL		Analogue	No	Romero et al., 2013. *Chem Biol.* 20:102-110. PMID: 23352144
69.	BS-1-28		Identical	No	
70.	BS-6-97		Analogue	No	Goswami et al., 2014. *ACS Appl Mater Interfaces.* 6:16384-16394 PMID: 25162678
71.	BS-6-81a		Identical	**Yes**	
72.	BS-6-76a (L-Tyrosine)		Identical	No	Kolodkin-Gal, et al. 2010. *Science.* 328:627-629 PMID: 20431016
73.	Pillarene BS-6-117		Identical	No	Joseph, R et al. 2016. *J Am Chem Soc.* 138:754-757. PMID: 26745311
74.	BS-6-91a		Identical	No	Williams, et al., 2012. *Biomaterials.* 33:8641-8656. PMID: 22940221
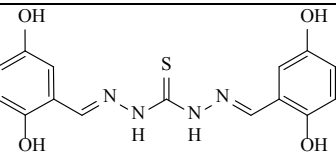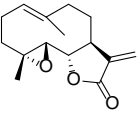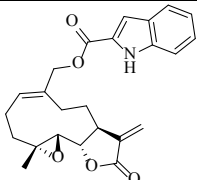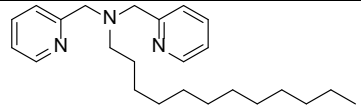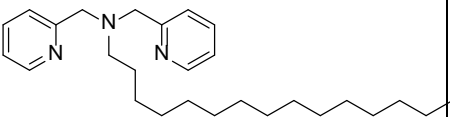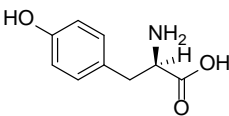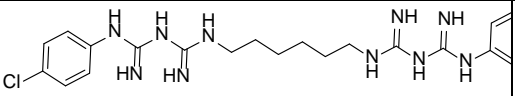
Data from these screens resulted in multiple hits but due to the fact that some of these compounds were reported as biofilm inhibitors, and not specifically inhibitors of *sarA*, we decided to do biofilm assays on each of the literature based compounds. Biofilm assays were performed using microtiter plates in the same fashion as described in Task 4. The compound indicated in orange (BS-7-39a) indicates an intermediate level of inhibition of growth and thus was excluded from further analysis.
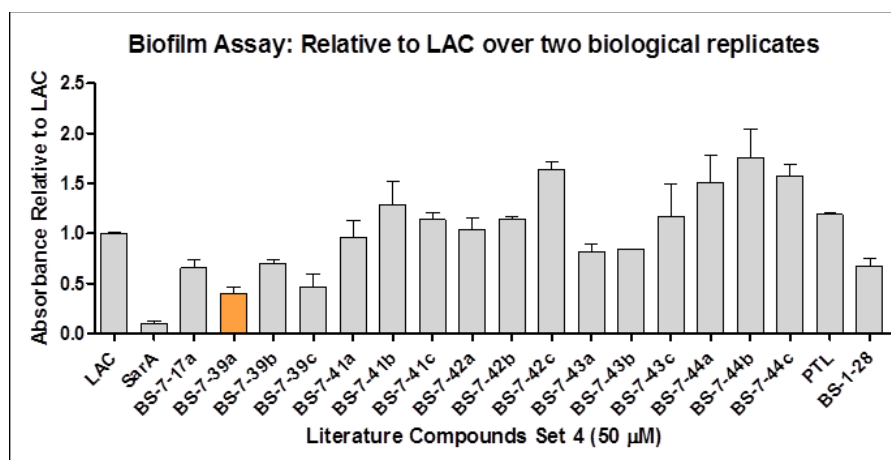
The results from these experiments led us to believe that BS-7-39c is a viable biofilm inhibitor in the context of our assays and thus deserving priority over other literature related compounds. This logic was further validated by showing that in the presence of BS-7-39c the LAC parent strain formed a biofilm at a level comparable to that observed in the isogenic LAC *sarA* mutant in the absence of this compound.
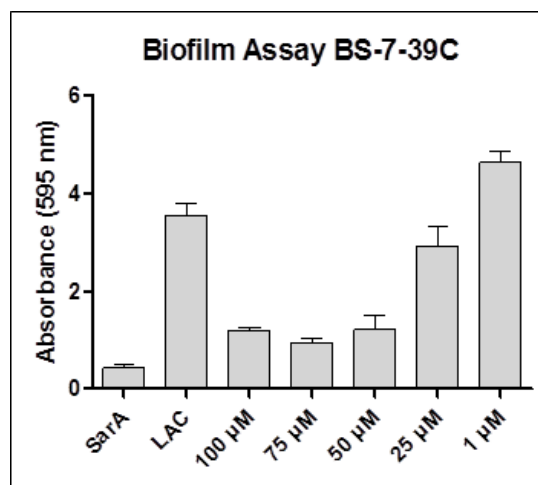
Identifying BS-7-39c as a viable inhibitor allowed us to then focus our attention on generating analogues of this compound to further optimize the anti-biofilm activity. These were evaluated using our reporter assay, but as mentioned in Task 4, due to working with a smaller number of test compounds, this allowed us to focus on identifying compounds that inhibited biofilm formation irrespective of whether they function through *sarA* as suggested by our reporter assay. For this reason, newly synthesized compounds were evaluated using our biofilm assay instead of our reporter assay. We then took the top analogues along with BS-7-39c and compared them with respect to biofilm reduction in our LAC and UAMS-1 strains.

Biofilm Assay: 50 μM — Absorbance Relative to LAC; Biofilm Assay: 50 μM — Absorbance Relative to U1
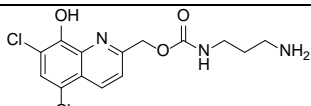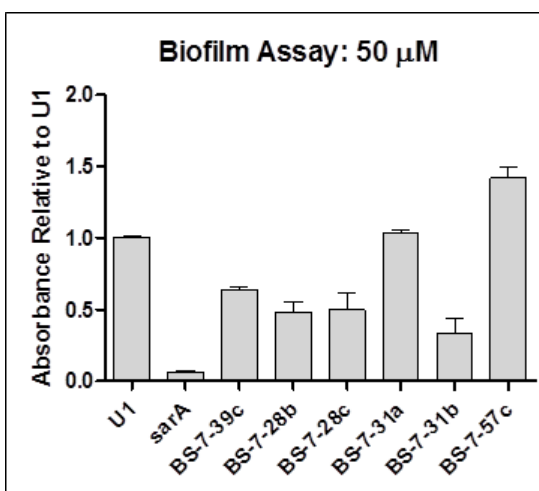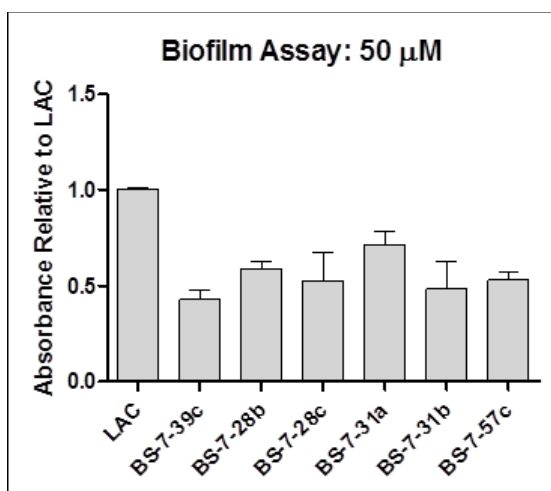
Compound	Biofilm Reduction (compared to LAC)	Biofilm Reduction (compared to U1)
BS-7-39c	57%	36%
BS-7-28b	41%	52%
BS-7-28c	48%	50%
BS-7-31a	29%	-4%
BS-7-31b	52%	67%
BS-7-57c	47%	-42%

This data showed that BS-7-28b, BS-7-28c, and BS-7-31b displayed anti-biofilm activity to levels of ~50% in both our LAC and UAMS-1 strains without inhibiting growth kinetics in either strain. These results would suggest that these three compounds are promising biofilm inhibitors.

Thus, we assessed relative antibiotic susceptibility as described in the context of Task 4. However, as with the compounds identified from our library, none of these compounds were found to significantly enhance antibiotic susceptibility in the context of daptomycin at either 24 or 72 hours.

BS-7-28c: 24 hr

BS-7-28c: 72 hr
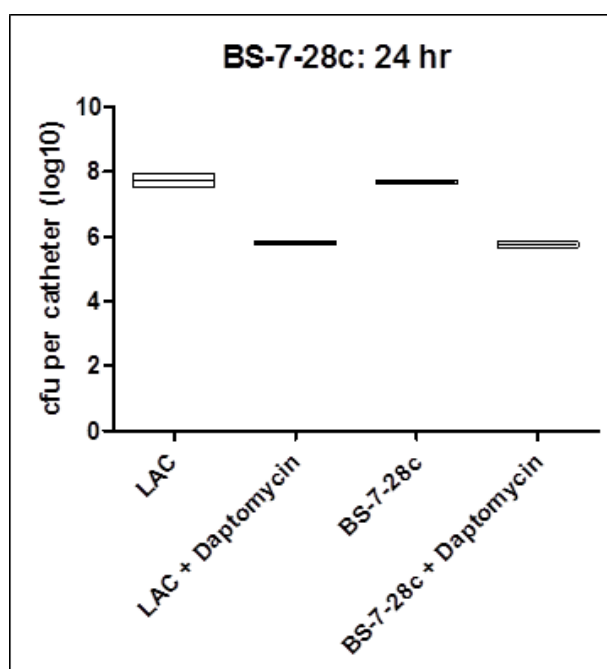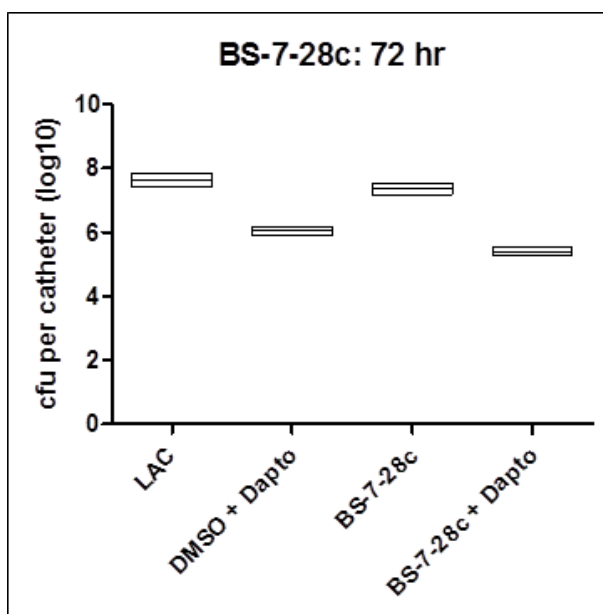
We put forth a tremendous effort to identify small molecule inhibitors of *sarA*-mediated regulation, and we did so both by screening the library available in the Crooks' laboratory and by mining the literature to identify promising compounds. We also extended both of these efforts to include analogues of these compounds. As judged by relative antibiotic susceptibility, we have not yet identified an inhibitor that we believe warranted efforts to conjugate it to BT2-peg2 and proceed with *in vivo* pharmacological and therapeutic efficacy studies. However, this does not mean that we failed to make significant progress. To emphasize this, in the following section we summarized the data from both Tasks 4 and 5 into a single table and indicated the degree of biofilm inhibition observed with both LAC and UAMS-1:

ID		Structure
YTR-2-66		
BS-6-123C	**57% (LAC), 53% (U1)**	
BS-7-61B	**44% (LAC), 62% (U1)**	
BS-7-62A		

BS-7-62B		
BS-7-39C		
BS-7-28B	**41% (LAC), 52% (U1)**	
BS-7-28C	**48% (LAC), 50% (U1)**	
BS-7-31a		
BS-7-31B	**52% (LAC), 67% (U1)**	
BS-7-57C		

What is most important about this compilation is that careful examination reveals that the five most promising compounds all fall into one of two categories represented by different chemical scaffolds:
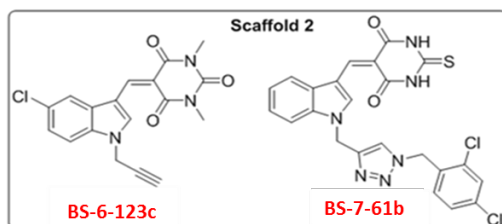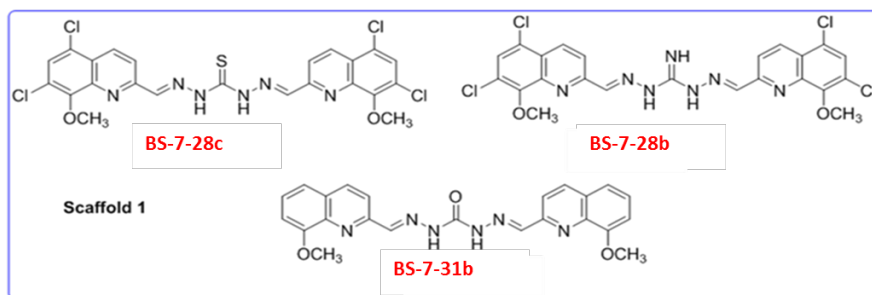
This is important because allows us to synthesize additional compounds based on these scaffolds, several of which are illustrated below:
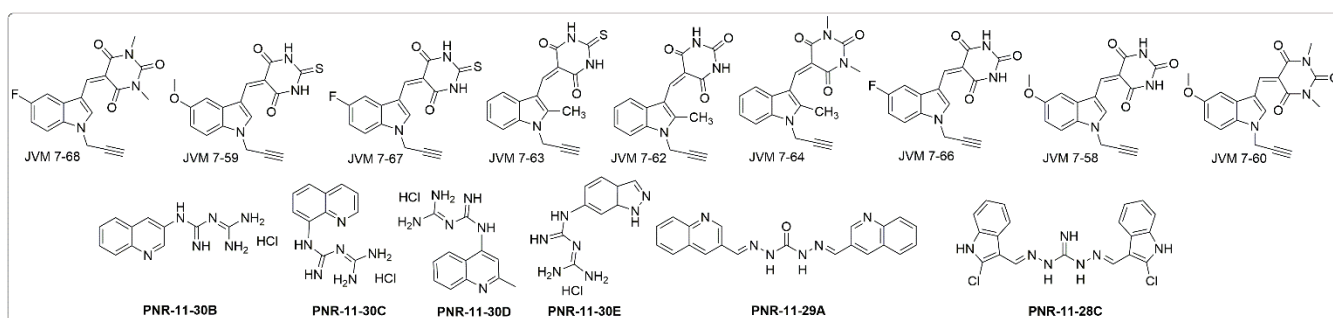
As these have become available, we have also begun to assess their impact on biofilm formation. One of these compounds (shown in red) was excluded from further analysis because it was found to inhibit bacterial growth, thereby precluding the possibility of forming a biofilm. However, several of these compounds showed promise, and three (JVM-7-68, JVM-7-59, and JVM-7-60) inhibited biofilm formation to a degree comparable to that observed in the *sarA* mutant itself:
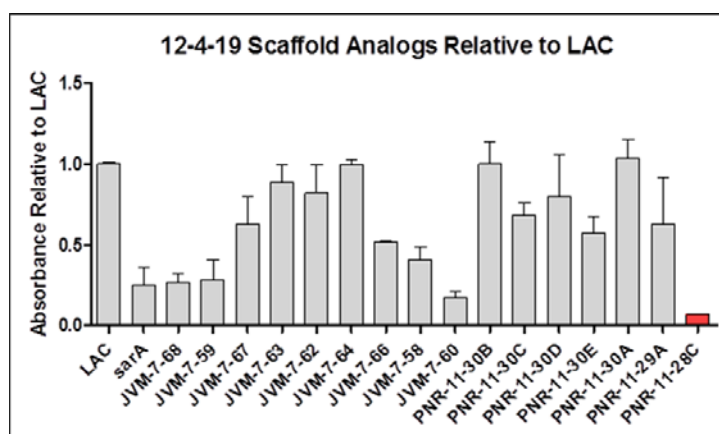
Task 6. Expand the screen of small molecule inhibitors to include additional staphylococcal strains and species. Our primary focus has been on *Staphylococcus aureus* as an orthopaedic pathogen for the reasons discussed above. We have attempted to take the diversity of *S. aureus* strains into account, particularly with respect to the relative capacity to form a biofilm, cause bone infection, and antibiotic susceptibility, by purposefully including the divergent strains LAC and UAMS-1 as our studies progressed. A primary reason we decided to include paenipeptin analogue 17 in our studies was its activity against *S. aureus* as detailed above. However, another reason is that this compound also had a minimum inhibitory concentration (MIC) ranging from 0.5 to 8.0 µg per ml across a wide spectrum of bacterial pathogens including *Acinetobacter baumannii* (ATCC 19606), *Escherichia coli* (ATCC 25922), *Klebsiella pneumoniae* (ATCC 13883), *Pseudomonas aeruginosa* (ATCC 27853), *Enterococcus faecium* (ATCC 19434), thus indicating that it represents a promising broad-spectrum antibiotic.

Task 7: Evaluate conjugation of the most promising *sarA* inhibitor to BT2-peg2. We have to yet undertaken experiments focused on accomplishing this task because we have not yet identified a *sarA* inhibitor from our primary screen (Task 4) or validated any described in the literature (Task 5) that exhibits sufficient activity in the context of an established biofilm to warrant this effort. We have, however, defined two chemical scaffolds that can serve as the starting point for moving forward to achieve this goal.

Task 8: Evaluate *in vivo* pharmacological properties of the most promising *sarA* inhibitor and its BT2-peg2 conjugate. These studies are pending awaiting the outcome of Task 7.

Task 9: Evaluate the efficacy of the most promising small molecule inhibitor and the most promising antibiotic *in vivo* with and without conjugation to BT2-peg2. We have completed this task with our BT2-minipeg-2 daptomycin conjugate, albeit with disappointing results. As detailed above in the context of Task 2, and are currently exploring alternative means of generating this conjugate as a means of restaining its bone-targeting properties. We have also successfully conjugated BT2-peg2 to

ciprofloxacin, but the antibacterial stability of this conjugate was compromised as detailed above. Thus, as with Task 8, we are not yet in a position to undertake our Task 9 experiments because we do not have BT2-minipeg-2 conjugates of antibiotics or *sarA* inhibitors that justify this effort.

What opportunities for training and professional development has the project provided?

Despite the difficulties encountered in accomplishing some of our key tasks, the efforts made during the course of the funding period offered tremendous opportunities for training and development to the entire research team and even to other trainees in the Smeltzer laboratory who were not directly involved in the effort. The most obvious of these is that the project was a collaboration between the Smeltzer and Crooks laboratories. The specific expertise of the Smeltzer laboratory is in the pathogenesis of *S. aureus* bone infection and treatment, while the specific expertise of the Crooks laboratory is on drug discovery in contexts other than infectious disease. Thus, personnel in both laboratories were exposed to areas of translational science beyond their specific areas of expertise. As emphasized throughout this final report, the difficulties we encountered do not detract from our resolve to overcome them, and the ability to do so will be greatly enhanced by the enthusiasm generated throughout the research team despite their recognition of the difficulties involved in our achieving ambitious goals.

How were the results disseminated to communities of interest?

The primary means of dissemination were through publication and presentations at appropriate meetings. The specific publications and meeting presentations are detailed below.

What do you plan to do during the next reporting period to accomplish the goals?

Technically, this is not applicable as this is a final report. However, we would emphasize again that our efforts to achieve the goals of this project will continue to the greatest extent possible.

IMPACT:

What was the impact on the development of the principal discipline(s) of the project?

While the impact of our efforts remains to be fully realized for the reasons detailed above, we remain confident that the effort is worthwhile and we remain committed to accomplishing our objectives. Doing so has the potential to transform the clinical approach to the prevention and treatment of bone infections arising as a consequence of traumatic injury including those impacting military personnel.

What was the impact on other disciplines?

This was a very targeted project focused on a specific and clinically relevant therapeutic problem. The impact on other disciplines is therefore difficult to define. However, we are confident that the results of our studies will impact other clinical disciplines in two respects. First, as detailed in our introduction, validation and optimization of BT2-peg2 could greatly facilitate the treatment of other bone diseases including cancer that would benefit from the enhanced delivery of appropriate therapeutic agents. Second, the ultimate results of our studies have the potential to validate the therapeutic importance and relevance of anti-biofilm and anti-virulence strategies targeted towards diverse bacterial pathogens.

What was the impact on technology transfer?

Nothing to report at this time.

What was the impact on society beyond science and technology?

Nothing to report at this time.

CHANGES/PROBLEMS:

Changes in approach and reasons for change

While we encountered unanticipated problems that caused us to shift our efforts toward overcoming these problems rather than evaluating *in vivo* relevance (Tasks 7-9), we have not changed our overall approach to accomplishing our ultimate objectives.

Actual or anticipated problems or delays and actions or plans to resolve them

Science is difficult, particularly in the context of translational science leading to changes that have a significant impact on clinical practice in the context of such a therapeutically-recalcitrant problem like that presented by traumatic bone infection. It is important that students and junior faculty understand this, and equally important that they understand the importance of overcoming these difficulties. We did encounter unanticipated difficulties in achieving our objectives, specifically with respect to Tasks 1-6. This precluded downstream accomplishments associated with Tasks 7-9, but it does not preclude the importance of overcoming these difficulties and ultimately achieving these objectives. We are fully confident that we put a valid experimental plan in place and that continuing to pursue this plan to the extent possible despite the expiration of the funding period of this grant will ultimately prove worthwhile.

Changes that had a significant impact on expenditures

The greatest expense of any scientific effort lies in the personnel required to carry out that effort. Thus, the only change that had a significant impact on expenditures was the need to shift the focus to supporting the personnel needed to overcome the difficulties encountered in Tasks 1-6 rather than being in a position to use these funds to pursue the *in vivo* experiments as outlined in Tasks 7-9.

Significant changes in use or care of human subjects, vertebrate animals, biohazards, and/or select agents

Significant changes in use or care of human subjects

Not applicable.

Significant changes in use or care of vertebrate animals

Nothing to report.

Significant changes in use of biohazards and/or select agents

Nothing to report.

PRODUCTS:

Publications, conference papers, and presentations

Journal publications

Directly associated with current grant:

Meeker, D.G., Loughran, A.J., Beenken, K.E., Spencer, H.J., Lynn, W.B., Mills, W.B., and *Smeltzer, M.S.* 2016. Evaluation of antibiotics effective against methicillin-resistant *Staphylococcus aureus* based on efficacy in the context of an established biofilm. *Antimicrobial Agents and Chemotherapy*, 60:5688-5694. PMCID: PMC5038242.

Atwood, D.N., Beenken, K.E., Lantz, T.L., Meeker, D.G., Lynn, W.B., Mills, W.B., Spencer, H.J., and *Smeltzer, M.S.* 2016. Regulatory mutations impacting antibiotic susceptibility in an established *Staphylococcus aureus* biofilm. *Antimicrobial Agents and Chemotherapy*, 60:1826-182. PMCID: PMC4775981.

Albayati, Z.A.F., Sunkara, M., Schimdt-Malan, S.M., Karau, M.J., Morris, A.J., Steckelberg, J.M, Patel, R., Breen, P., *Smeltzer, M.S.,* Taylor, K.G., Merten, K.E., Pierce, W.M., and Crooks, P.A. 2015. Use of a novel bone-targeting agent for the enhanced delivery of vancomycin to bone. *Antimicrobial Agents and Chemotherapy*. 60:1865-1868. PMCID: PMC4776008.

Atwood, D.N., Loughran, A.J., Courtney, A.P., Anthony, A.C., Meeker, D.G., Spencer, H.J., Gupta, R.K., Lee, C.Y., Beenken, K.E., *Smeltzer, M.S.* 2015. Comparative impact of diverse regulatory loci on *Staphylococcus aureus* biofilm formation. *MicrobiologyOpen.* 4:436-451. PMCID: PMC4475386.

Albayati, Z. A. F., Penthala, N., Bommagani, S., Post, G., Smeltzer, M. S., and Crooks, P.A. Evaluation of bone and kidney toxicity of BT2-peg2, a potential carrier for the targeted delivery of antibiotics to bone, under review. *Toxicology Reports* (TOXREP_2019_428), under review.

Supportive of the underlying hypothesis and experimental approach:

Ramirez, A.M., Bryrum, S.D., Beenken, K.E., Tackett, A.J., and *Smeltzer, M.S.* Exploiting correlations between protein abundance and the functional status of *saeRS* and *sarA* to identify virulence factors of potential importance in the pathogenesis of *Staphylococcus aureus* osteomyelitis. *ACS Infectious Disease,* in press. PMID: 31722523. doi: 10.1021/acsinfecdis.9b00291.

Rom, J.S., Ramirez, A.M., Beenken, K.E., Spencer, H.J., Sahukhal, G.S., Elasri, M.O. and *Smeltzer, M.S.* Defining the contribution of *msaABCR* to *sarA*-associated phenotypes in *Staphylococcus aureus*. *Infection and Immunity*, in press. PMID: 31740526. doi: 10.1128/IAI.00530-19.

Saeed, K., McLaren, A.C., Schwarz, E.M., Antoci, V., Arnold, W.V., Chen, A.F., Clauss, M., Esteban, J., Gant, V., Hendershot, E., Hickok, N., Higuera, C.A., Coraça-Huber, D.C., Choe, H., Jennings, J.A., Joshi, M., Li, W.T., Noble, P.C., Phillips, K.S., Pottinger, P.S., Restrepo, C., Rohde, H., Schaer, T.P., Shen, H., Smeltzer, M., Stoodley, P., Webb, J.C.J., Witsø, E. 2018. International consensus meeting on musculoskeletal infection: Summary from the biofilm workgroup and consensus on biofilm related musculoskeletal infections. Journal of Orthopaedic Research. 37:1007-1017. PMID: 30667567.

Rom, J.S., Atwood, D.N., Beenken, K.E., Meeker, D.G., Loughran, A.J., Spencer, H.J., and *Smeltzer, M.S.* 2017. Impact of *Staphylococcus aureus* regulatory mutations that modulate biofilm formation in the USA300 LAC on virulence in a murine bacteremia model. *Virulence*, 8:1776-1790. PMCID: PMC5810510.

Loughran, A.J., Gaddy, D., Beenken, K.E., Meeker, D.G., Morello, R., Zhao, H., Byrum, S.D., Tackett, A.J., Cassat, J.E., and Smeltzer, M.S. 2016. Impact of *sarA* and phenol-soluble modulins in the pathogenesis of osteomyelitis in diverse clinical isolates of *Staphylococcus aureus*. *Infection and Immunity*, 84:2586-2594. PMCID: PMC4995912.

Books or other non-periodical, one-time publications

Not applicable.

Other publications, conference papers and presentations

MALTO Meeting, 46th Annual Meeting, Memphis, TN, 2019. Poster Presentation.

Kerr and McCasland Lectureship, Oklahoma State University, Stillwater, OK. 2019. Keynote Lecture.

Military Health Sciences Research Symposium, Orlando, FL. 2018. Poster Presentation.

American Chemical Society Southwest Regional Meeting. Little Rock, AR. 2018. Oral presentation.

Drug Discovery and Development Colloquium (DDDC), 2018, Lexington, KY. Poster Presentation.

International Meeting of the American Academy of Orthopaedic Surgeons, San Diego, CA. 2017. Oral Presentation.

American Association of Pharmaceutical Sciences (AAPS), San Diego, CA. 2017. Poster presentation.

Drug Discovery and Development Colloquium. 2017, UAMS, Little Rock, AR. Poster Presentation.

MCBIOS XIV. 2017, UAMS, Little Rock, AR. Poster Presentation.

Military Health Sciences Research Symposium, Orlando, FL. 2016. Poster Presentation.

Military Health Sciences Research Symposium, Orlando, FL. 2016. Oral Presentation.

International Meeting of the American Academy of Orthopaedic Surgeons, Orlando, FL. 2016. Oral presentation.

Department of Defense State-of-the-Science meeting on Minimizing the Impact of Wound Infections Following Blast-Related Injuries, Washington, DC. 2016. Oral presentation.

International Meeting of the American Academy of Orthopaedic Surgeons, Las Vegas, NV. 2015. Oral presentation.

Website(s) or other Internet site(s)

Not applicable

Technologies or techniques

The primary technologies pursued with funding from this grant are the use of BT2-peg2 as a bone-targeting agent and the focus on *sarA* as a therapeutic target. While we did not achieve the results we hoped for, we did make significant progress toward establishing the experimental foundation to do so.

Inventions, patent applications, and/or licenses

Nothing to report.

Other Products

Nothing to report.

PARTICIPANTS AND OTHER COLLABORATING ORGANIZATIONS

What individuals have worked on the project?

Name: Mark S. Smeltzer
Project role: Principle investigator
ORCID ID: 0000-0002-0878-0692
Nearest person month worked: No change
Contribution to project: Oversight of overall project design and implementation of studies evaluating antibiotics, antibiotic conjugates, *sarA* inhibitors, and *sarA* inhibitor conjugates.

Name: Peter Crooks
Project Role: Co-investigator
ORCID ID: 0000-0002-1312-6150
Nearest person month worked: No change
Contribution to project: Oversight of chemical synthesis and BT2-peg2 conjugation studies

Name: Albayati Zaineb
Project Role: Instructor
ORCID ID: 0000-0003-1673-0756
Nearest person month worked: No change
Contribution to project: Oversight and implementation of *in vivo* pharmacological studies

Name: Narismha Penthala
Project Role: Research Instructor
ORCID ID: 0000-0001-6978-5588
Nearest person month worked: No change
Contribution to project: Synthesis and structural validation of antibiotic conjugates

Name: Shobanbabu Bommagani
Project Role: Post-doctoral research associate
ORCID ID: 0000-0002-8086-1753
Nearest person month worked: No change
Contribution to project: Synthesis and structural validation of *sarA* inhibitors

Name: Venumadhav Janganati
Project Role: Post-doctoral research associate
ORCID ID: 0000-0003-3641-2990
Nearest person month worked: 1
Contribution to project: Drug design and synthesis

Name: Suresh Kuarm Bowroju
Project Role: Post-doctoral research associate
ORCID ID: 0000-0001-9906-0625
Nearest person month worked: 1
Contribution to project: Drug design and synthesis
Funding support: No change

Name: Karen E. Beenken
Project Role: Research Assistant Professor
ORCID ID: 0000-0002-9152-8198
Nearest person month worked: No change
Contribution to project: Oversight of reporter screen and biofilm assays.

Name: Sonja Daily
Project Role: Laboratory technician
ORCID ID: Not applicable.
Nearest person month worked: No change
Contribution to project: Implementation of reporter screen and biofilm assays.

Name: Christopher Walker
Project Role: Laboratory technician
ORCID ID: Not applicable
Nearest person month worked: No change
Contribution to project: Implementation of reporter screen and biofilm assays.

Has there been a change in the active other support of the PD/PI(s) or senior/key personnel since the last reporting period?

Nothing to report.

What other organizations were involved as partners?

None.

COLLABORATIVE AWARDS:

Not applicable.

QUAD CHARTS:

Not applicable.

APPENDICES:

Meeker et al., 2015.

Atwood et al., 2016.

Albayati et al., 2015

Atwood et al., 2015

Albayati et al., manuscript submitted

Ramirez et al., in press

Rom et al., in press

Saeed et al., 2018

Rom et al., 2017

Loughran et al., 2016

Evaluation of Antibiotics Active against Methicillin-Resistant *Staphylococcus aureus* Based on Activity in an Established Biofilm

Daniel G. Meeker,[a] Karen E. Beenken,[a] Weston B. Mills,[a] Allister J. Loughran,[a] Horace J. Spencer,[b] William B. Lynn,[a] Mark S. Smeltzer[a]

Department of Microbiology & Immunology[a] and Department of Biostatistics,[b] University of Arkansas for Medical Sciences, Little Rock, Arkansas, USA

We used *in vitro* and *in vivo* models of catheter-associated biofilm formation to compare the relative activity of antibiotics effective against methicillin-resistant *Staphylococcus aureus* (MRSA) in the specific context of an established biofilm. The results demonstrated that, under *in vitro* conditions, daptomycin and ceftaroline exhibited comparable activity relative to each other and greater activity than vancomycin, telavancin, oritavancin, dalbavancin, or tigecycline. This was true when assessed using established biofilms formed by the USA300 methicillin-resistant strain LAC and the USA200 methicillin-sensitive strain UAMS-1. Oxacillin exhibited greater activity against UAMS-1 than LAC, as would be expected, since LAC is an MRSA strain. However, the activity of oxacillin was less than that of daptomycin and ceftaroline even against UAMS-1. Among the lipoglycopeptides, telavancin exhibited the greatest overall activity. Specifically, telavancin exhibited greater activity than oritavancin or dalbavancin when tested against biofilms formed by LAC and was the only lipoglycopeptide capable of reducing the number of viable bacteria below the limit of detection. With biofilms formed by UAMS-1, telavancin and dalbavancin exhibited comparable activity relative to each other and greater activity than oritavancin. Importantly, ceftaroline was the only antibiotic that exhibited greater activity than vancomycin when tested *in vivo* in a murine model of catheter-associated biofilm formation. These results emphasize the need to consider antibiotics other than vancomycin, most notably, ceftaroline, for the treatment of biofilm-associated *S. aureus* infections, including by the matrix-based antibiotic delivery methods often employed for local antibiotic delivery in the treatment of these infections.

Staphylococcus aureus is a leading cause of both hospital and community-acquired infections (1). *S. aureus* causes many different types of infections, but among the most common are infections associated with indwelling medical devices (2, 3). In fact, with the possible exception of *S. epidermidis*, *S. aureus* is easily the single most prominent cause of all types of implant-associated infection, and irrespective of overall prevalence, the virulence of *S. aureus* makes it by far the most clinically problematic pathogen (4, 5). This is particularly true in the context of implant-associated infections caused by methicillin-resistant *S. aureus* (MRSA) strains (6). Thus, the increasing prevalence of MRSA strains even among isolates causing community-associated infections (7) makes antibiotics effective against MRSA of particular clinical importance.

The prevalence of *S. aureus* as a cause of implant-associated infections is due in part to its ability to form a biofilm (5, 8–10). Biofilm formation not only contributes to the establishment and persistence of infection but also greatly complicates treatment owing to intrinsic antibiotic resistance, thus leading to infections that fail to respond to conventional antibiotic therapy even when acquired antibiotic resistance is not an issue (11). This often necessitates surgical intervention to remove the implant and any infected surrounding tissues, often accompanied by some form of local matrix-based antibiotic delivery (4). This is especially true in cases involving indwelling orthopedic devices (8, 12), which are particularly noteworthy in that they are increasing dramatically, with the number of both primary and revision total knee and hip replacement procedures continuing to increase without a decline in the overall infection rate (13).

Despite the increasing prevalence of biofilm-associated infections, antibiotics continue to be developed on the basis of their activity against planktonic bacterial cultures (14). This highlights the need to consider antibiotic activity in the context of a biofilm,

and in the case of *S. aureus*, it has become increasingly important to do so in the context of methicillin resistance. To this end, we previously used an *in vitro* model of catheter-associated biofilm formation to evaluate the relative activity of daptomycin, linezolid, and vancomycin (11). These studies led to the conclusion that the membrane-active antibiotic daptomycin exhibits greater activity in the context of a biofilm than either vancomycin or linezolid. Subsequent studies using a murine model of catheter-associated biofilm infection confirmed the activity of daptomycin under *in vivo* conditions (15). These studies support the hypothesis that daptomycin is a viable alternative and perhaps even a preferred alternative to vancomycin in the context of biofilm-associated infections. However, since these studies were done, a number of other antibiotics with activity against MRSA have been introduced into clinical practice. Thus, the purpose of the studies that we report on here was to use our established *in vitro* and *in vivo* models of catheter-associated biofilm formation (11, 15) as a first step toward evaluating the relative activity of these additional antibiotics.

MATERIALS AND METHODS

Bacterial strains and antibiotics tested. The strains included were the USA300 MRSA strain LAC and the USA200 methicillin-sensitive *S. aureus*

TABLE 1 Relationship between breakpoint MIC and MIC for each test strain

Antibiotic	BkPt[a] (µg/ml)	LAC			UAMS-1	
		MIC (µg/ml)	Ratio (MIC/BkPt)		MIC (µg/ml)	Ratio (MIC/BkPt)
Vancomycin	2.0	2.0	1.0		1.5	0.75
Daptomycin	1.0	0.5	0.5		0.5	0.5
Ceftaroline	1.0	0.5	0.5		0.5	0.5
Tigecycline	0.5	0.125	0.25		0.19	0.38
Telavancin	0.12	0.047	0.39		0.047	0.39
Oxacillin	2.0	128	64		1.5	0.75

[a] BkPt, breakpoint MIC. The breakpoint MICs cited are those defined by the United States Food and Drug Administration (FDA) for a susceptible strain of *S. aureus*.

(MSSA) strain UAMS-1. The primary antibiotics tested were daptomycin, vancomycin, telavancin, ceftaroline, and tigecycline, all of which are active against MRSA, as assessed under standard *in vitro* conditions (16). Oxacillin, which is not active against MSRA, was included as a control in these comparisons because the experiments included both the MRSA strain LAC and the MSSA strain UAMS-1. In separate experiments, we also directly compared the relative activity of the lipoglycopeptide antibiotics telavancin, oritavancin, and dalbavancin. All antibiotics were purchased from our hospital pharmacy, except for telavancin, which was kindly provided both in its pharmaceutical formulation (Vibativ) and as telavancin powder by Theravance Biopharma Antibiotics, Inc. (George Town, Cayman Islands).

Assessment of antibiotic susceptibility *in vitro*. Antibiotics were tested and compared using our established *in vitro* catheter model of biofilm formation (11). Briefly, 1-cm segments of fluorinated ethylene propylene catheters (14 gauge; Introcan safety catheter; B. Braun, Bethlehem, PA) were coated with human plasma before being placed into the wells of a 12-well microtiter plate containing 2 ml of tryptic soy broth supplemented with glucose and sodium chloride (biofilm medium [BM]). Each well was then inoculated with LAC or UAMS-1 at an optical density at 600 nm of 0.05. The plate was then incubated at 37°C for 24 h before the catheters were removed and transferred to fresh BM with and without the appropriate antibiotic. For *in vitro* experiments done with daptomycin, the BM was supplemented with calcium chloride, as previously described (11). In all cases, the medium used for *in vitro* assays was prepared fresh daily. Comparisons were done using multiple concentrations of each antibiotic. Specifically, the concentrations used corresponded to 5×, 10×, and 20× the breakpoint MIC for a susceptible strain of *S. aureus*, as defined by the United States Food and Drug Administration (FDA) (Table 1).

To compensate for the fact that telavancin has a much lower breakpoint MIC than the other antibiotics tested (Table 1), we also evaluated telavancin at 40×, 80×, and 160× its breakpoint MIC, thus allowing us to draw comparisons between approximately equal physical concentrations of telavancin and daptomycin. To make direct comparisons between the lipoglycopeptides, which have been reported to exhibit good penetration and relatively high efficacy in the context of a biofilm (17–19), we also evaluated oritavancin and dalbavancin at concentrations corresponding to 160× the telavancin breakpoint MIC, thus allowing us to draw comparisons between approximately equal physical concentrations of these antibiotics and daptomycin. In addition, a subset of antibiotics chosen for reasons discussed below was also tested at concentrations corresponding to multiples of the actual MICs for the test strains.

Antibacterial effects were assessed after 24 and 72 h of antibiotic exposure. For catheters exposed for 72 h, catheters were removed after 24 and 48 h, rinsed in sterile phosphate-buffered saline (PBS), and transferred to wells with fresh medium with and without antibiotics. After exposure for 24 or 72 h, catheters were removed, rinsed in sterile PBS to remove nonadherent bacteria, and sonicated in sterile PBS to remove adherent bacteria. After sonication, samples were serially diluted and 100-µl aliquots were plated on tryptic soy agar to quantify the number of viable CFU per catheter. Using this experimental method, the limit of detection was 50 CFU per catheter.

Assessment of antibiotic susceptibility *in vivo*. To test activity *in vivo*, we used a murine model of catheter-associated biofilm infection as previously described (15). Briefly, 1-cm catheter sections were implanted subcutaneously into the flanks of NIH Swiss mice. LAC (10^5 CFU) in a total volume of 100 µl was then injected into the lumen of each catheter. Beginning 24 h later, 100 µl of the test antibiotic at the concentrations indicated below was injected into the lumen daily for 5 days. Control mice were injected daily with 100 µl of sterile PBS. At the completion of each experiment, catheters were processed as previously described (15). The animal studies were approved by the University of Arkansas for Medical Sciences Institutional Animal Care and Use Committee.

Statistical methods. Statistical comparisons were made using the Mann-Whitney test. Using the same experimental model employed in these studies, we previously demonstrated that daptomycin has greater activity than vancomycin in the context of a biofilm formed by UAMS-1 (11). On the basis of this finding, statistical comparisons were made on the basis of activity relative to the activities of these two antibiotics. However, additional comparisons were made to assess the activities of lipoglycopeptide antibiotics relative to each other.

RESULTS AND DISCUSSION

After 24 h in the absence of antibiotic exposure, no significant difference with respect to the average colony counts per catheter was observed between UAMS-1 and LAC (Fig. 1). However, a significant difference was observed after 72 h, with the biofilms formed by UAMS-1 containing, on average, 2.5 times more viable bacterial cells than those formed by LAC ($1.16 \times 10^8 \pm 1.48 \times 10^8$ versus $4.58 \times 10^7 \pm 5.71 \times 10^7$; $n = 54$). The finding that there was no significant difference between the number of bacteria
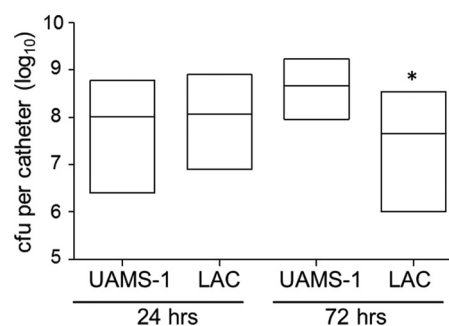
FIG 1 Relative capacity of UAMS-1 and LAC to form a biofilm *in vitro*. The relative capacity of each strain to form a biofilm was evaluated using our catheter model after 24 and 72 h of colonization without antibiotic exposure. Results are shown as the number of CFU per catheter, with each box illustrating the maximum and minimum values observed within each experimental group and the horizontal line indicating the mean for that group. *, statistically significant difference ($P < 0.05$) between the number of viable biofilm-associated bacteria formed by LAC relative to the number of viable biofilm-associated bacteria formed by UAMS-1 at 72 h.

FIG 2 Relative activity of different antibiotics against LAC and UAMS-1 at 24 h in the context of a biofilm *in vitro*. Activity was evaluated using daptomycin (DAP), vancomycin (VAN), ceftaroline (CPT), oxacillin (OXA), telavancin (TLV), and tigecycline (TGC) at concentrations corresponding to 5×, 10×, and 20× the breakpoint MIC for each antibiotic. Results are shown as the number of CFU per catheter, with each box illustrating the maximum and minimum values observed within each experimental group and the horizontal line indicating the mean for that group. Gray bars, results observed with catheters that were not exposed to any antibiotic; white bars, results observed after exposure of UAMS-1 (top) or LAC (bottom) biofilms to the indicated antibiotics; *, significant reduction in the number of viable bacteria (*P* ≤ 0.05) relative to that achieved with vancomycin at the equivalent concentration.

FIG 3 Relative activity of different antibiotics against LAC and UAMS-1 at 72 h in the context of a biofilm *in vitro*. Activity was evaluated using daptomycin (DAP), vancomycin (VAN), ceftaroline (CPT), oxacillin (OXA), telavancin (TLV), and tigecycline (TGC) at concentrations corresponding to 5×, 10×, and 20× the breakpoint MIC for each antibiotic. Results are shown as the number of CFU per catheter, with each box illustrating the maximum and minimum values observed within each experimental group and the horizontal line indicating the mean for that group. Gray bars, results observed with catheters that were not exposed to any antibiotic; white bars, results observed after exposure of UAMS-1 (top) or LAC (bottom) biofilms to the indicated antibiotics. *, significant reduction in the number of viable bacteria (*P* ≤ 0.05) relative to that achieved with vancomycin at the equivalent concentration; **, significant reduction relative to that achieved with daptomycin at the equivalent concentration.

within the biofilms formed by these two strains at 24 h suggests that biofilms formed by LAC become relatively static over time, while those formed by UAMS-1 continue to develop. This difference accounts in part for our inclusion of these two time points in our studies, with the other relevant consideration being the likelihood that the results would be impacted in an antibiotic-dependent manner by the time of exposure to the test antibiotic.

The number of potential comparisons in the experiments that we report is very large. Thus, we focused on the fact that vancomycin is the primary antibiotic used for the treatment of MRSA infections and our previous results demonstrating that daptomycin exhibits significantly greater activity than vancomycin in the context of a biofilm (11). Specifically, we based our statistical analysis on whether each antibiotic exhibited increased activity relative to that of each of these two antibiotics when tested at equivalent multiples of the breakpoint MIC for each antibiotic.

After 24 h of exposure of biofilms formed by UAMS-1, daptomycin was found to exhibit significantly greater activity than vancomycin at all concentrations tested (Fig. 2). This is consistent with the results observed in our previous study (11). A significant difference between vancomycin and both oxacillin and tigecycline at all concentrations tested and between ceftaroline and vancomycin at 20× the breakpoint MIC was also observed, with all of these antibiotics exhibiting significantly greater activity than vancomycin when the activities at corresponding concentrations were compared. However, no antibiotic was found to have activity greater than that of daptomycin at any concentration tested at the 24-h time point (Fig. 2).

After 24 h, the increased activity of daptomycin relative to that of vancomycin was also evident at all concentrations tested when these experiments were repeated using biofilms formed by LAC (Fig. 2). Additionally, while ceftaroline, tigecycline, and even oxacillin exhibited greater activity than vancomycin, depending on the antibiotic concentration, none exhibited greater activity than daptomycin at any of the concentrations tested (Fig. 2). The activity observed with oxacillin was surprising, given that LAC is an MRSA strain. However, when it was tested using UAMS-1, oxacillin exhibited greater activity than vancomycin at every concentration tested, and this was not the case with LAC.

When UAMS-1 biofilms were exposed to the same antibiotics for 72 h, daptomycin, ceftaroline, oxacillin, and tigecycline all exhibited greater activity than vancomycin at one or more of the concentrations tested (Fig. 3). No antibiotic tested exhibited greater activity than daptomycin at an equivalent concentration, with the exception of that activity of oxacillin at 5× the breakpoint MIC compared to that of daptomycin at 5× the breakpoint MIC. Additionally, ceftaroline, oxacillin, and tigecycline all exhibited activity comparable to that observed with daptomycin at one or more concentrations (Fig. 3). Most importantly, only daptomycin at 10× and 20× the breakpoint MIC and ceftaroline at 20× the breakpoint MIC were capable of clearing the catheters of viable biofilm-associated bacteria, as defined by the detection limit of our assay.

With the exception of oxacillin, the same general trends were
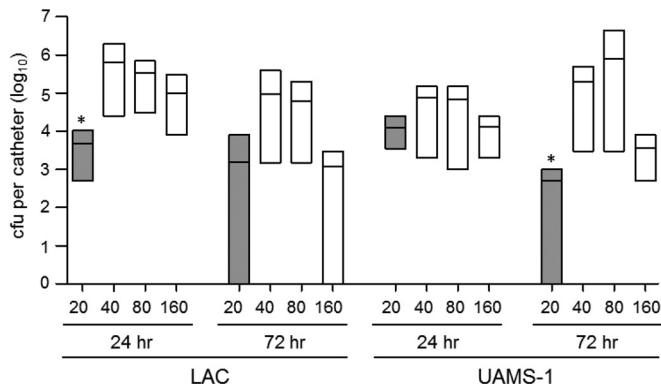
FIG 4 Evaluation of telavancin activity *in vitro*. Activity was evaluated by comparison of the activity of daptomycin at a concentration corresponding to 20× the breakpoint MIC (gray bars) to that of telavancin at 40×, 80×, and 160× the breakpoint MIC (white bars). Results are shown as the number of CFU per catheter, with each box illustrating the maximum and minimum values observed within each experimental group and the horizontal line indicating the mean for that group. *, significant reduction in the number of viable bacteria ($P \leq 0.05$) achieved with daptomycin at 20× the breakpoint MIC relative to that achieved with telavancin at 160× the breakpoint MIC.

FIG 5 Comparison of the activity of lipoglycopeptide antibiotics *in vitro*. The activities of telavancin (TLV), oritavancin (ORV), and dalbavancin (DBV) at an equal concentration corresponding to 160× the breakpoint MIC of telavancin (19.2 μg per ml) were compared. The results obtained with catheters that were exposed to antibiotic (white bars) for 72 h relative to those obtained with catheters that were not exposed to antibiotic (gray bars) are shown. Results are shown as the number of CFU per catheter, with each box illustrating the maximum and minimum values observed within each experimental group and the horizontal line indicating the mean for that group. *, significant reduction in the number of viable bacteria ($P \leq 0.05$) relative to that achieved with oritavancin; **, significant reduction relative to that achieved with dalbavancin.

observed when the 72-h experiments were repeated using biofilms formed by LAC. Specifically, daptomycin was shown to be superior to vancomycin at all concentrations tested. Ceftaroline at 20× the breakpoint MIC and tigecycline at 5× the breakpoint MIC were also found to exhibit greater activity than equivalent concentrations of vancomycin (Fig. 3). As with UAMS-1, daptomycin and ceftaroline were the only antibiotics found to clear any catheters of viable bacteria. In fact, 20× the breakpoint MICs of both daptomycin and ceftaroline were shown to reduce the number of viable bacteria to below the limit of detection in 50% of the catheters tested after 72 h of antibiotic exposure (data not shown). The increased clearance observed with LAC relative to that observed with UAMS-1 is likely a reflection of the fact that UAMS-1 formed a more robust biofilm than LAC at the 72-h time point (Fig. 1).

The lipoglycopeptide antibiotic telavancin includes a membrane-active component, in addition to its cell wall-inhibitory activity, and has shown promise in multiple animal models of infection (20, 21), but it exhibited relatively little activity by comparison to that of daptomycin and ceftaroline against both UAMS-1 and LAC biofilms at the concentrations initially tested *in vitro*. It is important to note in this respect that neither of these antibiotics was included for comparison in the previous studies focusing on telavancin (20, 21). However, telavancin also has a very low breakpoint MIC by comparison to the breakpoint MICs all of the other antibiotics that we tested (Table 1), thus leaving open the possibility that the results were skewed in favor of these other antibiotics by using multiples of the breakpoint MIC. To address this, we repeated the experiments using telavancin at 40×, 80×, and 160× its breakpoint MIC, with the last concentration (19.2 μg per ml) being comparable to 20× the breakpoint MIC of daptomycin (20 μg per ml). Under these circumstances, telavancin at 160× the breakpoint MIC did, in fact, exhibit activity comparable to that of daptomycin at 20× the breakpoint MIC at 72 h against LAC but not against UAMS-1 (Fig. 4). In fact, telavancin at 160× the breakpoint MIC was capable of reducing the number of viable bacteria to below the limit of detection. After 24 h of exposure, telavancin at 40×, 80×, and 160× the breakpoint MIC ex-

hibited activity comparable to that of daptomycin at 20× the breakpoint MIC when tested using biofilms formed by UAMS-1, but after 72 h, daptomycin at 20× the breakpoint MIC exhibited activity greater than that of telavancin at all of these concentrations (Fig. 4).

To determine whether similar results were observed with other lipoglycopeptides, we also carried out experiments comparing oritavancin and dalbavancin at physical concentrations equivalent to 160× the breakpoint MIC of telavancin (Table 1). In LAC biofilms, telavancin exhibited significantly greater activity than either of these other antibiotics (Fig. 5). Dalbavancin exhibited a level of activity that was greater than that observed with oritavancin but less than that observed with telavancin. In UAMS-1 biofilms, telavancin exhibited significantly greater activity than oritavancin and activity comparable to that of dalbavancin.

These experiments were done using the commercially available formulation of telavancin (Vibativ), which includes a number of inactive ingredients, including hydroxypropyl-beta-cyclodextrin and mannitol (Theravance Biopharma Antibiotics, Inc.), and a recent report demonstrated the need to reconsider the *in vitro* methods used for determining the MIC of telavancin in multiple bacterial species, including staphylococci (22). To address this, we reassessed the activity of telavancin in the context of a biofilm using the revised protocol recommended by the earlier report (22). The key element of this alternative approach is the use of telavancin powder rather than the commercial preparation and the use of dimethyl sulfoxide as the diluent in the presence of polysorbate 80 (22). The motivation for this was not only the observation that testing methods have a significant impact on the determination of MIC values for all lipoglycopeptides but also the need to consider the activity of antibiotics in alternative clinical contexts, including localized, matrix-based delivery, particularly in postdebridement and/or trauma-associated orthopedic procedures. However, we observed no differences in the results as a function of the drug formulation utilized (data not shown).
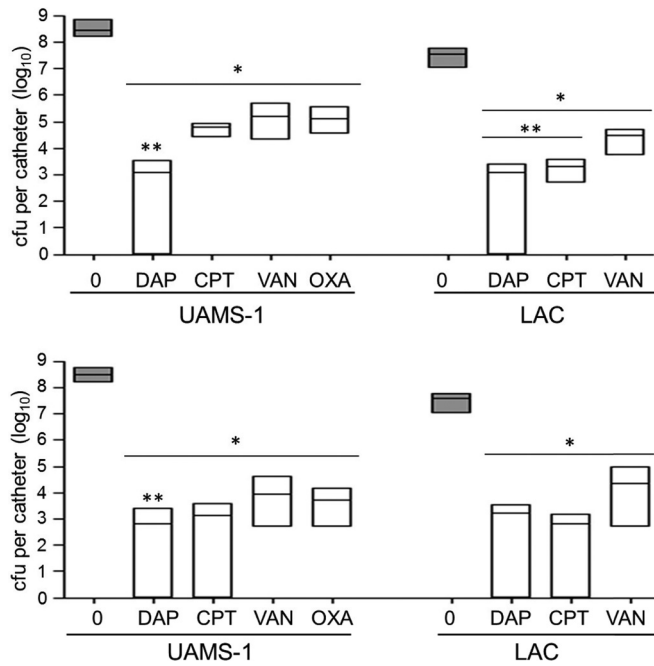
FIG 6 Relative activity of different antibiotics assessed *in vitro* based on the MIC. Activity was evaluated after 72 h of exposure using daptomycin (DAP), ceftaroline (CPT), vancomycin (VAN), and oxacillin (OXA) at concentrations corresponding to 20× (top) and 40× (bottom) the MIC for each test strain, as determined by Etest. Gray bars, results observed with catheters that were not exposed to any antibiotic; white bars, results observed after exposure to the indicated antibiotics. *, significant reduction in the number of viable bacteria ($P \leq 0.05$) relative to the number of untreated control bacteria; **, significant reduction relative to that achieved with vancomycin at the equivalent concentration.

Although comparison of the activities of antibiotics on the basis of their respective breakpoint MICs allows the broad applicability of the results, it is possible that this could skew the data in favor of those antibiotics for which a particular strain has a relatively low MIC compared to the breakpoint MIC. More directly, comparisons based on multiples of the breakpoint MIC result in lower multiples of the MIC for any antibiotic for which the ratio of the MIC to the breakpoint MIC is higher than that of another antibiotic. To assess this possibility, the MIC of each antibiotic for

each test strain was determined by the Clinical Microbiology Laboratory at Arkansas Children's Hospital. This information was then used to calculate a ratio of the MIC relative to the breakpoint MIC for each strain with each antibiotic (Table 1). We then focused our assessment on a comparison of daptomycin and ceftaroline, which were shown to have greater activity than the other antibiotics tested but also had relatively low ratios (0.5) that could have skewed the results for the reasons discussed above, to vancomycin and oxacillin, which were the only antibiotics that exhibited higher ratios. These antibiotics were compared at concentrations corresponding to 20× and 40× the MIC for each strain.

When tested at 20× the MIC, daptomycin was the only antibiotic found to have significantly greater activity than vancomycin against both UAMS-1 and LAC (Fig. 6). Ceftaroline was also found to have significantly greater activity than vancomycin against LAC but not UAMS-1. Against UAMS-1, daptomycin was also the only antibiotic found to exhibit significantly greater activity than vancomycin when they were tested at 40× the MIC, but this was not true against LAC. In fact, against LAC, even the difference observed between ceftaroline and vancomycin did not reach statistical significance when they were examined at 40× the MIC. However, both daptomycin and ceftaroline did demonstrate the ability to reduce the number of viable bacteria to below the limit of detection in some catheters, and this was not true with vancomycin or, with respect to UAMS-1, oxacillin (Fig. 6). These results are consistent with comparisons made on the basis of breakpoint MICs, thus confirming that daptomycin and ceftaroline do in fact exhibit greater activity than vancomycin in the context of a biofilm.

We next tested the efficacy of daptomycin, ceftaroline, and telavancin relative to that of vancomycin under *in vivo* conditions using concentrations corresponding to 20× and 40× the breakpoint MIC for each antibiotic. These three antibiotics were chosen because they were the only antibiotics capable of reducing the number of viable bacteria to below the limit of detection under any of the conditions tested. Interestingly, at 20× the breakpoint MIC, none of the differences observed between these antibiotics reached statistical significance, and only treatment with ceftaroline was found to result in a significant reduction in the number of bacteria relative to the number of bacteria for the PBS-treated control (Fig. 7). At 40× the breakpoint MIC, all antibiotics were found to have a significant effect relative to that of the PBS-treated

FIG 7 Relative activity of different antibiotics assessed *in vivo*. Catheters colonized with LAC were evaluated after 5 days of exposure to daptomycin (DAP), ceftaroline (CPT), vancomycin (VAN), and telavancin (TLV) at a concentration corresponding to 20× (left) or 40× (right) the breakpoint MIC for each antibiotic. Gray bars, results observed with catheters that were not exposed to any antibiotic; white bars, results observed after exposure to the indicated antibiotics. *, significant reduction in the number of viable bacteria ($P \leq 0.05$) relative to the number of untreated control bacteria; **, statistical significance by comparison to the results obtained with vancomycin.

control, but only ceftaroline was found to exhibit greater efficacy than vancomycin.

In summary, these results illustrate the intrinsic resistance that defines *S. aureus* biofilms, thus emphasizing the need to evaluate antibiotics in the context of an established biofilm. In fact, it is not clear if the concentrations used in our study can be achieved at the site of infection when antibiotics are administered systemically. However, antibiotics are also often administered locally using some form of matrix-based delivery system, particularly in orthopedic medicine (11, 23–25). We also recently described a novel nanocage-based system for the targeted local delivery of daptomycin (26). Thus, even if sufficient systemic levels cannot be achieved, it remains important to prioritize antibiotics for use in local antibiotic delivery systems.

In this respect, the results that we report confirm the greater activity of the membrane-active agent daptomycin relative to that of vancomycin. They also demonstrate that ceftaroline has activity comparable to that of daptomycin in the context of biofilms formed by both MSSA and MRSA strains, particularly at the higher concentrations tested, and even greater efficacy than daptomycin when tested under *in vivo* conditions. Indeed, the activity of these antibiotics relative to that of oxacillin suggests that they may offer a therapeutic advantage even in the context of MSSA infections. It is also worth noting that, in the context of biofilms formed by MRSA strain LAC, telavancin exhibited greater activity than any other lipoglycopeptide. This suggests that in at least some patients suffering from biofilm-associated infections caused by MRSA strains, telavancin may also be a viable therapeutic option, particularly since it was one of only three antibiotics shown to clear an established biofilm under any test condition. Most importantly, all of these results must be interpreted relative to those for vancomycin, which was relatively ineffective by comparison to daptomycin and ceftaroline yet remains the primary choice for the treatment of MRSA infections.

ACKNOWLEDGMENT

FUNDING INFORMATION

REFERENCES

1. **Brady RA, Leid JG, Calhoun JH, Costerton JW, Shirtliff ME.** 2013. Evaluation of genetically inactivated alpha toxin for protection in multiple mouse models of *Staphylococcus aureus* infection. PLoS One **8**:e63040. http://dx.doi.org/10.1371/journal.pone.0063040.
2. **Korol E, Johnston K, Waser N, Sifakis F, Jafri HS, Lo M, Kyaw MH.** 2013. A systematic review of risk factors associated with surgical site infections among surgical patients. PLoS One **8**:e83743. http://dx.doi.org/10.1371/journal.pone.0083743.
3. **Mootz JM, Benson MA, Heim CE, Crosby HA, Kavanaugh JS, Dunman PM, Kielian T, Torres VJ, Horswill AR.** 2015. Rot is a key regulator of *Staphylococcus aureus* biofilm formation. Mol Microbiol **96**:388–404. http://dx.doi.org/10.1111/mmi.12943.
4. **Darouiche RO.** 2004. Treatment of infections associated with surgical implants. N Engl J Med **350**:1422–1429. http://dx.doi.org/10.1056/NEJMra035415.
5. **Jorgensen NP, Meyer R, Dagnaes-Hansen F, Fuursted K, Peterson E.** 2014. A modified chronic infection model for testing treatment of *Staphylococcus aureus* biofilms on implants. PLoS One **9**:e103688. http://dx.doi.org/10.1371/journal.pone.0103688.
6. **Parvizi J, Pawasarat IM, Azzam KA, Joshi A, Hansen EN, Bozic KJ.** 2010. Periprosthetic joint infection: the economic impact of methicillin-resistant infections. J Arthroplasty **25**(Suppl 6):S103–S107. http://dx.doi.org/10.1016/j.arth.2010.04.011.
7. **DeLeo FR, Otto M, Kreiswirth BN, Chambers HF.** 2010. Community-associated methicillin-resistant *Staphylococcus aureus*. Lancet **375**:1557–1568. http://dx.doi.org/10.1016/S0140-6736(09)61999-1.
8. **Brady RA, Leid JG, Calhoun JH, Costerton JW, Shirtliff ME.** 2008. Osteomyelitis and the role of biofilms in chronic infection. FEMS Immunol Med Microbiol **52**:13–22. http://dx.doi.org/10.1111/j.1574-695X.2007.00357.x.
9. **Jennings JA, Carpenter DP, Troxel KS, Beenken KE, Smeltzer MS, Courtney HS, Haggard WO.** 2015. Novel antibiotic-loaded point-of-care implant coating inhibits biofilm. Clin Orthop Relat Res **473**:2270–2282. http://dx.doi.org/10.1007/s11999-014-4130-8.
10. **Römling U, Balsalobre C.** 2012. Biofilm infections, their resilience to therapy and innovative treatment strategies. J Intern Med **272**:541–561. http://dx.doi.org/10.1111/joim.12004.
11. **Weiss EC, Spencer HJ, Daily SJ, Weiss BD, Smeltzer MS.** 2009. Impact of *sarA* on antibiotic susceptibility of *Staphylococcus aureus* in a catheter-associated *in vitro* model of biofilm formation. Antimicrob Agents Chemother **53**:2475–2482. http://dx.doi.org/10.1128/AAC.01432-08.
12. **Cierny G.** 2011. Surgical treatment of osteomyelitis. Plast Reconstr Surg **127**(Suppl 1):190S–204S. http://dx.doi.org/10.1097/PRS.0b013e3182025070.
13. **Kurtz SM, Ong KL, Lau E, Bozic KJ.** 2014. Impact of the economic downturn on total joint replacement demand in the United States: updated projections to 2021. J Bone Joint Surg Am **96**:624–630. http://dx.doi.org/10.2106/JBJS.M.00285.
14. **Bjarnsholt T, Ciofu O, Molin S, Givskov M, Høiby N.** 2013. Applying insights from biofilm biology to drug development—can a new approach be developed? Nat Rev Drug Discov **12**:791–808. http://dx.doi.org/10.1038/nrd4000.
15. **Weiss EC, Zielinska A, Beenken KE, Spencer HJ, Daily SJ, Smeltzer MS.** 2009. Impact of *sarA* on daptomycin susceptibility of *Staphylococcus aureus* biofilms *in vivo*. Antimicrob Agents Chemother **53**:4096–4102. http://dx.doi.org/10.1128/AAC.00484-09.
16. **Holmes NE, Howden BP.** 2014. What's new in the treatment of serious MRSA infection? Curr Opin Infect Dis **27**:471–478. http://dx.doi.org/10.1097/QCO.0000000000000101.
17. **Baldoni D, Furustrand Tafin U, Aeppli S, Angevaare E, Oliva A, Haschke M, Zimmerli W, Trampuz A.** 2013. Activity of dalbavancin, alone and in combination with rifampicin, against methicillin-resistant *Staphylococcus aureus* in a foreign-body infection model. Int J Antimicrob Agents **42**:220–225. http://dx.doi.org/10.1016/j.ijantimicag.2013.05.019.
18. **Belley A, Neesham-Grenon E, McKay G, Arhin FF, Harris R, Beveridge T, Parr TR, Moeck G.** 2009. Oritavancin kills stationary-phase and biofilm *Staphylococcus aureus* cells *in vitro*. Antimicrob Agents Chemother **53**:918–925. http://dx.doi.org/10.1128/AAC.00766-08.
19. **Kirker KR, Fisher ST, James GA.** 2015. Potency and penetration of telavancin in staphylococcal biofilms. Int J Antimicrob Agents **46**:451–455. http://dx.doi.org/10.1016/j.ijantimicag.2015.05.022.
20. **Hegde SS, Janc JW.** 2014. Efficacy of telavancin, a lipoglycopeptide antibiotic, in experimental models of Gram-positive infection. Expert Rev Anti Infect Ther **12**:1463–1475. http://dx.doi.org/10.1586/14787210.2014.979789.
21. **Chan C, Hardin TC, Smart JI.** 2015. A review of telavancin activity in *in vitro* biofilms and animal models of biofilm-associated infections. Future Microbiol **10**:1325–1338. http://dx.doi.org/10.2217/fmb.15.53.
22. **Farrell DJ, Mendes RE, Rhomberg PR, Jones RN.** 2014. Revised

reference broth microdilution method for testing telavancin: effect on MIC results and correlation with other testing methodologies. Antimicrob Agents Chemother **58:**5547–5551. http://dx.doi.org/10.1128/AAC.03172-14.

23. **Beenken KE, Smith JK, Skinner RA, McLaren SG, Bellamy W, Gruenwald MJ, Spencer HJ, Haggard WO, Smeltzer MS.** 2014. Chitosan coating to enhance the therapeutic efficacy of calcium sulfate-based antibiotic therapy in the treatment of chronic osteomyelitis. J Biomater Appl **29:**514–523. http://dx.doi.org/10.1177/0885328214535452.

24. **Beenken KE, Bradney L, Bellamy W, Skinner RA, McLaren SG, Gruenwald MJ, Spencer HJ, Smith JK, Haggard WO, Smeltzer MS.** 2012. Use of xylitol to enhance the therapeutic efficacy of polymethyl-methacrylate-based antibiotic therapy in treatment of chronic osteo-myelitis. Antimicrob Agents Chemother **56:**5839–5844. http://dx.doi.org/10.1128/AAC.01127-12.

25. **Parker AC, Beenken KE, Jennings JA, Hittle L, Shirtliff ME, Bumgardner JD, Smeltzer MS, Haggard WO.** 2015. Characterization of local delivery with amphotericin B and vancomycin from modified chitosan sponges and functional biofilm prevention evaluation. J Orthop Res **33:**439–447. http://dx.doi.org/10.1002/jor.22760.

26. **Meeker DG, Jenkins SV, Miller EK, Beenken KE, Loughran AJ, Powless A, Muldoon TJ, Galanzha EI, Zharov VP, Smeltzer MS, Chen J.** 2016. Synergistic photothermal and antibiotic killing of biofilm-associated Staphylococcus aureus using targeted antibiotic-loaded gold nanoconstructs. ACS Infect Dis **2:**241–250. http://dx.doi.org/10.1021/acsinfecdis.5b00117.

Regulatory Mutations Impacting Antibiotic Susceptibility in an Established *Staphylococcus aureus* Biofilm

Danielle N. Atwood,[a] Karen E. Beenken,[a] Tamara L. Lantz,[a] Daniel G. Meeker,[a] William B. Lynn,[a] Weston B. Mills,[a] Horace J. Spencer,[d] Mark S. Smeltzer[a,b,c]

Department of Microbiology and Immunology,[a] Department of Orthopaedic Surgery,[b] Department of Pathology,[c] and Department of Biostatistics,[d] University of Arkansas for Medical Sciences, Little Rock, Arkansas, USA

We previously determined the extent to which mutations of different *Staphylococcus aureus* regulatory loci impact biofilm formation as assessed under *in vitro* conditions. Here we extend these studies to determine the extent to which those regulatory loci that had the greatest effect on biofilm formation also impact antibiotic susceptibility. The experiments were done under *in vitro* and *in vivo* conditions using two clinical isolates of *S. aureus* (LAC and UAMS-1) and two functionally diverse antibiotics (daptomycin and ceftaroline). Mutation of the staphylococcal accessory regulator (*sarA*) or *sigB* was found to significantly increase susceptibilities to both antibiotics and in both strains in a manner that could not be explained by changes in the MICs. The impact of a mutation in *sarA* was comparable to that of a mutation in *sigB* and greater than the impact observed with any other mutant. These results suggest that therapeutic strategies targeting *sarA* and/or *sigB* have the greatest potential to facilitate the ability to overcome the intrinsic antibiotic resistance that defines *S. aureus* biofilm-associated infections.

Biofilm formation is a defining factor in the clinical approach to many forms of *Staphylococcus aureus* infections owing to the fact that the presence of a biofilm confers a therapeutically relevant degree of intrinsic antibiotic resistance irrespective of the acquired resistance status of the offending bacterial strain (1). Thus, adjunct therapeutic approaches capable of limiting biofilm formation would offer a tremendous clinical advantage. A key component in the development of such approaches is to define the mechanism(s) by which *S. aureus* forms a biofilm, thus opening the door to the development of therapeutic approaches that limit biofilm formation and thereby limit the clinical impact of this intrinsic resistance.

We have focused our efforts in this regard on *S. aureus* regulatory elements, many of which have been shown to impact biofilm formation both negatively and positively, at least under *in vitro* conditions (2). This work has led us to place a primary emphasis on the staphylococcal accessory regulator (*sarA*), mutation of which limits biofilm formation to a degree that can be correlated with increased antibiotic susceptibility as assessed under both *in vitro* and *in vivo* conditions (3, 4). Moreover, our recent comparison to the impact of mutating *sarA* relative to that of mutating other *S. aureus* regulatory loci implicated in biofilm formation led us to conclude that mutation of *sarA* imposes a greater limitation on biofilm formation than mutation of any other *S. aureus* regulatory locus (2). However, these studies were limited to *in vitro* conditions and did not take into account relative antibiotic susceptibility.

To address this, we used *in vitro* (3) and *in vivo* (4) models of catheter-associated biofilm formation to assess the relative antibiotic susceptibility of those regulatory mutants previously shown to have the greatest impact, either positively or negatively, on biofilm formation (2). We did this by using the functionally distinct antibiotics daptomycin and ceftaroline and the genetically and phenotypically distinct *S. aureus* strains LAC (USA300, methicillin resistant) and UAMS-1 (USA200, methicillin sensitive) (4–7).

MATERIALS AND METHODS

Assessment of relative antibiotic susceptibility *in vitro*. Antibiotic susceptibility under *in vitro* conditions was assessed using a catheter-based model as previously described (3). Briefly, 1-cm segments of fluorinated ethylene propylene catheters (14-gauge Introcan Safety catheter; B. Braun, Bethlehem, PA) were first coated with human plasma before being placed into the wells of a 12-well microtiter plate containing 2 ml of tryptic soy broth supplemented with glucose and sodium chloride (biofilm medium [BM]). Each well was then inoculated with LAC, UAMS-1, or the appropriate isogenic mutant at an optical density at 600 nm of 0.05. The plate was then incubated at 37°C for 24 h before the catheters were removed and transferred to fresh BM with and without the appropriate antibiotic. After an additional 24-h incubation, catheters were removed, rinsed in phosphate-buffered saline (PBS) to remove nonadherent bacteria, and then placed in a test tube containing 5 ml of sterile PBS. To remove adherent bacteria, each catheter was then sonicated to remove adherent bacteria as previously described (3). Appropriately diluted samples were then plated on tryptic soy agar without antibiotic selection to determine the number of viable bacteria per catheter remaining.

Assessment of relative antibiotic susceptibility *in vivo*. Biofilm formation was assessed *in vivo* using a murine model of catheter-associated biofilm formation (4). Briefly, uncoated catheters were implanted into each flank of NIH Swiss mice and inoculated with 10^5 CFU of the test strain in a total volume of 100 µl of PBS by direct injection into the lumen of each catheter. After 24 h, the mice were randomly divided into experimental groups ($n = 5$). Because each mouse had two catheters implanted and because previous experiments have confirmed the absence of cross-

contamination between catheters in opposite flanks of the same mouse (4), each catheter was treated as an independent data point (n = 10). In untreated mice, 100 μl of sterile PBS was injected in the lumen of each catheter at daily intervals for 5 days. Catheters were then harvested and processed as described above to determine the number of CFU per catheter remaining after antibiotic treatment.

Antibiotics and *S. aureus* strains tested. For both *in vitro* and *in vivo* assays, daptomycin was tested at 5 times the Clinical and Laboratory Standards Institute (CLSI)-defined breakpoint MIC, while ceftaroline was tested at 10 times its CLSI-defined breakpoint concentration. The use of different concentrations of each antibiotic was based on preliminary studies indicating that ceftaroline exhibits somewhat reduced efficacy in the context of a biofilm in comparison to daptomycin (data not shown) and a desire to employ an antibiotic concentration that would allow us to detect differences in susceptibility that would not be apparent with antibiotic concentrations that were either too low or too high. The LAC mutants included were *sarA*, *atl*, *codY*, *fur*, *mgrA*, *rot*, *rsbU*, and *sigB*. UAMS-1 mutants examined were more limited but included *sarA*, *codY*, *mgrA*, *rot*, and *sigB*. As previously described (2), all of these mutants were generated by phage-mediated transduction from primary mutants available as part of the Nebraska Transposon Mutant Library (NTML).

Impact of regulatory mutations on MICs of relevant mutants. The relative daptomycin and ceftaroline susceptibilities of each strain were assessed by Etest (bioMérieux SA, Marcy l'Etoile, France) using tryptic soy agar as the growth medium.

Statistical analysis. Statistical comparisons were made between each parent strain and its isogenic mutant with and without antibiotic exposure. For each experimental setting, a set of contrasts that defined the comparisons of interest were created. Permutation tests, as described in Pallmann et al. (8), were performed to obtain the adjusted P values for each contrast. Briefly, using the observed data, t test statistics were calculated for each individual contrast, and the absolute values of the statistics were recorded. The data were then randomly permuted. The statistics from the permuted set were calculated, and the one resulting in the minimum P value across all contrasts was recorded. The data were permuted 50,000 times, presumably resulting in a distribution of test statistics from the null distribution. The number of times the permuted test statistic was larger than the observed test statistic was calculated for each contrast. The adjusted P value for a contrast is the aforementioned number divided by 50,001. A logarithmic transformation was applied to the CFU data prior to analysis. Adjusted P values of <5% were considered statistically significant. This analysis was performed using SAS 9.4 (SAS Institute Inc., Cary, NC).

RESULTS AND DISCUSSION

Using a microtiter plate-based assay, we previously examined the relative impact of mutating individual regulatory loci on *S. aureus* biofilm formation *in vitro* (2). These studies identified a number of mutants that exhibited either a decreased or increased capacity to form a biofilm, but they did not address the issue of whether these changes were sufficient to have an impact on antibiotic susceptibility in the context of an established biofilm. In this report, we examined this issue with a focus on those regulatory loci shown to have the greatest impact on biofilm formation in our previous study. This included LAC mutants *sarA*, *atl*, *codY*, *fur*, *mgrA*, *rot*, *rsbU*, and *sigB* as well as *sarA*, *codY*, *mgrA*, *rot*, and *sigB* mutants generated in the osteomyelitis isolate UAMS-1. To facilitate the ability to focus on the relative antibiotic susceptibility in a quantitative fashion, these studies were done using *in vitro* and *in vivo* models of catheter-associated biofilm formation (3, 4).

The only mutation that imposed a significant limitation on biofilm formation under *in vitro* conditions in the absence of antibiotic exposure was the *sarA* mutation, and this was true in both LAC and UAMS-1 (Fig. 1). However, exposure to 5X daptomycin
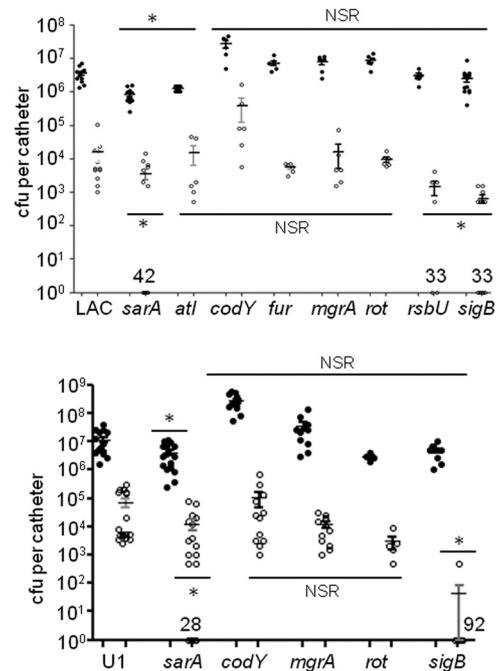
FIG 1 Relative daptomycin susceptibility *in vitro*. Daptomycin susceptibility in LAC, UAMS-1, and the indicated mutants was assessed using a catheter-based model of biofilm formation. The results indicate individual data points. The horizontal bar and error bars indicate the means ± standard errors of the mean (SEM) based on CFU per catheter remaining after antibiotic exposure. An asterisk above an experimental group indicates the statistical significance of each mutant relative to the isogenic parent strain in the absence of antibiotic exposure. An asterisk below a group indicates the significance of each mutant relative to the parent strain after antibiotic exposure. The number above a strain indicates the percentage of catheters cleared of bacteria as defined by the level of detection of our assay. NSR, no significant reduction.

was associated with significantly increased susceptibility in both UAMS-1 and LAC *sarA* and *sigB* mutants relative to the isogenic parent strain. Mutation of *rsbU* also resulted in a significant increase in susceptibility in LAC, but we did not have a UAMS-1 *rsbU* mutant. These reductions were reflected in colony counts per catheter and the percentage of catheters cleared of viable bacteria at least as defined by the limit of detection of our experimental method (50 CFU per catheter) (Fig. 1). Similar results were observed under *in vivo* conditions, although in this case none of the mutations, including the *sarA* mutation, were found to have a statistically significant impact in either strain in the absence of antibiotic exposure (Fig. 2). Additionally, under *in vivo* conditions, mutation of *sigB* had a significant impact in LAC but not in UAMS-1 (Fig. 2). Interestingly, mutation of *codY* resulted in a significant increase in daptomycin susceptibility *in vivo* in LAC but not in UAMS-1. This is consistent with the observation that mutation of *codY* resulted in a significant increase in biofilm formation in UAMS-1 *in vivo* but not in LAC (Fig. 2). To the extent that the goal is to identify potential *S. aureus* targets that can be exploited to therapeutic advantage, this emphasizes the importance of considering diverse clinical isolates in studies focusing on biofilm formation and relative antibiotic susceptibility.

To determine whether the results observed with daptomycin might be generalized to those with other antibiotics and thus likely to be a function of the impact of individual mutations on biofilm
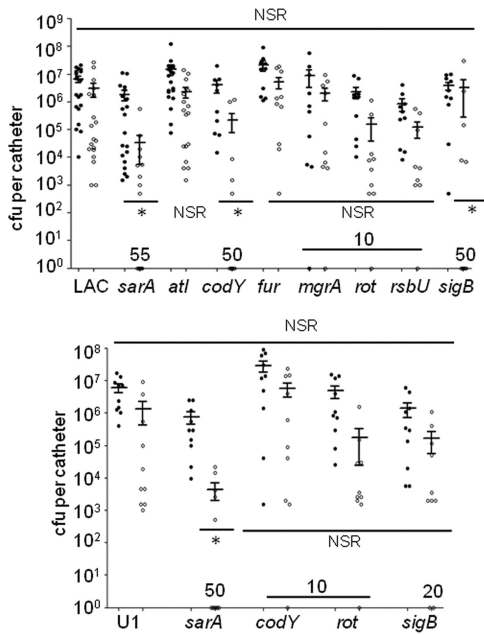
FIG 2 Relative daptomycin susceptibility *in vivo*. Daptomycin susceptibility was assessed using a murine model of a catheter-based model of biofilm formation. The results indicate individual data points. The horizontal bar and error bars indicate the means ± standard errors of the mean (SEM) based on CFU per catheter remaining after antibiotic exposure. An asterisk below a group indicates the significance after antibiotic exposure. The number above a mutant indicates the percentage of catheters cleared of bacteria below the level of detection. NSR, no significant reduction.

FIG 3 Relative ceftaroline susceptibility *in vivo*. Ceftaroline susceptibility was assessed using a murine model of a catheter-based model of biofilm formation. The results indicate individual data points. The horizontal bar and error bars indicate the means ± standard errors of the mean (SEM) based on CFU per catheter remaining after antibiotic exposure. An asterisk above an experimental group indicates the statistical significance relative to the isogenic parent strain in the absence of antibiotic exposure. An asterisk below a group indicates the significance after antibiotic exposure. The number above a mutant indicates the percentage of catheters cleared of bacteria below the level of detection. NSR, no significant reduction.

formation itself rather than a daptomycin-specific effect, we repeated the *in vivo* studies using ceftaroline. We chose ceftaroline rather than the more commonly used anti-methicillin-resistant *Staphylococcus aureus* (MRSA) antibiotic vancomycin because ceftaroline is a functionally distinct antibiotic in comparison to daptomycin and because our previous results have confirmed that vancomycin has relatively little efficacy in the context of an established biofilm (9). The results were essentially identical to those observed with daptomycin except that in this case mutation of *sarA* and *sigB* resulted in a significant increase in antibiotic susceptibility in both UAMS-1 and LAC (Fig. 3). As with daptomycin, this increased susceptibility was evident both in the average colony counts per catheter and the percentage of catheters cleared of viable bacteria as defined by the limit of detection of our experimental method. Importantly, mutation of *sarA* or *sigB* did not significantly alter the MIC of LAC or UAMS-1 to daptomycin or ceftaroline (Fig. 4), thus providing support for the hypothesis that the increased susceptibility we observed is a function of the impact of each mutation on the relative capacity to form a biofilm.

In summary, the primary clinical problem with *S. aureus* biofilm-associated infections is their intrinsic resistance to conventional antibiotic therapy, thus making the experimentally critical parameter the degree to which mutation of genes that impact biofilm formation also impact this intrinsic resistance. The results we report are significant in that they provide further support for the hypothesis that the staphylococcal accessory regulator (*sarA*) plays a critical role in this regard and that it does so in diverse strains of *S. aureus* irrespective of their methicillin-resistance status. At the same time, the results demonstrate that elements within

the *sigB* regulon also play a critical role. There is a report suggesting that *sigB* increases expression of *sarA* (9), and we confirmed that mutation of *sigB* in LAC results in a significant decrease in the accumulation of SarA (2), thus suggesting that the impact of *sigB* may be mediated at least in part through its impact on *sarA*. However, a recent report demonstrated that *sigB* is required for the
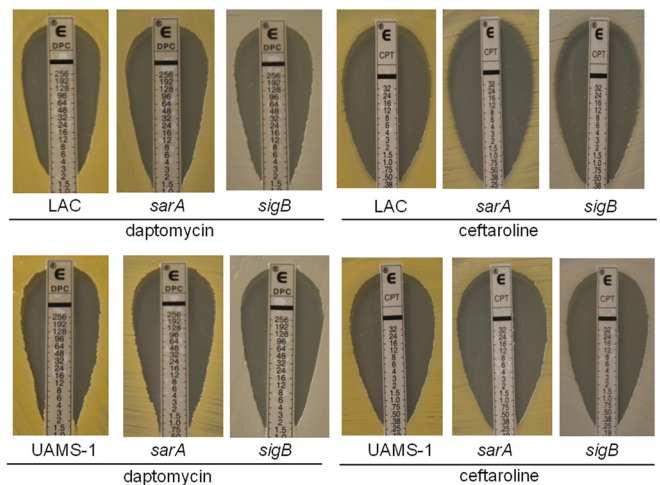
FIG 4 Impact of mutating *sarA* and *sigB* on MICs. The MICs of LAC and UAMS-1 *sarA* and *sigB* mutants was determined by Etest. DPC, daptomycin; CPT, ceftaroline.

establishment of chronic *S. aureus* infections and suggested that this was due to the fact that a functional SigB regulon promotes both the development of small colony variants (SCVs) and increased intracellular persistence (10). In contrast, mutations of *sarA* had relatively little impact on SCV formation. An independent report also concluded that *sarA*, but not *sigB*, is essential for biofilm development in *S. aureus* (11). Thus, the specific mechanistic basis that defines the comparable impact of *sarA* and *sigB* on antibiotic susceptibility *in vivo* remains unclear. Having said this, we previously reported one commonality: that protease production is increased in both *sarA* and *sigB* mutants to a degree that limits biofilm formation (2). However, the more important point in the context of this report is that these results confirm that both of these regulatory loci are potentially important targets for therapeutic intervention.

REFERENCES

1. **Lewis K.** 2008. Multidrug tolerance of biofilms and persister cells. Curr Top Microbiol Immunol **322:**107–131.
2. **Atwood DN, Loughran AJ, Courtney A, Anthony AC, Meeker DG, Gupta RK, Lee CY, Beenken KE, Smeltzer MS.** 2015. Comparative impact of diverse regulatory loci on *Staphylococcus aureus* biofilm formation. Microbiologyopen **4:**436–451. http://dx.doi.org/10.1002/mbo3.250.
3. **Weiss EC, Spencer HJ, Daily SJ, Weiss BD, Smeltzer MS.** 2009. Impact of *sarA* on antibiotic susceptibility of *Staphylococcus aureus* in a catheter-associated *in vitro* model of biofilm formation. Antimicrob Agents Chemother **53:**2475–2482. http://dx.doi.org/10.1128/AAC.01432-08.
4. **Weiss EC, Zielinska A, Beenken KE, Spencer HJ, Daily SJ, Smeltzer MS.** 2009. Impact of *sarA* on daptomycin susceptibility of *Staphylococcus aureus* biofilms *in vivo*. Antimicrob Agents Chemother **53:**4096–4102. http://dx.doi.org/10.1128/AAC.00484-09.
5. **Cassat JE, Dunman PM, Murphy EJ, Projan SJ, Beenken KE, Palm KJ, Yang S-J, Rice KC, Bayles KW, Smeltzer MS.** 2006. Transcriptional profiling of a *Staphylococcus aureus* clinical isolate and its isogenic *agr* and *sarA* mutants reveals global differences by comparison to the laboratory strain RN6390. Microbiology **152:**3075–3090. http://dx.doi.org/10.1099/mic.0.29033-0.
6. **Cassat JE, Dunman PM, McAleese F, Murphy E, Projan SJ, Smeltzer MS.** 2005. Comparative genomics of *Staphylococcus aureus* musculoskeletal isolates. J Bacteriol **187:**576–592. http://dx.doi.org/10.1128/JB.187.2.576-592.2005.
7. **Zielinska AK, Beenken KE, Joo HS, Mrak LN, Griffin LM, Loung TT, Lee CY, Otto M, Shaw LN, Smeltzer MS.** 2011. Defining the strain-dependent impact of the staphylococcal accessory regulator (*sarA*) on the alpha-toxin phenotype of *Staphylococcus aureus*. J Bacteriol **193:**2948–2958. http://dx.doi.org/10.1128/JB.01517-10.
8. **Pallmann P, Schaarschmidt F, Hothorn LA, Fischer C, Nacke H, Priesnitz KU, Schork NJ.** 2012. Assessing group differences in biodiversity by simultaneously testing a user-defined selection of diversity indices. Mol Ecol Resour **12:**1068–1078. http://dx.doi.org/10.1111/1755-0998.12004.
9. **Bischoff M, Entenza JM, Giachino P.** 2001. Influence of a functional *sigB* operon on the global regulators *sar* and *agr* in *Staphylococcus aureus*. J Bacteriol **183:**5171–5179. http://dx.doi.org/10.1128/JB.183.17.5171-5179.2001.
10. **Tuchscherr L, Bischoff M, Lattar SM, Noto Llana M, Pförtner H, Niemann S, Geraci J, Van de Vyver H, Fraunholz MJ, Cheung AL, Herrmann M, Völker U, Sordelli DO, Peters G, Löffler B.** 2015. Sigma factor SigB is crucial to mediate *Staphylococcus aureus* adaptation during chronic infections. PLoS Pathog **11:**e1004870. http://dx.doi.org/10.1371/journal.ppat.1004870.
11. **Valle J, Toledo-Arana A, Berasain C, Ghigo JM, Amorena B, Penadés JR, Lasa I.** 2003. SarA and not sigma B is essential for biofilm development in *Staphylococcus aureus*. Mol Microbiol **48:**1075–1087. http://dx.doi.org/10.1046/j.1365-2958.2003.03493.x.

CrossMark
click for updates

Novel Bone-Targeting Agent for Enhanced Delivery of Vancomycin to Bone

Zaineb A. F. Albayati,[a] Manjula Sunkara,[b] Suzannah M. Schmidt-Malan,[c] Melissa J. Karau,[c] Andrew J. Morris,[b] James M. Steckelberg,[d] Robin Patel,[c,d] Philip J. Breen,[a] Mark S. Smeltzer,[e] K. Grant Taylor,[f] Kevyn E. Merten,[g] William M. Pierce,[h] Peter A. Crooks[a]

College of Pharmacy, University of Arkansas for Medical Sciences, Little Rock, Arkansas, USA[a]; Saha Cardiovascular Research Center, University of Kentucky, Lexington, Kentucky, USA[b]; Department of Laboratory Medicine and Pathology Mayo Clinic, Rochester, Minnesota, USA[c]; Department of Medicine, Mayo Clinic, Rochester, Minnesota, USA[d]; Department of Microbiology and Immunology, College of Medicine, University of Arkansas for Medical Sciences, Little Rock, Arkansas, USA[e]; Department of Chemistry, University of Louisville, Louisville, Kentucky, USA[f]; Pradama, Inc., Louisville, Kentucky, USA[g]; Department of Pharmacology and Toxicology, University of Louisville, Louisville, Kentucky, USA[h]

We examined the pharmacokinetic properties of vancomycin conjugated to a bone-targeting agent (BT) with high affinity for hydroxyapatite after systemic intravenous administration. The results confirm enhanced persistence of BT-vancomycin in plasma and enhanced accumulation in bone relative to vancomycin. This suggests that BT-vancomycin may be a potential carrier for the systemic targeted delivery of vancomycin in the treatment of bone infections, potentially reducing the reliance on surgical debridement to achieve the desired therapeutic outcome.

Osteomyelitis is defined as any inflammatory process in bone, the most common cause of which is infection. Although many bacterial pathogens have been associated with osteomyelitis, *Staphylococcus aureus* is the predominant cause and the pathogen responsible for the most serious forms of bone infection (1). Given the increasing prevalence of *S. aureus* strains resistant to methicillin (2), vancomycin remains the most commonly used antibiotic for the treatment of these infections (3). While true vancomycin resistance is rare, *S. aureus* strains with reduced susceptibility are common and often arise as a consequence of the prolonged periods of vancomycin therapy required to treat bone infections (1, 4). Vancomycin acts by inhibiting bacterial cell wall biosynthesis (5, 6) and is a large hydrophilic molecule that has limited penetration into bone and therefore low bone bioavailability when administered systemically (7). These factors emphasize the need to develop methods to enhance delivery of vancomycin to bone in the treatment of osteomyelitis. One way to accomplish this is to employ local antibiotic delivery, which while

useful suffers from inherent limitations, not the least being the ability to gain direct access to the infection site (8–16). Thus, one of the major challenges to improve therapeutic outcomes for osteomyelitis patients is to develop methods for the systemic deliv-

FIG 1 Structures of vancomycin (left) and BT-vancomycin (right).

FIG 2 Plasma concentration-time profile of vancomycin (circles) and BT-vancomycin (squares) after i.v. administration of 50 mg/kg vancomycin or 63.85 mg/kg BT-vancomycin (molar equivalent to 50 mg/kg vancomycin). Results are the mean ± SEM ($n = 5$ rats). *, significantly higher than results for vancomycin, $P < 0.05$; **, significantly higher than results for vancomycin, $P < 0.01$; ***, significantly higher than results for vancomycin, $P < 0.0001$.

FIG 3 Concentration-time profile in bone of vancomycin (circles) and BT-vancomycin (squares) after i.v. administration of vancomycin (50 mg/kg) or BT-vancomycin (63.85 mg/kg). Results are the mean ± SEM ($n = 5$ rats per group). *, significantly higher than results for vancomycin, $P < 0.05$; **, significantly higher than results for vancomycin, $P < 0.01$; ***, significantly higher than results for vancomycin, $P < 0.001$.

ery of vancomycin, and potentially other antibiotics, in sufficient concentrations to achieve the desired therapeutic effect.

Previous studies in our laboratories have led to the development of bone-targeting agents (BT) based on their high affinity for hydroxyapatite and an enhanced tendency to accumulate in bone (17). We demonstrated that these compounds can be conjugated to vancomycin via a modified polyethylene glycol (PEG) linker (Fig. 1) to form BT-2-minipeg-2-vancomycin (BT-vancomycin) (18–20). Previous in vitro studies confirmed that the MICs of BT-vancomycin against methicillin-resistant and methicillin-susceptible S. aureus are comparable to those of vancomycin alone and that BT-vancomycin binds to hydroxyapatite to a greater extent than vancomycin (21). The objective of the present study was to define the pharmacokinetic (PK) profiles of vancomycin and BT-vancomycin after systemic administration via intravenous (i.v.) or intraperitoneal (i.p.) routes and to determine the plasma and bone content of vancomycin versus BT-vancomycin.

All experimental animal protocols were in strict accordance with the NIH "Guide for the Care and Use of Laboratory Animals" (24) and were approved by the Institutional Animal Care and Use Committees at the University of Kentucky, Lexington, KY, and Mayo Clinic, Rochester, MN. Thirty-five rats received a single i.v. injection via the tail vein of either vancomycin HCl (50 mg/kg of body weight) or BT-vancomycin (63.85 mg/kg; molar equivalent of 50 mg/kg of vancomycin HCl). Twenty rats were given an i.p. injection of either vancomycin HCl (50 mg/kg) or BT-vancomycin (63.85 mg/kg) twice daily for a total of seven doses. BT-vancomycin and vancomycin levels in plasma and bone were determined by liquid chromatography-tandem mass spectrometry (LC/MS-MS).

Bone samples (frozen tibiae) were pulverized, and the crushed bones were weighed, placed into 2-ml tubes, and stored at −80°C for further analysis. Analysis of vancomycin and BT-vancomycin was carried out using a Shimadzu LC unit coupled to an ABI 4000-Qtrap hybrid linear ion trap triple-quadrupole mass spectrometer in the multiple reaction monitoring (MRM) mode. Teicoplanin was used as an internal standard.
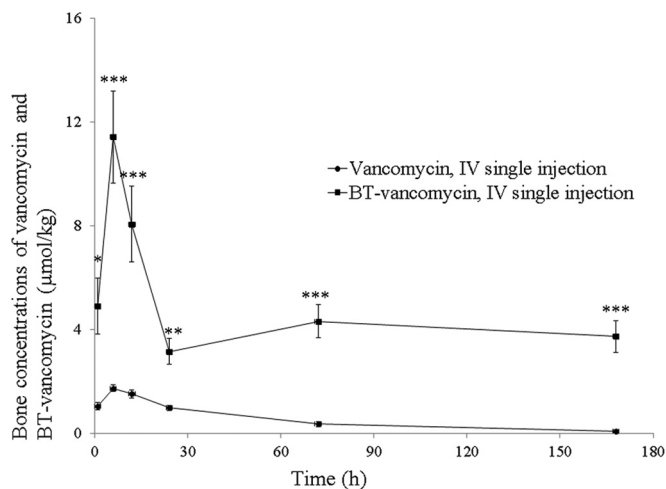
PK analysis was performed using data from individual rats, for which the mean and standard error of the mean (SEM) were calculated for each group. PK parameters were estimated using a noncompartmental model (Phoenix WinNonlin, Professional, version 6.2; Pharsight, Mountain View, CA). The levels of vancomycin and BT-vancomycin in plasma peaked at 13.00 ± 1.96 and 41.22 ± 8.71 μM, respectively, 1 h after administration (Fig. 2). The concentration of BT-vancomycin in plasma declined to its lowest levels (0.07 ± 0.02 μM) at 168 h, while vancomycin reached its lowest level 12 h after i.v. administration (Fig. 2). Compared to the peak concentrations in plasma, peak concentrations in bone were delayed, with peak concentrations occurring 6 h after i.v. administration (Fig. 3). The amount of BT-vancomycin in bone was approximately 5-fold higher than that of vancomycin during the initial 12-h period but increased progressively to approximately 47-fold at 168 h (Table 1).

Increased accumulation of BT-vancomycin was also confirmed after i.p. administration of seven doses of 50 mg/kg of vancomycin or the molar equivalent of BT-vancomycin at 12-h intervals. The ratios of BT-vancomycin to vancomycin were 7.8, 7.4, and 47.7 at 1, 6, and 12 h after the last i.p. administration

TABLE 1 Comparative concentrations of vancomycin and BT-vancomycin in bone after i.v. administration of 50 mg/kg vancomycin or 63.85 mg/kg BT-vancomycin[a]

Time (h)	Concn (μM) (mean ± SEM)[a]		BT-vancomycin/ vancomycin ratio
	Vancomycin	BT-vancomycin	
1	1.04 ± 0.14	4.89 ± 1.08[b]	4.7
6	1.73 ± 0.13	11.41 ± 1.79[c]	6.6
12	1.51 ± 0.15	8.06 ± 1.46[c]	5.3
24	0.97 ± 0.09	3.15 ± 0.49[b]	3.3
72	0.35 ± 0.10	4.31 ± 0.63[c]	12.3
168	0.08 ± 0.05	3.73 ± 0.61[c]	46.6

[a] $n = 5$ rats per group.
[b] Significantly higher than results for vancomycin ($P < 0.01$).
[c] Significantly higher than results for vancomycin ($P < 0.001$).

TABLE 2 Comparative concentrations of vancomycin and BT-vancomycin in plasma and bone after i.p. administration of 50 mg/kg vancomycin or 63.85 mg/kg BT-vancomycin

	Concn (μM) (mean $\pm$ SEM)[a] in plasma		Concn (μM) (mean $\pm$ SEM)[a] in bone		BT-vancomycin/
Time (h)	Vancomycin	BT-vancomycin	Vancomycin	BT-vancomycin	vancomycin ratio in bone
1	15.6 ± 2.0	21.1 ± 2.1[b]	7.3 ± 0.4	56.6 ± 8.4[c]	7.8
6	1.6 ± 0.2	37.7 ± 5.1[c]	7.9 ± 1.5	58.4 ± 9.2[d]	7.4
12	0.4 ± 0.04	27.4 ± 3.1[c]	0.9 ± 0.1	42.9 ± 11.1[c]	47.7

[a] $n = 5$ rats per group.
[b] Not significantly different from results for vancomycin.
[c] Significantly higher than results for vancomycin ($P < 0.0001$).
[d] Significantly higher than results for vancomycin ($P < 0.01$).

(Table 2). PK parameters obtained after i.v. administration are detailed in Table 3.

These data demonstrate that vancomycin and BT-vancomycin exhibit significant differences in their PK profiles. A decrease in total clearance (CL_{tot}) of 13.5-fold was observed for BT-vancomycin compared to vancomycin, with a 14.7-fold increase in half-life ($t_{1/2}$) allowing for a 10.8-fold enhancement in the area under the concentration-time curve (AUC). The significant changes in the AUC indicate a higher degree of *in vivo* exposure to BT-vancomycin, facilitating the accumulation of drug in bone due to an enhanced permeation and retention effect. Consequently, BT-vancomycin shows a longer systemic mean residence time (MRT) than vancomycin ($P < 0.001$). The higher MRT value of BT-vancomycin could be due in part to a more protracted steady state *in vivo*, resulting in improved delivery, dramatically increased access into bones, and prolonged exposure in bone tissue (Table 3).

The estimates of the maximum concentration of drug in serum (C_{max}) of vancomycin and BT-vancomycin determined in the present study were in agreement with previously published data, which include therapeutic peak and trough serum concentrations of 20.7 to 27.6 μM and 3.5 to 6.9 μM, respectively (22).

In our experiments, levels of BT-vancomycin in bone were above the MIC of vancomycin for up to 168 h after administration. These findings predict good antimicrobial outcomes, since the antimicrobial activity of vancomycin is time dependent and not concentration dependent (23).

In conclusion, our previously published work with BT-vancomycin showed that this novel molecule had *in vitro* activity similar to that of vancomycin against both methicillin-resistant and methicillin-susceptible *S. aureus* strains isolated from bone infections (21). Additionally, BT-vancomycin was shown to be more efficacious than an equimolar dose of vancomycin in a rat osteomyelitis model. However, the most efficacious dosing regimen used in these studies (i.p. injection every 12 h for 21 days) not only was associated with high BT-vancomycin levels in plasma but also caused a decrease in body weight, an elevation in white blood cell count, renal dysfunction, and evidence of tubulointerstitial nephritis. Although we did not examine toxicity in the current studies, we have demonstrated enhanced accumulation in bone, even after a single i.v. dose of an amount of BT-vancomycin equivalent to that used in the previous study (21). Thus, with further dose optimization, this toxicity can likely be minimized, making BT-vancomycin a useful BT therapy for the treatment of methicillin-resistant *S. aureus* (MRSA) osteomyelitis. More importantly, the results justify future studies to assess the utility of our promising BT agent in the context of other, less toxic antibiotics that have activity against MRSA.

TABLE 3 PK parameters in rats following i.v. administration of a single bolus of 50 mg/kg vancomycin or 63.85 mg/kg BT-vancomycin

	Result (mean $\pm$ SEM) for:	
Parameter[a]	Vancomycin	BT-vancomycin
$t_{1/2}$ (h)	1.44 ± 0.09	21.14 ± 4.86[d]
T_{max} (h)	1.00 ± 0.00	1.00 ± 0.00
C_{max} (μM)	12.63 ± 2.38	43.82 ± 9.45[b]
AUC (h $\cdot$ μM)	58.71 ± 10.33	631.39 ± 95.13[c]
V_z (liters/kg)	1.10 ± 0.18	1.13 ± 0.21
CL (liters/h/kg)	0.65 ± 0.12	0.048 ± 0.01[c]
AUMC (h $\cdot$ h $\cdot$ μM)	162.63 ± 25.67	$14,225.62 \pm 3,012.66$[e]
MRT (h)	1.93 ± 0.17	12.45 ± 1.63[d]
V_{ss} (liters/kg)	1.32 ± 0.35	0.80 ± 0.25

[a] T_{max}, time to maximum concentration of drug in serum; V_z, volume of distribution; CL, clearance; AUMC, area under the first moment of the concentration-time curve; V_{ss}, volume of distribution at steady state.
[b] Significantly higher than results for vancomycin ($P < 0.05$).
[c] Significantly higher than results for vancomycin ($P < 0.01$).
[d] Significantly higher than results for vancomycin ($P < 0.001$).
[e] Significantly higher than results for vancomycin ($P < 0.0001$).

REFERENCES

1. **Cierny G, III.** 2011. Surgical treatment of osteomyelitis. Plast Reconstr Surg 127(Suppl 1):190S–204S. http://dx.doi.org/10.1097/PRS.0b013e3182025070.
2. **Chambers HF, Deleo FR.** 2009. Waves of resistance: *Staphylococcus aureus* in the antibiotic era. Nat Rev Microbiol 7:629–641. http://dx.doi.org/10.1038/nrmicro2200.
3. **Lew DP, Waldvogel FA.** 2004. Osteomyelitis. Lancet 364:369–379. http://dx.doi.org/10.1016/S0140-6736(04)16727-5.
4. **Rodvold KA, McConeghy KW.** 2014. Methicillin-resistant *Staphylococcus aureus* therapy: past, present, and future. Clin Infect Dis 58(Suppl 1):S20–S27. http://dx.doi.org/10.1093/cid/cit614.
5. **Darley ES, MacGowan AP.** 2004. Antibiotic treatment of gram-positive bone and joint infections. J Antimicrob Chemother 53:928–935. http://dx.doi.org/10.1093/jac/dkh191.
6. **Rubinstein E, Keynan Y.** 2014. Vancomycin revisited—60 years later. Front Public Health 2:217. http://dx.doi.org/10.3389/fpubh.2014.00217.
7. **Massias L, Dubois C, de Lentdecker P, Brodaty O, Fischler M, Farinotti R.** 1992. Penetration of vancomycin in uninfected sternal bone. Antimi-

crob Agents Chemother **36:**2539–2541. http://dx.doi.org/10.1128/AAC
.36.11.2539.

8. **Cevher E, Orhan Z, Mülazimoğlu L, Sensoy D, Alper M, Yildiz A, Ozsoy Y.** 2006. Characterization of biodegradable chitosan microspheres containing vancomycin and treatment of experimental osteomyelitis caused by methicillin-resistant *Staphylococcus aureus* with prepared microspheres. Int J Pharm **317:**127–135. http://dx.doi.org/10.1016/j.ijpharm
.2006.03.014.

9. **Smith JK, Bumgardner JD, Courtney HS, Smeltzer MS, Haggard WO.** 2010. Antibiotic-loaded chitosan film for infection prevention: a preliminary *in vitro* characterization. J Biomed Mater Res B Appl Biomater **94:**203–211. http://dx.doi.org/10.1002/jbm.b.31642.

10. **Parker AC, Beenken KE, Jennings JA, Hittle L, Shirtliff ME, Bumgardner JD, Smeltzer MS, Haggard WO.** 2015. Characterization of local delivery with amphotericin B and vancomycin from modified chitosan sponges and functional biofilm prevention evaluation. J Orthop Res **33:**439–447. http://dx.doi.org/10.1002/jor.22760.

11. **Yang CC, Lin CC, Liao JW, Yen SK.** 2013. Vancomycin-chitosan composite deposited on post porous hydroxyapatite coated Ti6Al4V implant for drug controlled release. Mater Sci Eng C Mater Biol Appl **33:**2203–2212. http://dx.doi.org/10.1016/j.msec.2013.01.038.

12. **Shinsako K, Okui Y, Matsuda Y, Kunimasa J, Otsuka M.** 2008. Effects of bead size and polymerization in PMMA bone cement on vancomycin release. Biomed Mater Eng **18:**377–385. http://dx.doi.org/10.3233/BME
-2008-0554.

13. **Beenken KE, Bradney L, Bellamy W, Skinner RA, McLaren SG, Gruenwald MJ, Spencer HJ, Smith JK, Haggard WO, Smeltzer MS.** 2012. Use of xylitol to enhance the therapeutic efficacy of polymethylmethacrylate-based antibiotic therapy in treatment of chronic osteomyelitis. Antimicrob Agents Chemother **56:**5839–5844. http://dx.doi.org/10.1128
/AAC.01127-12.

14. **Beenken KE, Smith JK, Skinner RA, Mclaren SG, Bellamy W, Gruenwald MJ, Spencer HJ, Jennings JA, Haggard WO, Smeltzer MS.** 2014. Chitosan coating to enhance the therapeutic efficacy of calcium sulfate-based antibiotic therapy in the treatment of chronic osteomyelitis. J Biomater Appl **29:**514–523. http://dx.doi.org/10.1177/0885328214535452.

15. **Giavaresi G, Bertazzoni Minelli E, Sartori M, Benini A, Della Bora T, Sambri V, Gaibani P, Borsari V, Salamanna F, Martini L, Nicoli Aldini N, Fini M.** 2012. Microbiological and pharmacological tests on new antibiotic-loaded PMMA-based composites for the treatment of osteomyelitis. J Orthop Res **30:**348–355. http://dx.doi.org/10.1002/jor.21531.

16. **Jiang JL, Li YF, Fang TL, Zhou J, Li XL, Wang YC, Dong J.** 2012. Vancomycin-loaded nano-hydroxyapatite pellets to treat MRSA-induced chronic osteomyelitis with bone defect in rabbits. Inflamm Res **61:**207–215. http://dx.doi.org/10.1007/s00011-011-0402-x.

17. **Nasim S, Vartak AP, Pierce WM, Jr, Taylor KG, Smith N, Crooks PA.** 2010. 3-O-Phosphate ester conjugates of 17-β-O-{1-[2-carboxy-(2-hydroxy-4-methoxy-3-carboxamido)anilido]ethyl}1,3,5(10)-estratriene as novel bone-targeting agents. Bioorg Med Chem Lett **20:**7450–7453. http://dx.doi.org/10.1016/j.bmcl.2010.10.023.

18. **Neale JR, Richter NB, Merten KE, Taylor KG, Singh S, Waite LC, Emery NK, Smith NB, Cai J, Pierce WM, Jr.** 2009. Bone selective effect of an estradiol conjugate with a novel tetracycline-derived bone-targeting agent. Bioorg Med Chem Lett **19:**680–683. http://dx.doi.org/10.1016/j
.bmcl.2008.12.051.

19. **Pierce WM, Jr, Waite LC, Taylor KG.** July 2008.Bone targeting compounds for delivering agents to bone for interaction therewith.US patent 7,399,789.

20. **Pierce WM, Jr, Waite LC, Taylor KG.** December 2011. Bone targeting compounds for delivering agents to bone for interaction therewith (generation 2). US patent 8,071,575.

21. **Karau MJ, Schmidt-Malan SM, Greenwood-Quaintance KE, Mandrekar J, Cai J, Pierce WM, Jr, Merten K, Patel R.** 2013. Treatment of methicillin-resistant *Staphylococcus aureus* experimental osteomyelitis with bone-targeted vancomycin. SpringerPlus **2:**329. http://dx.doi.org/10.1186
/2193-1801-2-329.

22. **Lundstrom TS, Sobel JD.** 2004. Antibiotics for gram-positive bacterial infections: vancomycin, quinupristin-dalfopristin, linezolid, and daptomycin. Infect Dis Clin North Am **18:**651–668. http://dx.doi.org/10.1016
/j.idc.2004.04.014.

23. **Rybak MJ.** 2006. The pharmacokinetic and pharmacodynamic properties of vancomycin. Clin Infect Dis **42**(Suppl 1)**:**S35–S39. http://dx.doi.org/10
.1086/491712.

24. **National Research Council.** 2011. Guide for the care and use of laboratory animals, 8th ed. National Academies Press, Washington, DC.

MicrobiologyOpen

ORIGINAL RESEARCH

Comparative impact of diverse regulatory loci on *Staphylococcus aureus* biofilm formation

Danielle N. Atwood[1], Allister J. Loughran[1], Ashleah P. Courtney[1], Allison C. Anthony[1], Daniel G. Meeker[1], Horace J. Spencer[2], Ravi Kr. Gupta[1], Chia Y. Lee[1], Karen E. Beenken[1] & Mark S. Smeltzer[1,3,4]

[1]Department of Microbiology and Immunology, University of Arkansas for Medical Sciences, Little Rock, Arkansas
[2]Department of Biostatistics, University of Arkansas for Medical Sciences, Little Rock, Arkansas
[3]Department of Orthopaedic Surgery, University of Arkansas for Medical Sciences, Little Rock, Arkansas
[4]Department of Pathology, University of Arkansas for Medical Sciences, Little Rock, Arkansas .

Abstract

The relative impact of 23 mutations on biofilm formation was evaluated in the USA300, methicillin-resistant strain LAC. Mutation of *sarA*, *atl*, *codY*, *rsbU*, and *sigB* limited biofilm formation in comparison to the parent strain, but the limitation imposed by mutation of *sarA* was greater than that imposed by mutation of any of these other genes. The reduced biofilm formation of all mutants other than the *atl* mutant was correlated with increased levels of extracellular proteases. Mutation of *fur*- and *mgrA*-enhanced biofilm formation but in LAC had no impact on protease activity, nuclease activity, or accumulation of the polysaccharide intercellular adhesin (PIA). The increased capacity of these mutants to form a biofilm was reversed by mutation of *sarA*, and this was correlated with increased protease production. Mutation of *sarA*, *mgrA*, and *sigB* had the same phenotypic effect in the methicillin-sensitive strain UAMS-1, but mutation of *codY* increased rather than decreased biofilm formation. As with the UAMS-1 *mgrA* mutant, this was correlated with increased production of PIA. Examination of four additional clinical isolates suggests that the differential impact of *codY* on biofilm formation may be a conserved characteristic of methicillin-resistant versus methicillin-sensitive strains.

Introduction

Many forms of *Staphylococcus aureus* infection are characterized by formation of a bacterial biofilm, the presence of which confers a therapeutically relevant level of intrinsic resistance to both host defenses and conventional antibiotics (Brady et al. 2008; Lewis 2008; Trotonda et al. 2008; Bjarnsholt et al. 2013). Among these are infections

of bone and indwelling orthopedic devices, and given our specific interest in these infections, we have focused much of our effort on identifying factors that contribute to *S. aureus* biofilm formation (Tsang et al. 2008; Beenken et al. 2012, 2014; Cassat et al. 2013). Our results, as well as those from other laboratories, have led us to place a primary emphasis on the staphylococcal accessory regulator locus (*sarA*), mutation of which limits *S. aureus* biofilm formation to a degree that can be correlated with increased antibiotic susceptibility and an improved therapeutic outcome in relevant murine and rabbit models (Beenken et al. 2003; Valle et al. 2003; Weiss et al. 2009a, b; Abdelhady et al. 2014). However, *sarA* is part of a complex and highly interactive regulatory circuit that includes many other loci implicated in biofilm formation (Priest et al. 2012; Ibarra et al. 2013). This brings up two important questions, the first being whether other regulatory loci offer therapeutic potential comparable to or even greater than *sarA*, and the second being whether the functional status of other regulatory loci has the potential to compromise therapeutic strategies targeting *sarA*.

It is impossible to answer these questions because no comprehensive direct comparisons have been made under consistent experimental conditions. Indeed, there are reports that are directly contradictory by comparison to each other. For example, Tu Quoc et al. (2007) found that mutation of *mgrA* or *codY* limited biofilm formation, while other reports concluded that mutation of these same loci has the opposite effect (Majerczyk et al. 2008; Trotonda et al. 2008). One possible explanation for such disparate results is the use of different *S. aureus* strains, which is understandable, and in fact necessary, from a therapeutic point of view, particularly given the genetic and phenotypic diversity that exists among contemporary clinical isolates (Cassat et al. 2006; Wang et al. 2007; Klein et al. 2013). It has been suggested that methicillin resistance itself has a direct impact on the mechanism of biofilm formation, with methicillin-resistant strains relying primarily on surface proteins, most notably FnbA and FnbB, and methicillin-sensitive strains relying more heavily on the polysaccharide intercellular adhesin (PIA) (Pozzi et al. 2012).

It is also possible that such contradictory reports are due to the use of different in vitro methods of testing biofilm formation. Two primary examples include the medium used to assess biofilm formation and whether the substrate is first coated with human plasma proteins, the latter reflecting the fact that even abiotic medical implants are rapidly coated with host proteins after implantation (Francois et al. 1996). The in vitro assays that led to our initial focus on *sarA* employed tryptic soy broth (TSB) supplemented with both salt and glucose as well as a plasma-coated substrate (Beenken et al. 2003).

Subsequent studies have confirmed that the phenotypes we observed under these conditions translate to a reduced capacity to form a biofilm in vivo (Weiss et al. 2009b) and a reduced capacity to cause hematogenous bone and joint infection (Zielinska et al. 2012). Nevertheless, it remains important to consider alternative assay conditions if for no other reason than to clarify discrepancies in the literature. Thus, we compared the relative capacity of 23 mutants to form a biofilm in vitro under different conditions. Primary experiments were done with the USA300 methicillin-resistant strain LAC and expanded to additional clinical isolates including the methicillin-sensitive strain UAMS-1. We also investigated the mechanistic basis for mutations correlated with an altered biofilm phenotype.

Experimental Procedures

Generation of primary mutants

Regulatory mutants generated in the plasmid cured JE2 derivative of the USA300, methicillin-resistant strain LAC (Fey et al. 2013) were obtained from the Nebraska Transposon Mutant Library (NTML) through the Network on Antimicrobial Resistance in *S. aureus* (NARSA, now available from BEI Resources, Manassas, VA, http://www.beiresources.org). To ensure consistency with our previous studies, and because the NTML consists of primary mutants that have not been characterized beyond their transposon insertion sites, each mutation was first transduced into the derivative of LAC and its isogenic *sarA* mutant employed in our previous studies (Zielinska et al. 2011). To generate the NTML, JE2 was cured of both its larger plasmid conferring resistance to erythromycin and its smaller cryptic plasmid (Fey et al. 2013), while the derivative of LAC we employ was cured only of the larger plasmid (Wormann et al. 2011). This allowed erythromycin selection of transductants, with confirmation subsequently obtained by PCR analysis of the targeted gene (data not shown) and by comparison of *Eco*RI-digested genomic DNA, which confirmed the presence of the small cryptic plasmid in the LAC recipients but not in the JE2 donors (Fig. S1). However, analysis of a subset of strains using our standard assay conditions (Beenken et al. 2003) demonstrated that the impact of individual mutations on biofilm formation was consistent in JE2 and our derivative of LAC (Fig. S1).

We also examined *codY*, *mgrA*, and *sigB* mutants generated in the MSSA osteomyelitis isolate UAMS-1, isogenic *sarA* mutants generated in both LAC and UAMS-1, and an isogenic mutant of LAC unable to produce all extracellular proteases other than those encoded by the *spl* operon (Beenken et al. 2003, 2014; Zielinska et al. 2011,

2012). This was necessitated by the fact that the *spl* mutation is defined by resistance to erythromycin, thus precluding the ability to use our LAC derivative unable to produce any extracellular protease (Zielinska et al. 2011) as a transduction recipient. However, previous studies confirmed that biofilm formation is comparable in LAC *sarA* mutants unable to produce any extracellular protease versus those that retain the capacity to produce only the *spl*-encoded proteases (Loughran et al. 2014). Phage-mediated transduction was also used to generate *codY* mutants in each of four additional clinical isolates. However, because these strains were resistant to erythromycin, and because all of the mutants obtained from the NTML are defined by erythromycin resistance, it was first necessary to exchange the erythromycin resistance cassette in JE2 to an alternative antibiotic resistance cassette (Bose et al. 2013). All mutations, and the identity of the recipient strain, were confirmed by PCR of the targeted gene and additional genes and/or mutations that define each recipient strain (data not shown). Mutants were then maintained at −80°C in TSB containing 25% (v/v) glycerol.

Genetic complementation

Construction of an *rsbU* complementation plasmid was done by PCR amplification of the *rsbU* open reading frame (ORF) together with 556 bp of upstream DNA (forward oligonucleotide primer: GCGAAAATACCGACA CATGTAG; reverse primer: GGGTTTTGAAGCTTTAAAA TTGCTTC). The amplification product was cloned into the pCR2.1 TOPO vector (Invitrogen, Grand Island, NY) and transformed into Z-Competent *Escherichia coli* cells (Zymo Research Corp., Irvine, CA). After verification by DNA sequencing (data not shown), the plasmid was digested with *Eco*RI (New England Biolabs, Ipswitch, MA) and the insert ligated into the *E. coli-S. aureus* shuttle vector pLI50 (Blevins et al. 1999).

Construction of the *sigB* complementation plasmid was done by PCR amplification using a forward primer with an *Nde*I cut site (GGG<u>CATATG</u>GCGAAATAATGGCGA AAG) and a reverse primer that included a *Bam*HI cut site (CCC<u>GGATCC</u>CGTATCATTAATAAACAAATTC). The amplification product was ligated into pCR2.1, verified as described above, and the insert cloned into the shuttle vector pOS1 (Bubeck Wardenburg et al. 2006) such that expression of *sigB* was under the control of the lipoprotein diacylglycerol transferase promoter (pOS1-p*lgt*) (Torres et al. 2010). Amplification of *rsbU* and *sigB* was done using genomic DNA from the USA300 strain LAC as template.

The *mgrA* complementation plasmid was generated by PCR using a forward primer containing a *Hind*III restriction site and an N-terminal 6XHis tag (GGATCC

<u>AAGCTT</u>ATGCATCATCACCATCACCATGGATCTGATC AACATAATTTAAAAGAACAGCTATGC), the latter being added for purposes outside the scope of the experiments reported here, together with a reverse primer containing a *Hind*III restriction site (GGATCC<u>AAGCTT</u>TTATTTTTT CCTTTGTTTCATCAAATGCATGAATGAC). The amplification product was cloned into the shuttle vector pLL48 under the control of an isopropyl β-D-1-thiogalactopyranoside (IPTG)-inducible promoter. Specifically, pLL48 was generated by cloning P*spac-lacI* promoter from pCL15 into pLL47 plasmid (Luong and Lee 2006; Luong et al. 2011). In this case, amplification was done using genomic DNA from the *S. aureus* strain Newman. Induction was done using 1 mmol/L IPTG.

The plasmid constructs used to complement the *atl, codY, fur,* and *sarA* mutations were all described previously (Blevins et al. 1999; Torres et al. 2010; Luong et al. 2011; Bose et al. 2012). Where appropriate, complementation plasmids were first used to transform the *S. aureus* strain RN4220 by electroporation. Once in *S. aureus*, plasmids were then introduced into the appropriate strains by phage-mediated transduction. Complemented strains were also maintained at −80°C in TSB containing 25% (v/v) glycerol. For each experiment, strains under study were retrieved from cold storage by plating on tryptic soy agar (TSA) with appropriate antibiotic selection. Antibiotics were used at the following concentrations: erythromycin, 10 μg mL^{-1}; tetracycline, 5 μg mL^{-1}; kanamycin, 50 μg mL^{-1}; neomycin, 50 μg mL^{-1}, spectinomycin, 1000 μg mL^{-1}; chloramphenicol, 10 μg mL^{-1}. Kanamycin and neomycin were always used together to avoid selection of spontaneously resistant strains.

Assessment of biofilm formation

Biofilm formation was assessed in vitro using a microtiter plate assay. To explore the impact of different assay conditions, the medium consisted of TSB with and without supplementation with 3% sodium chloride and 0.5% glucose (biofilm medium, BFM), while the substrate was used with and without coating with 20% human plasma as previously described (Beenken et al. 2003). Briefly, bacterial cultures were grown at 37°C to stationary phase (16 h) in TSB or BFM with antibiotics when appropriate. Cultures were standardized to an OD$_{560}$ = 0.05 in the appropriate test medium (TSB or BFM) without antibiotics. IPTG (1 mmol/L) or Dispersin B (Kane Biotech Inc, Winnipeg, Manitoba, Canada, 5 μmol/L) was included as appropriate. Wells of a 96-well microtiter plate were then inoculated with 200 μL and incubated at 37°C for 24 h, at which point they were washed three times with 200 μL PBS, fixed with 200 μL 100% EtOH, stained with 200 μL crystal violet, and washed three times with 200 μL PBS.

Stain was then eluted with 150 μL 100% EtOH for 10 min before diluting the eluent with an equal volume of PBS. Absorbance was measured using a BioTek Synergy 2 microplate reader (BioTek Instruments, Winooski, VT). For mixed culture biofilm assays with LAC, UAMS-1, and their *sarA* mutants, each strain was grown overnight in BFM, standardized as described above, and mixed in equal volumes prior to inoculation of the wells. All assays were performed using at least two biological replicates, each containing a minimum of three experimental replicates.

Western blotting

SarA production was assessed using whole-cell lysates prepared from stationary phase cells and a rabbit polyclonal anti-SarA IgG antibody as previously described (Blevins et al. 1999). Secondary antibody was horseradish peroxidase (HRP)-conjugated goat anti-rabbit IgG (Sigma Chemical Co., St Louis, MO). Blots were performed in triplicate using different biological replicates. Blots were developed with SuperSignal West Femto Chemiluminescent Substrate (Thermo Scientific, Rockford, IL) and quantified using a Bio-Rad ChemiDocMP Imaging System and Image Lab Software (Bio-Rad Laboratories, Inc., Hercules, CA).

Protease activity

Protease activity was assessed in standardized samples of cell-free supernatant from stationary phase (16 h) cultures grown without antibiotics using a Protease Fluorescent Detection Kit (Sigma Chemical Co.) as previously described (Zielinska et al. 2012). Results are reported as relative fluorescence units and represent at least two biological replicates, each of which included four experimental replicates.

Nuclease activity

Nuclease activity was assessed using a fluorescence resonance energy transfer (FRET)-based assay as previously described (Beenken et al. 2012). Briefly, 25 μL sterilized, standardized supernatants from stationary phase cultures (16 h) grown without antibiotic selection were mixed with an equal volume of FRET substrate (5′-/5HEX/CCCCGGATCCACCCC/3BHQ_2/-3′; Integrated DNA Technologies, Coralville, IA) diluted to 2 μmol/L in buffer consisting of 20 mmol/L Tris, pH 8.0, and 10 mmol/L $CaCl_2$. Results were assessed after 5 min at 30°C using an excitation wavelength of 530 nm and an emission wavelength of 590 nm. Results are reported as relative fluorescence units. Nuclease activity was also assessed using

D'NASE Test Agar (REMEL, Lenexa, KS) (Tsang et al. 2008).

PIA immunoblot

Production of the polysaccharide intercellular adhesion (PIA) was assessed as previously described with slight modifications (Beenken et al. 2004). Specifically, cultures were grown overnight in TSB supplemented with 3.0% sodium chloride and 0.5% glucose and antibiotics as appropriate. After standardization to $OD_{660} = 5.0$, cells were harvested by centrifugation and resuspended in 60 μL 0.5 mol/L EDTA. Cell suspensions were boiled at 105°C for 8 min followed by centrifugation. Forty microliters of the supernatant was then incubated for 30 min with 5 μL proteinase K (10 mg per mL) at 48°C to reduce nonspecific background levels. Twenty microliter of Tris-buffered saline (20 mmol/L Tris-HCl, 150 mmol/L NaCl [pH 7.4]) was added to the samples, which were then stored at −20°C. For analysis, 20 μL of this sample was mixed with 60 μL TBS. Using a BIO-dot microfiltration apparatus (Bio-Rad Laboratories, Inc.), 50 μL was spotted onto a nylon membrane presoaked with TBS (Roche Diagnostics Corp., Indianapolis, IN). Each well was then rinsed with 200 μL tris-buffered saline (TBS). The membrane was then removed, dried, and blocked in 0.5% skim milk overnight at 4°C. PIA production was assessed using anti-PIA antiserum (kindly provided by Michael Otto, National Institute of Allergy and Infectious Disease) diluted 1:500 in 0.5% skim milk. Primary antibody was detected using HRP-conjugated goat anti-rabbit IgG secondary antibody (Sigma Chemical Co.). Blots were developed and quantified as described above after subtracting the background observed with a UAMS-1 *ica* mutant.

Statistical analysis

Statistical comparisons were done using the unpaired *t*-test or where appropriate one-way analysis of variance with Tukey's Multiple Comparison Test. Statistical analysis was done using GraphPad Prism 5.0 (La Jolla, CA).

Results and Discussion

Comparison of different assay conditions

LAC mutants were generated by phage-mediated transduction from JE2 donor strains obtained from the NTML (Fig. S1). A microtiter plate assay was then used to assess the relative capacity of these mutants to form a biofilm under different assay conditions. Neither LAC nor any of its regulatory mutants formed a biofilm when the assay
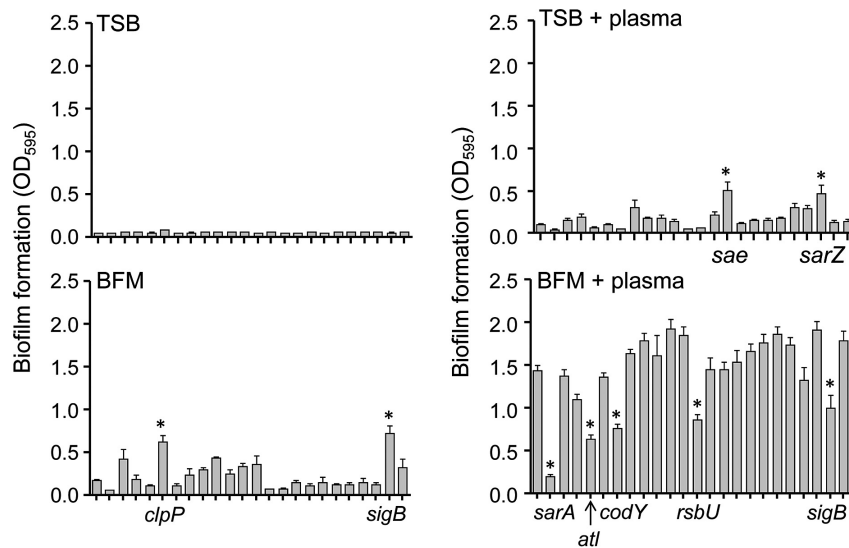
Figure 1. Biofilm phenotypes as a function of assay conditions. Biofilm formation was assessed in LAC and its isogenic mutants under four different assay conditions. To allow direct comparisons between conditions, the results shown in all panels are shown as raw data and represent the average ± standard error of the mean (SEM) from a minimum of two experiments, each of which was repeated with at least three replicates. Mutants that exhibit a statistically significant difference under each assay condition (asterisk; $P < 0.05$) are indicated in each panel. For every individual strain, including the *sarA* mutant, the results observed with BFM and plasma coating were statistically significant by comparison to the same strain assayed under all other conditions. Overall order in all panels is LAC followed by isogenic strains with mutations in *sarA*, *agr*, *arl*, *atl*, *clpP*, *codY*, *fur*, *lyt*, *mgrA*, *msa*, *rot*, *rsbU*, *rsr*, *sae*, *sarS*, *sarT*, *sarU*, *sarV*, *sarX*, *sarY*, *sarZ*, *sigB*, and *srr*.

was done in TSB without media supplementation and without plasma coating of the substrate (Fig. 1). A statistically significant increase was observed with two mutants (*saeRS* and *sarZ*) when the assay was done in TSB with plasma coating but without media supplementation, as well as two different mutants (*clpP* and *sigB*) when the assay was done using uncoated plates and TSB supplemented with NaCl and glucose (BFM). However, under all three of these experimental conditions, biofilm formation was extremely limited by comparison to the results observed when the assay was performed using BFM and the substrate was coated with human plasma (Fig. 1). In fact, biofilm formation was significantly increased under these conditions in every mutant, including the *sarA* mutant, by comparison to the same strain examined under all other assay conditions (Fig. 1). Our original studies identifying *sarA* as a primary mediator of biofilm formation were done using BFM and a plasma-coated substrate, and subsequent studies confirmed its importance under in vivo conditions, thus suggesting that these in vitro conditions accurately reflect the likelihood of in vivo relevance (Weiss et al. 2009a,b; Beenken et al. 2010, 2014; Zielinska et al. 2012). Additionally, indwelling medical devices are rapidly coated with host proteins (Steckelberg and Osmon 1994; Gotz 2002), and it has been demonstrated that biofilm-associated bacteria encounter unique growth conditions that include

increased osmolarity (Prigent-Combaret et al. 1999), both of which provide further support for the hypothesis that, by comparison to the other assay conditions we examined, the use of BFM and a plasma-coated substrate is more likely to reflect in vivo relevance. Thus, we employed these assay conditions in all subsequent experiments.

Relative impact of regulatory mutations

We examined the biofilm phenotype of LAC and each of 22 regulatory mutants and an *atl* mutant using our optimized assay conditions. While not a regulatory element, Atl has been shown to play a critical role in the initial attachment stage of biofilm formation and the subsequent release of extracellular DNA (eDNA) further enhancing the process (Houston et al. 2011). As such, we felt it was necessary to include Atl in our comparative studies. Comparisons included a minimum of six biological replicates per strain, each of which included at least three experimental replicates. To make the biological replicates comparable to one another, the results observed with LAC were set to 1.0, with the results observed with each regulatory mutant shown relative to this value. Results from all replicates were then combined for statistical analysis. These studies identified seven mutants in which the capacity to form a biofilm was significantly different from

Figure 2. Relative impact of *Staphylococcus aureus* regulatory loci on biofilm formation in vitro. Biofilm formation was assessed in LAC (WT) and its isogenic regulatory mutants using a microtiter plate assay with BFM and plasma coating of the substrate. Results shown represent the average ± SEM from a minimum of six experiments, each of which was repeated with at least three technical replicates. Single asterisk indicates statistical significance by comparison to the parent strain ($P < 0.05$). Double asterisks indicate statistical significance by comparison to the isogenic *sarA* mutant ($P < 0.05$).
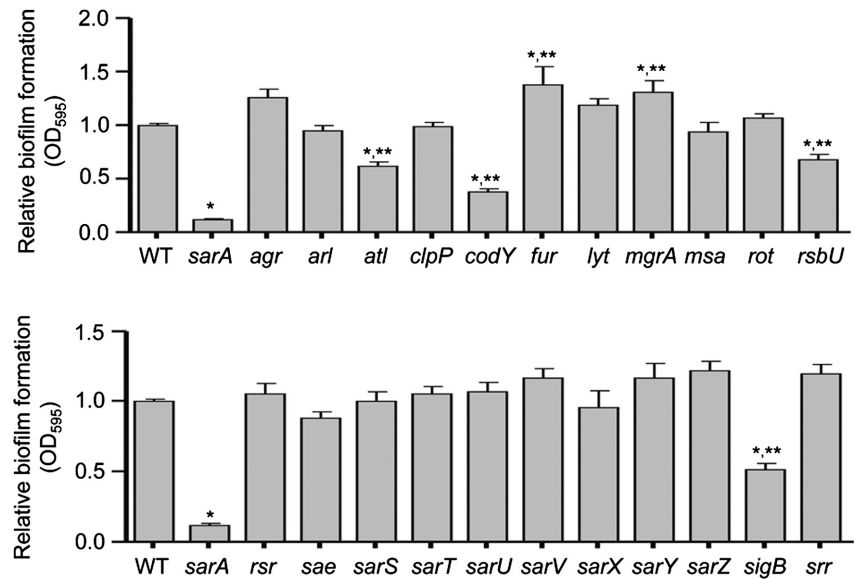
that observed in the LAC parent strain (Fig. 2). Five of these (*sarA*, *atl*, *codY*, *rsbU*, and *sigB*) had a reduced capacity to form a biofilm, while two (*fur* and *mgrA*) had an increased capacity to form a biofilm (Fig. 2). The cause-and-effect relationship between all mutations and their biofilm phenotypes was confirmed by genetic complementation (Fig. 3).

Although *atl*, *codY*, *rsbU*, and *sigB* mutants exhibited a decreased capacity to form a biofilm by comparison to the parent strain, they also exhibited a significantly increased capacity to form a biofilm by comparison to the isogenic *sarA* mutant (Fig. 2). The fact that mutation of *sarA* had a greater impact on biofilm formation than mutation of these other genes was confirmed by demonstrating that concomitant mutation of *sarA* reduced biofilm formation still further in all of these mutants (Fig. 3). Concomitant mutation of *sarA* also reversed the increased biofilm formation observed in the *fur* and *mgrA* mutants (Fig. 3), thus confirming that the impact of mutating *sarA* is epistatic to that of mutating these other regulatory loci.

Impact of regulatory mutations on accumulation of SarA

Eliminating the production of an effector protein like SarA typically has a greater phenotypic impact than mutation of genes that modulate the production or activity of that effector protein. One explanation for the intermediate impact of mutating *atl*, *codY*, *rsbU*, and *sigB* on biofilm formation is that mutation of these loci limits, but does not eliminate, the production of SarA itself. The only mutations found to have a statistically significant impact in this regard were the *rsbU* and *sigB* mutations (Fig. 4).

This is consistent with the current *S. aureus* regulatory paradigm indicating that RsbU is a positive regulator of SigB, and SigB an activator of *sarA* expression (Bischoff et al. 2001; Cheung et al. 2008; Pane-Farre et al. 2009). This suggests that the impact of these loci is likely to be mediated, at least in part, via a *sarA*-dependent pathway, while that of *atl* and *codY* is mediated via a *sarA*-independent pathway. Similarly, mutation of *fur* or *mgrA* had no impact on the accumulation of SarA (Fig. 4).

Impact of extracellular protease production on biofilm formation

Mutation of *sarA* is known to result in greatly increased levels of extracellular protease production, and this has been directly correlated with the reduced capacity of a LAC *sarA* mutant to form a biofilm under both in vitro and in vivo conditions (Tsang et al. 2008; Zielinska et al. 2011, 2012). To assess relative levels of protease activity, we used the Protease Fluorescent Detection Kit (Sigma Chemical Co.) which employs a fluorescein isothiocyanate (FITC)-casein substrate. These experiments confirmed that mutation of *rsbU*, *sigB*, and *codY*, all of which had a reduced capacity to form a biofilm (Fig. 1), also resulted in increased protease production in LAC (Fig. 5). Additionally, by comparison to the isogenic mutants, limiting the production of extracellular proteases by mutagenesis of the genes encoding aureolysin, SspA, SspB, and ScpA enhanced biofilm formation in all of these mutants (Fig. 5). Collectively, these results strongly support the hypothesis that increased protease production makes a significant contribution to the biofilm-deficient phenotype of *sarA*, *codY*, *rsbU*, and *sigB* mutants.

Figure 3. Relative impact of *sarA* versus other regulatory loci in LAC. (A) Biofilm formation was assessed in each regulatory mutant found to have a significant impact on biofilm formation with (+) and without (−) plasmid-based genetic complementation. Results shown represent the average ± SEM from a minimum of two experiments, each of which was repeated with at least three replicates. Single asterisk indicates that the results observed with the indicated mutant were significantly different from those observed with the LAC parent strain ($P < 0.05$). Double asterisks indicate that the results observed with the complemented strain were significantly different by comparison to those observed with the uncomplemented isogenic mutant ($P < 0.05$). (B) Biofilm formation was assessed in each regulatory mutant found to have a significant impact on biofilm formation with (−) and without (+) concomitant mutation of *sarA*. Single asterisk indicates statistical significance by comparison to the LAC parent strain ($P < 0.05$). Double asterisks indicate significance of the double mutant relative to the corresponding isogenic single mutant ($P < 0.05$).

Figure 4. Impact of LAC regulatory mutations on accumulation of SarA. Relative amounts of SarA were assessed by western blot. Graphs illustrate quantitative results from three separate blots. Single asterisk indicates statistical significance by comparison to the LAC parent strain ($P < 0.05$).

These results demonstrate a correlation between increased protease production and decreased biofilm in all biofilm-deficient mutants other than the *atl* mutant. It has been suggested that the autolysin encoded by *atl* facilitates the initial attachment stage of biofilm formation both directly by functioning as an adhesin, and indirectly by promoting the release of eDNA, with FnbA and FnbB subsequently being required for biofilm maturation, particularly in methicillin-resistant *S. aureus* (MRSA) strains (Houston et al. 2011). The fibronectin-binding proteins are recognized targets of protease-mediated degradation in *sarA* mutants (Karlsson et al. 2001; Mrak et al. 2012), but in this scenario relative levels of protease production would presumably be irrelevant owing to the reduced capacity of an *atl* mutant to initiate the process of biofilm formation. Even so, increased protease production would be relevant in an *atl/sarA* mutant because it would limit FnbA/FnbB-associated accumulation. This provides a likely explanation for why concomitant mutation of *sarA* further reduced biofilm formation in the *atl* mutant, par-

Figure 5. Impact of extracellular proteases in LAC. (A) Total protease activity was assessed in LAC mutants with (−) and without (+) concomitant mutation of *sarA*. Results shown represent the average ± SEM from a minimum of two experiments, each of which was repeated with at least four replicates. Single asterisk indicates statistical significance of the individual mutants by comparison to the LAC parent strain (*P* < 0.05). Double asterisks indicate significance of the double mutant relative to the appropriate isogenic single mutant (*P* < 0.05). (B) Biofilm formation was assessed in LAC and its regulatory mutants as a function of the relative capacity to produce extracellular proteases. Protease positive refers to strains with the capacity to produce all extracellular proteases. Protease deficient refers to strains unable to produce aureolysin, SspA, SspB, and ScpA. Results shown represent the average ± SEM from a minimum of two experiments, each of which was repeated with at least six replicates. Asterisk indicates statistical significance of protease-deficient derivatives relative to the respective isogenic protease-positive strains (*P* < 0.05).

ticularly since protease activity was increased in the *atl/sarA* mutant by comparison to both the isogenic *atl* mutant and LAC itself (Fig 5). Mutation of *sarA* has also been shown to result in reduced accumulation of Atl itself owing to protease-mediated degradation (Zielinska et al. 2012), but this is unlikely to play a primary role in defining the biofilm-deficient phenotype of an *atl/sarA* mutant because, if it did, mutation of *sarA* would not further decrease biofilm formation by comparison to an *atl* mutant (Fig. 3).

Mutation of *mgrA* or *fur* also had no impact on protease production by comparison to LAC (Fig. 5). However, limiting the production of proteases did enhance biofilm formation in the *mgrA* mutant. To the extent that concomitant mutation of *sarA* in the *mgrA* mutant also resulted in increased protease production by comparison to the isogenic *mgrA* mutant, this also provides a likely explanation for why concomitant mutation of *sarA* reversed the increased capacity of the *mgrA* mutant to form a biofilm (Fig. 3). Mutation of *sarA* also reversed the increased biofilm formation observed in the LAC *fur* mutant (Fig. 3), and resulted in a statistically significant increase in protease production, but the relative capacity of the *fur* mutant to form a biofilm under our assay conditions was not altered to a statistically significant extent

by limiting the production of extracellular proteases (Fig. 5). This suggests the involvement of other factors in defining the enhanced biofilm phenotype of a LAC *fur* mutant.

Mutation of *fur* in the commonly studied strain Newman, which notably does not produce surface-anchored fibronectin-binding proteins (Grundmeier et al. 2004), also enhanced biofilm formation under iron-limiting conditions, but only during the early stages of biofilm formation (Johnson et al. 2005). The mechanistic basis for these phenotypes was not explained although it appeared to be independent of any impact on accumulation of the PIA. To the extent that our assays were done using a nutrient-rich medium, and the results assayed after a 24 h incubation period, the increased capacity of the LAC *fur* mutant to form a biofilm under our assay conditions is in contrast to this report, although we did confirm that mutation of *fur* had no detectable impact on the accumulation of PIA in LAC (see below). A previous paper described a number of conserved surface Fur-regulated proteins (Frp) and suggested that at least two of these (FrpA and FrpB) are involved in the initial attachment stage of biofilm formation (Morrissey et al. 2002). Since Fur represses the production of these proteins in the presence of iron, one could hypothesize that mutation

of *fur* would result in an increase in Frp expression and consequently biofilm formation. Eap and Emp have also been implicated in biofilm formation (Palma et al. 1999; Hussain et al. 2001), but both of these are positively regulated by Fur at least under iron-restricted conditions, thus suggesting that they would be produced in decreased amounts in a *fur* mutant (Johnson et al. 2008).

Impact of extracellular nuclease production on biofilm formation

The results discussed above demonstrate an important role for extracellular proteases in defining the biofilm phenotype of most but not all of the regulatory mutants we examined. To determine whether the production of extracellular nucleases may account for at least some of these exceptions, we also assessed nuclease activity using a FRET-based assay (Kiedrowski et al. 2014). The only mutants that exhibited a significant increase in nuclease activity were the *rsbU* and *sigB* mutants (Fig. 6). This raises the possibility that this also contributes to the biofilm-deficient phenotype of these mutants. However, limiting protease production enhanced biofilm formation in both of these mutants (Fig. 3). Additionally, mutation of

sarA reversed the increase in nuclease production in the *rsbU* and *sigB* mutants (Fig. 6), and this was correlated with a further decrease, rather than an increase, in biofilm formation (Fig. 1). Indeed, mutation of *sarA* resulted in reduced nuclease activity in LAC, and we confirmed that this is reversed by eliminating the ability of *sarA* mutants to produce extracellular proteases (Fig. 6), thus demonstrating that the impact of *sarA* on nuclease activity in LAC occurs via an indirect mechanism involving protease-mediated degradation. More importantly, biofilm formation was increased in a protease-deficient *sarA* mutant (Fig. 5) despite the increase in nuclease activity (Fig. 6). Taken together, these results suggest that the increased production of proteases plays the more important role, by comparison to the increased production of extracellular nucleases, in defining the biofilm-deficient phenotype of *sarA*, *rsbU* and *sigB* mutants.

Nuclease activity was unchanged in *atl*, *fur*, or *mgrA* mutants (Fig. 6), but this does not preclude a role for eDNA in at least some of these mutants. In fact, in some cases the more relevant consideration may be that nuclease production was not increased. For instance, Trotonda et al. (2008) proposed that mutation of *mgrA* increases expression of *cidA* and decreases expression of *lrgAB*, the
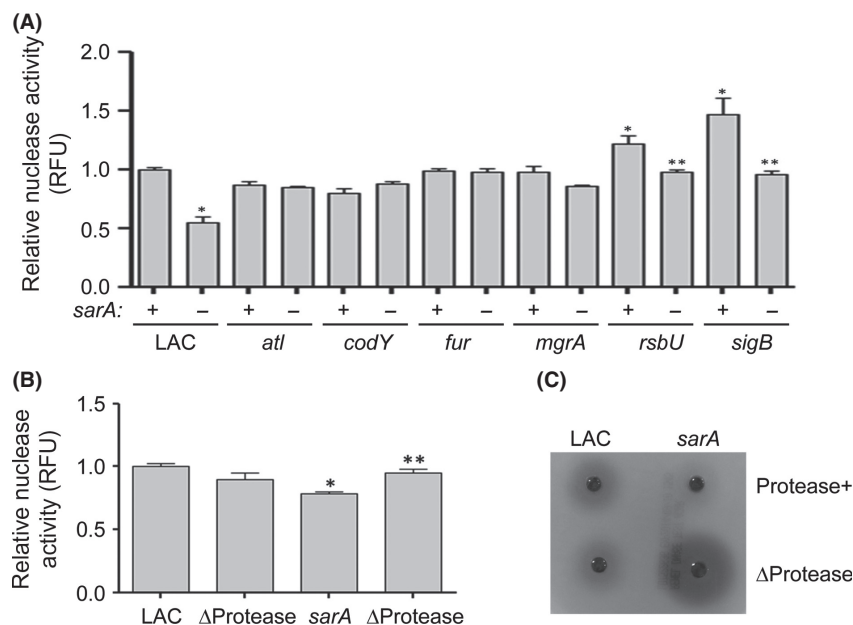
Figure 6. Impact of extracellular nucleases in LAC. (A) Total nuclease activity was assessed in LAC regulatory mutants with (−) and without (+) concomitant mutation of *sarA* using a FRET-based assay. Results shown represent the average ± SEM from a minimum of two experiments, each of which was repeated with at least four replicates. Single asterisk indicates statistical significance of the individual mutants by comparison to the LAC parent strain (*P* < 0.05). Double asterisks indicate significance of the double mutant relative to the corresponding isogenic single mutant (*P* < 0.05). (B) Relative levels of nuclease activity were assessed as above, but as a function of the production of extracellular proteases. Single asterisk indicates statistical significance of the individual mutants by comparison to the LAC parent strain (*P* < 0.05). Double asterisks indicate significance of the *sarA*/ΔProtease mutant relative to the corresponding isogenic *sarA* mutant (*P* < 0.05). (C) For comparison, relative levels of nuclease activity were also assessed using DNase Agar assay.

combined result of which is increased autolysis and increased availability of eDNA, and under these circumstances it is potentially important that mutation of *mgrA* did not result in increased nuclease activity. This same report also found that mutation of *sarA* reversed the increased biofilm formation observed in the *mgrA* mutant, but it was concluded that this was independent of the increased production of aureolysin or SspA (Trotonda et al. 2008). However, this report examined the impact of these proteases independently of each other, and our studies confirm that the impact of *sarA* on biofilm formation involves the increased production of multiple proteases (Loughran et al. 2014). In the case of the *atl* mutant, nuclease production would presumably be irrelevant owing to the reduced availability of eDNA as detailed above. In the case of *fur*, there is a report demonstrating that the mutation of *fur* represses expression of the genes encoding extracellular nucleases (Johnson et al. 2011), and this would presumably promote biofilm formation. Mutation of *fur* did enhance biofilm formation in LAC under the experimental conditions we employed, but the fact that nuclease production was unchanged in the LAC *fur* mutant suggests that extracellular nucleases cannot account for this phenotype. It is also important to recognize that the impact of *fur* on *S. aureus* phenotypes is dependent to a large extent on iron availability (Morrissey et al. 2002; Johnson et al. 2011), and we have not yet addressed this issue.

Impact of PIA production on biofilm formation

We next assessed whether production of the PIA (also known as poly-*N*-acetyl-*β*-(1–6)-glucosamine or PNAG) might contribute to the biofilm phenotypes we observed. This was complicated by the fact that we could not detect appreciable amounts of PIA in immunoblots with LAC or any of its mutants (Fig. 7). As an alternative approach, we examined the impact of Dispersin B, a known inhibitor of PIA-mediated biofilm formation (Donelli et al. 2007; Sugimoto et al. 2013). The only strains in which Dispersin B had a significant impact were the *rsbU* and *sigB* mutants, and in both cases biofilm formation was increased rather than decreased in the presence of Dispersin B (Fig. 7). Although the reasons PIA would limit biofilm formation remain unclear, we have observed this phenotype before (Loughran et al. 2014), and it is generally consistent with the suggestion that biofilm formation in *S. aureus*, particularly in MRSA strains such as LAC, is largely independent of PIA production (O'Neill et al. 2008; Pozzi et al. 2012). Indeed, one possible explanation for the increase in biofilm formation observed in LAC in the presence of Dispersin B is that the abundance of PIA, or other exopolysaccharides, was reduced to the point of increasing the exposure of surface proteins that promote biofilm formation.

Impact of select mutations in UAMS-1

The results discussed above are consistent with the following conclusions: (1) *sarA* plays a primary role in *S. aureus* biofilm formation in the USA300 strain LAC owing to its ability to repress the production of extracellular proteases; (2) protease production also plays an important role in limiting biofilm formation in *rsbU*, *sigB*, and *codY* mutants; (3) in those cases in which this is not the case, including those in which a mutation is associated with an enhanced capacity to form a biofilm, the impact of *sarA* on biofilm formation is epistatic to the impact of these other regulatory loci. However, these studies were limited to the MRSA strain LAC, and as noted above, it has been suggested that the mechanism of
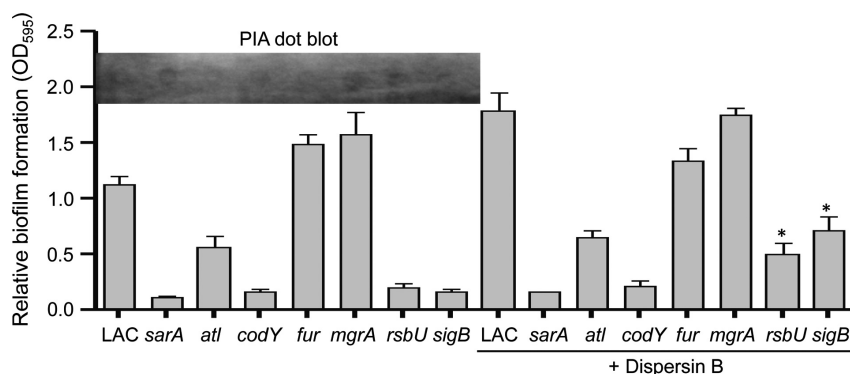
Figure 7. Impact of PIA in LAC. Biofilm formation was assessed using a microtiter plate assay with and without the addition of Dispersin B. Results shown represent the average ± SEM from a minimum of two experiments, each of which was repeated with at least three replicates. Asterisks indicate mutants in which the addition of Dispersin B had a statistically significant impact by comparison to the same strain in the absence of Dispersin B ($P < 0.05$). Inset illustrates levels of PIA production in LAC and its indicated isogenic mutants in the absence of Dispersin B.
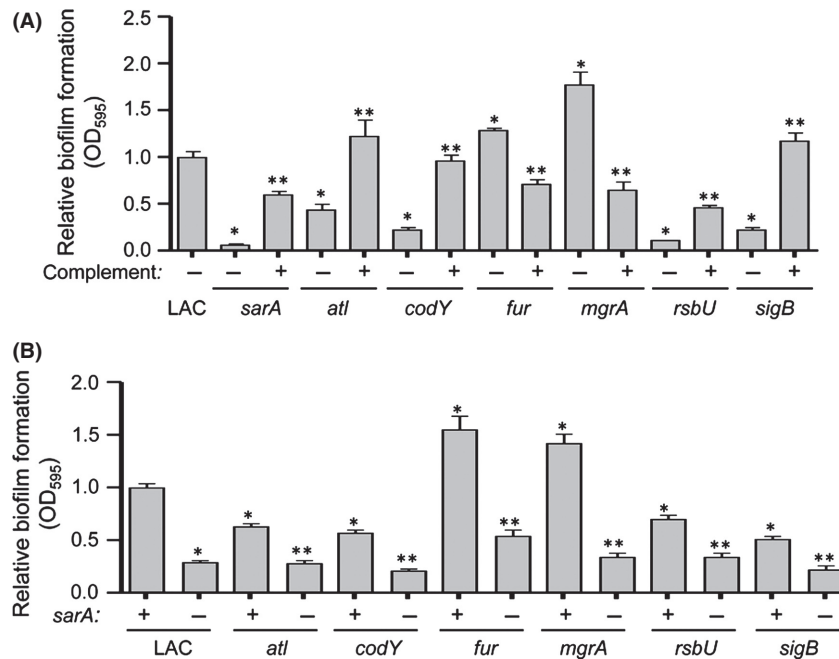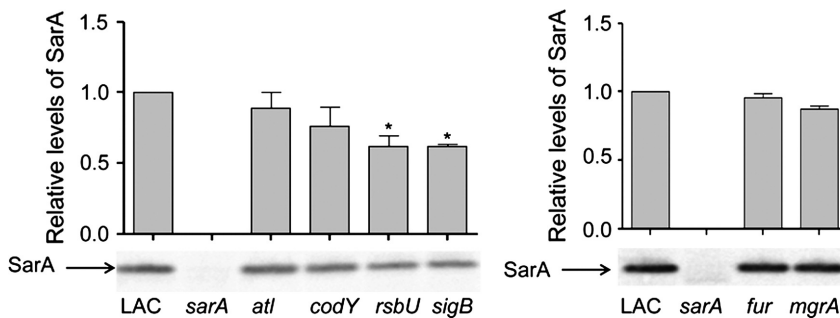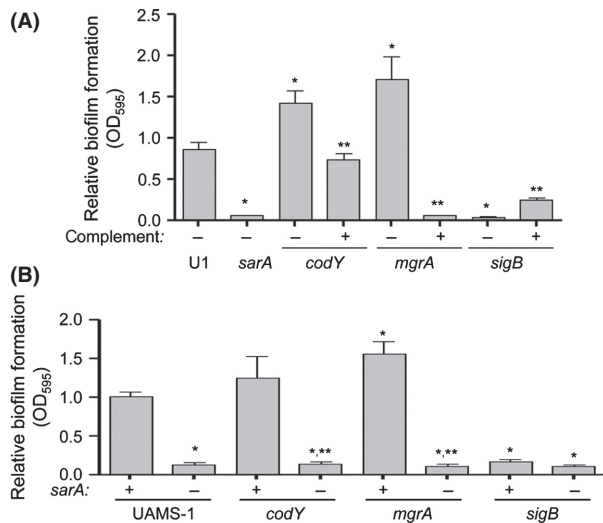
Figure 8. Relative impact of *sarA* versus other regulatory loci in UAMS-1. (A) Biofilm formation was assessed in each regulatory mutant found to have a significant impact on biofilm formation with (+) and without (−) plasmid-based genetic complementation. Results shown represent the average ± SEM from a minimum of three experiments, each of which was repeated with at least three replicates. Single asterisk indicates that the results observed with the indicated mutant were significantly different from those observed with the UAMS-1 (U1) parent strain (*P* < 0.05). Double asterisks indicate that the results observed with the complemented strain were significantly different by comparison to those observed with the uncomplemented isogenic mutant (*P* < 0.05). (B) Biofilm formation was assessed in each regulatory mutant found to have a significant impact on biofilm formation with (−) and without (+) concomitant mutation of *sarA*. Single asterisk indicates statistical significance of the individual mutants by comparison to the UAMS-1 parent strain (*P* < 0.05). Double asterisks indicate significance of the double mutant relative to the corresponding isogenic single mutant (*P* < 0.05).

biofilm formation differs as a function of methicillin resistance (Houston et al. 2011). We therefore examined the impact of a subset of these mutations in the MSSA strain UAMS-1. These studies were limited by difficulties in transducing mutations from the JE2 NTML derivatives, or their LAC transductants, into UAMS-1, but we had previously generated *codY*, *mgrA*, and *sigB* mutations in both UAMS-1 and its isogenic *sarA* mutant. Mutation of *sigB* and *mgrA* was found to have the same impact on biofilm formation in UAMS-1 and LAC (i.e., decreased in the former and increased in the latter). Similarly, Bose et al. (2012) previously demonstrated that mutation of *atl* limits biofilm formation in UAMS-1. Thus, the same general trends were observed in the context of these loci in both UAMS-1 and LAC.

In contrast, mutation of *codY* in UAMS-1 increased rather than decreased biofilm formation (Fig. 8). Our results are consistent with a previous report demonstrating that mutation of *codY* increased biofilm formation in UAMS-1, a phenotype that was attributed to the increased production of PIA (Majerczyk et al. 2008). This possibility is consistent with the observation that protease activity was not significantly increased in a UAMS-1 *codY* mutant (Fig. 9). Mutation of *codY* in UAMS-1 did result in increased nuclease activity (Fig. 10), which is interesting given that it had the opposite effect in LAC, but this is unlikely to be important in that a UAMS-1 *codY* mutant had an increased capacity to form a biofilm. Additionally, Dispersin B limited biofilm formation not only in a UAMS-1 *codY* mutant, but also in the isogenic *mgrA* mutant (Fig. 11). This implicates PIA production in the biofilm phenotype of both of these mutants. This was confirmed by demonstrating the PIA production was increased in both UAMS-1 *codY* and *mgrA* mutants (Fig. 11).
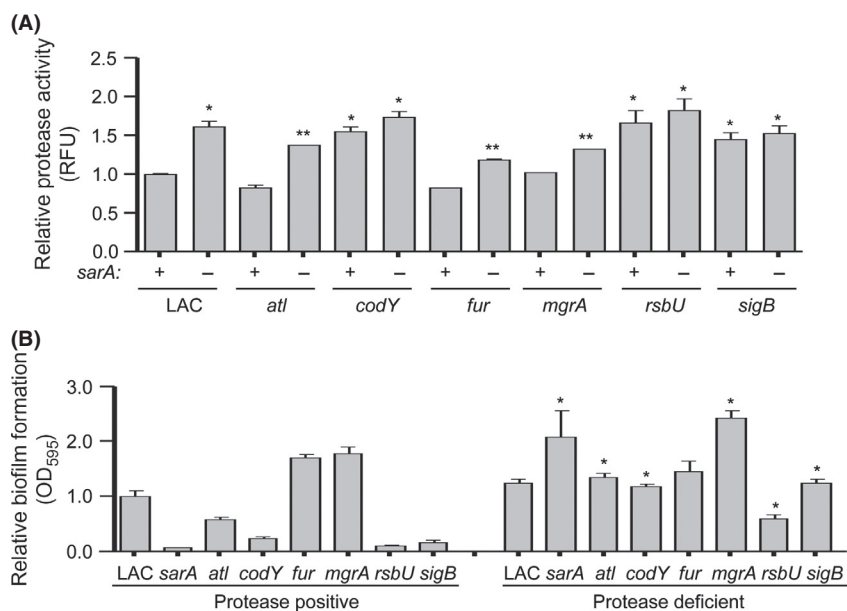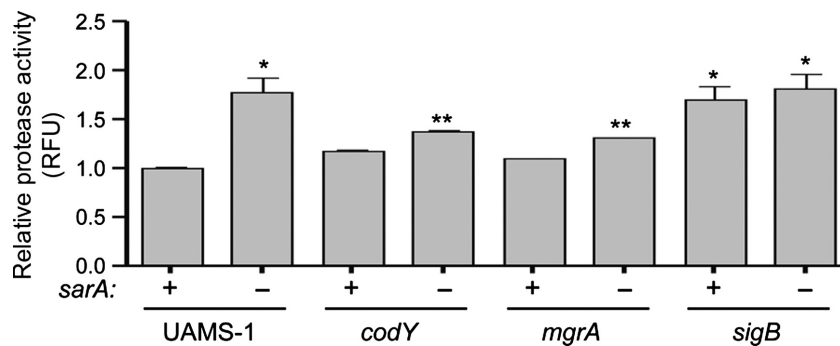

Figure 9. Impact of extracellular proteases in UAMS-1. Total protease activity was assessed in UAMS-1 mutants with (−) and without (+) concomitant mutation of *sarA*. Results shown represent the average ± SEM from a minimum of two experiments, each of which was repeated with at least four replicates. Single asterisk indicates statistical significance by comparison to the UAMS-1 parent strain (*P* < 0.05). Double asterisks indicate significance of the double mutant relative to the corresponding isogenic single mutant (*P* < 0.05).
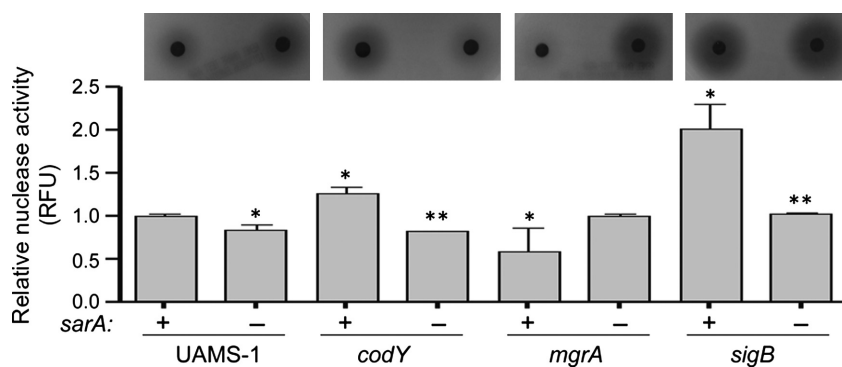
Figure 10. Impact of extracellular nucleases in UAMS-1. Total nuclease activity was assessed in UAMS-1 and its isogenic mutants with (−) and without (+) concomitant mutation of *sarA* using a FRET-based assay. Results shown represent the average ± SEM from a minimum of two experiments, each of which was repeated with at least four replicates. Single asterisk indicates statistical significance by comparison to the isogenic parent strain ($P < 0.05$). Double asterisks indicate significance of the double mutant relative to the respective isogenic single mutant ($P < 0.05$). Inset illustrates results observed using DNase agar.

Concomitant mutation of *sarA* reversed both the increased production of PIA (Fig. 11) and increased the capacity of *codY* and *mgrA* mutants to form a biofilm (Fig. 8). This suggests a cause-and-effect relationship. However, the limitation of PIA production observed in UAMS-1 *codY/sarA* and *mgrA/sarA* mutants relative to their isogenic *codY* and *mgrA* mutants was modest by comparison to the biofilm phenotypes of these mutants, and the level of PIA production was comparable in UAMS-1 and its *sarA* mutant (Fig. 11) despite their dramatically different biofilm phenotypes (Fig. 8). These results confirm that *sarA* plays a defining role in both the MRSA strain LAC and the MSSA strain UAMS-1 and that, in both strains, the primary phenotypic impact of *sarA* is a function of its impact on the production of extracellular proteases. Further support for this hypothesis comes from the observations that biofilm formation was limited in mixed culture assays consisting of either LAC or UAMS-1 together with *sarA* mutants generated in either strain (Fig. 12). Additionally, coculture with the LAC *sarA* mutant limited biofilm formation in both LAC and UAMS-1 to a lesser degree than co-culture with the UAMS-1 *sarA* mutant, which is consistent with the observation that mutation of *sarA* resulted in a greater increase in protease production in UAMS-1 than in LAC (Fig. 12).

These results provide further support for the importance of limiting protease production as a means of promoting biofilm formation in both the MRSA strain LAC and the MSSA strain UAMS-1. Nevertheless, they also reveal an important strain-dependent difference in the context of *codY*. To investigate this further, we transduced the *codY* mutation into additional clinical isolates and examined the impact on biofilm formation. We were limited in this case, owing to antibiotic resistance issues in
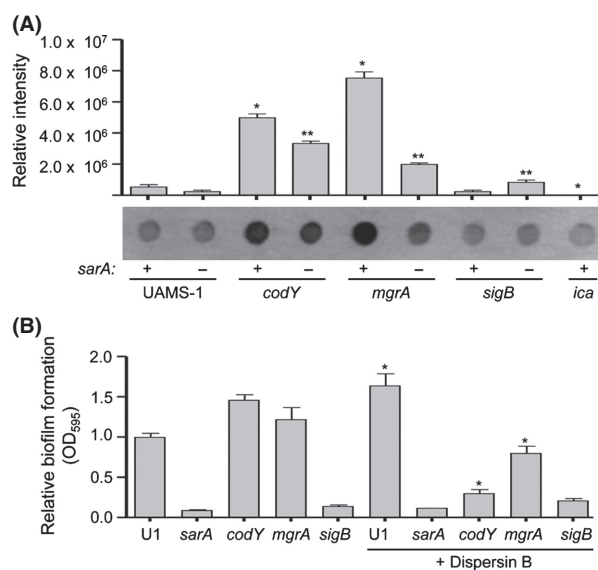
Figure 11. Impact of PIA in UAMS-1. (A) PIA production as assessed by dot blot. Graph illustrates quantitative results obtained from three independent blots, with a representative dot blot shown below the graph. Single asterisk indicates statistical significance by comparison to the isogenic UAMS-1 (U1) parent strain ($P < 0.05$). Double asterisks indicate significance of the double mutant relative to the appropriate isogenic single mutant ($P < 0.05$). (B) Biofilm formation was assessed with and without Dispersin B. Results shown represent the average ± SEM from a minimum of two experiments, each of which was repeated with at least three replicates. Asterisk indicates mutants in which the addition of Dispersin B had a statistically significant impact by comparison to the same strain in the absence of Dispersin B ($P < 0.05$).

the targeted clinical isolates, but we were able to successfully transduce this mutation into three additional MRSA strains and one additional MSSA strain. Biofilm formation was reduced in the *codY* mutants generated in all
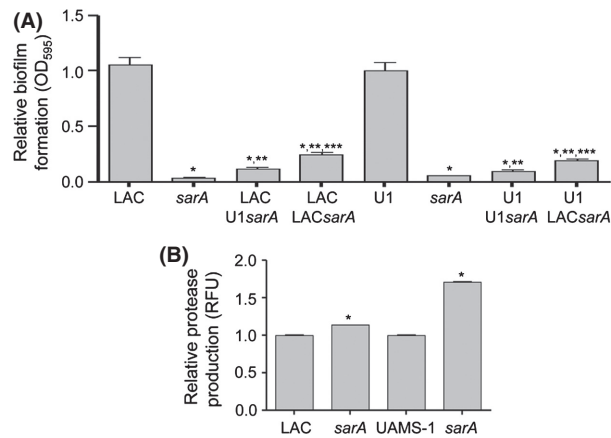
Figure 12. Impact of *sarA* mutants on wild-type biofilm phenotypes. (A) Biofilm formation was assessed in LAC or UAMS-1 (U1) after coculture with the indicated *sarA* mutants, with each parent strain and its isogenic *sarA* mutant included as controls. Results shown represent the average ± SEM from a minimum of three experiments, each of which was repeated with at least three replicates. Single asterisk indicates statistical significance by comparison to the respective parent strain ($P < 0.05$). Double asterisks indicate statistical significance by comparison to the isogenic *sarA* mutant ($P < 0.05$). Triple asterisks indicate a statistically significant difference between results observed with the LAC *sarA* mutant by comparison to the UAMS-1 *sarA* mutant ($P < 0.05$). (B) Total protease activity was assessed in LAC, its isogenic *sarA* mutant, UAMS-1, and its isogenic *sarA* mutant. WT parent strains, LAC, and UAMS-1, were set to 1.0 with the respective *sarA* mutants set relative to that. Results shown represent the average ± SEM from a minimum of two experiments, each of which was repeated with at least four replicates. Single asterisk indicates statistical significance by comparison to the respective parent strain ($P < 0.05$).

Figure 13. Strain-dependent impact of *codY* on biofilm formation. The impact of mutating *codY* on biofilm formation was assessed as a function of methicillin resistance status, with the strains shown in the upper panel being MRSA isolates, and those shown in the lower panel being MSSA isolates. Results shown represent the average ± SEM from a minimum of two experiments, each of which was repeated with at least six replicates. Asterisk indicates statistical significance by comparison to the respective parent strain ($P < 0.05$).

three MRSA strains and increased in the additional MSSA strain (Fig. 13). This suggests that the differential impact of mutating *codY* on biofilm formation may be directly correlated with methicillin resistance status, and that this is likely a function of the impact of mutating *codY* on the production of PIA. However, there are contradictory reports in the literature regarding the impact of *codY* on biofilm formation, with Majerczyk et al. (2008) concluding as we observed that mutation of *codY* in UAMS-1 enhances biofilm formation, and Tu Quoc et al. (2007) concluding that mutation of *codY* in the *S. aureus* strain S30 has the opposite effect, and both of these are methicillin-sensitive strains. Thus, this potential correlation warrants further study and is an area of active investigation in our laboratory.

Conclusion

In summary, the only mutation we identified that significantly impacts biofilm formation in a manner that could not be correlated with protease or PIA production is the LAC *fur* mutant, and even in this case mutation of *sarA* reversed the phenotypic impact of mutating *fur*. Thus, our results confirm the primary importance of *sarA* in the context of biofilm-associated *S. aureus* infections. Based on this, we believe the results we report strongly support the hypothesis that inhibitors of *sarA*-mediated regulation would have tremendous potential in the context of overcoming the pathology and therapeutic recalcitrance of these infections owing to their ability to increase the production of extracellular proteases, and that this would be true irrespective of the functional status of other *S. aureus* regulatory loci.

Acknowledgments

Research Institute (UL1TR000039) through the NIH National Center for Research Resources and National Center for Advancing Translational Sciences. The content is solely the responsibility of the authors and does not necessarily represent the views of the NIH.

Conflict of Interest

None declared.

References

Abdelhady, W., A. S. Bayer, K. Seidl, D. E. Moormeier, K. W. Bayles, A. Cheung, et al. 2014. Impact of vancomycin on sarA-mediated biofilm formation: role in persistent endovascular infections due to methicillin-resistant *Staphylococcus aureus*. J. Infect. Dis. 209:1231–1240.

Beenken, K. E., J. S. Blevins, and M. S. Smeltzer. 2003. Mutation of sarA in *Staphylococcus aureus* limits biofilm formation. Infect. Immun. 71:4206–4211.

Beenken, K. E., P. M. Dunman, F. McAleese, D. Macapagal, E. Murphy, S. J. Projan, et al. 2004. Global gene expression in *Staphylococcus aureus* biofilms. J. Bacteriol. 186:4665–4684.

Beenken, K. E., L. N. Mrak, L. M. Griffin, A. K. Zielinska, L. N. Shaw, K. C. Rice, et al. 2010. Epistatic relationships between sarA and agr in *Staphylococcus aureus* biofilm formation. PLoS ONE 5:e10790.

Beenken, K. E., H. Spencer, L. M. Griffin, and M. S. Smeltzer. 2012. Impact of extracellular nuclease production on the biofilm phenotype of *Staphylococcus aureus* under in vitro and in vivo conditions. Infect. Immun. 80:1634–1638.

Beenken, K. E., L. N. Mrak, A. K. Zielinska, D. N. Atwood, A. J. Loughran, L. M. Griffin, et al. 2014. Impact of the functional status of saeRS on in vivo phenotypes of *Staphylococcus aureus* sarA mutants. Mol. Microbiol. 92:1299–1312.

Bischoff, M., J. M. Entenza, and P. Giachino. 2001. Influence of a functional sigB operon on the global regulators sar and agr in *Staphylococcus aureus*. J. Bacteriol. 183:5171–5179.

Bjarnsholt, T., O. Ciofu, S. Molin, M. Givskov, and N. Hoiby. 2013. Applying insights from biofilm biology to drug development - can a new approach be developed? Nat. Rev. Drug Discov. 12:791–808.

Blevins, J. S., A. F. Gillaspy, T. M. Rechtin, B. K. Hurlburt, and M. S. Smeltzer. 1999. The Staphylococcal accessory regulator (sar) represses transcription of the *Staphylococcus aureus* collagen adhesin gene (cna) in an agr-independent manner. Mol. Microbiol. 33:317–326.

Bose, J. L., M. K. Lehman, P. D. Fey, and K. W. Bayles. 2012. Contribution of the *Staphylococcus aureus* Atl AM and GL murein hydrolase activities in cell division, autolysis, and biofilm formation. PLoS ONE 7:e42244.

Bose, J. L., P. D. Fey, and K. W. Bayles. 2013. Genetic tools to enhance the study of gene function and regulation in *Staphylococcus aureus*. Appl. Environ. Microbiol. 79:2218–2224.

Brady, R. A., J. G. Leid, J. H. Calhoun, J. W. Costerton, and M. E. Shirtliff. 2008. Osteomyelitis and the role of biofilms in chronic infection. FEMS Immunol. Med. Microbiol. 52:13–22.

Bubeck Wardenburg, J., W. A. Williams, and D. Missiakas. 2006. Host defenses against *Staphylococcus aureus* infection require recognition of bacterial lipoproteins. Proc. Natl Acad. Sci. USA 103:13831–13836.

Cassat, J., P.M. Dunman, E. Murphy, S.J. Projan, K.E. Beenken, K.J. Palm, et al. 2006. Transcriptional profiling of a *Staphylococcus aureus* clinical isolate and its isogenic agr and sarA mutants reveals global differences in comparison to the laboratory strain RN6390. Microbiology (Reading, England) 152: 3075–3090.

Cassat, J. E., N. D. Hammer, J. P. Campbell, M. A. Benson, D. S. Perrien, L. N. Mrak, et al. 2013. A secreted bacterial protease tailors the *Staphylococcus aureus* virulence repertoire to modulate bone remodeling during osteomyelitis. Cell Host Microbe 13:759–772.

Cheung, A. L., K. A. Nishina, M. P. Trotonda, and S. Tamber. 2008. The SarA protein family of *Staphylococcus aureus*. Int. J. Biochem. Cell Biol. 40:355–361.

Donelli, G., I. Francolini, D. Romoli, E. Guaglianone, A. Piozzi, C. Ragunath, et al. 2007. Synergistic activity of dispersin B and cefamandole nafate in inhibition of staphylococcal biofilm growth on polyurethanes. Antimicrob. Agents Chemother. 51:2733–2740.

Fey, P.D., J.L. Endres, V.K. Yajjala, T.J. Widhelm, R.J. Boissy, J.L. Bose, et al. 2013. A genetic resource for rapid and comprehensive phenotype screening of nonessential *Staphylococcus aureus* genes. mBio 4: e00537–12.

Francois, P., P. Vaudaux, N. Nurdin, H. J. Mathieu, P. Descouts, and D. P. Lew. 1996. Physical and biological effects of a surface coating procedure on polyurethane catheters. Biomaterials 17:667–678.

Gotz, F. 2002. Staphylococcus and biofilms. Mol. Microbiol. 43:1367–1378.

Grundmeier, M., M. Hussain, P. Becker, C. Heilmann, G. Peters, and B. Sinha. 2004. Truncation of fibronectin-binding proteins in *Staphylococcus aureus* strain Newman leads to deficient adherence and host cell invasion due to loss of the cell wall anchor function. Infect. Immun. 72:7155–7163.

Houston, P., S. E. Rowe, C. Pozzi, E. M. Waters, and J. P. O'Gara. 2011. Essential role for the major autolysin in the fibronectin-binding protein-mediated *Staphylococcus aureus* biofilm phenotype. Infect. Immun. 79:1153–1165.

Hussain, M., K. Becker, C. von Eiff, J. Schrenzel, G. Peters, and M. Herrmann. 2001. Identification and characterization of a novel 38.5-kilodalton cell surface protein of

Staphylococcus aureus with extended-spectrum binding activity for extracellular matrix and plasma proteins. J. Bacteriol. 183:6778–6786.

Ibarra, J. A., E. Perez-Rueda, R. K. Carroll, and L. N. Shaw. 2013. Global analysis of transcriptional regulators in *Staphylococcus aureus*. BMC Genom. 14:126.

Johnson, M., A. Cockayne, P. H. Williams, and J. A. Morrissey. 2005. Iron-responsive regulation of biofilm formation in *staphylococcus aureus* involves fur-dependent and fur-independent mechanisms. J. Bacteriol. 187:8211–8215.

Johnson, M., A. Cockayne, and J. A. Morrissey. 2008. Iron-regulated biofilm formation in *Staphylococcus aureus* Newman requires ica and the secreted protein Emp. Infect. Immun. 76:1756–1765.

Johnson, M., M. Sengupta, J. Purves, E. Tarrant, P. H. Williams, A. Cockayne, et al. 2011. Fur is required for the activation of virulence gene expression through the induction of the sae regulatory system in *Staphylococcus aureus*. IJMM 301:44–52.

Karlsson, A., P. Saravia-Otten, K. Tegmark, E. Morfeldt, and S. Arvidson. 2001. Decreased amounts of cell wall-associated protein A and fibronectin-binding proteins in *Staphylococcus aureus* sarA mutants due to up-regulation of extracellular proteases. Infect. Immun. 69:4742–4748.

Kiedrowski, M. R., H. A. Crosby, F. J. Hernandez, C. L. Malone, J. O. II McNamara, and A. R. Horswill. 2014. *Staphylococcus aureus* Nuc2 is a functional, surface-attached extracellular nuclease. PLoS ONE 9:e95574.

Klein, E. Y., L. Sun, D. L. Smith, and R. Laxminarayan. 2013. The changing epidemiology of methicillin-resistant *Staphylococcus aureus* in the United States: a national observational study. Am. J. Epidemiol. 177:666–674.

Lewis, K. 2008. Multidrug tolerance of biofilms and persister cells. Curr. Top. Microbiol. Immunol. 322:107–131.

Loughran, A. J., D. N. Atwood, A. C. Anthony, N. S. Harik, H. J. Spencer, K. E. Beenken, et al. 2014. Impact of individual extracellular proteases on *Staphylococcus aureus* biofilm formation in diverse clinical isolates and their isogenic sarA mutants. MicrobiologyOpen 3:897–909.

Luong, T.T., and C.Y. Lee. 2006. The arl locus positively regulates *Staphylococcus aureus* type 5 capsule via an mgrA-dependent pathway. Microbiology (Reading, England) 152:3123–3131.

Luong, T. T., K. Sau, C. Roux, S. Sau, P. M. Dunman, and C. Y. Lee. 2011. *Staphylococcus aureus* ClpC divergently regulates capsule via sae and codY in strain newman but activates capsule via codY in strain UAMS-1 and in strain Newman with repaired saeS. J. Bacteriol. 193:686–694.

Majerczyk, C. D., M. R. Sadykov, T. T. Luong, C. Lee, G. A. Somerville, and A. L. Sonenshein. 2008. *Staphylococcus aureus* CodY negatively regulates virulence gene expression. J. Bacteriol. 190:2257–2265.

Morrissey, J. A., A. Cockayne, J. Hammacott, K. Bishop, A. Denman-Johnson, P. J. Hill, et al. 2002. Conservation, surface exposure, and in vivo expression of the Frp family of iron-regulated cell wall proteins in *Staphylococcus aureus*. Infect. Immun. 70:2399–2407.

Mrak, L. N., A. K. Zielinska, K. E. Beenken, I. N. Mrak, D. N. Atwood, L. M. Griffin, et al. 2012. saeRS and sarA act synergistically to repress protease production and promote biofilm formation in *Staphylococcus aureus*. PLoS ONE 7: e38453.

O'Neill, E., C. Pozzi, P. Houston, H. Humphreys, D. A. Robinson, A. Loughman, et al. 2008. A novel *Staphylococcus aureus* biofilm phenotype mediated by the fibronectin-binding proteins, FnBPA and FnBPB. J. Bacteriol. 190:3835–3850.

Palma, M., A. Haggar, and J. I. Flock. 1999. Adherence of *Staphylococcus aureus* is enhanced by an endogenous secreted protein with broad binding activity. J. Bacteriol. 181:2840–2845.

Pane-Farre, J., B. Jonas, S. W. Hardwick, K. Gronau, R. J. Lewis, M. Hecker, et al. 2009. Role of RsbU in controlling SigB activity in *Staphylococcus aureus* following alkaline stress. J. Bacteriol. 191:2561–2573.

Pozzi, C., E. M. Waters, J. K. Rudkin, C. R. Schaeffer, A. J. Lohan, P. Tong, et al. 2012. Methicillin resistance alters the biofilm phenotype and attenuates virulence in *Staphylococcus aureus* device-associated infections. PLoS Pathog. 8:e1002626.

Priest, N. K., J. K. Rudkin, E. J. Feil, J. M. van den Elsen, A. Cheung, S. J. Peacock, et al. 2012. From genotype to phenotype: can systems biology be used to predict *Staphylococcus aureus* virulence? *Nature reviews*. Microbiology 10:791–797.

Prigent-Combaret, C., O. Vidal, C. Dorel, and P. Lejeune. 1999. Abiotic surface sensing and biofilm-dependent regulation of gene expression in *Escherichia coli*. J. Bacteriol. 181:5993–6002.

Steckelberg, J.M., and D. R. Osmon. 1994. Prosthetic joint infections. Pp. 259–290 In A. L. Bisno, F. A. Waldvogel, ed. Infections associated with indwelling medical devices. ASM Press, Washington, DC.

Sugimoto, S., T. Iwamoto, K. Takada, K. Okuda, A. Tajima, T. Iwase, et al. 2013. Staphylococcus epidermidis Esp degrades specific proteins associated with *Staphylococcus aureus* biofilm formation and host-pathogen interaction. J. Bacteriol. 195:1645–1655.

Torres, V. J., A. S. Attia, W. J. Mason, M. I. Hood, B. D. Corbin, F. C. Beasley, et al. 2010. *Staphylococcus aureus* fur regulates the expression of virulence factors that contribute to the pathogenesis of pneumonia. Infect. Immun. 78:1618–1628.

Trotonda, M. P., S. Tamber, G. Memmi, and A. L. Cheung. 2008. MgrA represses biofilm formation in *Staphylococcus aureus*. Infect. Immun. 76:5645–5654.

Tsang, L. H., J. E. Cassat, L. N. Shaw, K. E. Beenken, and M. S. Smeltzer. 2008. Factors contributing to the biofilm-deficient phenotype of *Staphylococcus aureus* sarA mutants. PLoS ONE 3:e3361.

Tu Quoc, P. H., P. Genevaux, M. Pajunen, H. Savilahti, C. Georgopoulos, J. Schrenzel, et al. 2007. Isolation and characterization of biofilm formation-defective mutants of *Staphylococcus aureus*. Infect. Immun. 75:1079–1088.

Valle, J., A. Toledo-Arana, C. Berasain, J. M. Ghigo, B. Amorena, J. R. Penades, et al. 2003. SarA and not sigmaB is essential for biofilm development by *Staphylococcus aureus*. Mol. Microbiol. 48:1075–1087.

Wang, R., K. R. Braughton, D. Kretschmer, T. H. Bach, S. Y. Queck, M. Li, et al. 2007. Identification of novel cytolytic peptides as key virulence determinants for community-associated MRSA. Nat. Med. 13:1510–1514.

Weiss, E. C., H. J. Spencer, S. J. Daily, B. D. Weiss, and M. S. Smeltzer. 2009a. Impact of sarA on antibiotic susceptibility of *Staphylococcus aureus* in a catheter-associated in vitro model of biofilm formation. Antimicrob. Agents Chemother. 53:2475–2482.

Weiss, E. C., A. Zielinska, K. E. Beenken, H. J. Spencer, S. J. Daily, and M. S. Smeltzer. 2009b. Impact of sarA on daptomycin susceptibility of *Staphylococcus aureus* biofilms in vivo. Antimicrob. Agents Chemother. 53:4096–4102.

Wormann, M. E., N. T. Reichmann, C. L. Malone, A. R. Horswill, and A. Grundling. 2011. Proteolytic cleavage inactivates the *Staphylococcus aureus* lipoteichoic acid synthase. J. Bacteriol. 193:5279–5291.

Zielinska, A. K., K. E. Beenken, H. S. Joo, L. N. Mrak, L. M. Griffin, T. T. Luong, et al. 2011. Defining the strain-dependent impact of the Staphylococcal accessory regulator (sarA) on the alpha-toxin phenotype of *Staphylococcus aureus*. J. Bacteriol. 193:2948–2958.

Zielinska, A.K., K.E. Beenken, L.N. Mrak, H.J. Spencer, G.R. Post, R.A. Skinner, et al. 2012. sarA-mediated repression of protease production plays a key role in the pathogenesis of *Staphylococcus aureus* USA300 isolates. Mol. Microbiol. 86 (5):1183–96.

Supporting Information

Additional Supporting Information may be found in the online version of this article:

Figure S1. Verification of LAC mutants and biofilm phenotypes in select mutants generated in JE2 and LAC. (A) Comparative analysis of EcoRI-digested genomic DNA from strains derived from JE2 or LAC. Arrow indicates the small plasmid present in our derivative of LAC but absent in JE2 and its NTML derivatives. (B) Biofilm formation was assessed using a microtiter plate assay. Results shown represent the average ± standard error of the mean (SEM) from a minimum of three experiments, each of which was repeated with at least six replicates. Results with LAC were set to 1.0. The results observed with all other strains, including JE2, shown relative to this value. Asterisk indicates significance by comparison to the corresponding parent strain ($P < 0.05$).

Manuscript Details

Manuscript number	TOXREP_2019_428_R1
Title	Evaluation of bone and kidney toxicity of BT2-peg2, a potential carrier for the targeted delivery of antibiotics to bone
Article type	Full Length Article

Abstract

Previous studies have demonstrated that the bone targeting agent BT2-peg2 (BT2-minipeg2, 9), when conjugated to vancomycin and delivered systemically by intravenous (IV) or intraperitoneal (IP) injection accumulates in bone to a greater degree than vancomycin alone, but that this accumulation is associated with severe nephrotoxicity. To determine whether this nephrotoxicity could be attributed to BT2-peg2 itself, we used a rat model to assess the distribution and toxicity of BT2-peg2 after IP injection of 11 mg/kg twice daily for 21 days. The results demonstrated that BT2-peg2 accumulates in bone but there was no evidence of nephrotoxicity or any histopathological abnormalities in the bone. This suggests the nephrotoxicity observed in previous studies is likely due to the altered pharmacokinetics of vancomycin when conjugated to BT2-peg2 rather than to BT2-peg2 itself. Thus, BT2-peg2 may be a safe carrier for the enhanced delivery of antibiotics other than vancomycin to the bone as a means of combating bone infection. However, the data also emphasizes the need to carefully examine the pharmacokinetic characteristics of any BT2-peg2-antibiotic conjugate utilized for treatment of bone infections

Keywords	BT2-peg2, Rat plasma, Bone delivery, Bone pathology, Nephrotoxicity
Corresponding Author	Peter Crooks
Corresponding Author's Institution	University of Arkansas for Medical Sciences
Order of Authors	Zaineb Albayati, Narsimha Reddy Penthala, Shobanbabu Bommagani, Ginell Post, Mark Smeltzer, Peter Crooks
Suggested reviewers	Pavan Puligujja, Satya Prakash Shukla, Rajesh Karuturi

Submission Files Included in this PDF

File Name [File Type]

Albayati Tox Reports Cover letter 100819 (002).doc [Cover Letter]

Responses to the reviewer comments.docx [Response to Reviewers]

Graphical Abstract BT2 paper revised.docx [Graphical Abstract]

Zaineb Rev-BT2Peg2 manuscript Crooks FINAL 100919 (7).docx [Manuscript File]

Fig 2 Kidneys.jpg [Figure]

Fig 3-Kidneys.jpg [Figure]

Fig 4-Bone-2.jpg [Figure]

coi_disclosure (1).pdf [Conflict of Interest]

declaration-of-competing-interests.docx [e-Component]

Supplementary Information.docx [Supporting File]

To view all the submission files, including those not included in the PDF, click on the manuscript title on your EVISE Homepage, then click 'Download zip file'.

Research Data Related to this Submission

There are no linked research data sets for this submission. The following reason is given:
No data was used for the research described in the article

To:
Dr. Aristidis M. Tsatsakis
Editor-in-Chief
Toxicology Reports,

Ref: "Resubmission of manuscript no. TOXREP_2019_428 for publication in *Toxicology Reports*

Dear Dr. Tsatsakis:

Please find attached a revised submission of our manuscript no. TOXREP_2019_428 entitled "Evaluation of bone and kidney toxicity of BT2-peg2, a potential carrier for the targeted delivery of antibiotics to bone". We thank the reviewer for his valuable comments on our manuscript and we have provided our responses to his questions below with the appropriate changes we have made to the manuscript. We trust that these modifications meet with your approval and that our manuscript is now suitable for publication in *Toxocology Reports*.

Sincerely

Peter A. Crooks, M.Sc., Ph.D., D.Sc.

Professor and Chairman

Department of Pharmaceutical Sciences

College of Pharmacy

University of Arkansas for Medical Sciences

4301 West Markham Street, Slot 522-3

Little Rock, AR 72205

phone: 501.686.6495

fax: 501.686.6057

PACrooks@uams.edu

Responses to the reviewer's comments

Comment 1: there is no mention to the LC/mass data to describe the content of BT2-preg 2 in a plasma or bone samples.

Response: We thank the reviewer for bringing this to our attention. A discussion of the LC-MS analysis data carried out on plasma and bone samples from animals treated with BT2-peg2 has now been added to the Discussion Section, page 6, lines column 1 lines 392 to column 2 lines 415.

Comment 2: The discussion based on non-obvious data.

Response: We have extensively modified the Discussion Section of our manuscript to provide a more comprehensive summary of the results of our study in the context of the nephrotoxic potential of our bone-targeting agent, BT2-peg2.

Comment 3: There is no data for vancomycin in this research it is better to examined also the effect of vancomycin in the same condition of BT2-peg 2 The effect of vancomycin and BT2-vancomycin on the kidney was tested in the previous MS, therefore the aim of this study was to determine the nephrotoxicity of BT2-Peg2 if there is any after treatment with BT2-peg2.

Response: We did not carry out a vancomycin study under the same conditions as in our BT2-peg2-treated rat study, since this has previously been reported in the Karau et al. (2013) study [reference 14 in our manuscript]. The Karau study was done in the same animal species (male albino Wistar rats) used in our study, and at the same molar dose and frequency of dosing of vancomycin as in our BT2-peg2 dosing study. Karau et al. found that no nephrotoxicity was observed when vancomycin was administered under these exact same conditions that were utilized in our current BT2-peg2 study. We have added additional discussion on this topic in the text of the manuscript (page 6, column 1 lines 369-382).

Comment 4: The discussion BT2-peg2B T2BT2-peg2

Response: We have now corrected the spelling of BT2-peg2 in the Discussion Section.

Responses to the reviewer's comments

Comment 1: there is no mention to the LC/mass data to describe the content of BT2-preg 2 in a plasma or bone samples.

Response: We thank the reviewer for bringing this to our attention. A discussion of the LC-MS analysis data carried out on plasma and bone samples from animals treated with BT2-peg2 has now been added to the Discussion Section, page 6, lines column 1 lines 392 to column 2 lines 415.

Comment 2: The discussion based on non-obvious data.

Response: We have extensively modified the Discussion Section of our manuscript to provide a more comprehensive summary of the results of our study in the context of the nephrotoxic potential of our bone-targeting agent, BT2-peg2.

Comment 3: There is no data for vancomycin in this research it is better to examined also the effect of vancomycin in the same condition of BT2-peg 2 The effect of vancomycin and BT2-vancomycin on the kidney was tested in the previous MS, therefore the aim of this study was to determine the nephrotoxicity of BT2-Peg2 if there is any after treatment with BT2-peg2.

Response: We did not carry out a vancomycin study under the same conditions as in our BT2-peg2-treated rat study, since this has previously been reported in the Karau et al. (2013) study [reference 14 in our manuscript]. The Karau study was done in the same animal species (male albino Wistar rats) used in our study, and at the same molar dose and frequency of dosing of vancomycin as in our BT2-peg2 dosing study. Karau et al. found that no nephrotoxicity was observed when vancomycin was administered under these exact same conditions that were utilized in our current BT2-peg2 study. We have added additional discussion on this topic in the text of the manuscript (page 6, column 1 lines 369-382).

Comment 4: The discussion BT2-peg2B T2BT2-peg2

Response: We have now corrected the spelling of BT2-peg2 in the Discussion Section.

Graphical Abstract

Evaluation of bone and kidney toxicity of BT2-peg2, a potential carrier for the targeted delivery of antibiotics to bone

Zaineb A.F. Albayati, Narsimha R. Penthala, Shobanbabu Bommagani, Ginell R. Post, Mark S. Smeltzer and Peter A. Crooks[*]

Leave this area blank for abstract info.

The bone-targeting agent BT2-peg2, when conjugated to vancomycin and delivered systemically to Albino Wister rats, results in severe nephrotoxicity. We have now shown that BT2-peg2 alone accumulates in rat bone and that there is no evidence of nephrotoxicity or any kidney or bone histopathological abnormality. These data indicate that BT2-peg2 is likely a safe carrier for the enhanced delivery of antibiotics other than vancomycin to bone as a means of combating bone infection.

Histological analysis of Albino Wister rat kidneys as a function of BT2-peg2 treatment (11mg ip 2 x daily x 21 days). Periodic acid–Schiff (PAS) stained histopathologic sections from untreated (left) and BT2-peg2-treated kidneys (right) showing no discernible evidence of microscopic glomerular or renal tubular damage.

Evaluation of bone and kidney toxicity of BT2-peg2, a potential carrier for the targeted delivery of antibiotics to bone

Zaineb A.F. Albayati[a], Narsimha R. Penthala[a], Shobanbabu Bommagani[a], Ginell R. Post[b], Mark S. Smeltzer[c] and Peter A. Crooks[a*]

[a]Department of Pharmaceutical Sciences, College of Pharmacy, University of Arkansas for Medical Sciences, Little Rock, AR 72205
[b]Department of Clinical Pathology, College of Medicine, University of Arkansas for Medical Sciences, Little Rock, AR 72205
[c]Department of Microbiology & Immunology, College of Medicine, University of Arkansas for Medical Sciences, Little Rock, AR 72205

ABSTRACT

Previous studies have demonstrated that the bone targeting agent BT2-peg2 (BT2-minipeg2, **9**), when conjugated to vancomycin and delivered systemically by intravenous (IV) or intraperitoneal (IP) injection accumulates in bone to a greater degree than vancomycin alone, but that this accumulation is associated with severe nephrotoxicity. To determine whether this nephrotoxicity could be attributed to BT2-peg2 itself, we used a rat model to assess the distribution and toxicity of BT2-peg2 after IP injection of 11 mg/kg twice daily for 21 days. The results demonstrated that BT2-peg2 accumulates in bone but there was no evidence of nephrotoxicity or any histopathological abnormalities in the bone. This suggests the nephrotoxicity observed in previous studies is likely due to the altered pharmacokinetics of vancomycin when conjugated to BT2-peg2 rather than to BT2-peg2 itself. Thus, BT2-peg2 may be a safe carrier for the enhanced delivery of antibiotics other than vancomycin to the bone as a means of combating bone infection. However, the data also emphasizes the need to carefully examine the pharmacokinetic characteristics of any BT2-peg2-antibiotic conjugate utilized for treatment of bone infections.

*Corresponding author. Tel.: +1-501-686-6495; fax: +1-501-686-6057; e-mail: pacrooks@uams.edu

1. Introduction

Osteomyelitis is a serious inflammatory condition of bone that is most often associated with infection by the bacterial pathogen *Staphylococcus aureus* [1]. Treatment of these infections is extremely challenging owing in part to the increasing prevalence of *S. aureus* strains resistant to methicillin and other beta-lactam antibiotics [2]. Despite the development of a number of newer antibiotics with efficacy against methicillin-resistant *S. aureus* (MRSA), vancomycin remains the antibiotic of choice in the clinical treatment of bone and joint infections [3-5]. Moreover, bone infections are characterized by formation of a biofilm, which confers a therapeutically-relevant level of intrinsic resistance to all conventional antibiotics, including vancomycin [6]. *S. aureus* can also be internalized by osteoblasts, which complicates conventional antibiotic therapy even further [7].

Thus, at a minimum it is necessary to administer high doses of antibiotics for long periods of time, but even then surgical debridement is most often also required [8]. Additionally, such prolonged antibiotic administration, particularly with vancomycin is associated with nephrotoxicity and the emergence of *S. aureus* strains that exhibit intermediate but therapeutically relevant levels of resistance to vancomycin (vancomycin intermediate *S. aureus* or VISA) [9]. At present, the primary means of overcoming these limitations is the use of localized, carrier-based antibiotic delivery as part of the surgical debridement protocol [8]. Thus, there is an urgent need for improved methods for the more effective systemic delivery of antimicrobial agents to bone. Indeed, such methods could limit the degree of debridement required to ensure the desired therapeutic effect or perhaps, at least in some cases, eliminate the need for debridement entirely.

BT2-peg2 (**9**) is derived from the hydroxyapatite-binding moiety of tetracycline and was used successfully to enhance the delivery of estradiol and other bioactive compounds to bone [10-13] Karau et al. [14] demonstrated that, under *in vitro* test conditions, vancomycin conjugated to BT2-peg2 had similar activity to vancomycin itself against MRSA, an observation that we subsequently confirmed [15]. Moreover, treatment of experimental osteomyelitis with vancomycin and the molar equivalent of BT2-peg2-vancomycin using the same dosing regimen confirmed that BT2-peg2-vancomycin exhibits enhanced therapeutic efficacy by comparison to vancomycin alone [14]. It was also confirmed by pharmacokinetic (PK) analysis that BT2-peg2-vancomycin significantly accumulates in bone and plasma after systemic administration by comparison to the systemic administration of vancomycin alone [15].

While promising, Karau et al. [14] also found that systemic administration of BT2-peg2-vancomycin in rats was associated with high plasma concentrations of this drug, elevated levels of serum creatinine and blood urea nitrogen (BUN), decreased serum albumin, leukocytosis, and severe nephrotoxicity, as has been reported with exposure to high plasma concentrations of vancomycin [16]. However, these investigators determined that systemic administration of an equimolar amount of vancomycin under similar conditions did not result in nephrotoxicity. Karau et al. hypothesized from these observations that the adverse consequences after systemic administration of BT2-peg2-vancomycin were likely due to an altered PK of BT2-peg2-vancomycin compared to vancomycin, resulting in prolonged accumulation of the former compound in plasma causing nephrotoxicity. To test this hypothesis, the present study was aimed at determining whether BT2-peg2 (**9**) alone, administered systemically under the same conditions and concentrations as in the Karau et al. study exhibits significant nephrotoxicity and/or histopathological changes in the bone itself.

2. Materials and Methods

2.1 Chemicals

All chemicals used in this study were of LC/MS grade or equivalent quality. Acetonitrile, methanol, formic acid, and normal saline were obtained from Fisher Scientific (Pittsburgh, PA, USA). Benzophenone was obtained from Sigma-Aldrich (St. Louis, MO, USA). Heparin sodium injection (10,000 USP units/mL) was purchased from Baxter Healthcare Corporation (Deerfield, IL, USA). The raw materials for the synthesis of BT2-peg2 were purchased from the AK scientific product catalog (Union City, CA, USA).

2.2 Synthesis of BT2-peg2 (9)

It is noteworthy to mention that BT2-peg2 (**9**) is stereochemically, structurally and functionally similar to the BT2-peg2 that has been discussed by Karau et al. and Albayati et al. [14, 15]. Synthesis of BT2-peg2 requires the preparation of the key raw material BT2 (**6**), which can be made in five steps via a modification of the procedures described by Neale et al. [10] and Brooke [17] from the readily available starting material, 2,6-dihydroxy benzoic acid (**1**) (Scheme 1). Esterification of **1** to methyl 2,6-dihydroxybenzoic acid (**2**) is the first step in the synthesis of BT2. Neale et al. have reported on the esterification of **1** using methyl iodide, NH_4OH, and $AgNO_3$ in 89% yield [10]. However, we were not able to obtain such yields using this methodology. By reacting **1** with dimethyl sulfate/sodium carbonate at room temperature over 12 h we were able to obtain a 95% yield of **2** which could be isolated in greater than 99% purity. The second step in the synthesis of BT2 is aminolysis of **2** with aqueous ammonia to form 2,6-dihydroxybenzamide (**3**), [10]. We found that by replacing aqueous ammonia with methanolic ammonia we were able to improve the yield of **3** to 84% with a simplified work-up procedure. For the *O*-methylation of **3** with dimethyl sulfate in acetone/potassium carbonate to afford 6-methoxybenzamide (**4**) we utilized the procedure of Brooke [17]. Nitration of **4** with nitric acid/acetic acid reagent then afforded 3-nitro-2-hydroxy-6-methoxybenzamide (**5**) [10]. Reduction of **5** is the final step in the synthesis of BT2 (**6**). Neale et al. has reported using Pd-C hydrogenation in methanol at 46 psig for the reduction of **5** to BT2 [10]. We modified this procedure by carrying out the reaction with 10 mole equivalents of 50-60% hydrazine hydrate and 10% w/w Pd-C in ethanol at reflux temperature and at atmospheric pressure. This procedure improved the yield of BT2 from 67% to 77%. The analytical data for intermediates **2-5** and BT2 (**6**) are in agreement with the reported literature [10]. The synthesis of BT2-peg2 (**9**) from BT2 (**6**) was carried out as per the reported literature procedure (Scheme 1) [17]. The overall yield of **9** from **1** utilizing the above procedures is improved by 43%. The H-1 and C-13 NMR spectra and other analytical data for BT2-peg2 (see Supplementary Information) were consistent with the reported analytical data [17].
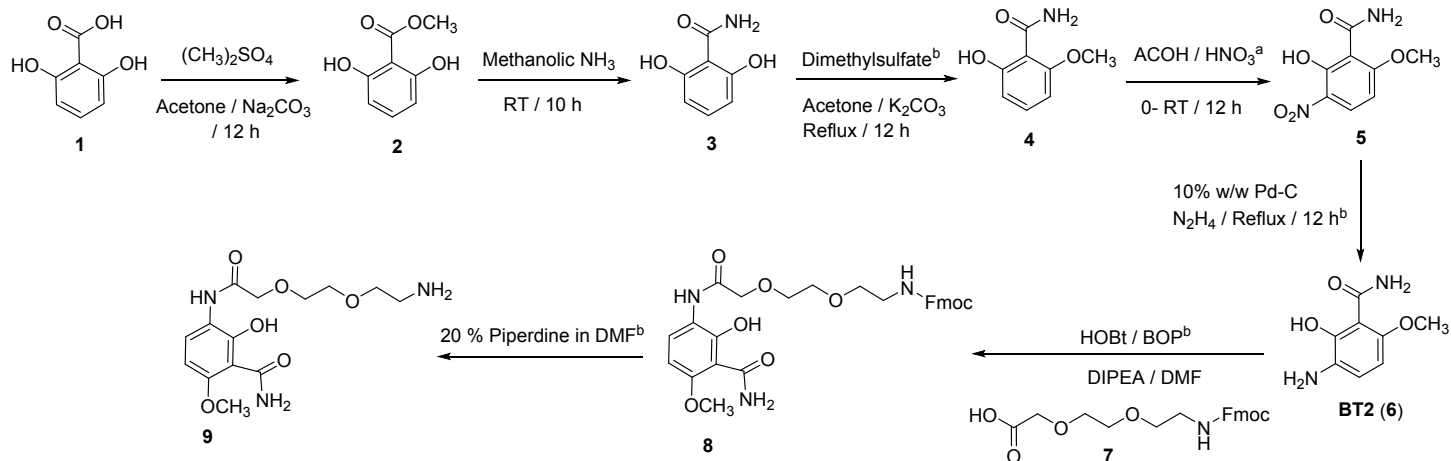
168 **Scheme 1.** Synthesis of BT2-peg2 conjugate (**9**)

2.3 Animal experimental protocol

All animal protocols were approved by the Institutional Animal Care and Use Committee of the University of Arkansas for Medical Sciences (UAMS) and the Animal Care and Use Review Office (ACURO) of the U.S. Army Medical Research and Material Command (USAMRMC).

BT2-peg2 (**9**) was administered at a concentration of 11 mg/kg, which is the molar equivalent of the amount of BT2-peg2 present in the BT2-peg2-vancomycin conjugate. BT2-peg2 was formulated in phosphate buffered saline (PBS) and delivered by intraperitoneal (IP) injection into each of four Albino Wistar male rats (200-250 gm, Charles River, Wilmington, MA). Administration was carried out twice daily for 21 days for a total of 42 doses, as employed in the study by Karau et al. [14]. Control rats were administered PBS IP injections twice daily for 21 days. BT2-peg2-treated and untreated rats were weighed daily throughout this period. Twelve hours after the last dose, rats were humanely euthanized using CO_2, and blood, kidneys and the right and left tibia harvested from each rat. Blood was collected via cardiac puncture and placed into sodium heparin blood collection tubes for hematology. Plasma was obtained by centrifugation at 10,000 rpm at room temperature (RT) for 5 min. Samples were stored at -80°C prior to analysis.

2.4 Histological, biochemical and hematological analysis

Kidneys from untreated and BT2-peg2-treated rats were collected, weighed, observed for abnormalities in size and color and fixed in neutralized buffered formalin (NBF) for 24 h prior to more detailed histological analysis. Histological analysis of the kidney was performed using Hematoxylin and Eosin (H&E) and Periodic acid–Schiff (PAS) stained sections. The left and right tibia were cleaned of soft tissues, washed with PBS and weighed. Right tibia samples were fixed in NBF for 24 h and decalcified using 10% EDTA (pH 7.0) prior to histological analysis of H&E stained sections. Plasma and the left tibia were used for quantitative determination of BT2-peg2 (**9**) concentrations by LC/MS/MS, as detailed below. Hematological analysis of blood was performed to determine white blood cell (WBC) count. UV/visible colorimetric analysis was used to determine plasma creatinine, blood urea nitrogen (BUN) and albumin levels, as previously described [18-20].

2.5 Preparation of plasma samples for LC/MS/MS analysis of BT2-peg2 (**9**) levels

A hundred µL of plasma from untreated and BT2-peg2-treated rats was spiked with benzophenone (10 µL of a 0.1 µg/mL solution in acetonitrile) as an internal standard. Protein precipitation was performed by adding 400 µL of acetonitrile. After 30 s of vortex mixing, the solution was centrifuged at 10,000 rpm for 10 min at RT. The supernatant was evaporated to dryness under nitrogen and each pellet was reconstituted with 60 µL of a 2:1 mixture of acetonitrile:water. Re-suspended pellets were vortexed, sonicated for 1 min, and centrifuged at 10,000 rpm for 10 min at RT prior to analysis by LC/MS/MS, as detailed below.

2.6 Preparation of bone samples and extraction procedure for analysis of BT2-peg2 (**9**)

Stainless steel balls (3.5 mm, Next Advance Inc, Troy, NY, USA) were placed in a 5 ml tube along with the tibia, 0.5 mL hexane, and 1 mL of water. Bone samples were homogenized for 3 min using a Bullet Blender Storm 5 homogenizer (Next Advance, Inc. Troy, NY, USA). Ten µL (0.1 µg/mL) of benzophenone was added to 0.2 mL of each bone homogenate as an internal standard. Samples were vortexed and extracted with 600 µL acetonitrile, followed by the addition of 400 µL water. Samples were then vortexed for 30 s and centrifuged at RT for 10 min at 10,000 rpm. Supernatants were then processed as described above for analysis by LC/MS/MS.

2.7 LC/MS/MS analysis of BT2-peg2 (**9**) in plasma and bone samples

3

Analysis of BT2-peg2 (**9**) in plasma and bone samples was performed using an Agilent LC/MS/MS Triple Quad 6430 instrument (Santa Clara, CA, USA) utilizing positive electrospray ionization (ESI) in the multiple reaction monitoring (MRM) mode with optimal ion source settings determined by standards of BT2-peg2 (**9**), and benzophenone as the internal standard. A curtain gas of 20 psi, an ion spray voltage of 4000 V, an ion source gas1/gas2 of 35 psi and a temperature of 300°C were employed in the collection of chromatographic data. Chromatographic separation was carried out on an Alltech Altima C-18 column (150 mm×3.0 mm, 5.0 μm) fitted with an Alltech Altima C-18 guard column (7.5 X 3.0 mm, 5μ, Grace Discovery Sciences, IL, USA). A gradient method was used with the mobile phase consisting of water containing 0.1% v/v formic acid as solvent A and ACN as solvent B. The separation was achieved using a gradient of 10 to 90% solvent B over 3.50 min, which was maintained at 90% B for a further 3.50 min, and then equilibrated back to the initial conditions over 3.20 min. The flow rate was 0.8 mL/min and injection volume through the auto sampler unit for all the samples was 5 μL. BT2-peg2 and the benzophenone internal standard (IS) exhibited retention times of 3.2 and 5.6 min, respectively. MRM transitions monitored were m/z 328.1/166.0 for BT2-peg2, and m/z 183.1/105.1 and m/z 183.1/77.1 for benzophenone.

2.8 Calibration standards

Calibration standards for BT2-peg2 in plasma and bone samples were constructed by spiking 100 μL of drug free plasma or bone homogenate samples with 10 μL of freshly prepared standard solutions of BT2-peg2 (0, 1, 10, 20, 40, 100, and 200 ng/mL. Calibration curves of BT2-peg2 in plasma and bone were established by plotting the peak area ratios of BT2-peg2 and IS vs. concentrations of BT2-peg2. Linear regression equations were obtained by using the least-squares method. The calibration curves of BT2-peg2 in plasma showed excellent linearity between 10-200 ng/mL with correlation coefficient (R^2) of 0.975 and 10-200 ng/mL with correlation coefficient of 0.982 for bone. The lower limit of detection (LOD) and lower limit of quantitation (LOQ) values were 1 and 10 ng/mL for plasma and 10-20 ng/mL for bone, respectively.

2.9 Histopathology

Kidney and bone samples were fixed in 10% NBF. Bone samples were decalcified in 10% EDTA buffer, pH 7.0. Tissues were then placed in cassettes and embedded in paraffin. Samples were then sectioned at 5 μM and stained with H&E. For kidney sections, the periodic acid-Schiff (PAS) stain was also used to highlight the tubular brush border cells. Histologic sections prepared from the kidneys and right tibia were evaluated microscopically by a pathologist in a blinded fashion.

2.10 Statistical analysis

Data are presented as mean ± standard error of the mean (mean ± SEM). The data were analyzed for statistical significance using the unpaired Student's t-test with Welch's correction factor for unequal variances with $p \leq 0.05$ as the criterion of significance.

3. Results

The percent change in body weight over the course of 21 days treatment for the untreated and groups were not statistically different ($p \geq 0.05$, Fig. 1). The kidneys from the untreated and the BT2-peg2-treated rats exhibited a deep maroon color and were indistinguishable visually (Fig. 2), and their size and weight indicated no significant difference between the two groups (Table 1). Most importantly, histologic evaluation of the renal sections from BT2-peg2-treated and untreated rats showed unremarkable glomeruli, tubules, vessels and interstitium. There were also no histopathologic features of renal injury, including tubular dilatation, apical budding, brush border or tubular loss (Fig. 3). In addition, biochemical results indicated normal values for blood urea nitrogen (BUN), plasma albumin and creatinine in both the untreated and BT2-peg2-treated animals (Table 1).

There was also no statistical difference in total white blood cell counts for the untreated and BT2-peg2 treated groups, which exhibited values of $8.9 \pm 0.9 \times 10^3$ and $9.3 \pm 0.8 \times 10^3/\mu L$, respectively. Significant amounts of BT2-peg2 were detected in the left tibia, while BT2-peg2 was undetectable in plasma (LOD < 1 ng/mL, Table 1). Microscopic examination of the right tibia from BT2-peg2-treated and untreated rats showed similar features, including intact cortical and paratrabecular bone with morphologically unremarkable trilineage hematopoiesis. There was no evidence of cellular or stromal injury in either experimental group (Fig. 4).

Table 1

Kidney weights, BUN, plasma albumin, creatinine values, and plasma and bone BT2-peg2 levels after treatment with BT2-peg2 at a dose of 11 mg/kg (the molar equivalent of BT2-peg2 used in the BT2-peg2-vancomycin study [14]).

Group	Untreated	BT2-peg2-treated
Kidney weight (g)	2.5 ± 0.22	2.4 ± 0.35
BUN (mg/dl)	22.1 ± 2.5	23.0 ± 0.9
Albumin (gm/dl)	3.4 ± 0.02	3.5 ± 0.01
Creatinine (mg/dl)	0.5 ± 0.01	0.6 ± 0.01
Plasma (ng/mL)	-	< 1
Bone (ng/g)	-	235.0 ± 96.8

Fig. 1. Percent body weight change over the 21-day course of treatment with BT2-peg2 (11 mg/kg twice daily) in Albino Wistar male rats.

4
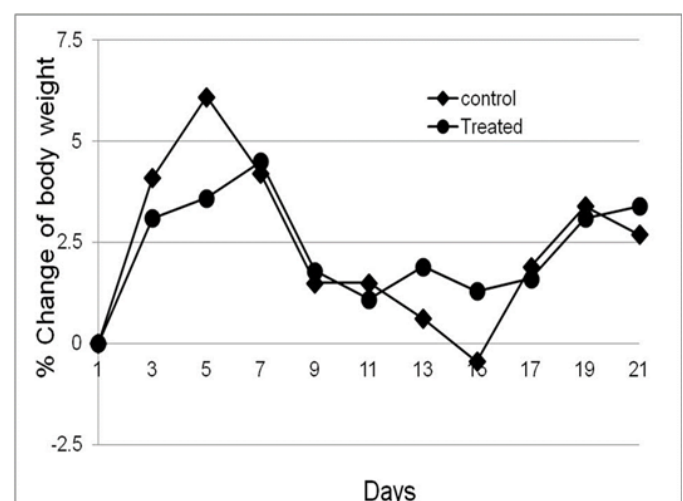
Untreated BT2-peg2

Fig. 2. Representative kidneys from untreated and BT2-peg2-treated rats.
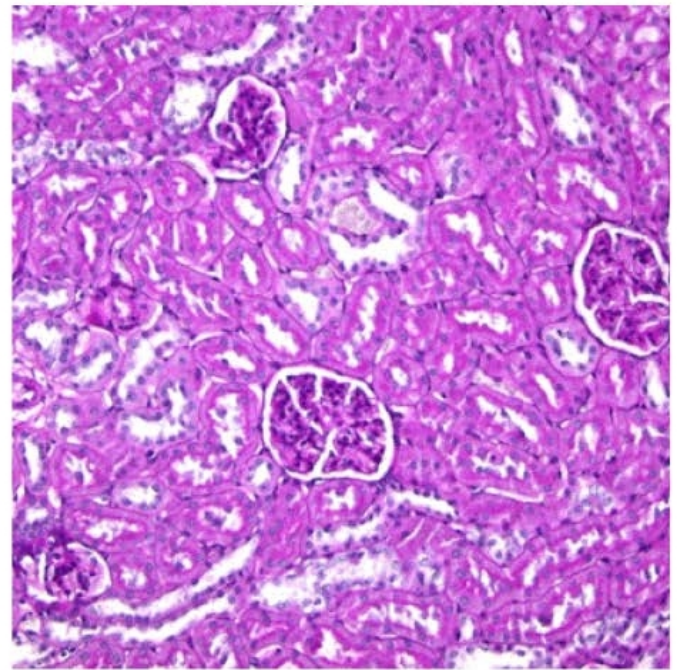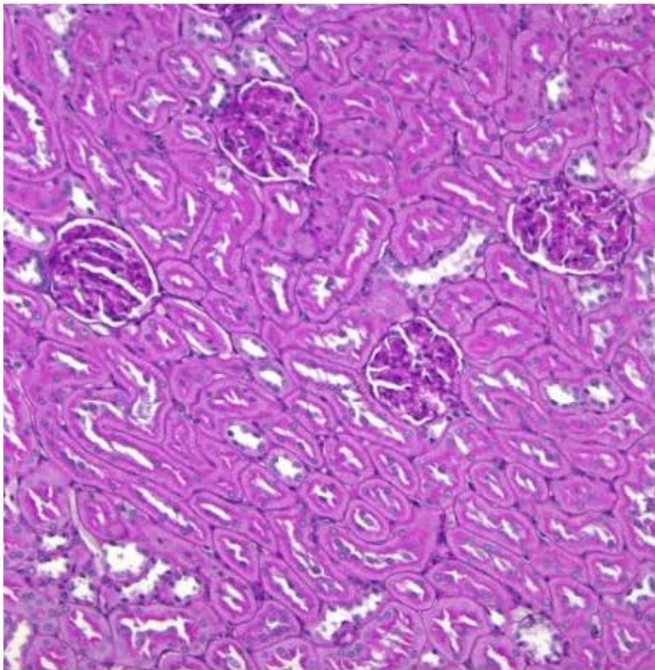
Fig. 3. Histological analysis of kidneys as a function of BT2-peg2 treatment. Periodic acid–Schiff (PAS) stained histopathologic sections from untreated (left) and BT2-peg2-treated kidneys (right). There was no discernible evidence of microscopic glomerular or renal tubular damage as evidenced by tubular dilatation, apical budding, or brush border and tubular loss. The absence of demonstrable histopathology was also confirmed by H&E staining (data not shown).
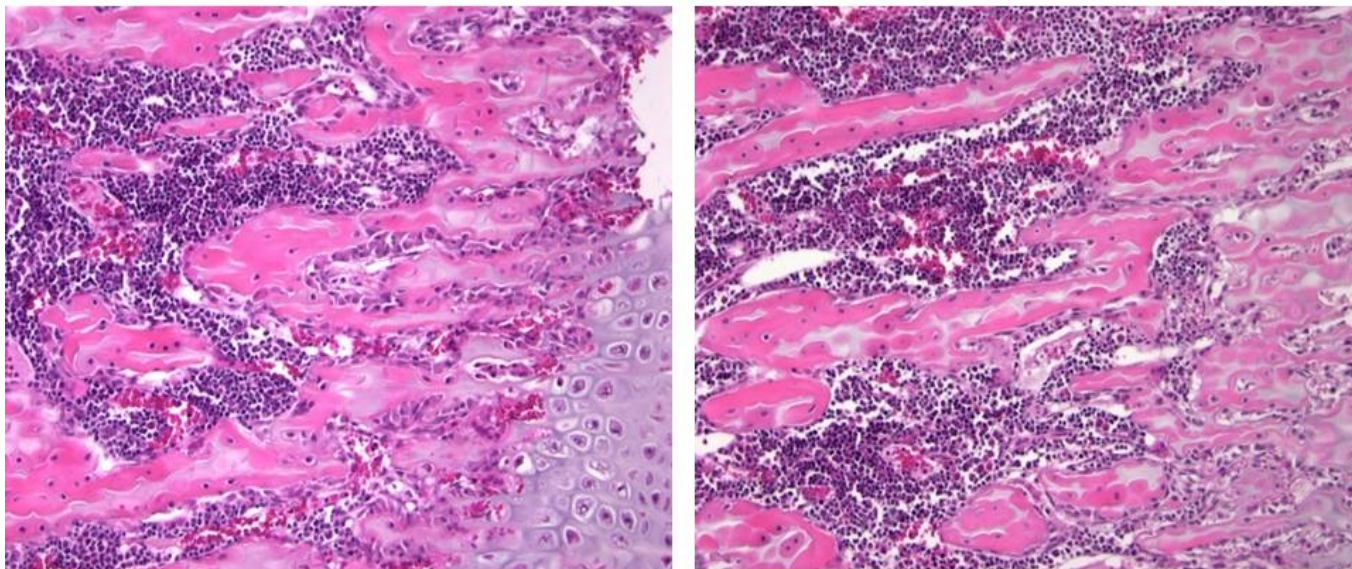
Fig. 4. Bone histology as a function of BT2-peg2 treatment. Representative images of H&E stained sections of the right tibia are shown from untreated (left) and BT2-peg2-treated rats.

4. Discussion

Previous studies employing a rat model of experimental osteomyelitis provided evidence that BT2-peg2-vancomycin delivered systemically by intravenous (IV) or intraperitoneal (IP) injection exhibits greater therapeutic efficacy in the context of bone than an equivalent dose of vancomycin [14]. However, the use of BT2-peg2-vancomycin was also associated with a profound change in pharmacokinetic profile characterized by high plasma levels of BT2-peg2-vancomycin, decreased animal weight, increased kidney size, and severe tubulointerstitial nephritis. Subsequent chemical analysis also confirmed that administration of BT2-peg2-vancomycin resulted in elevated levels of serum creatinine and blood urea nitrogen (BUN), and decreased serum albumin.

It is noteworthy that vancomycin administered via conservative dosing and/or via more intense dosing (twice/day for 21 days) was not nephrotoxic in any of the doses and protocols used. In this respect it should be noted that nephrotoxicity associated with BT2-peg2-vancomycin was minimized if not eliminated using more conservative dosing regimens (i.e. every 12 hrs for 3.5 days followed by once daily every fourth day or once per week), but these more conservative regimens were not demonstrably associated with an enhanced therapeutic effect [14]. It should also be noted that plasma levels of BT2-peg2-vancomycin were dramatically elevated using the more intensive dosing regimen and this was not the case with either of the more conservative dosing regimens [14]. This suggests a direct correlation between high plasma levels of BT2-peg2-vancomycin and nephrotoxicity.

Since this study was aimed at determining whether BT2-peg2 itself contributed to the above adverse effects, in order to test this hypothesis as stringently as possible, we employed the maximum dosing regimen used by Karau et al. [14], which was twice daily administration of drug for 21 days. To this end, we administered 11 mg/kg of BT2-peg2 (which is the molar equivalent of the BT2-peg2 component of BT2-peg2-vancomycin) to rats using the same dosing regimen (i.e. IP injection twice daily for 21 days) shown to enhance therapeutic efficacy in the study by Karau et al [14].

As presented in Table 1, we found that plasma levels of BT2-peg2 were below the limit of detection (< 1 ng/mL) despite the clear accumulation of BT2-peg2 in the bone, indicating that BT2-peg2 is targeting bone tissue. The latter finding is consistent with the high affinity of BT2-peg2 for hydroxyapatite and an enhanced tendency to accumulate in bone [17]. Despite vancomycin antibacterial efficacy against both methicillin-resistant and methicillin-susceptible *S. aureus* strains, vancomycin ability to penetrate bone tissue is limited. Also, vancomycin exhibits poor pharmacokinetics that makes it insufficiently bioavailable in bone tissue, thus limiting its *in vivo* use for bone infections. Our previous studies have sought to optimize vancomycin bioavailability by conjugating the bone targeting agent BT2-peg2 to deliver vancomycin to the bone as BT2-peg2-vancomycin, a strategy of potential clinical use in the treatment of bone infection. We demonstrated that BT2-peg2 can be chemically conjugated to vancomycin via a modified polyethylene glycol (PEG) linker to form BT2-peg2-vancomycin, which retains the antibacterial activity of vancomycin [10, 12, 14]. Previous *in vitro* studies have confirmed that the MICs of BT2-peg2-vancomycin against methicillin-resistant and methicillin-susceptible *S. aureus* are comparable to those of vancomycin, and that BT2-peg2-vancomycin binds to hydroxyapatite to a greater extent than vancomycin [14].

In summary, the results from the current study demonstrate that systemic administration of BT2-peg2 via the IP route is not associated with any of the nephrotoxic side effects observed in previous studies employing BT2-peg2-vancomycin [14]. Specifically, there was no statistically significant difference between the untreated and BT2-peg2-treated experimental groups, as assessed by weight loss, kidney size and overall morphology, histopathological changes in the kidney, or changes in blood urea nitrogen (BUN), albumin or creatinine levels. All of these results are consistent with the hypothesis that BT2-peg2 itself was not responsible for the nephrotoxicity observed in the earlier studies of Karau et al. [14].

In addition, a hypothetical assumption, if vancomycin is released, in vivo from the BT2-peg2-vancomycin conjugate, an equivalent molar amount of BT2-peg2 would have been also released. Neither vancomycin nor free BT2-peg2 was released, since the levels of free vancomycin and/or BT2-peg2 in plasma and bone tissues from BT2-peg2-vancomycin-treated (molar equivalent dose of 50 mg/kg of vancomycin) rats were undetectable after IV or IP

treatment with BT2-peg2-vancomycin, indicating either no hydrolysis of BT2-peg2-vancomycin had occurred or their levels were not significant or unquantifiable [15].

It was suggested by Karau et al. that the high plasma levels of BT2-peg2-vancomycin compared to vancomycin observed with the high dosing regimen were likely due to the pegylation component of the BT2-peg2-vancomycin formulation in that pegylation is known to increase drug half-life, although the possibility that release of BT2-peg2-vancomycin from the bone into the systemic circulation also contributed to the high levels observed in plasma could not be ruled out [14].

While certainly not definitive, this suggests that the 183-fold elevated plasma levels of BT2-peg2-vancomycin compared to vancomycin observed by Karau et al. [14] were due to altered pharmacokinetic parameters and reduced clearance of BT2-peg2-vancomycin rather than sustained release from the bone. This is consistent with our previous PK studies demonstrating that vancomycin was first detectable in blood 1 hr after administration and was cleared within 12 hrs [15]. In contrast, plasma BT2-peg2-vancomycin was also first detected at 1 hr, but remained detectable for at least 168 h, demonstrating a significant decrease in total clearance (Cl_{tot}) from the body [15]. This significant change in the PK properties of vancomycin when conjugated to BT2-peg2 resulted in a higher plasma concentration and a longer in $vivo$ exposure to BT2-peg2-vancomycin. In fact, a decrease of 13.5-fold in Cl_{tot} and a 14.7-fold increase in half-life ($t_{1/2}$) was exhibited by BT2-peg2-vancomycin compared to vancomycin with for the former compound producing a 10.8-fold enhancement in the area-under-the-curve (AUC) for BT2-peg2-vancomycin when compared to vancomycin [15].

Finally, in this current study we not only confirmed the targeting efficiency of BT2-peg2 in the context of bone, but also that its accumulation in bone is not associated with adverse bone pathology or leukocytosis. Thus, both histological and hematological results indicate normal bone marrow function. Overall, we conclude that BT2-peg2 has tremendous potential as a safe and effective bone targeting agent and that the nephrotoxicity observed in earlier experiments is in fact a function of its conjugation to vancomycin, likely owing to prolonged persistence in the blood. This suggests that BT2-peg2 could be used to enhance the systemic delivery of antibiotics other than vancomycin to bone. However, the results we report also emphasize the need to carefully evaluate dose, PK parameters and potential toxicity of alternative BT2-peg2 conjugates in addition to their therapeutic efficacy in the context of bone infection.

Conflict of interest Statement

None of the authors have any financial interests to declare.

References and notes

[1] G. Cierny, 3rd, Surgical treatment of osteomyelitis, Plastic and Reconstructive Surgery, 127 Suppl 1 (2011) 190S-204S.
[2] H.F. Chambers, F.R. Deleo, Waves of resistance: Staphylococcus aureus in the antibiotic era, Nature Reviews Microbiology, 7 (2009) 629-641.
[3] E.S. Darley, A.P. MacGowan, Antibiotic treatment of gram-positive bone and joint infections, Journal of Antimicrobial Chemotherapy, 53 (2004) 928-935.
[4] L. Morata, J. Mensa, A. Soriano, New antibiotics against gram-positives: present and future indications, Current Opinion in Pharmacology, 24 (2015) 45-51.
[5] E. Rubinstein, Y. Keynan, Vancomycin revisited - 60 years later, Front Public Health, 2 (2014) 217.
[6] R.A. Brady, J.G. Leid, J.H. Calhoun, J.W. Costerton, M.E. Shirtliff, Osteomyelitis and the role of biofilms in chronic infection, FEMS Immunology and Medical Microbiology, 52 (2008) 13-22.
[7] J. Josse, F. Velard, S.C. Gangloff, Staphylococcus aureus vs. Osteoblast: Relationship and Consequences in Osteomyelitis, Frontiers in Cellular and Infection Microbiology, 5 (2015) 85.
[8] D.P. Lew, F.A. Waldvogel, Osteomyelitis, Lancet, 364 (2004) 369-379.
[9] K. Hiramatsu, Y. Kayayama, M. Matsuo, Y. Aiba, M. Saito, T. Hishinuma, A. Iwamoto, Vancomycin-intermediate resistance in Staphylococcus aureus, Journal of Global Antimicrobial Resistance, 2 (2014) 213-224.
[10] J.R. Neale, N.B. Richter, K.E. Merten, K. Grant Taylor, S. Singh, L.C. Waite, N.K. Emery, N.B. Smith, J. Cai, W.M. Pierce, Bone selective effect of an estradiol conjugate with a novel tetracycline-derived bone-targeting agent, Bioorganic & Medicinal Chemistry Letters, 19 (2009) 680-683.
[11] S. Nasim, A.P. Vartak, W.M. Pierce, Jr., K.G. Taylor, N. Smith, P.A. Crooks, 3-O-phosphate ester conjugates of 17-beta-O-{1-[2-carboxy-(2-hydroxy-4-methoxy-3-carboxamido)anilido]ethyl}1,3,5(10)-estratriene as novel bone-targeting agents, Bioorganic & Medicinal Chemistry Letters, 20 (2010) 7450-7453.
[12] W.M.L. Pierce, KY, US), Waite, Leonard C. (Corydon, IN, US), Taylor, Grant K. (Louisville, KY, US), Bone targeting compounds for delivering agents to bone for interaction therewith, University of Louisville Research Foundation (Louisville, KY, US), United States, 2008.
[13] W.M.L. Pierce Jr., KY, US), Taylor, Grant K. (Louisville, KY, US), Waite, Leonard C. (Corydon, IN, US), Methods and compounds for the targeted delivery of agents to bone for interaction therewith, University of Louisville Research Foundation (Louisville, KY, US), United States, 2011.
[14] M.J. Karau, S.M. Schmidt-Malan, K.E. Greenwood-Quaintance, J. Mandrekar, J. Cai, W.M. Pierce, Jr., K. Merten, R. Patel, Treatment of Methicillin-resistant Staphylococcus aureus experimental Osteomyelitis with bone-targeted Vancomycin, Springerplus, 2 (2013) 329.
[15] Z.A. Albayati, M. Sunkara, S.M. Schmidt-Malan, M.J. Karau, A.J. Morris, J.M. Steckelberg, R. Patel, P.J. Breen, M.S. Smeltzer, K.G. Taylor, K.E. Merten, W.M. Pierce, P.A. Crooks, Novel Bone-Targeting Agent for Enhanced Delivery of Vancomycin to Bone, Antimicrobial Agents and Chemotherapy, 60 (2015) 1865-1868.
[16] E.J. Filippone, W.K. Kraft, J.L. Farber, The Nephrotoxicity of Vancomycin, Clinical Pharmacology & Therapeutics, 102 (2017) 459-469.
[17] R.N. Brooke, I. Studies of cyclic peptides containing the arginine-glycine-aspartic acid pharmacophore; II. Targeting drugs to bone, Chemistry, University of Louisville, 2008.
[18] A. Krishnegowda, N. Padmarajaiah, S. Anantharaman, K. Honnur, Spectrophotometric assay of creatinine in human serum sample, Arabian Journal of Chemistry, 10 (2017) S2018-S2024.
[19] D.R. Wybenga, J. Di Giorgio, V.J. Pileggi, Manual and automated methods for urea nitrogen measurement in whole serum, Clinical Chemistry, 17 (1971) 891-895.
[20] A.E. Pinnell, B.E. Northam, New automated dye-binding method for serum albumin determination with bromcresol purple, Clinical Chemistry, 24 (1978) 80-86.

Untreated   BT2-peg2
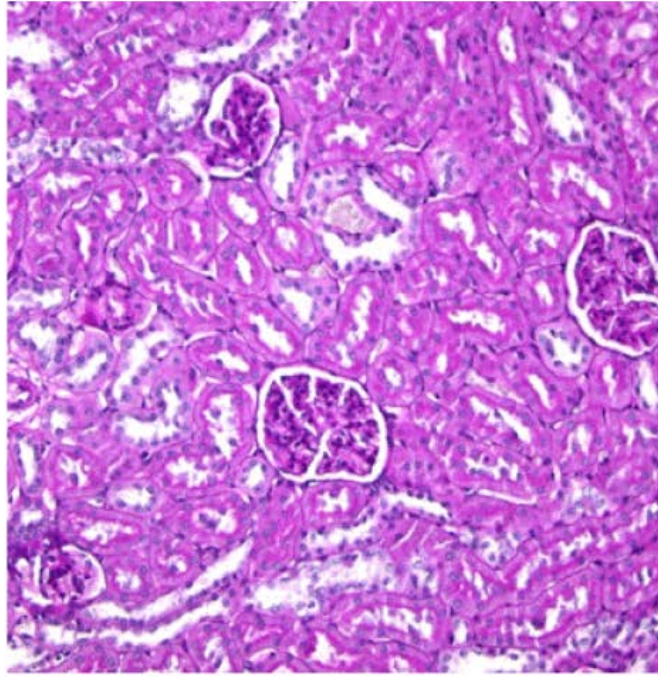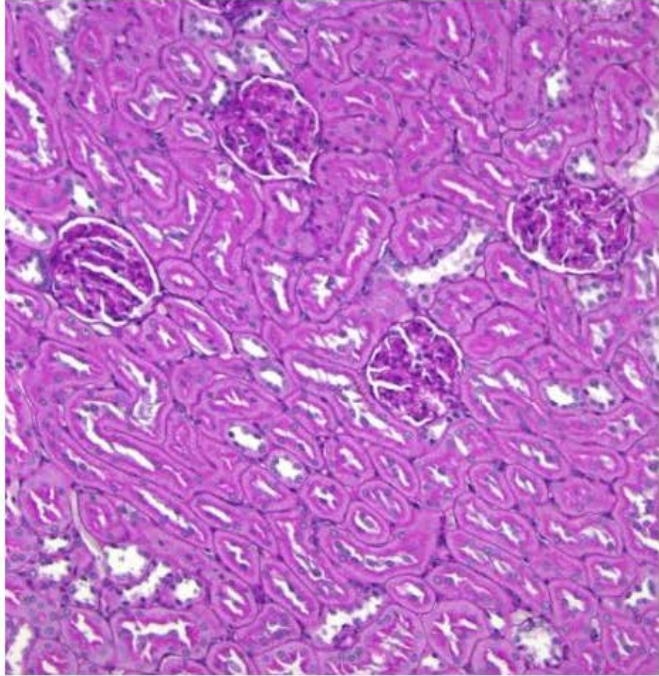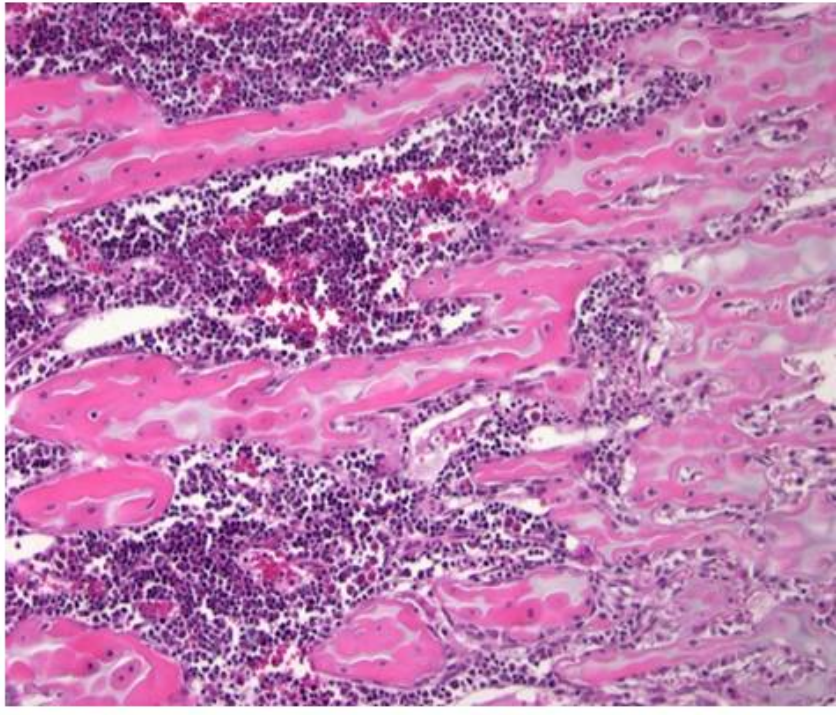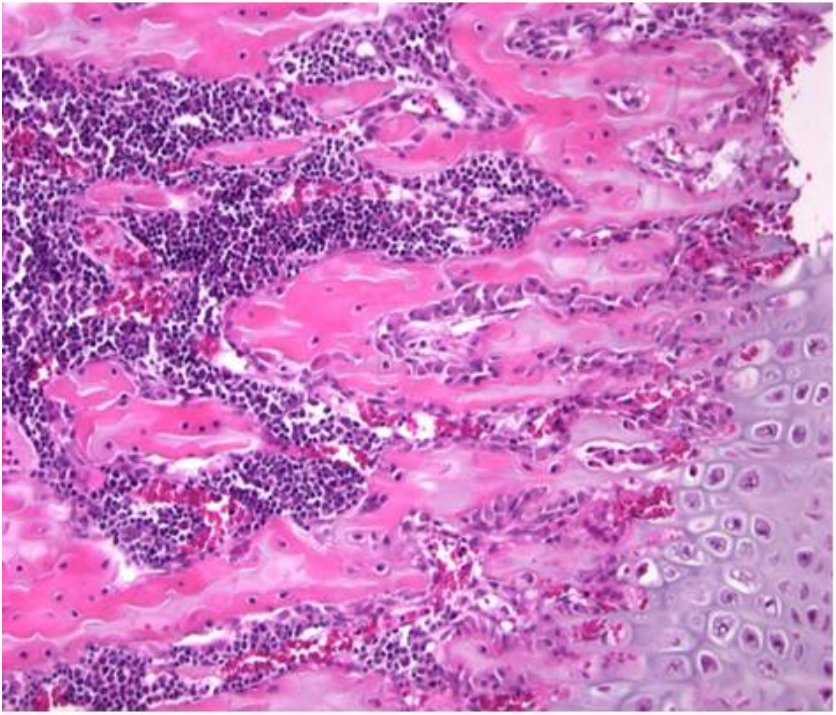
ICMJE Form for Disclosure of Potential Conflicts of Interest

The purpose influence how they receive and understand your work. The form is designed to be completed electronically and stored electronically. It contains programming that allows appropriate data display. Each author should submit a separate form and is responsible for the accuracy and completeness of the submitted information. The form is in six parts.

1. Identifying information.

The work under consideration for publication.

This section asks for information about the work that you have submitted for publication. The time frame for this reporting is that of the work itself, from the initial conception and planning to the present. The requested information is about resources that you received, either directly or indirectly (via your institution), to enable you to complete the work. Checking "No" means that you did the work without receiving any financial support from any third party -- that is, the work was supported by funds from the same institution that pays your salary and that institution did not receive third-party funds with which to pay you. If you or your institution received funds from a third party to support the work, such as a government granting agency, charitable foundation or commercial sponsor, check "Yes"

2.

Relevant financial activities outside the submitted work.

This section asks about your financial relationships with entities in the bio-medical arena that could be perceived to influence, or that give the appearance of potentially influencing, what you wrote in the submitted work. You should disclose interactions with ANY entity that could be considered broadly relevant to the work. For example, if your article is about testing an epidermal growth factor receptor (EGFR) antagonist in lung cancer, you should report all associations with entities pursuing diagnostic or therapeutic strategies in cancer in general, not just in the area of EGFR or lung cancer.

Report all sources of revenue paid (or promised to be paid) directly to you or your institution on your behalf over the 36 months prior to submission of the work. This should include all monies from sources with relevance to the submitted work, not just monies from the entity that sponsored the research. Please note that your interactions with the work's sponsor that are outside the submitted work should also be listed here. If there is any question, it is usually better to disclose a relationship than not to do so.

3. For grants you have received for work outside the submitted work, you should disclose support ONLY from entities that could be perceived to be affected financially by the published work, such as drug companies, or foundations supported by entities that could be perceived to have a financial stake in the outcome. Public funding sources, such as government agencies, charitable foundations or academic institutions, need not be disclosed. For example, if a government agency sponsored a study in which you have been involved and drugs were provided by a pharmaceutical company, you need only list the pharmaceutical company.

Intellectual Property.

This section asks about patents and copyrights, whether pending, issued, licensed and/or receiving royalties.

Relationships not covered above.

Use this section to report other relationships or activities that readers could perceive to have influenced, or that give the appearance of potentially influencing, what you wrote in the submitted work.

Definitions.

4.

5.

Entity: government agency, foundation, commercial sponsor, academic institution, etc.
Grant: A grant from an entity, generally [but not always] paid to your organization
Personal Fees: Monies paid to you for services rendered, generally honoraria, royalties, or fees for consulting , lectures, speakers bureaus, expert testimony, employment, or other affiliations
Non-Financial Support: Examples include drugs/equipment supplied by the entity, travel paid by the entity, writing assistance, administrative support, etc**.**

Other: Anything not covered under the previous three boxes
Pending: The patent has been filed but not issued
Issued: The patent has been issued by the agency
Licensed: The patent has been licensed to an entity, whether earning royalties or not
Royalties: Funds are coming in to you or your institution due to your patent

ICMJE Form for Disclosure of Potential Conflicts of Interest

Section 1. Identifying Information

1. Given Name (First Name) 2. Surname (Last Name) 3. Date

4. Are you the corresponding author? ☐ Yes ☐ No

5. Manuscript Title

6. Manuscript Identifying Number (if you know it)

Section 2. The Work Under Consideration for Publication

Did you or your institution **at any time** receive payment or services from a third party (government, commercial, private foundation, etc.) for any aspect of the submitted work (including but not limited to grants, data monitoring board, study design, manuscript preparation, statistical analysis, etc.)?

Are there any relevant conflicts of interest? ☐ Yes ☐ No

ADD

Section 3. Relevant financial activities outside the submitted work.

Place a check in the appropriate boxes in the table to indicate whether you have financial relationships (regardless of amount of compensation) with entities as described in the instructions. Use one line for each entity; add as many lines as you need by clicking the "Add +" box. You should report relationships that were **present during the 36 months prior to publication**.

Are there any relevant conflicts of interest? ☐ Yes ☐ No

ADD

Section 4. Intellectual Property -- Patents & Copyrights

Do you have any patents, whether planned, pending or issued, broadly relevant to the work? ☐ Yes ☐ No

Section 5. Relationships not covered above

Are there other relationships or activities that readers could perceive to have influenced, or that give the appearance of potentially influencing, what you wrote in the submitted work?

☐ Yes, the following relationships/conditions/circumstances are present (explain below):

☐ No other relationships/conditions/circumstances that present a potential conflict of interest

ICMJE Form for Disclosure of Potential Conflicts of Interest

At the time of manuscript acceptance, journals will ask authors to confirm and, if necessary, update their disclosure statements. On occasion, journals may ask authors to disclose further information about reported relationships.

Section 6. Disclosure Statement

Based on the above disclosures, this form will automatically generate a disclosure statement, which will appear in the box below.

Generate Disclosure Statement

Evaluation and Feedback

Please visit http://www.ICMJE.org/cgi-bin/feedback to provide feedback on your experience with completing this form.

Declaration of interests

☒ The authors declare that they have no known competing financial interests or personal relationships that could have appeared to influence the work reported in this paper.

☐The authors declare the following financial interests/personal relationships which may be considered as potential competing interests:

Evaluation of bone and kidney toxicity of BT2-peg2, a potential carrier for the targeted delivery of antibiotics to bone

Zaineb A.F. Albayati[a], Narsimha R. Penthala[a], Shobanbabu Bommagani[a], Ginell R. Post[b], Mark S. Smeltzer[c] and Peter A. Crooks[a]*

[a]Department of Pharmaceutical Sciences, College of Pharmacy, University of Arkansas for Medical Sciences, Little Rock, AR 72205
[b]Department of Clinical Pathology, College of Medicine, University of Arkansas for Medical Sciences, Little Rock, AR 72205
[c]Department of Microbiology & Immunology, College of Medicine, University of Arkansas for Medical Sciences, Little Rock, AR 72205

BT2-peg2 (9)

^{1}H NMR (400 MHz, DMSO-d_6): δ 2.94 (t, J = 4.8, Hz, s, 2H, 6′ CH$_2$), 3.63 (m, 4H, 4′,5′ CH$_2$), 3.73 (m, 2H, 3′, CH$_2$), 3.88 (s, 3H, C$_6$-OCH$_3$), 4.11 (s, 2H, 2′ CH$_2$), 6.54 (d, J = 8.8 Hz, 1H, C$_5$-H), 8.05 (brs, 2H, NH$_2$),8.15 (d, J = 9.2 Hz, 1H, C$_4$-H), 8.30 (s, 1H, C$_1$-amide H), 8.35 (s, 1H, C$_1$-amide H), 8.87 (s, 1H, C$_3$-amide H) *ppm*. ^{13}C NMR (100 MHz, DMSO-d_6): δ 38.85, 56.59, 67.12, 69.90, 70.52, 70.70, 100.70, 102.95, 120.59, 124.66, 154.66, 155.19, 167.93, 172.26 *ppm*. M/z calculated, 328.3370, found: 328.200.

172.26
167.93
155.19
154.66
124.66
120.59
102.95
100.70
70.70
70.52
69.90
67.12
56.59
40.57
40.36
40.15
39.94
39.73
39.52
39.31
38.85

f1 (ppm)

200 190 180 170 160 150 140 130 120 110 100 90 80 70 60 50 40 30 20 10 0
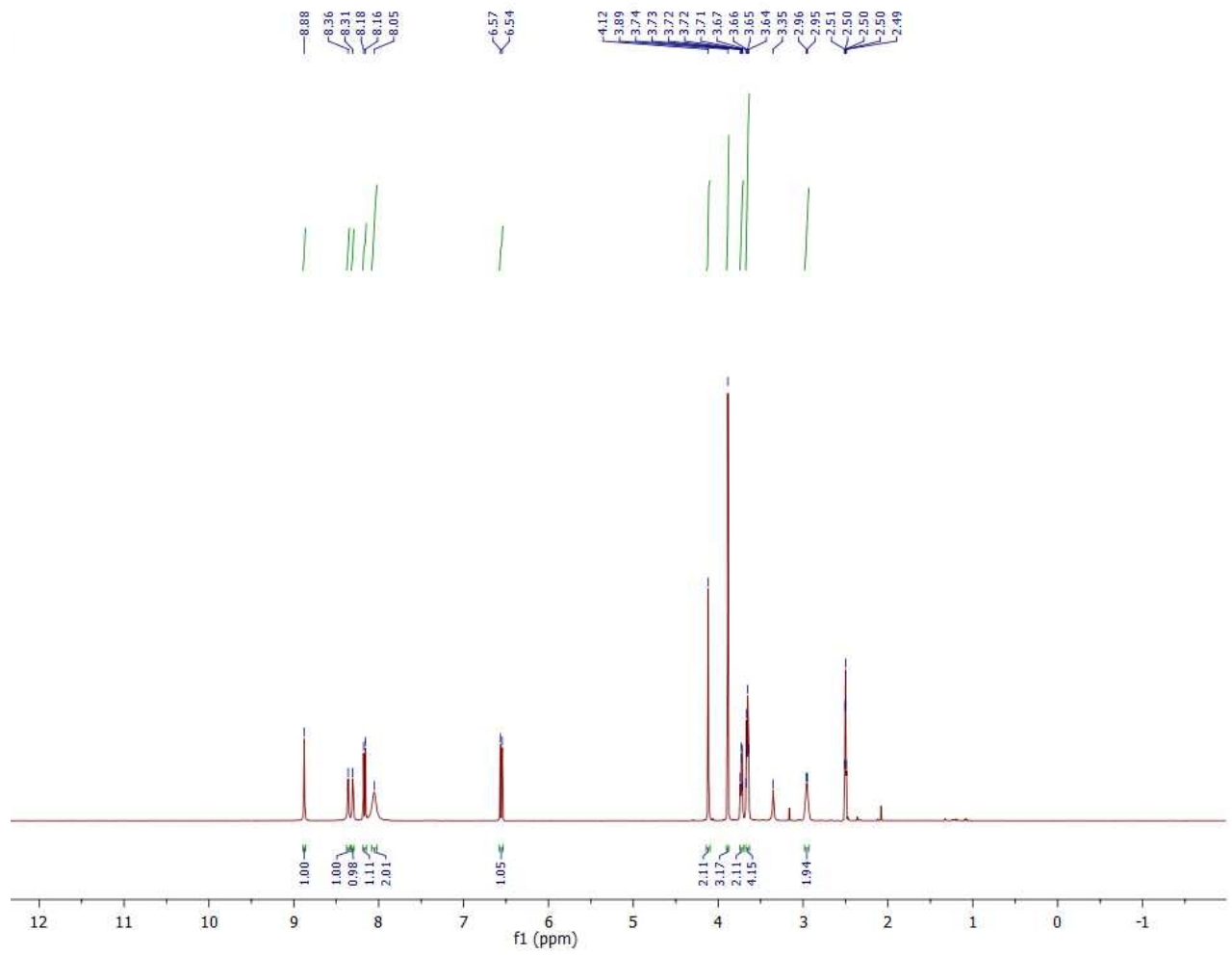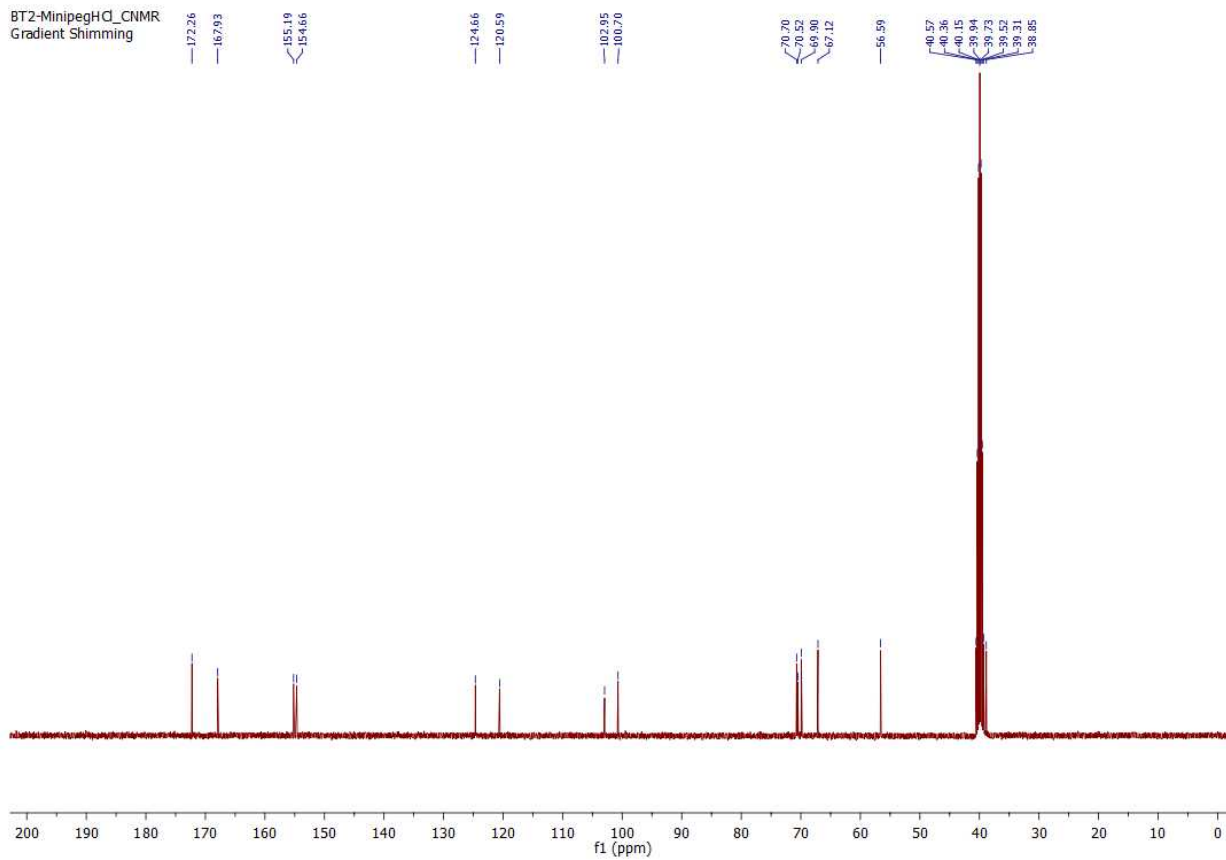
Sample Name	Unavailable	Position	Unavailable	Instrument Name	Unavailable	User Name	
Inj Vol	Unavailable	InjPosition	Unavailable	SampleType	Unavailable	IRM Calibration Status	
Data Filename	BT2-minipeg2-MP-5uL-	ACQ Method		Comment	Sample information is unavailable	Acquired Time	
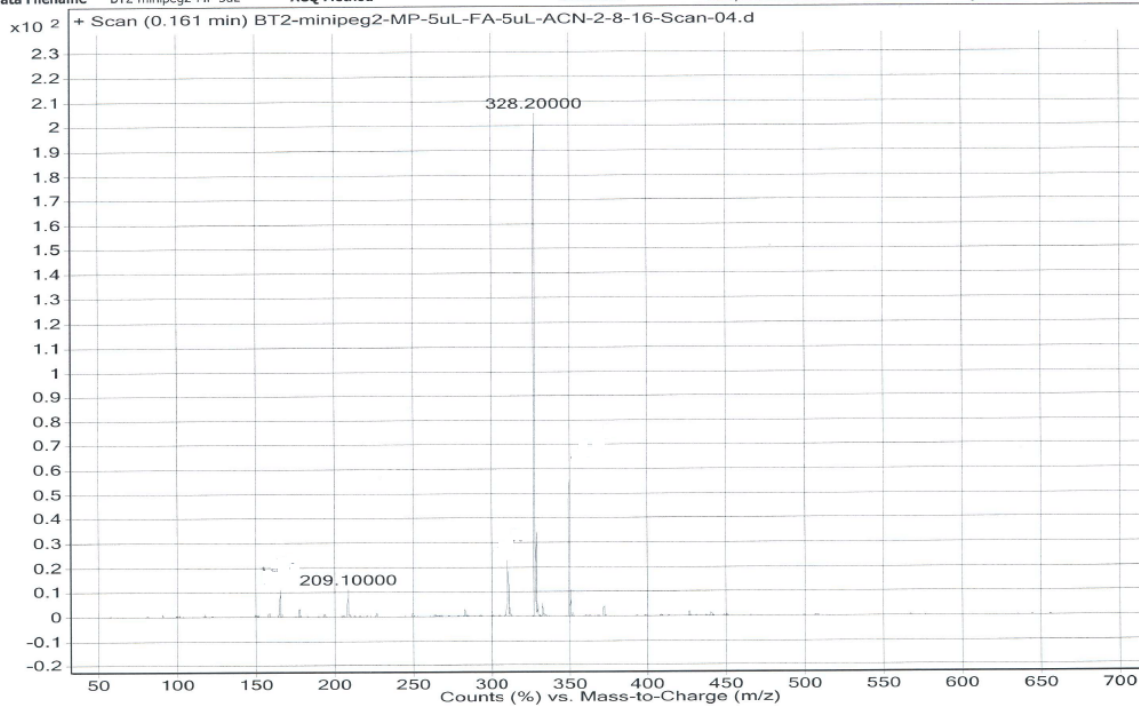
x10 2 + Scan (0.161 min) BT2-minipeg2-MP-5uL-FA-5uL-ACN-2-8-16-Scan-04.d

328.20000

209.10000

Counts (%) vs. Mass-to-Charge (m/z)

Exploiting Correlations between Protein Abundance and the Functional Status of *saeRS* and *sarA* To Identify Virulence Factors of Potential Importance in the Pathogenesis of *Staphylococcus aureus* Osteomyelitis

Aura M. Ramirez,[†] Stephanie D. Byrum,[‡,§] Karen E. Beenken,[†] Charity Washam,[‡,§] Rick D. Edmondson,[‡] Samuel G. Mackintosh,[‡] Horace J. Spencer,[∥] Alan J. Tackett,[‡,§] and Mark S. Smeltzer*,[†,⊥]

[†]Department of Microbiology and Immunology, College of Medicine, University of Arkansas for Medical Sciences, 4301 W. Markham Street, Slot 511, Little Rock, Arkansas 72205, United States

[‡]Department of Biochemistry and Molecular Biology, University of Arkansas for Medical Sciences, 4301 W. Markham Street, Slot 516, Little Rock, Arkansas 72205, United States

[§]Arkansas Children's Research Institute, 1 Children's Way, Little Rock, Arkansas 72202, United States

[∥]Department of Biostatistics, University of Arkansas for Medical Sciences, 4301 W. Markham Street, Little Rock, Arkansas 72205, United States

[⊥]Department of Orthopaedic Surgery, University of Arkansas for Medical Sciences, 4301 W. Markham Street, Slot 531, Little Rock, Arkansas 72205, United States

ⓢ *Supporting Information*

ABSTRACT: We used a murine model of postsurgical osteomyelitis (OM) to evaluate the relative virulence of the *Staphylococcus aureus* strain LAC and five isogenic variants that differ in the functional status of *saeRS* and *sarA* relative to each other. LAC and a variant in which *saeRS* activity is increased (*sae*[C]) were comparably virulent to each other, while Δ*saeRS*, Δ*sarA*, Δ*saeRS*/Δ*sarA*, and *sae*[C]/Δ*sarA* mutants were all attenuated to a comparable degree. Phenotypic comparisons including a mass-based proteomics approach that allowed us to assess the number and abundance of full-length proteins suggested that mutation of *saeRS* attenuates virulence in our OM model owing primarily to the decreased production of *S. aureus* virulence factors, while mutation of

sarA does so owing to protease-mediated degradation of these same virulence factors. This was confirmed by demonstrating that eliminating protease production restored virulence to a greater extent in a LAC *sarA* mutant than in the isogenic *saeRS* mutant. Irrespective of the mechanism involved, mutation of *saeRS* or *sarA* was shown to result in reduced accumulation of virulence factors of potential importance. Thus, using our proteomics approach we correlated the abundance of specific proteins with virulence in these six strains and identified 14 proteins that were present in a significantly increased amount (log$_2$ ≥ 5.0) in both virulent strains by comparison to all four attenuated strains. We examined biofilm formation and virulence in our OM model using a LAC mutant unable to produce one of these 14 proteins, specifically staphylocoagulase. The results confirmed that mutation of *coa* limits biofilm formation and, to a lesser extent, virulence in our OM model, although in both cases the limitation was reduced by comparison to the isogenic *sarA* mutant.

KEYWORDS: *Staphylococcus aureus, osteomyelitis, virulence factors, biofilm, protease, proteomics*
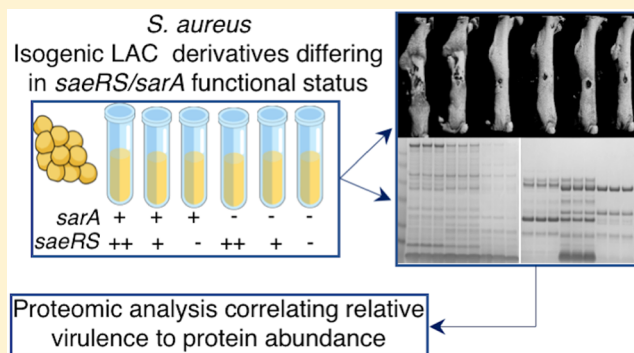
*S*taphylococcus aureus is the principal cause of osteomyelitis (OM) and other forms of orthopedic infection including those associated with the presence of an indwelling prosthesis. The medical treatment of these infections is complicated by a compromised localized vasculature, the presence of a biofilm, and the presence of bacterial variants (e.g., persister cells) with reduced metabolic activity and consequently increased anti-

biotic tolerance.[1] The continued emergence of antibiotic resistant strains, most notably methicillin-resistant *S. aureus* (MRSA), further complicates the success of traditional antibiotic-based therapies.[1] For these reasons, the majority of
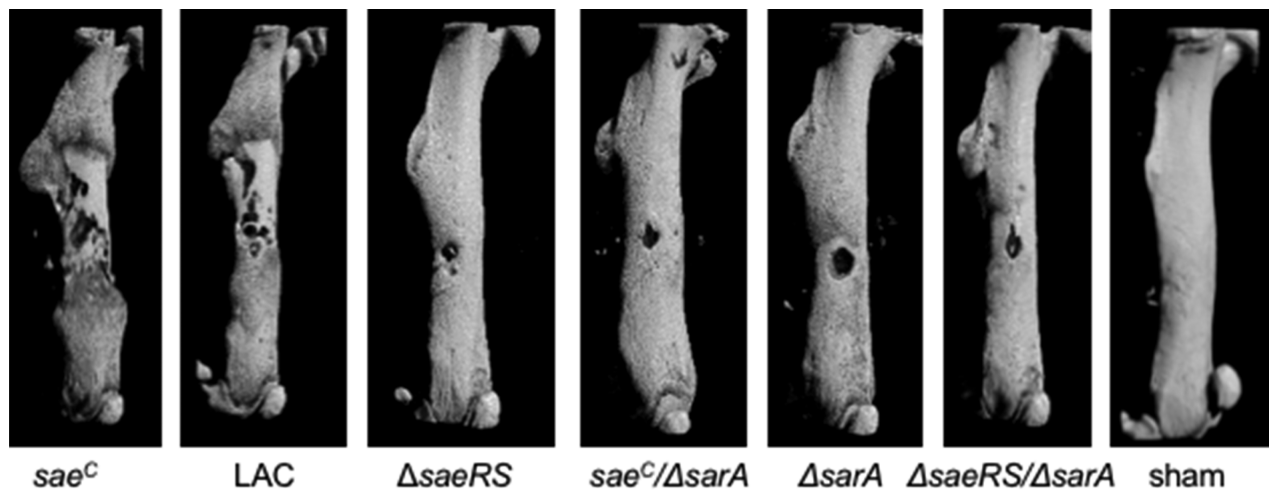
Figure 1. Impact of the functional status of *saeRS* and *sarA* in post-traumatic osteomyelitis. A murine model of post-traumatic osteomyelitis was used to assess the relative virulence of LAC, its *sarA* mutant (Δ*sarA*), and isogenic derivatives of each of these strain in which *saeRS* was either mutated (Δ*sae*) or exhibited enhanced activity (*sae*^C). Bones were imaged by *μ*CT 14 days after initiation of the infection. The sham was subjected to the surgical procedure in the absence of infection. Representative images are shown from mice in each experimental group of these seven experimental groups.

OM cases caused by *S. aureus* require surgical intervention in addition to long-term, intensive antibiotic therapy.[2] Even after such intensive medical and surgical intervention the recurrence rate remains unacceptably high.[1] Identifying critical *S. aureus* virulence factors, and improving our understanding of how these factors impact pathogenesis in OM, is key to potentially finding new therapeutic targets that can be exploited to better address this clinical problem.

One approach to identifying such virulence factors is to exploit the impact of regulatory loci in the specific context of the pathogenesis of OM. Regulatory circuits in *S. aureus* are complex and highly interactive, thus allowing the bacterium to adjust the production of its many virulence factors to diverse microenvironments within the host.[3] In the specific case of OM, it has been demonstrated that mutation of the staphylococcal accessory regulator (*sarA*) or the *S. aureus* exoprotein (*saeRS*) regulatory locus attenuates virulence in a murine model of postsurgical OM as assessed by both cortical bone loss and reactive bone (callus) formation.[4,5] Mutation of both loci has also been shown to result in the increased production of extracellular proteases and decreased accumulation of specific virulence factors including alpha toxin, phenol-soluble modulins (PSMs) and protein A (Spa).[5−9] In fact, the increased production of extracellular proteases, specifically aureolysin, has been shown to play a significant role in defining the attenuation of a LAC *saeRS* mutant owing to the decreased accumulation of PSMs.[6]

Mutation of *sarA* also results in reduced accumulation of PSMs owing to protease-mediated degradation, and in fact mutation of *sarA* results in a much greater increase in protease production than mutation of *saeRS*.[7−9] This suggests that mutation of *sarA* may attenuate the virulence of LAC to an even greater extent than mutation of *saeRS*. However, the accumulation of any protein is a function of its production vs its degradation, and our studies suggest that the primary impact of mutating *saeRS* on virulence is due to reduced production of *S. aureus* virulence factors, while that of mutating *sarA* is due to protease-mediated degradation of these virulence factors.[7,8] Thus, the relative impact of these two regulatory loci in the context of OM remains unknown. To

assess this experimentally, we evaluated the virulence of LAC and five isogenic derivatives that differ with respect to the functional status of *saeRS* and *sarA* relative to each other. Comparisons were made using a murine model of postsurgical OM.[4,5] We then took advantage of the results of these studies to identify and prioritize specific virulence factors of potential relevance by correlating relative virulence with the accumulation of full-length proteins present in conditioned medium (CM) from stationary phase cultures of the same strains.

■ RESULTS

Mutation of *saeRS* or *sarA* Attenuates the Virulence of LAC in OM to a Comparable Degree. We previously generated five derivatives of LAC that vary with respect to the functional status of *saeRS* and *sarA* relative to each other.[6,7] To assess the relative virulence of these strains, we employed a murine model of postsurgical osteomyelitis.[4,5] Briefly, a unicortical defect was created in the femur of mice. LAC or one of these five isogenic derivatives was then inoculated directly into the medullary canal. After 14 days, infected bones were harvested and analyzed by microcomputed tomography (*μ*CT). Duplicate samples were also harvested and processed to determine bacterial burdens in the femur. By comparison to uninfected mice subjected to the same surgical procedure (sham), the femurs of all infected mice showed marked callus formation adjacent to the inoculation site and extending to the proximal and distal ends of the femur (Figure 1). In sham mice, the unicortical defect was almost completely sealed, while this was not the case with any of the infected mice irrespective of the strain used to initiate the infection.

To quantitatively assess virulence differences between these strains, *μ*CT images were analyzed to assess relative levels of callus formation and cortical bone destruction. As assessed based on both parameters, LAC and its derivative with increased activation of *saeRS* (*sae*^C) were comparably virulent (Figure 2). As previously reported,[4,5] mutation of *saeRS* (Δ*saeRS*) and/or *sarA* (Δ*sarA*) resulted in decreased callus formation and cortical bone destruction. The functional status of *saeRS* did not have a statistically significant effect in the *sarA* mutant with respect to either of these parameters, but there did
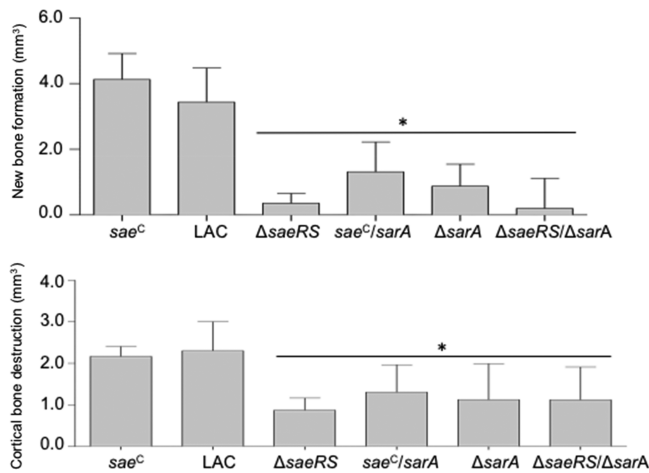
Figure 2. Quantitative assessment of reactive bone formation and cortical bone destruction as a function of *saeRS* and *sarA*. Analysis of μCT images was used to assess reactive new bone formation (top) and cortical bone destruction (bottom) in each of 5 mice infected with the indicated strains. Statistical analysis was done by one-way ANOVA with Dunnett's correction. Asterisk (*) indicates a significant difference relative to LAC.

appear to be a trend suggesting that reactive bone formation decreased as the combined activity of both *sae* and *sarA* decreased (Figure 2). Similarly, while the difference did not reach statistical significance, mutation of *saeRS* appeared to limit callus formation to a greater extent than mutation of *sarA*.

In addition to μCT analysis, we also quantified bacterial burdens in the femur. By comparison to LAC, we did not observe a statistically significant difference in bacterial burdens in the femurs of mice infected with the *sae*[C] derivative, the Δ*sarA* mutant, or the *sae*[C]/Δ*sarA* mutant (Figure 3). Significantly reduced bacterial burdens were observed in the femurs of mice infected with the Δ*saeRS* mutant. Specifically, no bacteria were recovered from the femurs of 60% of the mice infected with this strain. The number of bacteria recovered from the remaining 40% of these mice ranged from 10^4 to 10^5
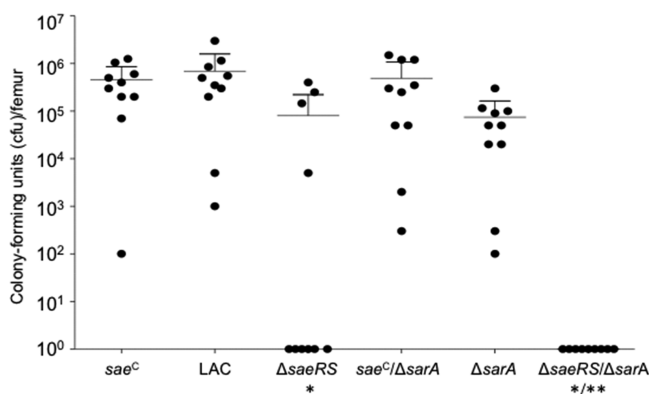
Figure 3. Bacterial burdens in the bone as a function of *saeRS* and *sarA*. Femurs were harvested from mice infected with each of the indicated strains 14 days after infection. Femurs were flash frozen, pulverized, and sonicated before removing tissue debris by low speed centrifugation. Supernatants were then serially diluted and plated on TSA to determine the number of viable bacteria per femur. Single asterisk (*) indicates a significant difference relative to LAC. Double asterisks (**) indicates a statistical significance relative to the Δ*saeRS* mutant.

cfu per femur. The reasons for this variability are unclear. However, these experiments were done as two independent biological replicates, and most, but not all, of the mice in which no viable bacteria were recovered were included in the first replicate. Nevertheless, these results are consistent with a previous report that also found that bacterial burdens were reduced in a LAC Δ*sae* mutant.[5] Moreover, no viable bacteria were recovered from any of the femurs of mice infected with the Δ*saeRS*/Δ*sarA* double mutant (Figure 3). This suggests that *sarA*, which had not been previously examined in this regard, also contributes to the ability of *S. aureus* to persist in the bone as defined by the 14-day postinfection period we employed and that concomitant mutation of *saeRS* and *sarA* has an additive effect in this regard. Taken together with the μCT data, our results indicate that *saeRS* and *sarA* contribute to the pathogenesis of OM to a comparable degree.

Correlations between Virulence, Protease Production, and Protein Abundance. Mutation of *saeRS* or *sarA* has been shown to result in the increased production of extracellular proteases, and this has been correlated with reduced accumulation of specific virulence factors and reduced virulence.[6−8] We confirmed that mutation of *saeRS* or *sarA* results in increased protease activity and that mutation of *sarA* has a much greater impact in this regard than mutation of *saeRS* (Figure 4). The impact of mutating *saeRS* and *sarA* on
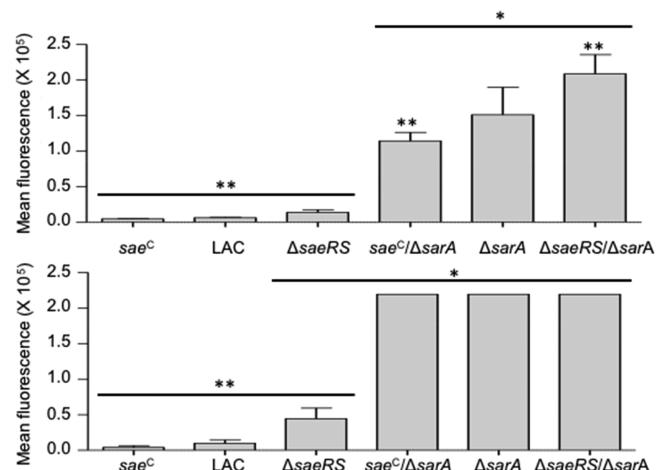
Figure 4. Impact of *saeRS* and *sarA* on protease activity. Overall protease activity was determined in conditioned medium (CM) from stationary phase cultures of LAC, its *sarA* mutant (Δ*sarA*), and isogenic derivatives of each in which *saeRS* was either constitutively expressed (*sae*[C]) or mutated (Δ*saeRS*). Protease activity was determined using a FRET based assay (EnzChek Gelatinase/Collagenase Assay Kit, Molecular Probes) after incubation for 2 h (top) or 16 h (bottom). Statistical analysis was done by one-way ANOVA with Dunnett's correction. A single asterisk (*) indicates a significant difference relative to LAC. Double asterisks (**) indicate statistical significance relative to the *sarA* mutant.

protease production was additive in that a statistically significant difference was observed between the *sarA* and *saeRS*/*sarA* mutants. Conversely, protease production was reduced in the Δ*sae*[C]/*sarA* mutant relative to the isogenic Δ*sarA* mutant. Although the difference in virulence between the Δ*sae*[C]/*sarA* and *sarA* mutants did not reach statistical significance (Figure 2), this is consistent with the trends we observed in our OM comparisons, and in this case the

difference between the $\Delta sae^C/sarA$ and $\Delta sarA$ mutants was statistically significant (Figure 4).

The relative levels of protease production were inversely correlated with the accumulation of high-molecular weight proteins as assessed by SDS-PAGE analysis of conditioned medium (CM) from stationary phase cultures of each of these strains. CM samples from stationary phase cultures were chosen because protease production is highest in this growth phase. We also believe that stationary phase cultures are most likely to be representative of in vivo growth conditions. Evidence to support this hypothesis comes from the observation that protease-deficient mutants have been shown to be hypervirulent in vivo in diverse animal models of infection.[9,10] The abundance of high molecular weight proteins was dramatically reduced in CM from the $\Delta sarA$ mutant, with a corresponding increase in the abundance of lower molecular weight proteins (Figure S1). This was true irrespective of the functional status of saeRS, although overall protein profiles of CM from the $sae^C/\Delta sarA$ and $\Delta saeRS/\Delta sarA$ mutants did differ from each other and from that observed in the isogenic $\Delta sarA$ mutant. This is consistent with the relative level of protease production in these strains, and it provides an additional indication that the functional status of saeRS has an impact on the phenotype of a LAC $\Delta sarA$ mutant. In contrast, the abundance of many proteins, including high molecular weight proteins, was reduced in CM from a $\Delta saeRS$ mutant, but the overall distribution of these proteins was largely unaffected (Figure S1). These observations are consistent with the hypothesis that mutation of saeRS impacts the abundance of *S. aureus* exoproteins primarily at the level of their production, while mutation of sarA does so primarily at the level of their accumulation owing to protease-mediated degradation.

To further examine this hypothesis, we carried out gel-based proteomic studies employing a novel mass-based approach that allowed us to focus specifically on spectral counts derived from full-length proteins to the exclusion of spectral counts derived from degradation products of those proteins.[11] On the basis of triplicate samples, and irrespective of the abundance of each protein, we identified an average of 1090 full-length proteins in CM from LAC and 1007 in CM from its sae^C derivative (Figure 6). An average of 763 ($\geq$70%) of these were detectable in CM from the $\Delta saeRS$ mutant. In contrast, an average of 145 and 160 full-length proteins ($\leq$15.9%) were detected in CM from the isogenic $\Delta sarA$ and $\Delta saeRS/\Delta sarA$ mutants, respectively. This number was more than doubled to an average of 349 in the $sae^C/\Delta sarA$ mutant (Figure 5), likely owing to increased protein production associated with the sae^C allele.

To assess the abundance of individual proteins, we carried out an analysis based on total spectral counts derived from full-length proteins rather than the total number of detectable proteins. The number of spectral counts was highest in the sae^C derivative (average = 21 356), slightly lower in LAC (18 709) and decreased progressively through the $\Delta saeRS$ (8485), $sae^C/\Delta sarA$ (5478), $\Delta sarA$ (3223), and $\Delta saeRS/\Delta sarA$ mutants (1746) (Figure 5). The fact that $\geq$70% of full-length proteins that were detectable in LAC and its sae^C derivative were also detectable in the $\Delta saeRS$ mutant, while this proportion was reduced to $\leq$45% when comparisons were made based on total spectral counts, is consistent with the hypothesis that the primary mechanism by which saeRS impacts exoprotein accumulation is at the level of production. Similarly, the fact
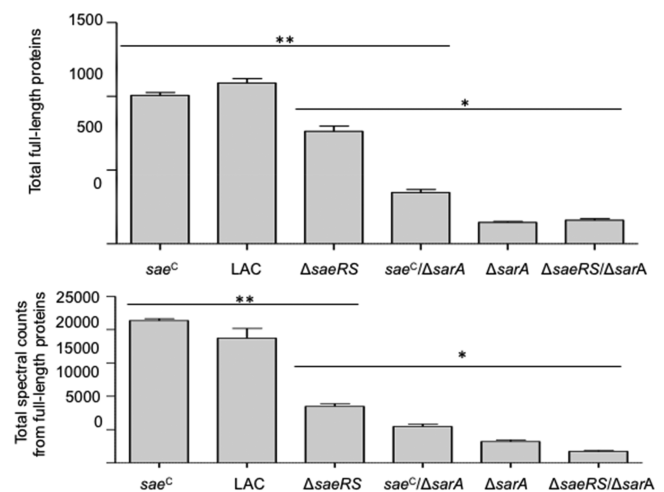
Figure 5. Impact of *sarA* and *saeRS* on relative abundance of full-length proteins. CM from LAC and five derivatives that differ with respect to the functional status of *saeRS* and *sarA* was analyzed in triplicate using a novel mass-based proteomics approach that allows us to focus on quantifying only full-length functional proteins.[11] The top panel illustrates the average number of full-length proteins identified in CM from each strain irrespective of the amount of each protein. The bottom panel illustrates the average number of spectral counts obtained from full-length proteins in CM from each strain. Statistical analysis was done by one-way ANOVA with Dunnett's correction. A single asterisk (*) indicates a significant difference relative to LAC. Double asterisks (**) indicate statistical significance relative to the *sarA* mutant.

that the decrease observed with the $\Delta sarA$ mutant was comparable whether assessed by total proteins ($\leq$14%) or spectral counts ($\leq$17%) is consistent with the hypothesis that the impact of mutating sarA occurs primarily at the level of protease-mediated degradation. However, irrespective of the mechanism responsible, the association between relative virulence (Figure 2) and the number of spectral counts derived from full-length proteins (Figure 5) suggests that defining correlations among these strains between relative virulence and protein abundance as defined based on spectral counts derived from full-length proteins has the potential to identify *S. aureus* virulence factors that are potentially important in the pathogenesis of OM.

To this end, we explored two different methods of data analysis to identify proteins that were increased in abundance in LAC and its sae^C by comparison to all four of the attenuated strains ($\Delta saeRS$, $saeRS^C/\Delta sarA$, $\Delta sarA$, $\Delta saeRS/\Delta sarA$). In the first approach, we did individual pairwise comparisons (t test) between each of the two most virulent strains and each of the four attenuated strains. Comparisons were made on the basis of statistical significance ($p \leq 0.05$) using a $\log_2$ fold-change (FC) cutoff of $\geq$2, which corresponds to an absolute FC $\geq$ 4. The list of proteins meeting these criteria in each pairwise comparison was then compared, using Venny 2.1,[12] to identify proteins that were increased in both virulent strains by comparison to all four attenuated mutants. This resulted in the identification of a common set of 114 proteins (Figure 6 and Table S1).

To prioritize among these 114 proteins, we increased the stringency to a $\log_2$ FC $\geq$ 5, which corresponds to an absolute FC $\geq$ 32. This narrowed the list of high priority targets that differed between virulent and attenuated strains from 114 to 10. To validate these results, we also analyzed the entire
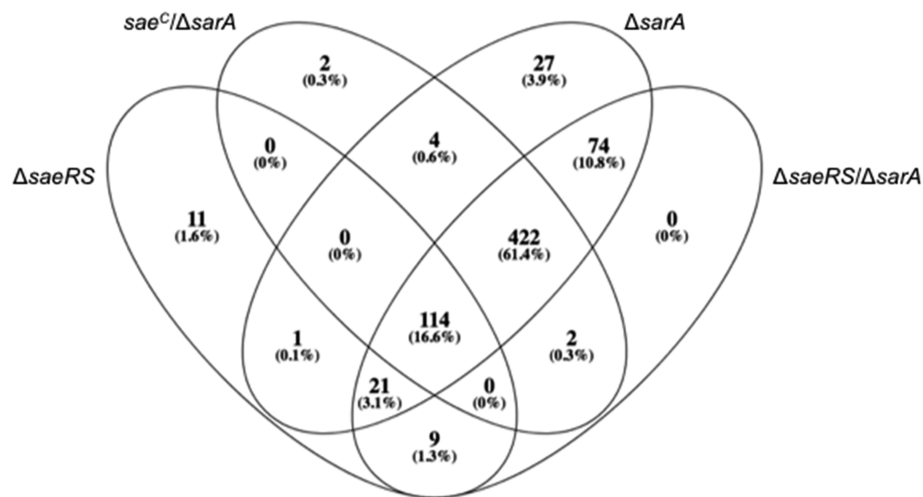
Figure 6. Venn diagram indicating overlap between proteins present in conditioned medium from LAC and its *saeRS* and *sarA* mutants. Conditioned medium (CM) from three independent stationary phase cultures of each strain were resolved by SDS-PAGE and stained with Coomassie Blue (Figure S1). The number of proteins identified as significantly differing ($p \leq 0.05$; $\log_2$ FC ≥ 2) between both of the virulent strains (*sae*^{C} and LAC) compared to each attenuated strain are shown.

proteome data set using the edgeR generalized linear model quasi-likelihood (glmQLT) method.[13,14] This statistical analysis allowed us to compare spectral counts obtained from full-length proteins present in CM from the virulent (LAC and its *sae*^{C} derivative) vs attenuated (*sae*^{C} and LAC vs Δ*saeRS*, *sae*^{C}/Δ*sarA*, Δ*sarA*, Δ*saeRS*/Δ*sarA*). Using this approach, we identified 333 proteins that were significantly increased ($p \leq 0.05$; $\log_2$ FC ≥ 2) in both virulent strains by comparison to all four attenuated strains (Figure 7 and Table S2). To further prioritize among these, we then selected those proteins exhibiting a $\log_2$ FC ≥ 5. Using this approach, 11 proteins were identified that differed in abundance between virulent and attenuated strains.
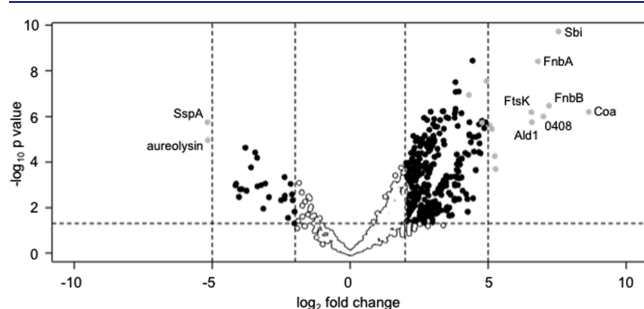
Figure 7. Differential protein accumulation in virulent versus attenuated strains. Volcano plot showing the $\log_2$ fold change (*x*-axis) and $-\log_{10}$ FDR-adjusted *p*-value (*y*-axis) of each protein identified in each strain. Inner vertical lines indicate a $\log_2$ fold change of 2.0. Outer vertical lines indicate a $\log_2$ fold change of 5.0. Proteins that were not found to differ significantly (as defined by an FDR corrected *p*-value ≥0.05 and a fold change ≤2) between virulent and attenuated strains using the quasi-likelihood analysis method are shown as open circles. Proteins in which the abundance was statistically significant ($p \leq 0.05$) and the $\log_2$ fold change ≥2.0 but ≤5.0 as defined by both data analysis methods are shown in black. Proteins in which the $\log_2$ fold change was ≥5.0 as defined by at least one data analysis method are shown in gray. The 7 proteins identified as present in significantly increased amounts in both virulent strains by comparison to all four attenuated strains by both analysis methods are labeled in the upper right quadrant.

The list of proteins prioritized with each analysis method were similar but not identical. Thus, using both analysis methods we identified a total of 14 proteins that differed in abundance by a $\log_2$ FC ≥ 5 in both virulent strains vs all four attenuated strains (Table 1). Of these, 3 were identified using the pairwise analysis method but not the quasi-likelihood GLM method (Table 1). Similarly, 4 were identified using the quasi-likelihood GLM method but not the pairwise analysis method. The other 7 proteins were identified using both data analysis methods (Table 1, Figure 7). These 7 proteins were the fibronectin-binding proteins FnbA and FnbB, Sbi, staphylocoagulase, an FtsK/SpoIII family protein, alanine dehydrogenase 1, and an uncharacterized putative surface protein encoded by SAUSA300_0408. All 7 of these were also identified in our previous study focusing solely on identifying proteins that are present in reduced amounts in a LAC *sarA* mutant owing to protease-mediated degradation,[11] an observation that we believe further validates our experimental approach. It is also interesting to note that the only two proteins found to be present at a level $\log_2$ FC ≥ 5 in all four attenuated strains vs both of the more virulent strains were the extracellular proteases aureolysin and SspA (Figure 7).

Investigating the Role of Staphylocoagulase. As a first step toward ultimately examining the hypothesis that the specific proteins identified in our studies play a role in the pathogenesis of OM, we began the process of generating mutations in the genes encoding these proteins. We initially employed transduction from existing mutants in the Nebraska Transposon Mutant Library (NTML),[15] and among the first of our successful transductions was the mutation in the gene encoding staphylocoagulase (*coa*). We chose to move forward with these mutants based on previous reports suggesting that coagulase plays an important role in immune evasion, biofilm formation[16] and osteoblast physiology.[17] We confirmed that all 7 LAC Δ*coa* mutants generated by transduction from the NTML *coa* mutant exhibited a reduced capacity to form a biofilm by comparison to LAC, albeit to a lesser extent than was observed in the isogenic *sarA* mutant (Figure 8). We also assessed the relative virulence of one of these Δ*coa* mutants in our OM model, and while trends were evident with respect to a reduction in both new bone formation and cortical bone

Table 1. Proteins Selected as Priority Targets for Further Studies

protein	gene	accession number	localization	molecular weight (kDa)	method
Immunoglobulin-binding protein sbi	sbi	SBI_STAA3	unknown	50	both
Staphylocoagulase	coa	A0A0H2XHP9_STAA3	extracellular	69	both
Fibronectin binding protein B	fnbB	A0A0H2XKG3_STAA3	cell wall	104	both
Alanine dehydrogenase 1	ald1	DHA1_STAA3	cytoplasmic	40	both
FtsK/SpollE family protein	SAUSA300_1687	A0A0H2XK12_STAA3	membrane	145	both
Fibronectin-binding protein A	fnbA	FNBA_STAA3	cell wall	112	both
Putative surface protein	SAUSA300_0408	A0A0H2XJZ9_STAA3	unknown	57	both
Uncharacterized leukocidin-like protein 2	SAUSA300_1975	LUKL2_STAA3	extracellular	40	pairwise
Uncharacterized leukocidin-like protein 1	SAUSA300_1974	LUKL1_STAA3	extracellular	39	pairwise
Putative staphylocoagulase	SAUSA300_0773	A0A0H2XEN7_STAA3	extracellular	59	pairwise
Transcriptional regulatory protein WalR	walR	WALR_STAA3	cytoplasmic	27	GLM
Uncharacterized protein	SAUSA300_0198	A0A0H2XFU2_STAA3	unknown	36	GLM
Serine protease HtrA-like	SAUSA300_0923	HTRAL_STAA3	unknown	86	GLM
Protein RecA	recA	A0A0H2XFW9_STAA3	cytoplasmic	35	GLM
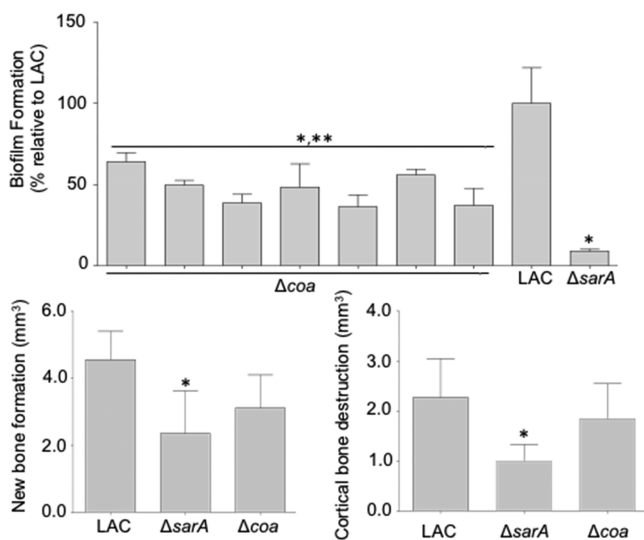
Figure 8. Impact of staphylocoagulase on biofilm formation and osteomyelitis. The top panel illustrates the relative levels of biofilm formation in LAC, its isogenic sarA mutant, and each of 7 independently generated LAC coa mutants. Assays were performed in 3 replicates and the average observed with LAC set to 100%. All other results are shown relative to this value. The bottom panel illustrates quantitative assessment of reactive bone formation (left) and cortical bone destruction (right) in ΔsarA and Δcoa mutants relative to the LAC parent strain. Statistical analysis was done by one-way ANOVA with Dunnett's correction. A single asterisk (*) indicates a significant difference relative to LAC. Double asterisks (**) indicate statistical significance relative to the ΔsarA mutant.

Figure 9. Impact of the functional status of saeRS and sarA on biofilm formation. Biofilm formation was assessed in each of the indicated strains. Assays were performed in 6 replicates and the average observed with LAC set to 100%. All other results, including each of the 6 individual LAC replicates, are shown relative to this value. Statistical analysis was done by one-way ANOVA with Dunnett's correction. A single asterisk (*) indicates a significant difference relative to LAC. Double asterisks (**) indicate statistical significance relative to the ΔsarA and ΔsaeRS/ΔsarA mutants.

destruction, neither of these differences were found to be statistically significant by comparison to LAC (Figure 8).

Investigating Potential Mechanisms of Attenuation Associated with Mutation of saeRS and/or sarA. The pathogenesis of OM is complex and incompletely understood, but two phenotypes that have been implicated as important contributing factors are biofilm formation and cytotoxicity for osteoblast and/or osteoclasts.[6,9,18−20] These are difficult phenotypes to assess directly in vivo, but they can be readily assessed in vitro. Thus, we examined each of these to determine whether the impact of saeRS and sarA on these phenotypes could be correlated with relative virulence. As previously demonstrated,[6,7] we found that mutation of sarA limited biofilm formation to a much greater extent than

mutation of saeRS, and this was true irrespective of the functional status of saeRS (Figure 9). However, biofilm

formation was increased to a statistically significant extent in the saeᶜ/ΔsarA mutant relative to the ΔsarA and ΔsaeRS/ΔsarA mutants. Similar trends were observed in the context of osteoblast and osteoclast cytotoxicity. Specifically, CM from stationary phase cultures of LAC, its saeᶜ derivative, and its ΔsaeRS mutant were comparably cytotoxic for both cell types, while mutation of sarA largely eliminated this cytotoxicity (Figure 10).

A primary reason we carried out these in vitro studies was to determine whether any of these phenotypes could be definitively correlated with differences in virulence we observed in our OM model. If so, this would greatly facilitate the ability to examine a large number of potential targets prior to proceeding to in vivo analysis. However, while biofilm formation and cytotoxicity were significantly reduced in 3 of the 4 attenuated strains, neither was significantly reduced in the ΔsaeRS mutant. One possible explanation for this is that the magnitude of the impact of mutating sarA on protease production as assessed under in vitro conditions is sufficient to be apparent in the context of biofilm formation and cytotoxicity, while the impact of mutating saeRS on protease production is not. However, this does not preclude the
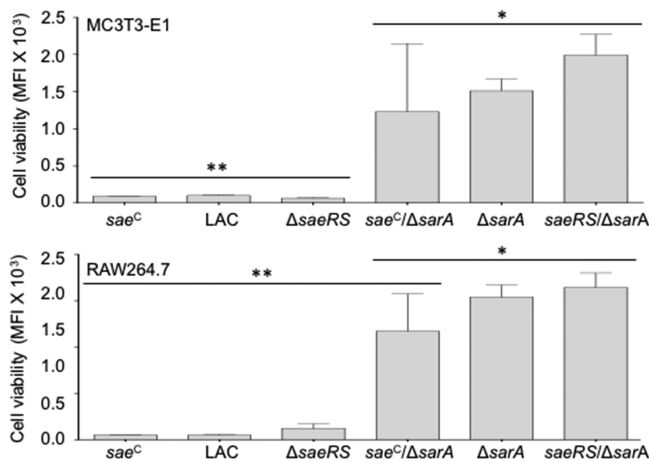
Figure 10. Impact of the functional status of *saeRS* and *sarA* on osteoblast and osteoclast cytotoxicity. Conditioned medium (CM) from stationary phase cultures of the indicated strains were added to monolayers of osteoblast (MC3T3-E1) or osteoclast-like cell lines (RAW264.7) and incubated at 37 °C for 24 h. Cell viability was then determined using a Live/Dead assay kit (Molecular Probes) in which mean fluorescence intensity (MFI) is an indication of cell viability. Statistical analysis was done by one-way ANOVA with Dunnett's correction. A single asterisk (*) indicates a significant difference relative to LAC. Double asterisks (**) indicate statistical significance relative to the Δ*sarA* and Δ*saeRS*/Δ*sarA* mutants.

possibility that mutation of *saeRS* has a greater impact in vivo in the specific microenvironment of bone.

The alternative explanation is that the mechanism by which mutation of *saeRS* attenuates virulence differs by comparison to the mechanism by which mutation of *sarA* attenuates virulence. On the basis of this possibility, we extended our analysis to identify proteins that were present in increased amounts in a LAC Δ*sarA* mutant relative to a Δ*saeRS* mutant and vice versa. Relatively few proteins were present in increased amounts in a Δ*sarA* mutant by comparison to a Δ*saeRS* mutant, but among these were all six of the *spl*-encoded proteases (Figure 11). This is consistent with our
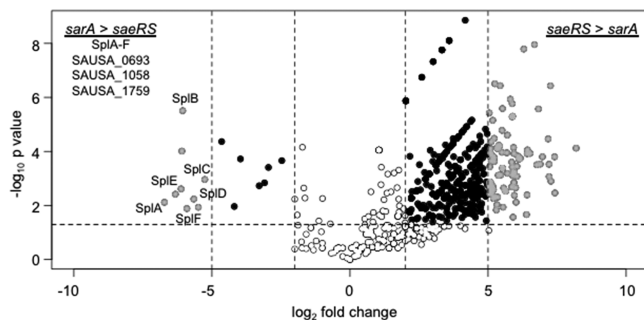
Figure 11. Differential protein accumulation in Δ*saeRS* and Δ*sarA* mutants. Volcano plot showing the $\log_2$ fold change (*x*-axis) and $-\log_{10}$ FDR-adjusted *p*-value (*y*-axis) of each protein identified in each strain. Inner vertical lines indicate a $\log_2$ fold change of 2.0. Outer vertical lines indicate a $\log_2$ fold change of 5.0. Proteins that were not found to differ significantly between the Δ*saeRS* and Δ*sarA* mutants as defined by an FDR corrected *p*-value ≥0.05 and a fold change ≤2 are shown as open circles. Proteins in which the abundance was statistically significant ($p \leq 0.05$) and the $\log_2$ fold change ≥2.0 but ≤5.0 are shown in black. Proteins in which the $\log_2$ fold change was ≥5.0 are shown in gray.

previous reports demonstrating that these proteases are present in reduced amounts in a Δ*saeRS* mutant but increased amounts in an isogenic Δ*sarA* mutant.[7] In contrast, we identified 91 proteins that were present in an increased amount in a Δ*saeRS* mutant by comparison to a Δ*sarA* mutant (Figure 11, Table S3).

Of these, 36 were present in equivalent amounts in CM from the Δ*saeRS* mutant and LAC, thus suggesting that Spl-mediated degradation may be a limiting factor in the accumulation of these proteins in a Δ*sarA* mutant. This also suggests that these proteases, or specific targets of these proteases that are present in decreased amounts in CM from a Δ*sarA* mutant, may contribute to biofilm formation and/or cytotoxicity for osteoblasts and osteoclasts as assessed under in vitro conditions. The remaining 55 proteins were present in decreased amounts in the Δ*saeRS* mutant relative to LAC and its *sae*[C] derivative. This leaves open the possibility that they contribute to the attenuation of both the Δ*saeRS* and Δ*sarA* mutants in our murine OM model, but are unlikely to contribute to the attenuation of the Δ*saeRS* mutant and not the Δ*sarA* mutant.

Finally, to further examine the hypothesis that mutation of *saeRS* limits virulence in our OM model owing primarily to its impact on protein production, while *sarA* does so owing primary to its impact on protease production and the degradation of *S. aureus* proteins, we generated derivatives of LAC and each of these mutants with a limited capacity to produce extracellular proteases. Specifically, protease-deficient derivatives of LAC and its *sarA* mutant were unable to produce aureolysin, ScpA, SspA, SspB, or any of the *spl*-encoded proteases, while the *saeRS* mutant retained the capacity to produce the *spl*-encoded proteases. However, as discussed above, mutation of *saeRS* does not result in the increased production of these proteases. Eliminating protease production restored biofilm formation and cytotoxicity in the Δ*sarA* mutant, but had little impact in the Δ*saeRS* mutant (Figure 12). This was also true in a LAC Δ*saeRS*/Δ*sarA* mutant. Moreover, as evidenced by visual assessment of μCT images, eliminating protease production restored virulence to a greater extent in the Δ*sarA* mutant than in the Δ*saeRS* mutant, and enhanced the virulence of LAC itself (Figure 13). In fact, the increased virulence observed in the protease-deficient derivatives of LAC and its Δ*sarA* mutant resulted in broken bones to an extent that precluded accurate quantitative analysis of these μCT images.

■ DISCUSSION

Osteomyelitis is a relatively infrequent form of *S. aureus* infection, but it is one that presents a unique clinical problem that demands an equally unique, multidisciplinary clinical approach.[18] This also applies to infections associated with indwelling orthopedic devices, and in this respect, it is important to recognize that the number of such infections is predicted to increase dramatically in the immediate future. Indeed, it has been estimated that the number of periprosthetic joint infections associated with total hip and knee arthroplasty in the United States will surpass 60 000 by 2020 at an annual cost that will exceed $1.62 billion.[19] This makes it imperative to develop prophylactic and therapeutic strategies that can be used to combat these infections either alone or as a means of enhancing the efficacy of conventional antibiotic therapy.

The studies we report are based on the scientific premise that a key component required for the development of such
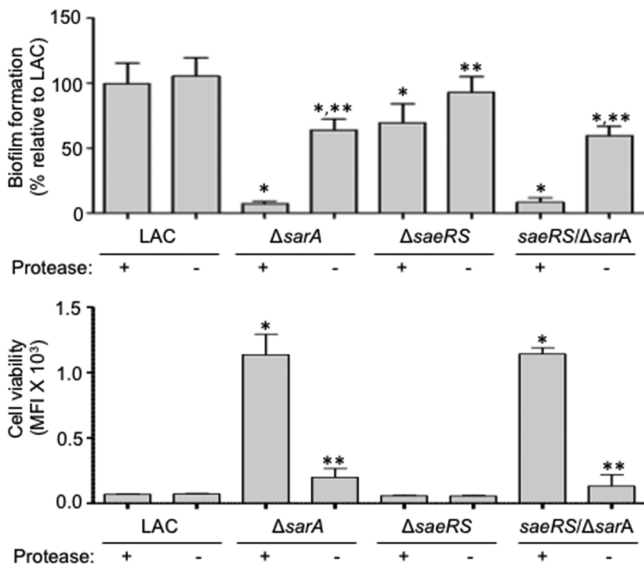
Figure 12. Impact of protease production in Δ*sarA* and Δ*saeRS* mutants in vitro. Biofilm formation (top) and osteoblast cytotoxicity (bottom) were assessed in each of the indicated strains (+) and their protease-deficient derivatives (−). Biofilm assays were performed in 6 replicates and the average observed with LAC set to 100%. All other results, including each of the 6 individual LAC replicates, are shown relative to this value. Cell viability was determined using a Live/Dead assay kit (Molecular Probes) in which mean fluorescence intensity (MFI) is an indication of cell viability. Statistical analysis was done by one-way ANOVA with Dunnett's correction. A single asterisk (*) indicates a significant difference relative to LAC. Double asterisks (**) indicate statistical significance relative to the Δ*sarA* and Δ*saeRS*/Δ*sarA* mutants.

strategies is a clear understanding of the pathogenesis of orthopedic infections that takes into consideration the specific microenvironment of bone. In this respect it is important to note that *S. aureus* is overwhelmingly the primary clinical concern based on both the frequency and severity of the infections caused by this bacterial pathogen.[18,20] It has been demonstrated that expression of *sarA* and *saeRS* is increased during the acute and chronic phases of osteomyelitis,[21,22] and previous reports have demonstrated that mutation of *saeRS* or *sarA* attenuates virulence in a murine model of postsurgical OM.[4,5] This accounts for our experimental focus on these regulatory loci in this report.

In addition, the attenuation of a LAC Δ*saeRS* mutant has been correlated with the increased production of extracellular proteases, specifically aureolysin, and the resulting decrease in the accumulation of phenol-soluble modulins (PSMs), although this could not fully explain the attenuation of a LAC Δ*saeRS* mutant.[4,5] As demonstrated in previous reports,[7,23] and confirmed in the studies reported here, mutation of *sarA* results in a much greater increase in protease production than mutation of *saeRS*. This suggests that mutation of *sarA* would attenuate virulence in OM even by comparison to a Δ*saeRS* mutant.

To address this, we took advantage of our previous studies demonstrating that mutation of *saeRS* or *sarA* attenuates virulence to a comparable degree in a murine bacteremia model[6] to define the relative virulence of LAC and five isogenic derivatives that differ with respect to the functional status of *saeRS* and *sarA* in a murine model of postsurgical OM. The results demonstrated that mutation of *saeRS* or *sarA* also attenuates virulence in this model to a comparable degree (Figure 2). The attenuation observed with the LAC Δ*sarA* mutant was reversed to a limited extent in the *sae*[C]/*sarA* mutant, but the difference was not statistically significant in the
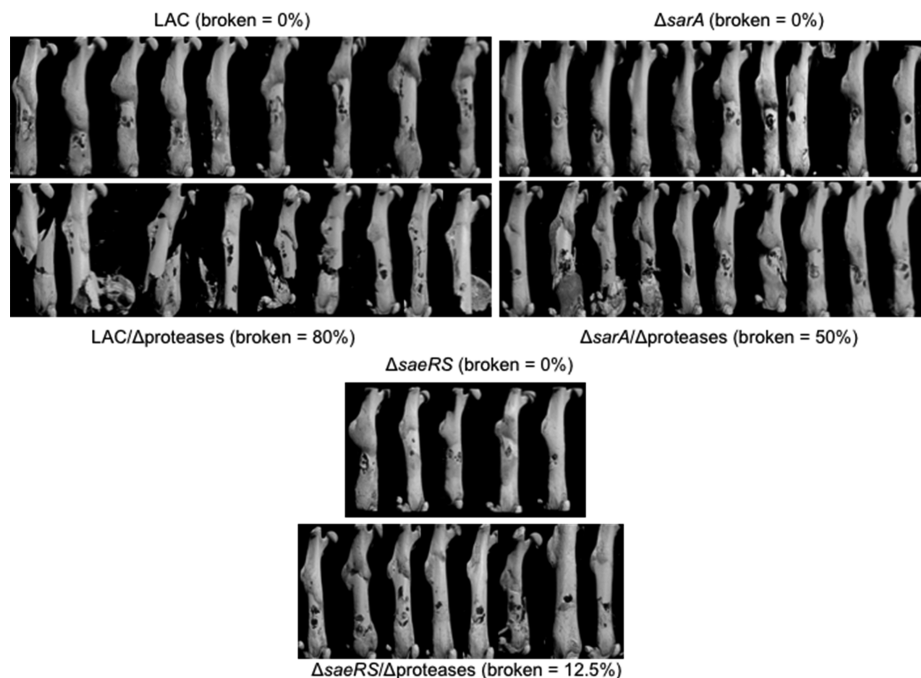
Figure 13. Impact of protease production in Δ*sarA* and Δ*saeRS* mutants in vivo. A murine model of post-traumatic osteomyelitis was used to assess the relative virulence of LAC, its Δ*sarA* and Δ*sae* mutants, and protease-deficient derivatives of each strain (Δprotease). All images from all mice in each experimental group are shown for comparison along with the percentage of femurs from all animals within each group in which the femur was broken.

context of either μCT analysis or bacteriological burdens in the femur. Mutation of *saeRS* did have a greater impact than mutation of *sarA* on bacterial burdens in the femur (Figure 3). However, mutation of *saeRS* and *sarA* had an additive effect in this regard, thus suggesting that both loci contribute to the ability of *S. aureus* to colonize and persist in the bone.

Although mutation of *saeRS* and mutation of *sarA* had a comparable impact on virulence but not on protease production, the accumulation of any protein is a function of its production vs its degradation. Indeed, we previously proposed that the primary impact of mutating *saeRS* on the virulence of *S. aureus* is mediated at the level of virulence factor production while that of mutating *sarA* is mediated at the level of the protease-mediated degradation of these virulence factors. The results we report here provide further support for this hypothesis. Specifically, mutation of *saeRS* resulted in a protein profile that included the majority of proteins present in LAC and its *sae*^C derivative, albeit in reduced amounts, while the protein profile of the isogenic Δ*sarA* mutant was characterized by a lack of high-molecular weight proteins (Figure S1). However, differences in the relative impact of extracellular proteases in a Δ*sarA* mutant vs a Δ*saeRS* mutant do not preclude the possibility that mutation of these loci impacts the accumulation of an overlapping set of proteins that are relevant in the pathogenesis of OM. Indeed, there are reports describing transcriptional changes associated with OM,[21,22] but the results we report suggest that a better approach would be to consider virulence differences in the context of protein accumulation rather than transcriptional changes alone.

To address this, we utilized a novel mass-based proteomic approach recently developed and validated in our laboratories that allows us to focus on spectral counts derived from full-length proteins to the exclusion those derived from degradation products of those proteins.[11] The results confirmed that the accumulation of full-length proteins is significantly reduced in all four of the strains found to be attenuated in our murine OM model compared to the virulent strains LAC and its *sae*^C derivative (Figure 5). Using a stringent cutoff of a $\log_2$ fold-change of ≥ 5.0 (absolute fold-change ≥ 32) and each of two data analysis methods, we identified 14 proteins that were more abundant in both virulent strains by comparison to all four attenuated strains (Table 1, Figure 7). This suggests to us that these proteins are of potential interest in the pathogenesis of OM. However, we are not suggesting that these 14 proteins are the only proteins of potential interest. For instance, staphylococcal protein A (Spa) was not included among the priority list of 14 proteins, and it has been implicated in the pathogenesis of OM.[24−28] Moreover, the abundance of Spa was reduced to a statistically significant extent in all four attenuated strains (Figure S2) and did not meet the highly stringent standards we chose to employ only because of its relatively high abundance in the Δ*saeRS* mutant. Thus, it could be argued that these standards are too stringent. However, we believe that the methods we employed are appropriate in that they increase the likelihood of identifying high-priority targets that warrant further examination. In fact, we used two different data analysis methods to further increase the stringency of our approach, and this reduced this group of high-priority targets from 14 to 7 based on the fact that they were identified using both methods.

Included among these 7 proteins were the fibronectin-binding proteins FnbA and FnbB. This is potentially relevant in that these proteins have been implicated in biofilm formation, which is a key component of many types of *S. aureus* infection including OM.[29−31] An FtsK/SpoIII family protein was also identified using both analysis methods. The other two proteins included in the list of 7 that were identified by both analysis methods were an uncharacterized putative surface protein (SAUSA300_0408), which was also identified in a previous report focusing solely on the role of *saeRS* OM,[5] and alanine dehydrogenase 1. The latter is a cytoplasmic protein, but this does not preclude the possibility that it may act as a "moonlighting" virulence factor, particularly given that other dehydrogenases have been reported to moonlight on the cell surface promoting adhesion to extracellular matrix proteins.

Also included were the immunoglobulin binding protein Sbi and staphylocoagulase, both of which have been implicated as important components of immune evasion.[32−38] Other reports have concluded that coagulase production contributes to biofilm formation[16] and, at least as assessed under in vitro conditions, osteoblast physiology and bone destruction.[17] As further validation of our experimental approach, we demonstrated that LAC Δ*coa* mutants have a reduced capacity to form a biofilm and exhibit a modest reduction in virulence in our OM model (Figure 8). The fact that mutation of *coa* had less impact on biofilm formation and virulence in our OM model than mutation of *sarA* is not unexpected given that mutation of *sarA* limits the accumulation of many *S. aureus* proteins of potential relevance. This was also true with respect to osteoblast and osteoclast cytotoxicity, which was significantly reduced in a *sarA* mutant but not in a *coa* mutant (Figure S3). Nevertheless, these results suggest that coagulase does play a role in OM as previously suggested.[16,17] They also suggest that the impact of mutating *saeRS* or *sarA* on the pathogenesis of OM is likely to be multifactorial.

From a mechanistic point of view, there are two considerations that we tried to take into account. The first is whether we could identify any in vitro phenotypes that could be directly correlated with virulence. This was based on the hope such phenotypes could be used to further prioritize *S. aureus* proteins of potential interest before pursuing in vivo studies. However, while there were clear correlations, none of the in vitro phenotypes we examined could be definitively correlated with relative virulence. This includes protease production, biofilm formation and cytotoxicity for osteoblasts and osteoclasts. The second consideration is the manner by which mutation of *saeRS* and *sarA* limits virulence in our OM model, and in this respect we believe the results we report provide further support for the hypothesis that mutation of *saeRS* does so by limiting the production of important virulence factors, while *sarA* does so by limiting their accumulation owing to the increased production of extracellular proteases. Thus, in effect mutation of *saeRS* vs *sarA* represent two distinct means to the same end, that being reduced virulence in the specific clinical context of osteomyelitis.

This is consistent with the observation that eliminating protease production restored virulence in the Δ*sarA* mutant to a greater extent than was observed in the isogenic Δ*saeRS* mutant (Figure 13). In fact, eliminating the production of extracellular proteases in the Δ*sarA* mutant and even in LAC itself enhanced virulence in our OM model to an extent to

which the proportion fractured bones precluded accurate quantitative μCT analysis (Figure 13). However, protein production vs degradation are not mutually exclusive functions, and this does not mean that increased protease production is irrelevant in a LAC $\Delta saeRS$ mutant. Rather, it just suggests that the relatively modest impact of mutating $saeRS$ on protease production may be phenotypically apparent only because the amount of many *S. aureus* proteins is already limited in the Δsae mutant. Nevertheless, this does not preclude the possibility that mutation of $saeRS$ and/or $sarA$ results in the reduced accumulation of common *S. aureus* proteins that contribute to the pathogenesis of OM either alone or in combination with each other, and we believe the results of the experiments we report have allowed us to identify and prioritize specific proteins of interest in this regard.

At the same time, it is also possible that the attenuation of LAC $\Delta sarA$ and $\Delta saeRS$ mutants can be attributed to the impact of these mutations on different *S. aureus* proteins, and the experimental approach we describe would preclude the identification of such proteins. This possibility prompted us to make proteomic comparisons between the $\Delta sarA$ and $\Delta saeRS$ mutants themselves (Figure 11). The results confirmed that the abundance of 91 proteins was elevated in the $\Delta saeRS$ mutant by comparison to the $\Delta sarA$ mutant. However, the abundance of the majority of these was still reduced by comparison to LAC itself. The extent to which the abundance of any given protein must be reduced to have a phenotypic impact in vivo is not known, thus leaving open the possibility that the reduced abundance of these proteins contributes to the attenuation of the $\Delta saeRS$ mutant by comparison to LAC and its sae^{C} derivative. However, since these 91 proteins were more abundant in $\Delta saeRS$ than $\Delta sarA$ mutants, it seems unlikely they would contribute to the attenuation of the $\Delta saeRS$ mutant but not the $\Delta sarA$ mutant.

In contrast, very few proteins were present in increased amounts in the $\Delta sarA$ mutant by comparison to the $\Delta saeRS$ mutant. Interestingly, this did include all six of the *spl*-encoded proteases. This is consistent with previous reports demonstrating that the abundance of these proteases is increased in a $\Delta sarA$ mutant but not in a $\Delta saeRS$ mutant.[5,9] This suggests that specific targets of these proteases, or the proteases themselves, may contribute to the reduced biofilm formation and cytotoxicity observed with the $\Delta sarA$ mutant as assessed under in vitro conditions.

Finally, the proteomic approach we described can also be used to identify *S. aureus* proteins that are less likely to be involved in the pathogenesis of OM (Table S4). For instance, LukD, LukF, and LukS were all present in increased amounts in a LAC $\Delta sarA$ mutant by comparison to the isogenic $\Delta saeRS$ mutant. The abundance of these proteins in the $\Delta saeRS$ mutant was comparable to LAC itself. This suggests that these exotoxins are unlikely to contribute to the attenuation of the $\Delta sarA$ or $\Delta saeRS$ mutants. With respect to LukF and LukS, this is consistent with the observation that mutation of $sarA$ also limits virulence in the methicillin-sensitive strain UAMS-1,[4] which does not encode either of these genes.

CONCLUSION

The results we report demonstrate that mutation of $saeRS$ or $sarA$ in the USA300 strain LAC attenuates virulence to a comparable degree in a murine model of postsurgical OM to a comparable degree. Our results also support the conclusion that the primary impact of mutating $saeRS$ is mediated at the

level of protein production, while that of mutating $sarA$ is mediated at the level of protease-mediated protein degradation. Irrespective of the underlying mechanism that limits their accumulation, this opens up the possibility of identifying and prioritizing *S. aureus* virulence factors of potential relevance in the specific context of OM based on a correlation between their relative abundance in *S. aureus* strains that are demonstrably different with respect to virulence in this important clinical context. Because mutation of $saeRS$ or $sarA$ impacts the accumulation of a large number of possible virulence factors, prioritization is a key element of our approach, and in this regard, we purposefully applied a very stringent standard in the analysis of our proteomic comparisons. This accounts for our primary focus on 7 proteins, but it certainly does not preclude the possibility that other proteins not among this primary group are also important. Nevertheless, we believe the results we report clearly indicate that these proteins warrant direct examination as virulence factors of potential relevance in the pathogenesis of OM.

EXPERIMENTAL SECTION

Ethics Statement. All experiments involving animals were reviewed and approved by the Institutional Animal Care and Use Committee of the University of Arkansas for Medical Sciences and performed according to NIH guidelines, the Animal Welfare Act, and United States federal law.

Bacterial Strains and Growth Conditions. The bacterial strains used in this study were previously described.[6,39,40] Briefly, an erythromycin-sensitive derivative of the USA300 strain LAC was used as the parent strain from which the isogenic derivatives sae^{C}, $\Delta saeRS$, $sae^{C}/\Delta sarA$, $\Delta sarA$, and $\Delta saeRS/\Delta sarA$ were generated. The $\Delta saeRS/\Delta$protease mutant was made by transduction of the $saeRS$ mutation into a LAC derivative containing mutations in $sspAB$, $scpA$, and the gene encoding aureolysin (*aur*). These mutations were generated using the pKOR derivative pJB38 for $sspAB$ and $scpA$ and the pKOR1::*aur* construct for *aur*. The $\Delta sarA/\Delta$protease mutant was made by transduction of the $sarA$ mutation[20] into a LAC derivative unable to produce these same proteases as well as those encoded by the *spl* operon.[40] Strains were maintained at $-80\,^{\circ}$C in tryptic soy broth (TSB) containing 25% (v/v) glycerol. For each experiment, strains were retrieved from cold storage by plating on tryptic soy agar[41] with appropriate antibiotic selection. Antibiotics used were erythromycin (5 μg/mL), tetracycline (5 μg/mL), kanamycin (50 μg/mL), and neomycin (50 μg/mL).

Murine Model of Osteomyelitis. Induction of OM was done as previously described.[5,6] Briefly, 6–8 week-old C57BL/6 female mice were anesthetized and an incision made in the right hind limb to expose the femur. Using a precision needle, a unicortical defect was created at the midfemur. The intramedullary canal was inoculated via the unicortical defect with 2 μL of a bacterial suspension containing 1×10^6 cells harvested from midexponential phase ($OD_{560} = 1.0$) cultures. Muscle and skin were sutured, and the infection allowed to proceed for 14 days. After this time, mice were euthanized and the infected femurs harvested for microcomputed tomography (μCT) analysis or quantitation of the bacterial burden.

Microcomputed Tomography (μCT). Image acquisition and analysis were done according to protocols described elsewhere with minor modifications.[4,5] Briefly, imaging was be performed with the Skyscan 1174 X-ray Microtomograph

(Bruker, Kontich, Belgium) using an isotropic voxel size of 6.7 μm, an X-ray voltage of 50 kV (800 μA) and a 0.25 mm aluminum filter. Reconstruction was carried out using the Skyscan Nrecon software. The reconstructed cross-sectional slices were processed using the Skyscan CT-analyzer software as follows: first, bone tissue was isolated from the soft tissue and background using a global thresholding (low = 85; high = 255). Using the bone-including binarized images a semi-automated protocol was run to delineate regions of interest where the reactive new bone (callus) was isolated from the cortical bone (this protocol is a morphological escalator that separates the reactive bone structures using multiple rounds of opening and closing of gaps using increasing preset diameters for each round). The resulting images were loaded as ROI and corrected by drawing inclusive or exclusive contours on the periosteal surface to keep only and strictly the cortical bone. Using these defined ROI, the volume of cortical bone was calculated, and the amount of cortical bone destruction estimated by subtracting the value obtained from each bone from the average obtained from sham operated bones inoculated with PBS. New bone formation was quantified using the subtractive ROI function on the previously delineated cortical bone-including ROI images and calculating the bone volume included in the newly defined ROI. Statistical analysis of data from each experimental group was done by one-way ANOVA with Dunnett's correction. Separate comparisons were made with all strains relative to LAC or to its $\Delta sarA$ mutant. A p-value ≤ 0.05 was considered statistically significant.

Bacterial Burdens in the Femur. Bacterial loads in each femur were determined as previously reported.[5] Briefly, femurs were separated from surrounding soft tissue, frozen in liquid nitrogen, and homogenized. Homogenized bones were resuspended in 1 mL PBS. Subsequently, homogenates were sonicated, vortexed, serially diluted and plated on TSB solidified with 1.5% agar. Colony forming units (cfu) were counted and differences between groups of mice assessed using a one-way analysis of variance (ANOVA) model. Briefly, cfu data was logarithmically transformed prior to analysis. For samples with no bacterial counts, a number near 1 was added to each cfu value before the transformation was applied. Contrasts were defined to assess the comparisons of interest. Adjustments for multiple comparisons were made using simultaneous general linear hypothesis testing procedures.[42] Adjusted p-values ≤ 0.05 were considered significant. Analyses were done using R (version 3.4.3, R Foundation for Statistical Computing, Vienna, Austria). Multiple comparison procedures were implemented using the R library multcomp.

Extracellular Protease Activity. Overnight cultures grown in 5.0 mL of TSB without antibiotic selection were standardized relative to each other based on optical density (OD$_{560}$ = 10) and cells removed by centrifugation. Supernatants were then filter sterilized (0.2 μm) to obtain conditioned media (CM). Protease activity in these samples was assessed using the EnzChek Gelatinase/Collagenase Assay Kit (Thermo). Fluorescence was measured after 2 and 16 h of incubation. Statistical analysis was done by one-way ANOVA with Dunnett's correction. Separate comparisons were made with all strains relative to LAC or to its $\Delta sarA$ mutant. A p-value ≤ 0.05 was considered statistically significant.

Biofilm Formation. These assays were done as previously described.[43] Briefly, overnight cultures grown in biofilm media (TSB supplemented with glucose and sodium chloride)

without antibiotic selection were standardized (OD$_{540}$ = 0.05) and inoculated into a microtiter plate where the wells were coated with human plasma proteins beforehand.[6,7,23,41,43,44] Biofilm formation was then assessed after 24 h. Statistical analysis was done by one-way ANOVA with Dunnett's correction. Separate comparisons were made with all strains relative to LAC or to its $\Delta sarA$ mutant. A p-value ≤ 0.05 was considered statistically significant.

Cytotoxicity Assay. These assays were done according to a previously reported protocol.[4] Briefly, MC3T3-E1 and RAW 264.7 cells were seeded into black 96 well microtiter plates with a clear bottom at densities of 10 000 and 50 000 cells/well, respectively. After 24 h the media was replaced with a 1:1 mixture of cell media and CM standardized as described above (OD$_{540}$ = 10). Plates were incubated for 24 h. Cytotoxicity was determined using the LIVE/DEAD Viability/Cytotoxicity Kit for mammalian cells (Thermo Fisher Scientific). Statistical analysis was done by one-way ANOVA with Dunnett's correction. Separate comparisons were made with all strains relative to LAC or to its $\Delta sarA$ mutant. A p-value ≤ 0.05 was considered statistically significant.

Exoprotein Profile Analysis. Assessment of the secreted proteome was performed in triplicate as previously described.[11] Briefly, an equal volume of standardized CM from each sample was resolved by one-dimensional SDS-PAGE and visualized by Coomassie-staining. Each gel lane was sliced into 24 equiv bands of 2 mm each. Gel bands were destained, reduced, alkylated, dehydrated, and trypsin digested. Acidified tryptic peptides were separated using reverse phase UPLC. Eluted peptides were ionized by electrospray (2.15 kV) followed by MS/MS analysis using higher-energy collisional dissociation (HCD) on an Orbitrap Fusion Tribrid mass spectrometer (Thermo) in top-speed data-dependent mode. MS/MS data were acquired using the ion trap analyzer and proteins were identified by database search using Mascot (Matrix Science, version 2.5.1) against the USA300 *S. aureus* database (2653 entries, GenBank accession JTJK01000002). A decoy database (based on the reverse of the protein sequences) was used in the search to calculate the FDR for the search algorithm. Scaffold (Proteome Software) was used to verify MS/MS based peptide and protein identifications (FDR < 1%; identified peptides $\geq$ 2). Total spectral counts for each replicate were exported from Scaffold into Microsoft Excel and R for further analysis.

Data analysis was done as previously described.[11] Briefly, spectral count data collected from wild-type was used to locate the gel band with the maximum spectral count for a given protein. Spectral count observed in this band were added to spectral count observed in the gel bands immediately above and below to obtain total spectral count in a 3-band continuous window corresponding to the overall spectral peak for each full-length protein. A counts matrix for all samples including each of the replicates was generated based on this 3-band window. For the first analysis method the spectral count for each identified protein in each of the virulent strains was compared to the spectral count in each of the attenuated strains using two tailed t tests. Proteins with p > 0.05 were filtered out from each comparison. For the proteins with $p \leq 0.05$, the fold change was determined, first with a cutoff of log$_2$ FC $\geq$ 2 and, then with a cutoff of log$_2$ FC $\geq$ 5. The resulting lists of the proteins meeting these criteria in each pairwise comparison were then compared using Venny (version 2.1) to identify commonalities and differences

between each set of comparisons. For the second analysis method, the spectral counts were imported into R for statistical analysis using the EdgeR Bioconductor package.[13,14] The spectral counts were normalized using Trimmed Mean of M-values (TMM) prior to performing the generalized linear model quasi-likelihood ratio test. Data visualization images were generated using R studio.

Mutation of *coa*. The mutated *coa* gene was moved to LAC via transduction from a donor strain obtained from the Nebraska Transposon Mutant Library (NTML)[15] through BEI Resources (Manassas, VA; http://www.beiresources.org). The isogenic LAC Δ*coa* mutants were validated with a PCR validated by PCR using primers specific for the *coa* gene (5′ GCTAGGCGCATTAGCAGTTG and 3′ TCGTAACTCT-TTCGCGTGCT). These oligos bind to sites flanking the transposon insertion site. The genetic background of these mutants was also verified with a PCR specific for the small cryptic plasmid present in LAC and absent in the plasmid curated LAC derivative strain, JE2, in which the NTML was generated (data not shown). The primers used for this PCR were 5′ CCGAGGCTCAACGTCAATAA, 3′ GCAGT-TGGTGGGAACTACAA.

ASSOCIATED CONTENT

Ⓢ Supporting Information

The Supporting Information is available free of charge at https://pubs.acs.org/doi/10.1021/acsinfecdis.9b00291.

Tables S1–S4; Figures S1–S3 (PDF)

AUTHOR INFORMATION

Corresponding Author

*Phone: 501-686-7958. E-mail: smeltzermarks@uams.edu.

ORCID Ⓞ

Alan J. Tackett: 0000-0002-3672-4460
Mark S. Smeltzer: 0000-0002-0878-0692

Author Contributions

Conceived and designed the experiments: AR, KB, MS. Performed the experiments: AR, KB, SB, CW, AJ. Analyzed the data: AR, SB, CW, AJ, HS, MS. Wrote the paper: AR, KB, MS.

Notes

The authors declare no competing financial interest.

ACKNOWLEDGMENTS

ABBREVIATIONS

OM, osteomyelitis; *sarA*, staphylococcal accessory regulator; *saeRS*, *S. aureus* exoprotein regulatory locus; PSMs, phenol-soluble modulins; Spa, taphylococcal protein A; CM, conditioned media; μCT, microcomputed tomography; FC, fold-change; glmQLT, generalized linear model quasi-like-lihood; NTML, Nebraska Transposon Mutant Library; *coa*, staphylocoagulase.

REFERENCES

(1) Monaco, M., Pimentel de Araujo, F., Cruciani, M., Coccia, E. M., and Pantosti, A. (2016) Worldwide Epidemiology and Antibiotic Resistance of Staphylococcus aureus. *Curr. Top. Microbiol. Immunol.* 409, 21−56.

(2) Jerzy, K., and Francis, H. (2018) Chronic Osteomyelitis - Bacterial Flora, Antibiotic Sensitivity and Treatment Challenges. *Open Orthop J.* 12, 153−163.

(3) Priest, N. K., Rudkin, J. K., Feil, E. J., van den Elsen, J. M., Cheung, A., Peacock, S. J., Laabei, M., Lucks, D. A., Recker, M., and Massey, R. C. (2012) From genotype to phenotype: can systems biology be used to predict Staphylococcus aureus virulence? *Nat. Rev. Microbiol.* 10 (11), 791−7.

(4) Loughran, A. J., Gaddy, D., Beenken, K. E., Meeker, D. G., Morello, R., Zhao, H., Byrum, S. D., Tackett, A. J., Cassat, J. E., and Smeltzer, M. S. (2016) Impact of sarA and Phenol-Soluble Modulins on the Pathogenesis of Osteomyelitis in Diverse Clinical Isolates of Staphylococcus aureus. *Infect. Immun.* 84 (9), 2586−94.

(5) Cassat, J. E., Hammer, N. D., Campbell, J. P., Benson, M. A., Perrien, D. S., Mrak, L. N., Smeltzer, M. S., Torres, V. J., and Skaar, E. P. (2013) A secreted bacterial protease tailors the Staphylococcus aureus virulence repertoire to modulate bone remodeling during osteomyelitis. *Cell Host Microbe* 13 (6), 759−72.

(6) Beenken, K. E., Mrak, L. N., Zielinska, A. K., Atwood, D. N., Loughran, A. J., Griffin, L. M., Matthews, K. A., Anthony, A. M., Spencer, H. J., Skinner, R. A., Post, G. R., Lee, C. Y., and Smeltzer, M. S. (2014) Impact of the functional status of saeRS on in vivo phenotypes of Staphylococcus aureus sarA mutants. *Mol. Microbiol.* 92 (6), 1299−312.

(7) Mrak, L. N., Zielinska, A. K., Beenken, K. E., Mrak, I. N., Atwood, D. N., Griffin, L. M., Lee, C. Y., and Smeltzer, M. S. (2012) saeRS and sarA act synergistically to repress protease production and promote biofilm formation in Staphylococcus aureus. *PLoS One* 7 (6), No. e38453.

(8) Zielinska, A. K., Beenken, K. E., Joo, H. S., Mrak, L. N., Griffin, L. M., Luong, T. T., Lee, C. Y., Otto, M., Shaw, L. N., and Smeltzer, M. S. (2011) Defining the strain-dependent impact of the Staphylococcal accessory regulator (sarA) on the alpha-toxin phenotype of Staphylococcus aureus. *J. Bacteriol.* 193 (12), 2948−58.

(9) Zielinska, A. K., Beenken, K. E., Mrak, L. N., Spencer, H. J., Post, G. R., Skinner, R. A., Tackett, A. J., Horswill, A. R., and Smeltzer, M. S. (2012) sarA-mediated repression of protease production plays a key role in the pathogenesis of Staphylococcus aureus USA300 isolates. *Mol. Microbiol.* 86 (5), 1183−96.

(10) Gimza, B., Larias, M., Budny, B., and Shaw, L. (2019) Mapping the global network of extracellular protease regulation in Staphylococcus aureus. *bioRxiv* DOI: 10.1101/764423.

(11) Byrum, S. D., Loughran, A. J., Beenken, K. E., Orr, L. M., Storey, A. J., Mackintosh, S. G., Edmondson, R. D., Tackett, A. J., and Smeltzer, M. S. (2018) Label-Free Proteomic Approach to Characterize Protease-Dependent and -Independent Effects of sarA Inactivation on the Staphylococcus aureus Exoproteome. *J. Proteome Res.* 17, 3384.

(12) Oliveros, J. (2007) *Venny: An Interactive Tool for Comparing Lists with Venn's Diagrams.*

(13) McCarthy, D. J., Chen, Y., and Smyth, G. K. (2012) Differential expression analysis of multifactor RNA-Seq experiments with respect to biological variation. *Nucleic Acids Res. 40* (10), 4288−97.

(14) Robinson, M. D., McCarthy, D. J., and Smyth, G. K. (2010) edgeR: a Bioconductor package for differential expression analysis of digital gene expression data. *Bioinformatics 26* (1), 139−40.

(15) Fey, P. D., Endres, J. L., Yajjala, V. K., Widhelm, T. J., Boissy, R. J., Bose, J. L., and Bayles, K. W. (2013) A genetic resource for rapid and comprehensive phenotype screening of nonessential Staphylococcus aureus genes. *mBio 4* (1), e00537−12.

(16) Zapotoczna, M., McCarthy, H., Rudkin, J. K., O'Gara, J. P., and O'Neill, E. (2015) An Essential Role for Coagulase in Staphylococcus aureus Biofilm Development Reveals New Therapeutic Possibilities for Device-Related Infections. *J. Infect. Dis. 212* (12), 1883−93.

(17) Jin, T., Zhu, Y. L., Li, J., Shi, J., He, X. Q., Ding, J., and Xu, Y. Q. (2013) Staphylococcal protein A, Panton-Valentine leukocidin and coagulase aggravate the bone loss and bone destruction in osteomyelitis. *Cell. Physiol. Biochem. 32* (2), 322−33.

(18) Cierny, G., 3rd (2011) Surgical treatment of osteomyelitis. *Plast. Reconstr. Surg. 127*, 190S−204S.

(19) Kurtz, S. M., Lau, E., Watson, H., Schmier, J. K., and Parvizi, J. (2012) Economic burden of periprosthetic joint infection in the United States. *J. Arthroplasty 27*, 61−65.

(20) Lew, D. P., and Waldvogel, F. A. (2004) Osteomyelitis. *Lancet 364* (9431), 369−79.

(21) Kalinka, J., Hachmeister, M., Geraci, J., Sordelli, D., Hansen, U., Niemann, S., Oetermann, S., Peters, G., Loffler, B., and Tuchscherr, L. (2014) Staphylococcus aureus isolates from chronic osteomyelitis are characterized by high host cell invasion and intracellular adaptation, but still induce inflammation. *Int. J. Med. Microbiol. 304* (8), 1038−49.

(22) Szafranska, A. K., Oxley, A. P., Chaves-Moreno, D., Horst, S. A., Rosslenbroich, S., Peters, G., Goldmann, O., Rohde, M., Sinha, B., Pieper, D. H., Loffler, B., Jauregui, R., Wos-Oxley, M. L., and Medina, E. (2014) High-resolution transcriptomic analysis of the adaptive response of Staphylococcus aureus during acute and chronic phases of osteomyelitis. *mBio*, DOI: 10.1128/mBio.01775-14.

(23) Beenken, K. E., Mrak, L. N., Griffin, L. M., Zielinska, A. K., Shaw, L. N., Rice, K. C., Horswill, A. R., Bayles, K. W., and Smeltzer, M. S. (2010) Epistatic relationships between sarA and agr in Staphylococcus aureus biofilm formation. *PLoS One 5* (5), No. e10790.

(24) Claro, T., Widaa, A., McDonnell, C., Foster, T. J., O'Brien, F. J., and Kerrigan, S. W. (2013) Staphylococcus aureus protein A binding to osteoblast tumour necrosis factor receptor 1 results in activation of nuclear factor kappa B and release of interleukin-6 in bone infection. *Microbiology 159* (1), 147−154.

(25) Claro, T., Widaa, A., O'Seaghdha, M., Miajlovic, H., Foster, T. J., O'Brien, F. J., and Kerrigan, S. W. (2011) Staphylococcus aureus protein A binds to osteoblasts and triggers signals that weaken bone in osteomyelitis. *PLoS One 6* (4), No. e18748.

(26) Mendoza Bertelli, A., Delpino, M. V., Lattar, S., Giai, C., Llana, M. N., Sanjuan, N., Cassat, J. E., Sordelli, D., and Gomez, M. I. (2016) Staphylococcus aureus protein A enhances osteoclastogenesis via TNFR1 and EGFR signaling. *Biochim. Biophys. Acta, Mol. Basis Dis. 1862* (10), 1975−83.

(27) Ren, L. R., Wang, H., He, X. Q., Song, M. G., Chen, X. Q., and Xu, Y. Q. (2017) Staphylococcus aureus Protein A induces osteoclastogenesis via the NFkappaB signaling pathway. *Mol. Med. Rep. 16* (5), 6020−6028.

(28) Widaa, A., Claro, T., Foster, T. J., O'Brien, F. J., and Kerrigan, S. W. (2012) Staphylococcus aureus protein A plays a critical role in mediating bone destruction and bone loss in osteomyelitis. *PLoS One 7* (7), No. e40586.

(29) Brady, R. A., Leid, J. G., Calhoun, J. H., Costerton, J. W., and Shirtliff, M. E. (2008) Osteomyelitis and the role of biofilms in chronic infection. *FEMS Immunol. Med. Microbiol. 52* (1), 13−22.

(30) O'Neill, E., Pozzi, C., Houston, P., Humphreys, H., Robinson, D. A., Loughman, A., Foster, T. J., and O'Gara, J. P. (2008) A novel Staphylococcus aureus biofilm phenotype mediated by the fibronec-tin-binding proteins. *FnBPA and FnBPB. J. Bacteriol 190* (11), 3835−50.

(31) Johansson, A., Flock, J. I., and Svensson, O. (2001) Collagen and fibronectin binding in experimental staphylococcal osteomyelitis. *Clin. Orthop. Relat. Res. 382*, 241−6.

(32) Burkholder, K. M., and Bhunia, A. K. (2010) Listeria monocytogenes uses Listeria adhesion protein (LAP) to promote bacterial transepithelial translocation and induces expression of LAP receptor Hsp60. *Infect. Immun. 78* (12), 5062−73.

(33) Daniely, D., Portnoi, M., Shagan, M., Porgador, A., Givon-Lavi, N., Ling, E., Dagan, R., and Nebenzahl, Y. M. (2006) Pneumococcal 6-phosphogluconate-dehydrogenase, a putative adhesin, induces protective immune response in mice. *Clin. Exp. Immunol. 144* (2), 254−263.

(34) Jin, H., Song, Y. P., Boel, G., Kochar, J., and Pancholi, V. (2005) Group A streptococcal surface GAPDH, SDH, recognizes uPAR/CD87 as its receptor on the human pharyngeal cell and mediates bacterial adherence to host cells. *J. Mol. Biol. 350* (1), 27−41.

(35) Kim, K. P., Jagadeesan, B., Burkholder, K. M., Jaradat, Z. W., Wampler, J. L., Lathrop, A. A., Morgan, M. T., and Bhunia, A. K. (2006) Adhesion characteristics of Listeria adhesion protein (LAP)-expressing Escherichia coli to Caco-2 cells and of recombinant LAP to eukaryotic receptor Hsp60 as examined in a surface plasmon resonance sensor. *FEMS Microbiol. Lett. 256* (2), 324−32.

(36) Molkanen, T., Tyynela, J., Helin, J., Kalkkinen, N., and Kuusela, P. (2002) Enhanced activation of bound plasminogen on Staphylococcus aureus by staphylokinase. *FEBS Lett. 517* (1−3), 72−8.

(37) Wampler, J. L., Kim, K. P., Jaradat, Z., and Bhunia, A. K. (2004) Heat shock protein 60 acts as a receptor for the Listeria adhesion protein in Caco-2 cells. *Infect. Immun. 72* (2), 931−6.

(38) Kim, H. K., Thammavongsa, V., Schneewind, O., and Missiakas, D. (2012) Recurrent infections and immune evasion strategies of Staphylococcus aureus. *Curr. Opin. Microbiol. 15* (1), 92−9.

(39) Kolar, S. L., Ibarra, J. A., Rivera, F. E., Mootz, J. M., Davenport, J. E., Stevens, S. M., Horswill, A. R., and Shaw, L. N. (2013) Extracellular proteases are key mediators of Staphylococcus aureus virulence via the global modulation of virulence-determinant stability. *MicrobiologyOpen 2* (1), 18−34.

(40) Wormann, M. E., Reichmann, N. T., Malone, C. L., Horswill, A. R., and Grundling, A. (2011) Proteolytic cleavage inactivates the Staphylococcus aureus lipoteichoic acid synthase. *J. Bacteriol. 193* (19), 5279−91.

(41) Tsang, L. H., Cassat, J. E., Shaw, L. N., Beenken, K. E., and Smeltzer, M. S. (2008) Factors contributing to the biofilm-deficient phenotype of Staphylococcus aureus sarA mutants. *PLoS One 3* (10), No. e3361.

(42) Hothorn, T., Bretz, F., and Westfall, P. (2008) Simultaneous inference in general parametric models. *Biom. J. 50* (3), 346−63.

(43) Beenken, K. E., Blevins, J. S., and Smeltzer, M. S. (2003) Mutation of sarA in Staphylococcus aureus limits biofilm formation. *Infect. Immun. 71* (7), 4206−11.

(44) Beenken, K. E., Spencer, H., Griffin, L. M., and Smeltzer, M. S. (2012) Impact of extracellular nuclease production on the biofilm phenotype of Staphylococcus aureus under in vitro and in vivo conditions. *Infect. Immun. 80* (5), 1634−8.

1
2
3
4
5
6 **The impact of *msaABCR* on *sarA*-associated phenotypes is different in divergent**
7 **clinical isolates of *Staphylococcus aureus***
8

9 Joseph S. Rom[a], Aura M. Ramirez[a], Karen E. Beenken[a], Gyan S. Sahukhal[c], Mohamed O.
10 Elasri[c], and Mark S. Smeltzer[a,b#]

11

12

13 [a]Department of Microbiology and Immunology, University of Arkansas for Medical Sciences,
14 Little Rock, AR 72205

15

16 [b]Department of Orthopaedic Surgery, University of Arkansas for Medical Sciences, Little Rock,
17 AR 72205

18

19 [c]Center for Molecular and Cellular Biosciences, University of Southern Mississippi, Hattiesburg,
20 MS 39406

21

22

23

24

25

26

27

28 Running title: Impact of *msaABCR* on *sarA* phenotypes

29

30

31
32

33 **#Corresponding author:**   Dr. Mark S. Smeltzer
34   Department of Microbiology and Immunology
35   University of Arkansas for Medical Sciences
36   4301 W. Markham
37   501-686-7958
38   smeltzermarks@uams.edu

1

39   **ABSTRACT**

40   The staphylococcal accessory regulator (*sarA*) plays an important role in *Staphylococcus*

41   *aureus* infections including osteomyelitis, and the *msaABCR* operon has been implicated as an

42   important factor in modulating expression of *sarA*. Thus, we investigated the contribution of

43   *msaABCR* to *sarA*-associated phenotypes in the *S. aureus* clinical isolates LAC and UAMS-1.

44   Mutation of *msaABCR* resulted in reduced production of SarA and a reduced capacity to form a

45   biofilm in both strains. Biofilm formation was enhanced in a LAC *msa* mutant by restoring the

46   production of SarA, but this was not true in a UAMS-1 *msa* mutant. Similarly, extracellular

47   protease production was increased in a LAC *msa* mutant but not a UAMS-1 *msa* mutant. This

48   difference was reflected in the accumulation and distribution of secreted virulence factors and in

49   the impact of extracellular proteases on biofilm formation in a LAC *msa* mutant. Most

50   importantly, it was reflected in the relative impact of mutating *msa* as assessed in a murine

51   osteomyelitis model, which had a significant impact in LAC but not in UAMS-1. In contrast,

52   mutation of *sarA* had a greater impact on all of these *in vitro* and *in vivo* phenotypes by

53   comparison to mutation of *msaABCR,* and it did so in both LAC and UAMS-1. These results

54   suggest that, at least in osteomyelitis, it would be therapeutically preferable to target *sarA* rather

55   than *msaABCR* to achieve the desired clinical result, particularly in the context of divergent

56   clinical isolates of *S. aureus.*

INTRODUCTION

Mutation of the staphylococcal accessory regulator (*sarA*) attenuates the virulence of divergent clinical isolates of *Staphylococcus aureus* in animal models of bacteremia, post-surgical osteomyelitis, and infective endocarditis (1-3). It also limits biofilm formation *in vitro* and *in vivo* to a degree that can be correlated with increased antibiotic susceptibility (2, 4-6). The effector molecule of the *sarA* regulatory system is a 15 kDa protein that has been shown to impact the production of multiple *S. aureus* virulence factors at a transcriptional level and by modulating the stability of mRNA (7-12). We have also demonstrated that an important factor contributing to the reduced virulence of *sarA* mutants, and their reduced capacity to form a biofilm, is the increased production of extracellular proteases and resulting decrease in the accumulation of multiple *S. aureus* proteins including both surface-associated and extracellular virulence factors (1, 13-17).

Thus, the *sarA* regulatory locus impacts both the production and the accumulation of *S. aureus* virulence factors, and this collectively makes an important contribution to diverse phenotypes that contribute to pathogenesis. This makes *sarA* a potential therapeutic target, and efforts have been made to exploit *sarA* in this regard (17-19). However, *S. aureus* regulatory circuits are complex and highly interactive (20), and mutation of other *S. aureus* regulatory loci within this circuit has also been shown to increase protease production to a degree that limits biofilm formation (21-25).

Among these other loci is *msa* (modulator of *sarA*), mutation of which was originally reported to limit the expression of *sarA* and the production of SarA itself (26). The *msa* gene was identified in the 8325-4 strain RN6390 by a transposon insertion in the open-reading frame SA1233 as designated in the N315 genome, but it was subsequently shown to be part of a four-gene operon now designated *msaABCR* (27). Genes within the *msa* operon encode a putative protein (MsaA) with no known function, a DNA binding protein (MsaB) shown to act as a transcription factor that regulates expression of numerous genes, and genes encoding a

3

83 regulatory RNA (*msaC*) and an antisense RNA (*msaR*) complementary to *msaB* (27). As would

84 be expected based on the phenotypes of *sarA* mutants (3, 4, 13, 15, 16, 28) and the role of

85 *msaABCR* in enhancing expression of *sarA*, mutation of *msaABCR* (hereinafter referred to as

86 *msa*) has been correlated with increased protease production and a decreased capacity to form

87 a biofilm (25, 27, 29).

88   Mutation of *msa* was also reported to result in decreased expression of the accessory gene

89 regulator (*agr*) in the 8325-4 strain RN6390 but to have the opposite effect in the clinical isolate

90 UAMS-1 (26). Expression levels of the well-characterized *agr*-regulated genes encoding alpha

91 toxin (*hla*) and protein A (*spa*) also differed between these two strains, while expression of the

92 genes encoding aureolysin (*aur*) and SspA (*sspA*) were increased in both strains. Differences

93 between these two strains have also been observed in the phenotype of their isogenic *sarA*

94 mutants (30-31). Such reports are not surprising given that RN6390 has a mutation in *rsbU* that

95 impacts the *sigB* regulatory pathway (32), which has also been shown to impact expression of

96 both *agr* and *sarA* as well as protease production (33-34). However, significant differences also

97 exist among clinical isolates, and to date, such strain-dependent differences have not been

98 adequately investigated. Thus, the overall impact of *msa* in divergent clinical isolates, and the

99 extent to which it is dependent on its interaction with *sarA*, remains unclear. In this report, we

100 addressed these issues by generating *msa*, *sarA*, and *msa/sarA* mutants in the methicillin-

101 resistant USA300 strain LAC and the methicillin-sensitive USA200 strain UAMS-1, and

102 assessed the impact these mutations had on well-defined phenotypes associated with their

103 isogenic *sarA* mutants.

104 **RESULTS AND DISCUSSION**

105   **Impact of *msa* on *sarA* expression.** Using an anti-SarA antibody (35), we first assessed

106 the production of SarA in *msa* mutants generated in LAC and UAMS-1 by western blot.

107 Experiments were done using whole cell lysates prepared from equal numbers of CFU

108 harvested from cultures in the mid-, late-, and post-exponential growth phases. The results were

4

109   comparable in both strains (Fig. 1) and confirmed that mutation of *msa* results in reduced

110   production of SarA, particularly during the mid- and late-exponential growth phases. However,

111   while the differences in the abundance of SarA were in most cases statistically significant, they

112   were also modest in that the amount of SarA present in lysates prepared from LAC and UAMS-

113   1 *msa* mutants was consistently >50% of that observed in the isogenic parent strain irrespective

114   of growth stage. This is consistent with transcriptional analysis, which demonstrated that

115   mutation of *msa* results in a modest but statistically significant decrease in the level of *sarA*

116   transcript in both LAC and UAMS-1 by comparison to the isogenic parent strain (Table 1).

117   These studies also confirmed that this transcriptional phenotype could be genetically

118   complemented. These results are consistent with the hypothesis that *msa* functions upstream to

119   modulate the expression of SarA.

120   **Impact of *msa* on biofilm formation.** Thus, the important question becomes whether the

121   reduction in the amount of SarA observed in *msa* mutants is phenotypically relevant. One of the

122   primary phenotypes that defines *sarA* mutants in divergent clinical isolates, including LAC and

123   UAMS-1, is the reduced capacity to form a biofilm (36). Using a well-established microtiter plate

124   assay (28), we confirmed that mutation of *msa* limits biofilm formation in both LAC and UAMS-1,

125   but to a limited extent by comparison to the isogenic *sarA* mutants (Fig. 2). The relative impact

126   of mutating *msa* vs. *sarA* was confirmed by demonstrating that concomitant mutation of both

127   *msa* and *sarA* limited biofilm formation to a level comparable to that observed in the isogenic

128   *sarA* mutant and well below that observed in the corresponding *msa* mutant (Suppl. Fig. 1).

129   These results are also consistent with the hypothesis that *msa* is upstream of SarA and the

130   observation that mutation of *msa* had only a modest impact on the accumulation of SarA, but

131   they also suggest that the reduced amount of SarA observed in *msa* mutants is phenotypically

132   relevant in the context of biofilm formation.

133   If this is true, then restoring the production of SarA in an *msa* mutant should restore biofilm

134   formation. To investigate this, we introduced the same plasmid (pSARA) used to genetically

5

135   complement the *sarA* mutation into an *msa* mutant. Western blot analysis confirmed that the

136   accumulation of SarA was restored in both LAC and UAMS-1 *msa* mutants (Fig. 3). Introducing

137   pSARA also restored biofilm formation in a LAC *msa* mutant but not in a UAMS-1 *msa* mutant

138   (Fig. 2). The reasons for this strain-dependent difference are unclear, but these results suggest

139   that *msa* limits biofilm formation in UAMS-1 owing to a *sarA*-independent regulatory effect.

140   **Impact of *msa* on protease production**. To investigate the mechanistic basis for these

141   biofilm phenotypes, we examined the relative impact of mutating *sarA* and *msa* on the

142   production of extracellular proteases. This was based on our previous demonstration that the

143   increased production of extracellular proteases plays a key role in defining the biofilm-deficient

144   phenotype of *S. aureus sarA* mutants (1). In LAC, mutation of *msa* resulted in a statistically

145   significant increase in overall protease activity as assessed using both casein- and gelatin-

146   based FRET assays, although the impact was more evident in the casein-based assay than the

147   gelatin-based assay (Fig. 4). This was not true in a LAC *sarA* mutant, where the impact of

148   mutating *sarA* on protease production was readily evident in both assays (Fig. 4). Additionally,

149   restoring SarA production in a LAC *msa* mutant decreased protease production, in the case of

150   the casein-based assay to wild-type levels. As might be expected based on the relative

151   sensitivity of the two assays, this was most evident when assessed using the casein-based

152   assay. However, mutation of *msa* in UAMS-1 did not have a significant impact on overall

153   protease activity as assessed using either casein- or gelatin-based FRET assays (Fig. 4). As in

154   LAC, mutation of *sarA* in UAMS-1 resulted in a statistically-significant increase in protease

155   production in both protease assays. These results are also consistent with the hypothesis that

156   the impact of mutating *msa* on biofilm formation in UAMS-1 occurs via a *sarA*-independent

157   regulatory effect.

158   This strain-dependent difference was also apparent in assays employing *gfp* transcriptional

159   reporter constructs generated with the promoters from each of the genes and/or operons

160   encoding *S. aureus* extracellular proteases (*aur*, *splA-F*, *sspABC* and *scpAB*). Specifically,

6

161 expression levels from all four reporters were significantly increased in a LAC *msa* mutant, but

162 not to the level observed in the isogenic *sarA* mutant (Fig. 5). In contrast, fluorescence was not

163 increased to a significant extent in a UAMS-1 *msa* mutant with any reporter other than the

164 *scp::gfp*, and even then, the increase was modest by comparison to fluorescence levels

165 observed with the same reporter in the LAC *msa* mutant and with all four reporters in the

166 UAMS-1 *sarA* mutant (Fig. 5). These results suggest that the strain-dependent impact of *msa* on

167 protease production is mediated at a transcriptional level.

168   These results also suggest the possibility of a cause-and-effect relationship between

169 increased protease production and decreased biofilm formation in a LAC *msa* mutant. Indeed,

170 there was an inverse and proportional relationship between protease production and biofilm

171 formation in LAC and its isogenic *sarA*, *msa*, and *sarA/msa* mutants (Suppl. Fig. 2). However,

172 this inverse relationship was not apparent in a UAMS-1 *msa* mutant. Mutation of *msa* in LAC

173 also resulted in the decreased accumulation of both Hla and extracellular protein A (eSpa) (Fig.

174 6). In contrast, in UAMS-1, which does not produce Hla, the accumulation of eSpa was greatly

175 reduced in a *sarA* mutant, but not in the isogenic *msa* mutant. The reduced accumulation of

176 eSpa observed in a LAC *msa* mutant was reversed by eliminating the production of extracellular

177 proteases, while in a UAMS-1 *msa* mutant, the abundance of eSpa was not affected by the

178 inability to produce these proteases (Fig. 6).

179   These results demonstrate that mutating *msa* results in a significant increase in protease

180 production in LAC but not in UAMS-1. SDS-PAGE analysis of conditioned medium (CM) from

181 overnight cultures confirmed the decreased accumulation of high molecular weight (HMW)

182 proteins in a LAC *msa* mutant, and that this was reversed by eliminating the production of

183 extracellular proteases (Fig. 7). As would be expected based on the results discussed above,

184 this effect was not apparent in a UAMS-1 *msa* mutant. In contrast, mutation of *sarA* limited the

185 accumulation of HMW proteins in CM in both LAC and UAMS-1, and in both cases this was

186 reversed by eliminating the ability of these mutants to produce extracellular proteases (Fig. 7).

7

187   **Impact of *msa* on PIA production**. To examine other possibilities, we assessed the

188   production of the polysaccharide intracellular adhesion (PIA) in *msa* and *sarA* mutants. PIA is

189   known to contribute to biofilm formation, and it has been suggested that it plays a particularly

190   important role in methicillin-sensitive strains like UAMS-1 (37). However, we were unable to

191   detect PIA above background levels in LAC, UAMS-1, or their isogenic *sarA* and *msa* mutants

192   (Suppl. Fig. 3).

193   **Impact of *msa* on extracellular nuclease**. Extracellular DNA and the production of

194   extracellular nucleases have also been implicated in biofilm formation in both methicillin-

195   resistant and methicillin-sensitive strains (38). *S. aureus* produces at least two nucleases, one

196   of which (Nuc1) is a secreted extracellular protein while the other (Nuc2) remains bound to the

197   cell surface (39). Mutation of *sarA* in UAMS-1 has been shown to result in the increased

198   production of these nucleases, and at least under *in vitro* conditions, this has been shown to

199   limit biofilm formation (40). Based on this, we examined the impact of mutating *msa* on nuclease

200   production with a specific focus on the Nuc1 extracellular nuclease. This was facilitated by the

201   availability of an anti-Nuc1 antibody (16), which allowed us to investigate this issue using

202   western blots of CM harvested from overnight cultures of each strain. It is important to recognize

203   that Nuc1 is produced in two forms, the smaller of which (NucA) is proteolytically derived from

204   the larger (NucB), and both of which are enzymatically active (41).

205   Relative to the parent strain, Nuc1 was present in increased amounts in a UAMS-1 *sarA*

206   mutant, and all of the Nuc1 present that could be detected by western blot was present in the

207   smaller NucA form (Fig. 8). This suggests that the increased production of extracellular

208   proteases in a UAMS-1 *sarA* mutant can be correlated with the absence of NucB. This was

209   confirmed in western blots with CM from a *sarA* mutant unable to produce these proteases, in

210   which case all of the Nuc1 detected was in the NucB form. Moreover, the overall abundance of

211   Nuc1 was increased in the protease-deficient UAMS-1 *sarA* mutant by comparison to the *sarA*

212   mutant (Fig. 8). The abundance of Nuc1 was also increased in a UAMS-1 *msa* mutant, and in

8

213 this case both NucA and NucB were detectable by western blot. While the overall amount of

214 Nuc1 was not increased in a protease-deficient UAMS-1 *msa* mutant, all of the Nuc1 present

215 was in the larger NucB form. This could be interpreted to suggest that mutation of *msa* does

216 result in an increase in protease production in UAMS-1 that is phenotypically apparent, but we

217 believe this would be an over-interpretation in that, unlike the isogenic protease-deficient *sarA*

218 mutant, the amount of Nuc1 did not increase appreciably in the UAMS-1 protease-deficient *msa*

219 mutant (Fig. 8).

220   The increased abundance of Nuc1 observed in a UAMS-1 *sarA* mutant was not apparent in

221 a LAC *sarA* mutant, but it was apparent in the isogenic *msa* mutant (Fig. 8). Unlike the UAMS-1

222 *msa* mutant, all of the Nuc1 detectable by western blot in the LAC *msa* mutant was present in

223 the smaller NucA form. This is consistent with the observation that mutating *msa* had a

224 significant impact on protease production in LAC but not in UAMS-1. As with the UAMS-1

225 protease-deficient *sarA* and *msa* mutants, only NucB could be detected in CM from the

226 protease-deficient LAC *sarA* and *msa* mutants (Fig. 8). As with a UAMS-1 *msa* mutant,

227 eliminating protease production in a LAC *msa* mutant limited proteolytic processing of Nuc1, but

228 did not appreciably alter the overall amount. In contrast, the abundance of NucB was also

229 enhanced in a protease-deficient LAC *sarA* mutant by comparison to the isogenic *sarA* mutant

230 itself. These results demonstrate that the production of Nuc1 is increased in LAC and UAMS-1

231 *sarA* and *msa* mutants. They also indicate that the abundance of Nuc1 is limited by increased

232 protease production in *sarA* mutants generated in both strains, but that this is not the case even

233 in a LAC *msa* mutants. However, the impact of *msa* on protease production was still evident in a

234 LAC *msa* mutant in that all of the Nuc1 present was present in the smaller NucA form (Fig. 8).

235   **Impact of protease and nuclease production on biofilm formation.** Given these

236 overlapping protease and nuclease phenotypes, we directly examined the impact of eliminating

237 the production of extracellular proteases or Nuc1 on the biofilm-deficient phenotype of LAC and

238 UAMS-1 *sarA* and *msa* mutants. In both strains, eliminating the ability to produce extracellular

9

239   proteases enhanced biofilm formation in both *sarA* and *msa* mutants to levels comparable to

240   those observed in the isogenic parent strain (Fig. 9). This could be interpreted to suggest that

241   the increased production of extracellular proteases limits biofilm formation in *msa* mutants, even

242   in UAMS-1. However, it is important to note that eliminating protease production also enhanced

243   biofilm formation in UAMS-1 itself to a greater extent than in LAC (Fig. 9). In fact, the increase in

244   biofilm formation observed in a protease-deficient derivative of UAMS-1 was comparable to that

245   observed in the UAMS-1 *msa* mutant, and this was not the case in the same derivatives of LAC.

246   Thus, we believe these results are also consistent with the conclusion that the increased

247   production of extracellular protease production limits biofilm formation in a LAC *msa* mutant but

248   not in a UAMS-1 *msa* mutant.

249   Biofilm formation was also enhanced in LAC and UAMS-1 *msa* mutants unable to produce

250   Nuc1, but once again, these results must be interpreted with caution because eliminating the

251   production of Nuc1 also enhanced biofilm formation in the LAC and UAMS-1 parent strains (Fig.

252   9). As with protease production, the increase in biofilm formation observed in the nuclease-

253   deficient UAMS-1 *msa* mutant was less than that observed in the nuclease-deficient LAC *msa*

254   mutant, and this was reflected in the relative impact of eliminating Nuc1 production on biofilm

255   formation (Fig. 9). In contrast, eliminating the production of Nuc1 did have a significant impact

256   on biofilm formation in a UAMS-1 *sarA* mutant, but not in a LAC *sarA* mutant (Fig. 9). This is

257   consistent with the observation that mutation of *msa* resulted in an increase in the abundance of

258   Nuc1 in a UAMS-1 *sarA* mutant but not in a LAC *sarA* mutant, although as previously discussed

259   protease production was shown to limit the abundance and processing of Nuc1 in *sarA* mutants

260   generated in both strains.

261   **Impact of *msa* on staphyloxanthin production.** All of the results discussed above are

262   consistent with a model in which *msa* functions upstream to enhance the production of SarA,

263   but also demonstrate that the impact of mutating *msa* on *sarA*-associated phenotypes is strain

264   dependent. There are also reports that mutation of *msa* in LAC has also been implicated in

265   phenotypes that have not been previously associated with *sarA*. One of these is that mutation of

266   *msa* in LAC has been reported to result in the reduced production of staphyloxanthin (27), which

267   has been implicated as an important virulence factor in *S. aureus* (42). We examined this in

268   LAC and UAMS-1 *sarA* and *msa* mutants, and the results confirmed that mutation of *msa* in

269   LAC results in a statistically significant reduction in the production of staphyloxanthin (Fig. 10)

270   and consequently reduced pigmentation of colonies on agar plates (data not shown).

271   Importantly, unlike the relative impact of mutating *sarA* and *msa* on biofilm formation and

272   protease production, the impact of mutating *msa* exceeded that of mutating *sarA* in this regard,

273   thus suggesting that the impact of mutating *msa* on staphyloxanthin production is primarily

274   independent of its impact on *sarA*. In UAMS-1 the results of these assays provided an even

275   more striking contrast. Specifically, staphyloxanthin production was increased in a UAMS-1 *sarA*

276   mutant but decreased in the isogenic *msa* mutant (Fig. 10). Although the decrease observed in

277   a UAMS-1 *msa* mutant was not statistically significant, this contrast nevertheless makes it

278   evident that the impact of mutating *msa* on staphyloxanthin production in UAMS-1 is

279   independent of its impact on *sarA*.

280   **Impact of *msa* in osteomyelitis**. The results discussed above provide insight into the

281   impact of *msa* on *sarA*-associated phenotypes in divergent clinical isolates of *S. aureus*.

282   However, they also suggest, specifically with respect to our staphyloxanthin assays, that *msa*

283   serves regulatory functions that are independent of its impact on *sarA*. Moreover, all of these

284   results are based on *in vitro* assays that do not necessarily reflect the unique microenvironment

285   of the bone. Thus, we wanted to directly assess the relative contribution of *msa* and *sarA* to

286   virulence in our murine osteomyelitis model (3, 43). As previously reported (3), mutation of *sarA*

287   limited virulence in both strains as assessed based on reactive bone formation and cortical bone

288   destruction, although in this experiment the reduction in cortical bone destruction observed with

289   the UAMS-1 *sarA* mutant did not reach statistical significance (Fig. 11). By comparison,

290   mutation of *msa* had only a modest impact on virulence in LAC, particularly in the context of

11

291 cortical bone destruction, and it had no significant impact in UAMS-1 in either reactive bone

292 formation or cortical bone destruction.

293 **CONCLUSIONS**

294   Most reports describing the impact of *S. aureus* regulatory loci on clinically relevant

295 phenotypes, including virulence, are based on examination of single loci in a single strain, and

296 this makes it difficult to reach conclusions regarding the relative potential of different regulatory

297 loci as therapeutic targets. We have attempted to address this by directly comparing different

298 regulatory mutants generated in divergent clinical isolates of *S. aureus* using both *in vitro* and *in*

299 *vivo* assays (3, 4, 44). The results of these studies have led us to focus on *sarA* and to

300 hypothesize that a primary factor contributing to the impact of mutating *sarA* on virulence and

301 virulence-associated phenotypes is the increased production of extracellular proteases and the

302 limitation this imposes on the accumulation of both surface-associated and extracellular

303 virulence factors (1,16). To date, we have not included the *msaABCR* operon in these studies,

304 and it is important to do so given that *msa* has been shown to function upstream of *sarA* and to

305 impact *sarA*-associated phenotypes including biofilm formation and protease production (25-27,

306 29). This raises the possibility that *msa* could also be a viable therapeutic target. Experimentally

307 addressing this possibility was the focus of the experiments we report. However, the results we

308 report lead us to conclude that this is not the case for two reasons. First, even in the genetically

309 and phenotypically divergent clinical isolates LAC and UAMS-1, the impact of mutating *msa* on

310 biofilm formation and virulence in our osteomyelitis model is limited by comparison to that of

311 mutating *sarA*. Second, the relative impact of mutating *msa* differed between these two strains

312 with respect to both of these phenotypes. This emphasizes the need for direct comparative

313 studies like those we report, particularly given the complexity of *S. aureus* regulatory circuits

314 and the diversity among *S. aureus* strains as represented by the USA300 isolate LAC and the

315 USA200 strain UAMS-1.

316 **MATERIALS AND METHODS**

317   **Bacterial strains and growth conditions.** The strains used in these experiments are

318   summarized in Tables 1 and 2. LAC and UAMS-1 mutants produced during the course of this

319   work were generated by Φ11-mediated transduction from existing mutants (1, 4, 13, 15, 27, 34,

320   44-53). Protease reporter plasmids were also introduced into the designated mutants by Φ11-

321   mediated transduction (23). All strains were maintained at −80°C in tryptic soy broth (TSB)

322   containing 25% (v/v) glycerol. For each experiment, strains under study were retrieved from cold

323   storage by plating on tryptic soy agar (TSA) with appropriate antibiotic selection. Antibiotics

324   were incorporated into the culture media as appropriate at the following concentrations:

325   chloramphenicol, 10 µg ml^{-1}; kanamycin, 50 µg ml^{-1}; and neomycin, 50 µg ml^{-1}; erythromycin, 10

326   µg ml^{-1}; spectinomycin, 1 mg ml^{-1}; or tetracycline 5 µg ml^{-1}. Kanamycin and neomycin were

327   always used together to avoid selection of spontaneously resistant strains.

328   **Preparation of *S. aureus* conditioned media.** To prepare conditioned medium (CM),

329   cultures of each strain were grown overnight (16 hr) in TSB at 37°C with constant shaking. The

330   optical density at 560 nm (OD$_{560}$) of each culture was determined and fresh TSB added to

331   standardize each culture to an equivalent optical density. Cells were then removed by

332   centrifugation and CM prepared by filter-sterilization. Samples were stored at -80°C until used.

333   **Preparation of whole-cell lysates.** Whole cell lysates were prepared as previously

334   described with minor modification (45). Briefly, strains were cultured at 37°C in TSB with

335   constant shaking and a medium-to-flask ratio of 0.5. Bacterial cells from a volume of each

336   culture calculated to obtain an equivalent number of cells were harvested by centrifugation at an

337   OD$_{560}$ of approximately 1.5, 4.0, and 10.0, which correspond to the mid-exponential, late-

338   exponential, and post-exponential growth phases, respectively. Cells were washed with sterile

339   phosphate-buffered saline (PBS) and re-suspended in 750 µl of TEG buffer (25 mM Tris-HCl,

340   pH 8.0, 25 mM EGTA). Cell suspensions were stored at -20°C until all samples had been

341   collected, at which point samples were thawed on ice, transferred to Fastprep Lysing Matrix B

342   tubes, and lysed in a FastPrep®-24 benchtop homogenizer (MP Biomedicals) using two 40 sec

13

343   intervals at a rate of 6.0 m/sec interrupted by a 5 min interval in which the homogenates were

344   chilled on ice. After centrifugation at 15,000 x g for 10 min at 4°C, supernatants were harvested

345   and stored at -80°C.

346   **Western blotting.** SarA western blots were done with an anti-SarA antibody and

347   appropriate secondary antibodies as previously described (1, 15, 16). Western blots included at

348   least two biological replicates. Densitometric values were obtained with a Bio-Rad

349   ChemiDocMP Imaging System and Image Lab Software (Bio-Rad Laboratories).

350   **RNA isolation and real-time qPCR.** Overnight cultures of *S. aureus* were diluted 1:10

351   times in fresh TSB and incubated at 37°C with shaking (200 rpm) for 2 hr. The cells were then

352   normalized to an OD_{600} of 0.05 in 25 ml TSB in 125 ml conical flask and incubated at 37°C with

353   shaking (200 rpm). The cells were collected at mid-exponential growth phase. Total RNA was

354   isolated from cells using a Qiagen RNeasy Maxi column (Qiagen), as previously described (27).

355   The quality of total RNA was determined by Nanodrop spectrometer readings and 1 µg RNA

356   was used to synthesize cDNA using iScript™ Reverse Transcription Supermix for RT-qPCR

357   (Biorad). RT-qPCR was done using iTaq™ Universal SYBR® Green Supermix (Biorad) as

358   described previously (27). The constitutively expressed gyrase A (*gyrA*) gene was used as an

359   endogenous control gene and was included in all experiments. The following primer sequences

360   were used to measure *sarA* expression: RT-*sarA*-F TTTGCTTCAGTGATTCGTTTATTTACTC

361   and RT-*sarA*-R GTAATGAGCATGATGAAAGAACTGTATT. Analysis of expression of each

362   gene was done based on at least three biological replicates.

363   **Static *in vitro* biofilm assay.** Biofilm formation was assessed *in vitro* using a microtiter

364   plate assay as previously described (28). Briefly, sterile 96-well microtiter plates were coated

365   with 100 µl of 20% carbonate/bicarbonate–reconstituted human plasma (Sigma) and incubated

366   overnight at 4°C. Bacterial cultures were grown overnight in TSB supplemented with 3% sodium

367   chloride and 0.5% glucose (biofilm medium, BFM) at 37°C. Cultures were standardized to an

368   OD_{560} = 0.05 in fresh BFM. Plasma was gently aspirated, and the microtiter plate inoculated with

14

369 200 μl of standardized culture per well. The plate was incubated statically overnight at 37°C.

370 Wells were gently washed three times with 200 μl PBS, fixed with 200 μl 100% EtOH, stained

371 with 200 μl Gram's crystal violet, and finally washed three times with 250 μl PBS. The stain was

372 eluted with 100 μl 100% EtOH for 10 min, the eluent diluted into a new 96-well plate, and the

373 absorbance was measured at 595 nm with a FLUOstar Omega microplate reader (BMG

374 Labtech).

375 **Total protease activity.** Total protease activity of CM was assessed using the FRET-

376 based Protease Fluorescent Detection Kit (Sigma) and the EnzChek® Gelatinase/Collagenase

377 Assay Kit (ThermoFisher Scientific), both according to the manufacturer instructions.

378 **Protease reporter assay.** Stains carrying each protease reporter (pCM13, pCM15,

379 pCM16, or pCM35) were cultured in TSB overnight as detailed above. Cultures were then

380 standardized to an OD_{560} of 10.0. 200 μl of each standardized culture was then aliquoted in

381 triplicate into a black clear-bottomed 96-well plate and the mean fluorescence intensity (MFI)

382 measured with a FLUOstar Omega microplate reader (excitation: 485 nm, emission: 520 nm)

383 (BMG Labtech).

384 **PIA immunoblot.** Production of the polysaccharide intercellular adhesion (PIA) was

385 assessed as previously described with minor modifications (44). Specifically, cultures were

386 grown overnight in BFM. After standardization to OD_{560} of 5.0, cells were harvested by

387 centrifugation and re-suspended in 60 μl 0.5 M EDTA. Cell suspensions were boiled for 5 min

388 followed by centrifugation (14,000 x g for 2 min). 40 μl of the supernatant was then incubated for

389 30 min at 48°C with 1 μl proteinase K (10 mg/ml) at 48°C. 20 μl of Tris-buffered saline (20 mM

390 Tris-HCl, 150 mM NaCl [pH 7.4]) was added to each sample, which was then stored at −20°C.

391 For analysis, 2 μl of each sample was spotted directly to a dry nitrocellulose membrane and PIA

392 detected using an anti-PIA antibody as previously described (44).

393 **Characterization of exoprotein profiles.** Exoprotein profiles were examined as previously

394 described (1). CM harvested as described above was resolved by SDS-PAGE using 4-12%

15

395   gradient Novex Bis-Tris Plus gels (Life Technologies). Proteins were visualized by staining with

396   SimplyBlue™ SafeStain (Life Technologies). Images were obtained using a Bio-Rad

397   ChemiDocMP Imaging System (Bio-Rad Laboratories).

398   **Staphyloxanthin production.** The relative production of staphyloxanthin was assessed

399   using bacterial cells harvested from overnight cultures as previously described (27). Briefly, cells

400   were harvested and standardized to an $OD_{560} = 10.0$ and washed twice with sterile water. Cells

401   were then re-suspended in 1.0 ml of 100% methanol and heated at 55°C for 5 min with

402   occasional vortexing. The cells were removed by centrifugation at 15,000 × g for 1 min and 100

403   µl of supernatant into a 96-well microtiter plate in triplicate. Absorbance values were read on a

404   FLUOstar Omega microplate reader (BMG Labtech) at a 465 nm and background corrected with

405   a methanol blank.

406   **Murine model of post-traumatic osteomyelitis.** The murine model of acute posttraumatic

407   osteomyelitis model was performed as previously described (43). Prior to surgery, 8-10 week

408   old C57BL/6 mice received 2.0 mg/kg of body weight meloxicam via subcutaneous injection and

409   were then anesthetized with isoflurane for the duration of the surgery. For each mouse, an

410   incision was made above the right hind limb. The periosteum was pulled apart with forceps and

411   using a 21-gauge Precision Glide needle (Becton Dickinson), a 1-mm uni-cortical bone defect

412   was made at the lateral mid-shaft of the femur. A bacterial inoculum of 1×10^6 CFU in 2 µl of

413   PBS was delivered into the intramedullary canal. The periosteum and skin were then closed

414   with sutures, and the mice were allowed to recover from anesthesia. Infection was allowed to

415   proceed for 14 days thereafter, at which time the mice were euthanized and the right femur was

416   removed and subjected to micro-computed tomography (micro-CT) analysis. All experiments

417   involving animals were reviewed and approved by the Institutional Animal Care and Use

418   Committee of the University of Arkansas for Medical Sciences and were performed according to

419   NIH guidelines, the Animal Welfare Act, and U.S. federal law.

16

420   **Micro-computed tomography.** The analysis of cortical bone destruction and new bone

421   formation was performed using micro-CT imaging with a Skyscan 1174 micro-CT (Bruker), and

422   scans were analyzed using the manufacturer's analytical software. Briefly, axial images of each

423   femur were acquired at a resolution of 6.7 μm at 50 kV and 800 μA through a 0.25-mm

424   aluminum filter. Bones were visualized using a scout scan and then scanned in three sections

425   as an oversize scan to image the entire femoral length. The volume of cortical bone was

426   isolated in a semi-automated process per the manufacturer's instruction. Briefly, cortical bone

427   was isolated from soft tissue and the background by global thresholding (low threshold, 89; high

428   threshold, 255). The processes of opening, closing, dilation, erosion, and de-speckling were

429   configured using the bones from sham-treated controls to separate the new bone from the

430   existing cortical bone, and a task list was created to apply the same process and values to all

431   bones in the data set. After processing of the bones using the task list, the volume of interest

432   (VOI) was corrected by drawing inclusive or exclusive contours on the periosteal surface.

433   Cortical bone destruction analysis consisted of approximately 1,800 slices between anatomical

434   landmarks at opposing ends of the femur. Destruction was determined by subtraction of the

435   volume of infected bones from the average bone volume from sham-treated controls. Reactive

436   new bone formation was assessed by first isolating the region of interest (ROI) that contained

437   only the original cortical bone (as described above). After cortical bone isolation, the new bone

438   volume was determined by subtraction of the cortical bone volume from the total bone volume.

439   All calculations were performed on the basis of direct voxel counts.

440   **Statistical analysis.** To allow for statistical comparison across biological and experimental

441   replicates, the results obtained for each experimental replicate with each strain were averaged

442   across all biological replicates. For densitometric analyses of western blots, protease assays,

443   biofilm assays and pigmentation assays, results observed with the isogenic wild-type strain

444   were set to 1.0, and these averages were then plotted relative to the results observed with this

445   strain. For protease reporter assays and μCT analysis, absolute values were plotted for all

17

446 replicates obtained with each strain. Analysis of variance (ANOVA) models with Dunnett's post-

447 test adjustment was used to assess statistical significance. P-values ≤ 0.05 were considered to

448 be statistically significant. Statistical analyses were performed using the statistical programming

449 language R version 3.3.3 (Vienna, Austria), SAS 9.4 (Cary, NC) and GraphPad Prism 5.0 (La

450 Jolla, CA).

451 **ACKNOWLEDGMENTS**

461 **REFERENCES**

462   1. Zielinska AK, Beenken KE, Mrak LN, Spencer HJ, Post GR, Skinner RA, Tackett AJ,

463   Horswill AR, Smeltzer MS. 2012. *sarA*-mediated repression of protease production plays

464   a key role in the pathogenesis of *Staphylococcus aureus* USA300 isolates. Mol Microbiol

465   86:1183-1196.

466   2. Abdelhady W, Bayer AS, Seidl K, Moormeier DE, Bayles KW, Cheung A, Yeaman MR,

467   Xiong YQ. 2014. Impact of vancomycin on *sarA*-mediated biofilm formation: role in

468   persistent endovascular infections due to methicillin-resistant *Staphylococcus aureus*. J

469   Infect Dis 209:1231–1240.

470   3. Loughran AJ, Gaddy D, Beenken KE, Meeker DG, Morello R, Zhao H, Byrum SD,

471   Tackett AJ, Cassat JE, Smeltzer MS. 2016. Impact of *sarA* and phenol-soluble modulins

18

472   in the pathogenesis of osteomyelitis in diverse clinical isolates of *Staphylococcus*
473   *aureus*. Infect Immun 84:2586-2594.

474   4. Atwood DN, Beenken KE, Lantz TL, Meeker DG, Lynn WB, Mills WB, Spencer, HJ,
475   Smeltzer, MS. 2016. Regulatory mutations impacting antibiotic susceptibility in an
476   established *Staphylococcus aureus* biofilm. Antimicrob Agents Chemother 60:1826-
477   1829.

478   5. Weiss EC, Zielinska A, Beenken KE, Spencer HJ, Daily SJ, Smeltzer MS. 2009. Impact
479   of *sarA* on daptomycin susceptibility of *Staphylococcus aureus* biofilms *in vivo*.
480   Antimicrob Agents Chemother 53:4096-4102.

481   6. Weiss EC, Spencer HJ, Daily SJ, Weiss BD, Smeltzer MS. 2009. Impact of *sarA* on
482   antibiotic susceptibility of *Staphylococcus aureus* in a catheter-associated *in vitro* model
483   of biofilm formation. Antimicrob Agents Chemother. 53:2475-2482.

484   7. Chien Y, Manna AC, Cheung AL. 1998. SarA level is a determinant of *agr* activation in
485   *Staphylococcus aureus*. Mol Microbiol 30:991-1001.

486   8. Chien Y, Manna AC, Projan SJ, Cheung AL. 1999. SarA, a global regulator of virulence
487   determinants in *Staphylococcus aureus*, binds to a conserved motif essential for *sar*-
488   dependent gene regulation. J Biol Chem 274:37169-37176.

489   9. Gao J, Stewart GC. 2004. Regulatory elements of the *Staphylococcus aureus* protein A
490   (Spa) promoter. J Bacteriol 186:3738-3748.

491   10. Roberts C, Anderson KL, Murphy E, Projan SJ, Mounts W, Hurlburt B, Smeltzer M,
492   Overbeek R, Disz T, Dunman PM. 2006. Characterizing the effect of the *Staphylococcus*
493   *aureus* virulence factor regulator, SarA, on log-phase mRNA half-lives. J Bacteriol
494   188:2593-2603.

495   11. Reyes D, Andrey DO, Monod A, Kelley WL, Zhang G, Cheung AL. 2011. Coordinated
496   regulation by AgrA, SarA, and SarR to control *agr* expression in *Staphylococcus aureus*.
497   J Bacteriol. 193:6020-6031.

19

498 12. Morrison JM, Anderson KL, Beenken KE, Smeltzer MS, Dunman PM. 2012. The
499   staphylococcal accessory regulator, SarA, is an RNA-binding protein that modulates the
500   mRNA turnover properties of late-exponential and stationary phase *Staphylococcus*
501   *aureus* cells. Front Cell Infect Microbiol 2:26.

502 13. Tsang LH, Cassat JE, Shaw LN, Beenken KE, Smeltzer MS. 2008. Factors contributing
503   to the biofilm-deficient phenotype of *Staphylococcus aureus sarA* mutants. PLoS One
504   3:e3361.

505 14. Mrak LN, Zielinska AK, Beenken KE, Mrak IN, Atwood DN, Griffin LM, Lee CY, Smeltzer
506   MS. 2012. *saeRS* and *sarA* act synergistically to repress protease production and
507   promote biofilm formation in *Staphylococcus aureus*. PLoS One. 7:e38453.

508 15. Beenken KE, Mrak LN, Zielinska AK, Atwood DN, Loughran AJ, Griffin LM, Matthews
509   KA, Anthony AC, Spencer HJ, Post GR, Lee CY, Smeltzer MS. 2014. Impact of the
510   functional status of *saeRS* on *in vivo* phenotypes of *sarA* mutants in *Staphylococcus*
511   *aureus*. Mol Microbiol 92:1299-1312.

512 16. Byrum, SD, Loughran, AJ, Beenken KE, Orr LM, Storey AJ, Mackintosh, SG,
513   Edmondson RD, Tackett AJ, Smeltzer MS. 2018 Label-free proteomic approach to
514   characterize protease-dependent and independent effects of *sarA* inactivation on the
515   *Staphylococcus aureus* exoproteome. ACS J Proteome Res 17:3384-3395.

516 17. Arya R, Princy SA. 2013. An insight into pleiotropic regulators *agr* and *sar*: Molecular
517   probes paving the new way for antivirulent therapy. Future Microbiol 8:1339-1353.

518 18. Arya R, Ravikumar R, Santhosh RS, Princy SA. 2015. SarA based novel therapeutic
519   candidate against *Staphylococcus aureus* associated with vascular graft infections. Front
520   Microbiol 6:416.

521 19. Chen Y, Liu T, Wang K, Hou C, Cai S, Huang Y, Du Z, Huang H, Kong J, Chen Y. 2016.
522   Baicalein inhibits *Staphylococcus aureus* biofilm formation and the quorum sensing
523   system *in vitro*. PLoS One 2016 11:e0153468.

524 20. Priest NK, Rudkin JK, Feil EJ, van den Elsen JM, Cheung A, Peacock SJ, Laabei M,

525   Lucks DA, Recker M, Massey RC. 2012. From genotype to phenotype: Can systems

526   biology be used to predict *Staphylococcus aureus* virulence? Nat Rev Microbiol 10:791-

527   797.

528 21. Tu Quoc PH, Genevaux P, Pajunen M, Savilahti H, Georgopoulos C, Schrenzel J, Kelley

529   WL. 2007. Isolation and characterization of biofilm formation-defective mutants of

530   *Staphylococcus aureus*. Infect Immun 75:1079-1088.

531 22. Lauderdale KJ, Boles BR, Cheung AL, Horswill AR. 2009. Interconnections between

532   Sigma B, agr, and proteolytic activity in *Staphylococcus aureus* biofilm maturation. Infect

533   Immun 77:1623–1635.

534 23. Mootz JM, Malone CL, Shaw LN, Horswill AR. 2013. Staphopains modulate

535   *Staphylococcus aureus* biofilm integrity. Infect Immun 81:3227-3238.

536 24. Mootz JM, Benson MA, Heim CE, Crosby HA, Kavanaugh JS, Dunman PM, Kielian T,

537   Torres VJ, Horswill AR. 2015. Rot is a key regulator of *Staphylococcus aureus* biofilm

538   formation. Mol Microbiol 96:388-404.

539 25. Sahukhal GS, Batte JL, Elasri MO. 2015. *msaABCR* operon positively regulates biofilm

540   development by repressing proteases and autolysis in *Staphylococcus aureus*. FEMS

541   Microbiol Lett 362.

542 26. Sambanthamoorthy K, Smeltzer MS, Elasri MO. 2006. Identification and characterization

543   of *msa* (SA1233), a gene involved in expression of SarA and several virulence factors in

544   *Staphylococcus aureus*. Microbiol 152:2559-2572.

545 27. Sahukhal GS, Elasri MO. 2014. Identification and characterization of an operon,

546   *msaABCR*, that controls virulence and biofilm development in *Staphylococcus aureus*.

547   BMC Microbiol 14:154.

548 28. Beenken KE, Blevins JS. Smeltzer MS. 2003. Mutation of *sarA* in *Staphylococcus*

549   *aureus* limits biofilm formation. Infect Immun 71:4206–4211.

21

550 29. Sambanthamoorthy K, Schwartz A, Nagarajan V, Elasri MO. 2008. The role of *msa* in
551   *Staphylococcus aureus* biofilm formation. BMC Microbiol 8:221.

552 30. Blevins JS, Beenken KE, Elasri MO, Hurlburt BK, Smeltzer MS. 2002. Strain-dependent
553   differences in the regulatory roles of *sarA* and *agr* in *Staphylococcus aureus*. Infect
554   Immun 70:470-480.

555 31. Beenken KE, Mrak LN, Griffin LM, Zielinska AK, Shaw LN, Rice KC, Horswill AR, Bayles
556   KW, Smeltzer MS. 2010. Epistatic relationships between *sarA* and *agr* in
557   *Staphylococcus aureus* biofilm formation. PLoS One 5:e10790.

558 32. Herbert S, Ziebandt AK, Ohlsen K, Schäfer T, Hecker M, Albrecht D, Novick R, Götz F.
559   2010. Repair of global regulators in *Staphylococcus aureus* 8325 and comparative
560   analysis with other clinical isolates. Infect Immun 78:2877-2889.

561 33. Giachino P, Engelmann S, Bischoff M. 2001. Sigma(B) activity depends on RsbU in
562   *Staphylococcus aureus*. J Bacteriol 183:1843–1852.

563 34. Rom JS, Atwood DN, Beenken KE, Meeker DG, Loughran AJ, Spencer HJ, Lantz TL,
564   Smeltzer MS. 2017. Impact of *Staphylococcus aureus* regulatory mutations that
565   modulate biofilm formation in the USA300 strain LAC on virulence in a murine
566   bacteremia model. Virulence 8:1776-1790.

567 35. Zielinska AK, Beenken KE, Joo HS, Mrak LN, Griffin LM, Luong TT, Lee CY, Otto M,
568   Shaw LN, Smeltzer MS. 2011. Defining the strain-dependent impact of the
569   staphylococcal accessory regulator (*sarA*) on the alpha-toxin phenotype of
570   *Staphylococcus aureus*. J Bacteriol 193:2948-2958.

571 36. Loughran AJ, Atwood DN, Anthony AC, Harik NS, Spencer HJ, Beenken KE, Smeltzer
572   MS. 2014. Impact of individual extracellular proteases on *Staphylococcus aureus* biofilm
573   formation in diverse clinical isolates and their isogenic *sarA* mutants. MicrobiologyOpen
574   3:897-909.

22

575   37. McCarthy H, Rudkin JK, Black NS, Gallagher L, O'Neill E, O'Gara JP. 2015. Methicillin

576   resistance and the biofilm phenotype in *Staphylococcus aureus*. Front Cell Infect

577   Microbiol 5:1.

578   38. Sugimoto S, Sato F, Miyakawa R, Chiba A, Onodera S, Hori S, Mizunoe Y. 2018. Broad

579   impact of extracellular DNA on biofilm formation by clinically isolated methicillin-resistant

580   and -sensitive strains of *Staphylococcus aureus*. Sci Rep 8:2254.

581   39. Kiedrowski MR, Crosby HA, Hernandez FJ, Malone CL, McNamara JO 2nd, Horswill AR.

582   2014. *Staphylococcus aureus* Nuc2 is a functional, surface-attached extracellular

583   nuclease. PLoS One 9:e95574.

584   40. Beenken KE, Spencer H, Griffin LM, Smeltzer MS. 2012. Impact of extracellular

585   nuclease production on the biofilm phenotype of *Staphylococcus aureus* under *in vitro*

586   and *in vivo* conditions. Infect Immun 80:1634–1638.

587   41. Kiedrowski MR, Kavanaugh JS, Malone CL, Mootz JM, Voyich JM, Smeltzer MS, Bayles

588   KW, Horswill AR. 2011. Nuclease modulates biofilm formation in community-associated

589   methicillin-resistant *Staphylococcus aureus*. PLoS One 6:e26714.

590   42. Song Y, Liu CI, Lin FY, No JH, Hensler M, Liu YL, Jeng WY, Low J, GY, Nizet V, Wang

591   AHJ, Oldfield E. 2009. Inhibition of staphyloxanthin virulence factor biosynthesis in

592   *Staphylococcus aureus*: *in vitro*, *in vivo*, and crystallographic results. J Med Chem

593   52:3869–3880.

594   43. Cassat JE, Hammer ND, Campbell JP, Benson MA, Perrien DS, Mrak LN, Smeltzer MS,

595   Torres VJ, Skaar EP. 2013. A secreted bacterial protease tailors the *Staphylococcus*

596   *aureus* virulence repertoire to modulate bone remodeling during osteomyelitis. Cell Host

597   Microbe 13:759-772.

598   44. Atwood DN, Loughran AJ, Courtney AP, Anthony AC, Meeker DG, Spencer HJ, Gupta

599   RK, Lee CY, Beenken KE, and Smeltzer MS. 2015. Comparative impact of diverse

600   regulatory loci on *Staphylococcus aureus* biofilm formation. MicrobiologyOpen 4:436–

601   451.

602   45. Blevins JS, Gillaspy AF, Rechtin TM, Hurlburt BK, Smeltzer MS. 1999. The

603   staphylococcal accessory regulator (*sar*) represses transcription of the *Staphylococcus*

604   *aureus* collagen adhesin gene (*cna*) in an *agr*-independent manner. Mol Microbiol

605   33:317-326.

606   46. Batte JL, Samanta D, Elasri MO. 2016. MsaB activates capsule production at the

607   transcription level in *Staphylococcus aureus*. Microbiol 162:575–589.

608   47. Wörmann ME, Reichmann NT, Malone CL, Horswill AR, Gründling A. 2011. Proteolytic

609   cleavage inactivates the *Staphylococcus aureus* lipoteichoic acid synthase. J Bacteriol

610   193:5279–5291.

611   48. Gillaspy AF, Hickmon SG, Skinner RA, Thomas JR, Nelson CL, Smeltzer MS. 1995.

612   Role of the accessory gene regulator (*agr*) in pathogenesis of staphylococcal

613   osteomyelitis. Infect Immun 63:3373–3380.

614   49. Beenken KE, Dunman PM, McAleese F, Macapagal D, Murphy E, Projan S, Blevins J,

615   Smeltzer M. 2004. Global gene expression in *Staphylococcus aureus* biofilms. J

616   Bacteriol 186:4665–4684.

617   50. Majerczyk CD, Sadykov MR, Luong TT, Lee C, Somerville GA, Sonenshein AL. 2008.

618   *Staphylococcus aureus* CodY negatively regulates virulence gene expression. J

619   Bacteriol 190:2257–2265.

620   51. Atwood DN, Beenken KE, Loughran AJ, Meeker DG, Lantz TL, Graham JW, Spencer

621   HJ, Smeltzer MS. 2016. XerC contributes to diverse forms of *Staphylococcus aureus*

622   infection via *agr*-dependent and *agr*-independent pathways. Infect Immun 84:1214–

623   1225.

24

624   52. Brann KR, Fullerton MS, Onyilagha FI, Prince AA, Kurten RC, Rom JS, Blevins JS,

625   Smeltzer MS, Voth DE. 2019. Infection of primary human alveolar macrophages alters

626   *Staphylococcus aureus* toxin production and activity. Infect Immun 87:e00167-19.

627   53. Bae T, Schneewind O. 2006. Allelic replacement in *Staphylococcus aureus* with

628   inducible counter-selection. Plasmid 55:58-63.

629

630

631

632

633

634

635

636

637

638   **FIGURE LEGENDS**

639   **Fig. 1. Impact of *msa* on the accumulation of SarA.** SarA accumulation was

640   assessed by western blot of whole cell lysates prepared from mid-, late- or post-

641   exponential phase cultures of LAC, UAMS-1 (U1), and their isogenic *msa* and *sarA*

642   mutants. Bar charts illustrate densitometry based on two biological replicates.

643   Densitometry results from samples prepared from each parent strain using cells

644   obtained at each growth phase were standardized to OD_{560} = 10. Error bars indicate

645   standard error of the mean. Single asterisk indicates statistical significance relative to

25

646 the isogenic parent strain. Double asterisks indicate statistical significance relative to

647 the isogenic *sarA* mutant.

648

649 **Fig. 2. Impact of *msa* and *sarA* on biofilm formation.** Biofilm formation was assessed

650 with the LAC, UAMS-1, their *sarA* and *msa* mutants, as well as mutants complemented

651 with *sarA* (^{S}) or *msa* (^{M}). Bar chart represents cumulative results from at least two

652 biological replicates, each of which included five experimental replicates. Error bars

653 indicate standard error of the mean. Single asterisk indicates statistical significance

654 relative to the isogenic parent strain. Double asterisks indicate statistical significance

655 relative to the isogenic *sarA* mutant.

656

657 **Fig. 3. SarA accumulation in *sarA*- and *msa*-complemented mutants.** SarA

658 accumulation was assessed by western blot of whole cell lysates prepared from mid-

659 exponential phase cultures of LAC, UAMS-1, their *sarA* and *msa* mutants, as well as

660 mutants complemented with *sarA* (^{S}) or *msa* (^{M}). Bar charts illustrate densitometry

661 based on at least two experimental replicates. Densitometry was performed using

662 samples prepared from cells obtained at mid-exponential growth phase (standardized to

663 OD_{560} = 1.5). Error bars indicate standard error of the mean. Single asterisk indicates

664 statistical significance relative to the isogenic parent strain. Double asterisks indicate

665 statistical significance relative to the isogenic *sarA* mutant.

666

667 **Fig. 4. Impact of *msa* and *sarA* on protease production.** Protease activity in

668 conditioned medium (CM) was assessed with LAC, UAMS-1, their *sarA* and *msa*

669 mutants, as well as mutants complemented with *sarA* (^{S}) or *msa* (^{M}). Protease activity

26

670 was assessed using a FITC-casein cleavage hydrolysis assay (left) and an FITC-gelatin

671 cleavage hydrolysis assay (right). Results are reported as mean fluorescence values

672 (MFI) ± the standard error of the mean. Bar charts are representative of results from at

673 least two biological replicates, each of which included three experimental replicates.

674 Error bars indicate standard error of the mean. Single asterisk indicates statistical

675 significance relative to the isogenic parent strain. Double asterisks indicate statistical

676 significance relative to the isogenic *sarA* mutant.

677

678 **Fig. 5. Impact of *msa* and *sarA* on protease gene expression.** Reporter constructs

679 were generated using the promoters from each of the four genes/operons encoding

680 extracellular proteases and the gene encoding green fluorescent protein (*gfp*). Each

681 construct was introduced into LAC, UAMS-1, and their isogenic *sarA* and *msa* mutants.

682 Mean fluorescence intensity (MFI) was assessed after overnight cultures were

683 standardized to an OD_{560} = 10. Bars represent average MFI ± standard error of the

684 mean from each of two independent biological replicates, each of which included three

685 experimental replicates. Statistical analysis was done independently for each strain and

686 each reporter. Single asterisk indicates statistical significance compared to the isogenic

687 parent strain. Double asterisk indicate statistical significance compared to the isogenic

688 *sarA* mutant.

689

690 **Fig. 6. Impact of extracellular proteases on accumulation of specific proteins.** The

691 abundance of alpha toxin (Hla) and extracellular protein A (eSpa) was assessed by

692 western blot of CM obtained from stationary phase cultures of LAC and UAMS-1, their

693 *sarA* and *msa* mutants, and isogenic derivatives of each strain unable to produce

27

694   extracellular proteases (*prot).* Purified Spa and Hla was included as positive controls.

695   CM from LAC *spa* and *hla* mutants were included as negative controls.

696

697   **Fig. 7. Impact of *sarA* and *msa* on accumulation of extracellular proteins.**

698   Extracellular protein profiles were assessed by SDS-PAGE analysis of CM obtained

699   from stationary phase cultures of LAC, UAMS-1, their *sarA* and *msa* mutants, and

700   isogenic derivatives of each strain unable to produce extracellular proteases (*prot*).

701

702   **Fig. 8. Impact of proteases on Nuc1 production and processing in *sarA* and *msa***

703   **mutants.** The amount of extracellular nuclease was assessed by western blot using CM

704   from LAC, UAMS-1, their isogenic *sarA* and *msa* mutants, *sarA* (^{S}) or *msa* (^{M})

705   complemented variants, and isogenic derivatives of regulatory mutants unable to

706   produce extracellular proteases (*prot*). A UAMS-1 *nuc1* (*nuc*) mutant was included as a

707   negative control in both blots.

708

709   **Fig. 9. Impact of extracellular proteases and nucleases on biofilm formation in**

710   ***msa* and *sarA* mutants.** Biofilm formation was assessed with LAC, UAMS-1, their *sarA*

711   and *msa* mutants, and isogenic derivatives of each strain unable to produce either

712   extracellular proteases (*prot*, top) or the extracellular nuclease Nuc1 (*nuc*, bottom). Bar

713   chart indicates cumulative results from at least two biological replicates, each of which

714   included five experimental replicates. Error bars indicate standard error of the mean.

715   Single asterisk indicates statistical significance relative to the isogenic parent strain.

716   Double asterisks indicate statistical significance relative to the isogenic *sarA* mutant.

717   Triple asterisks indicate statistical significance relative to the isogenic *msa* mutant.

28

718

Fig. 10. Staphyloxanthin production in *sarA* and *msa* mutants. Pigment was extracted from standardized samples of bacteria grown to stationary phase and measured at an absorbance of 465 nm. Bar charts represent cumulative results from at least four biological replicates, each of which included three experimental replicates. Error bars indicate standard error of the mean. Single asterisk indicates statistical significance relative to the isogenic parent strain. Double asterisks indicate values that are statistically significant relative to the isogenic *sarA* mutants.

726

Fig. 11. Impact of *sarA* and *msa* on the virulence of LAC and UAMS-1 in an osteomyelitis model. Images were analyzed for cortical bone destruction and reactive (new) bone formation in C57BL/6 mice infected with LAC, UAMS-1, or their isogenic *sarA* and *msa* mutants. Values are presented as volumes relative to mock-infected mice which underwent the surgical procedure but were injected only with sterile PBS. At least ten mice were analyzed for each mutant or respective parent strain. Single asterisk indicates statistical significance relative to the isogenic parent strain. Double asterisks indicate statistical significance relative to the isogenic *sarA* mutant.

735

TABLE 1. *sarA* expression at mid-exponential growth phase

Strain	Expression compared to WT
LAC *ΔmsaABCR*	0.493 ± 0.01
LAC *ΔmsaABCR,* pCN34::*msaABCR*	0.984 ± 0.0168
UAMS-1 *ΔmsaABCR*	0.753 ± 0.016
UAMS-1 *ΔmsaABCR*, pCN34::*msaABCR*	0.875 ± 0.019

737

TABLE 2. LAC *S. aureus* strains used in this study.

29

Strain	Genotype	References
UAMS-2279[a]	Wild type	1
UAMS-2294	*sarA*::*kan*/*neo*	1
UAMS-4001	*sarA*::*kan*/*neo*, pSARA	1
UAMS-4520	*ΔmsaABCR*	27
UAMS-4521	*ΔmsaABCR*, pCN34::*msaABCR*	27
UAMS-4601	*ΔmsaABCR*, pSARA	This work
UAMS-4545	*ΔmsaABCR*, *sarA*::*kan*/*neo*	This work
UAMS-4222	Wild type, pCM13 (*aur::sgfp*)	23
UAMS-4223	*sarA*::*kan*/*neo*, pCM13 (*aur::sgfp*)	This work
UAMS-4537	*ΔmsaABCR*, pCM13 (*aur::sgfp*)	This work
UAMS-4226	Wild type, pCM15 (*spl::sgfp*)	23
UAMS-4227	*sarA*::*kan*/*neo*, pCM15 (*spl::sgfp*)	This work
UAMS-4538	*ΔmsaABCR*, pCM15 (*spl::sgfp*)	This work
UAMS-4230	Wild type, pCM16 (*ssp::sgfp*)	23
UAMS-4231	*sarA*::*kan*/*neo*, pCM16 (*ssp::sgfp*)	This work
UAMS-4539	*ΔmsaABCR*, pCM16 (*ssp::sgfp*)	This work
UAMS-4234	Wild type, pCM35 (*scp::sgfp*)	23
UAMS-4235	*sarA*::*kan*/*neo*, pCM35 (*scp::sgfp*)	This work
UAMS-4446	*spa::erm*	34
UAMS-4552	*hla::erm*	52
UAMS-4540	*ΔmsaABCR*, pCM35 (*scp::sgfp*)	This work
UAMS-3001	*Δaur, ΔsspAB, ΔscpA, spl::erm*	47
UAMS-3002	*sarA*::*kan*/*neo*, *Δaur, ΔsspAB, ΔscpA, spl::erm*	1
UAMS-4557	*ΔmsaABCR*; *Δaur, ΔsspAB, ΔscpA, spl::erm*	This work
UAMS-2280	*nuc*::*ltrB*	41
UAMS-2295	*sarA*::*kan*/*neo*, *nuc*::*ltrB*	This work
UAMS-4582	*ΔmsaABCR*, *nuc*::*ltrB*	This work

739

740   [a] Variant of the clinical isolate LAC which has been cured of the erythromycin resistance

741   plasmid as previously described (1).

742

743   **Table 3. UAMS-1 *S. aureus* strains used in this study.**

Strain	Genotype	References

UAMS-1	Wild type	48
UAMS-929	*sarA*::*kan*/*neo*	30
UAMS-969	*sarA*::*kan*/*neo*, pSARA::*cat*	30
UAMS-4499	*ΔmsaABCR*	46
UAMS-4500	*ΔmsaABCR*, pCN34::*msaABCR*	46
UAMS-4603	*ΔmsaABCR*, pSARA	This work
UAMS-4549	*ΔmsaABCR*; *sarA*::*kan*/*neo*	This work
UAMS-4220	Wild type, pCM13 (*aur::sgfp*)	This work
UAMS-4221	*sarA*::*kan*/*neo*, pCM13 (*aur::sgfp*)	This work
UAMS-4541	*ΔmsaABCR*, pCM13 (*aur::sgfp*)	This work
UAMS-4224	Wild type, pCM15 (*spl::sgfp*)	This work
UAMS-4225	*sarA*::*kan*/*neo*, pCM15 (*spl::sgfp*)	This work
UAMS-4542	*ΔmsaABCR*, pCM15 (*spl::sgfp*)	This work
UAMS-4228	Wild type, pCM16 (*ssp::sgfp*)	This work
UAMS-4229	*sarA*::*kan*/*neo*, pCM16 (*ssp::sgfp*)	This work
UAMS-4543	*ΔmsaABCR*, pCM16 (*ssp::sgfp*)	This work
UAMS-4232	Wild type, pCM35 (*scp::sgfp*)	This work
UAMS-4233	*sarA*::*kan*/*neo*, pCM35 (*scp::sgfp*)	This work
UAMS-4544	*ΔmsaABCR*, pCM35 (*scp::sgfp*)	This work
UAMS-321	*ica::tet*	49
UAMS-1624	*codY::ermC*	50
UAMS-4412	*xerC::erm*	51
UAMS-1471	*Δnuc*	13
UAMS-1477	*sarA*::*kan*/*neo, Δnuc*	13
UAMS-4556	*ΔmsaABCR, Δnuc*	This work
UAMS-4574	*Δaur, ΔsspAB, scpA::tet*	This work
UAMS-4578	*sarA*::*kan*/*neo, Δaur, ΔsspAB, scpA::tet*	This work
UAMS-4583	*ΔmsaABCR, Δaur, ΔsspAB, scpA::tet*	This work

744
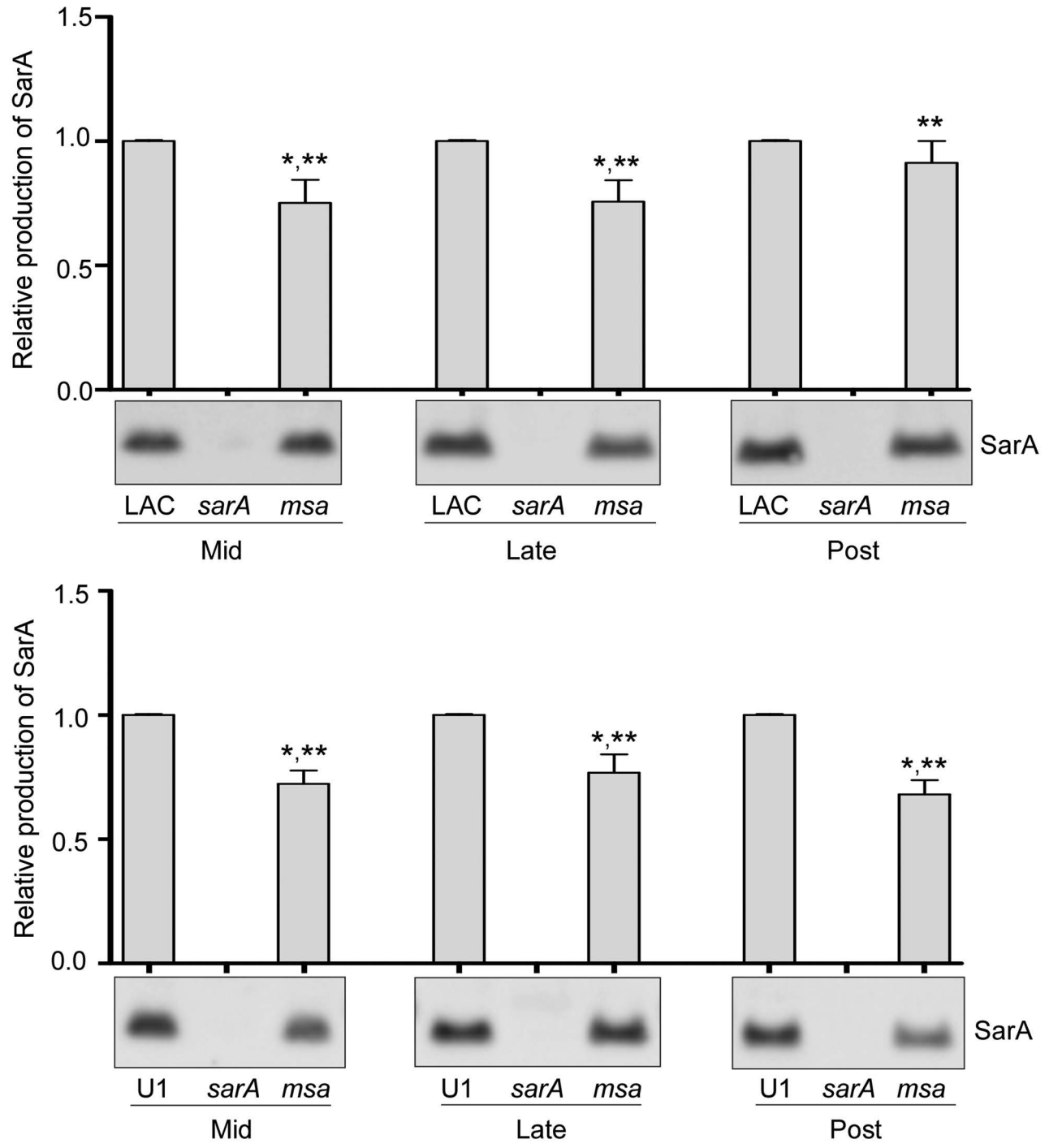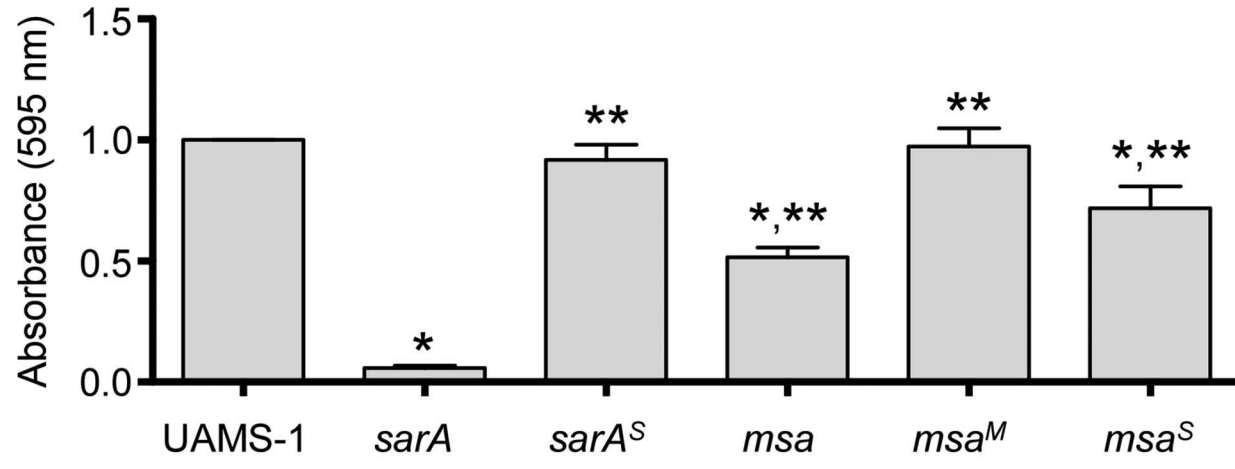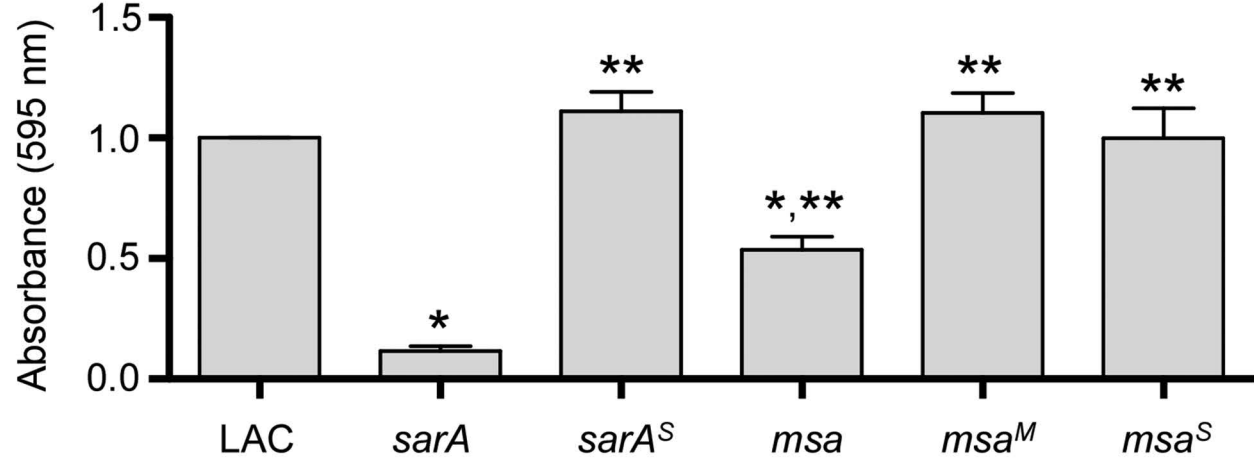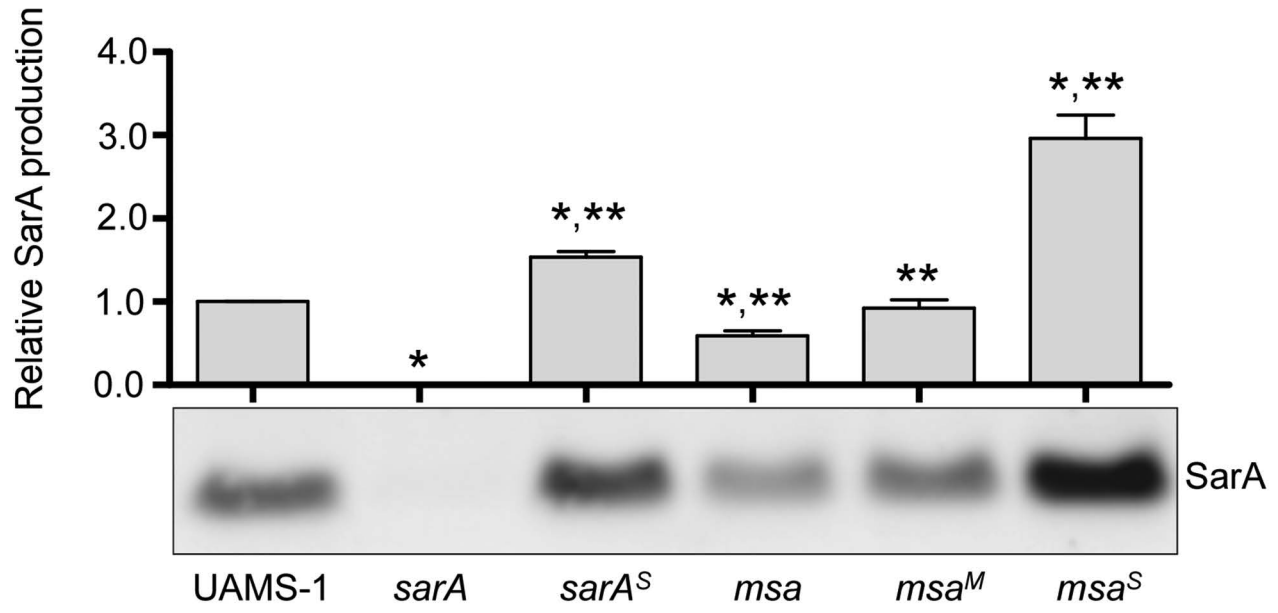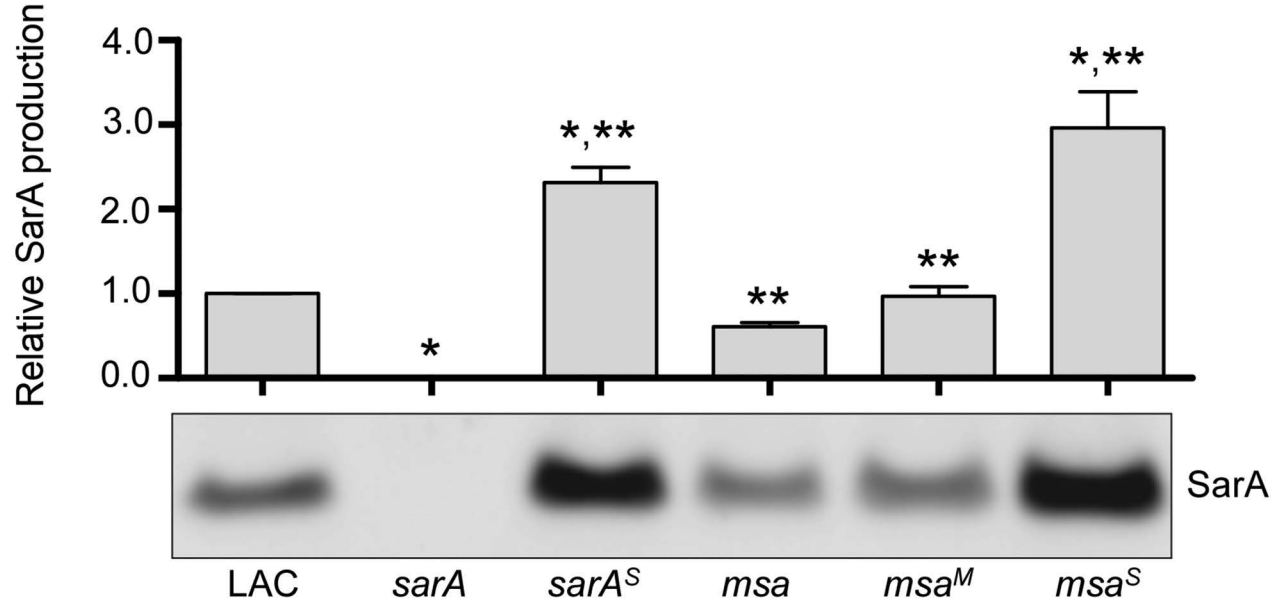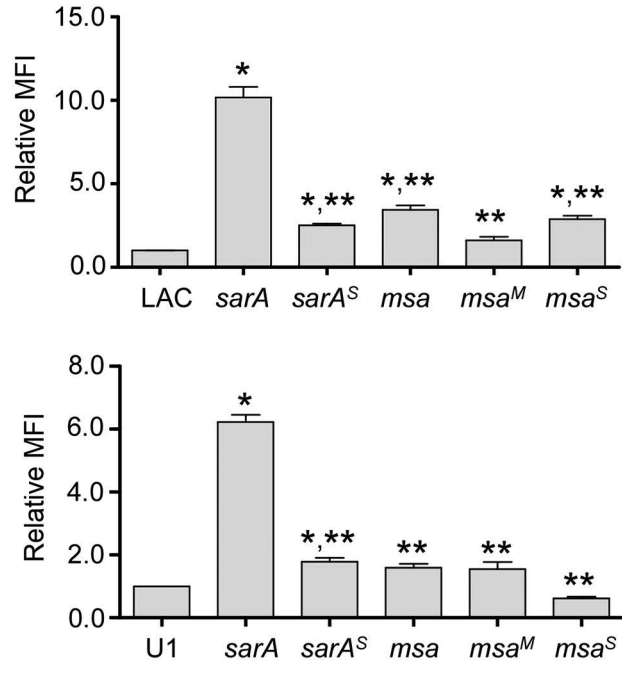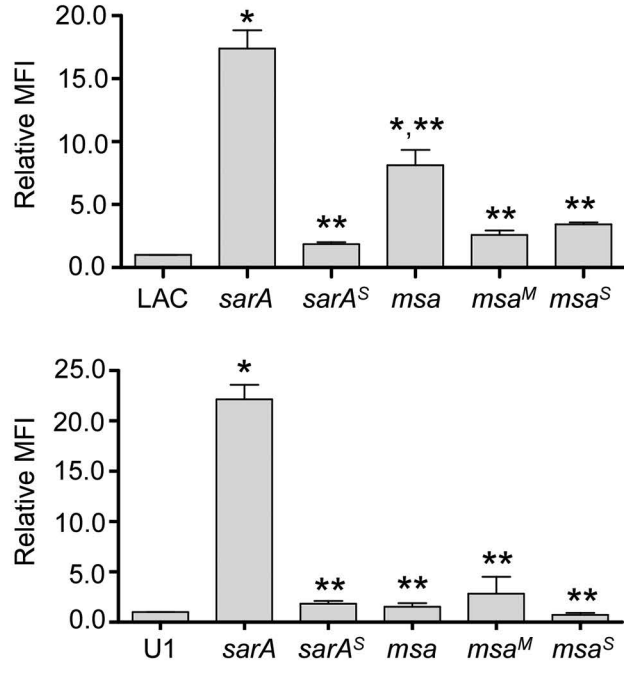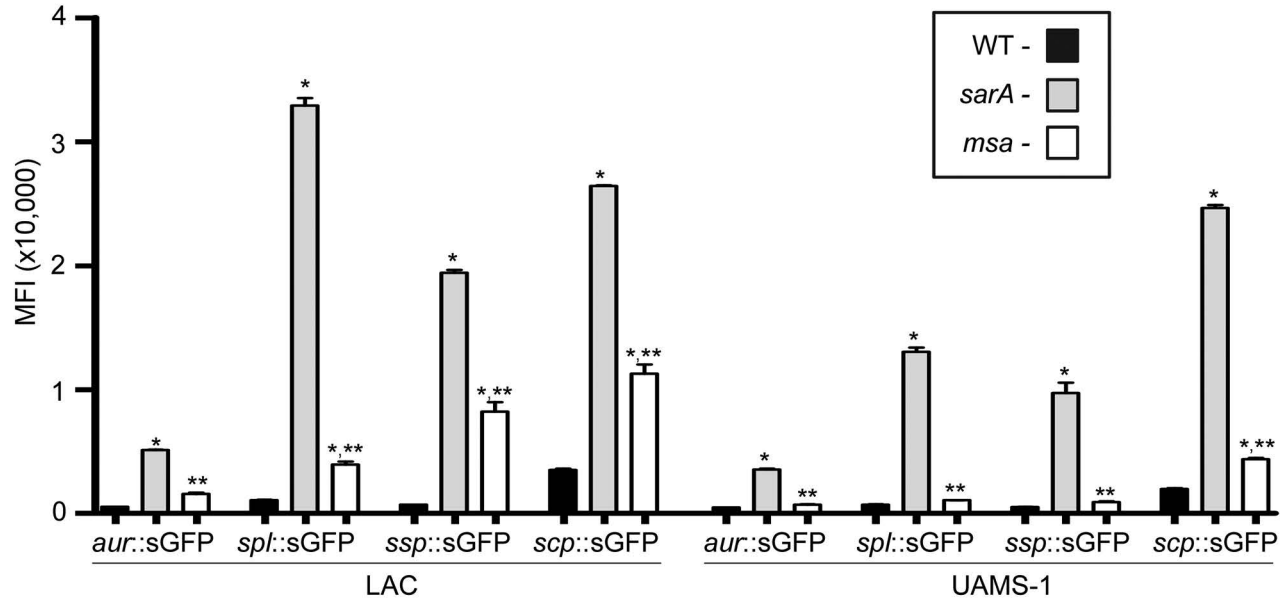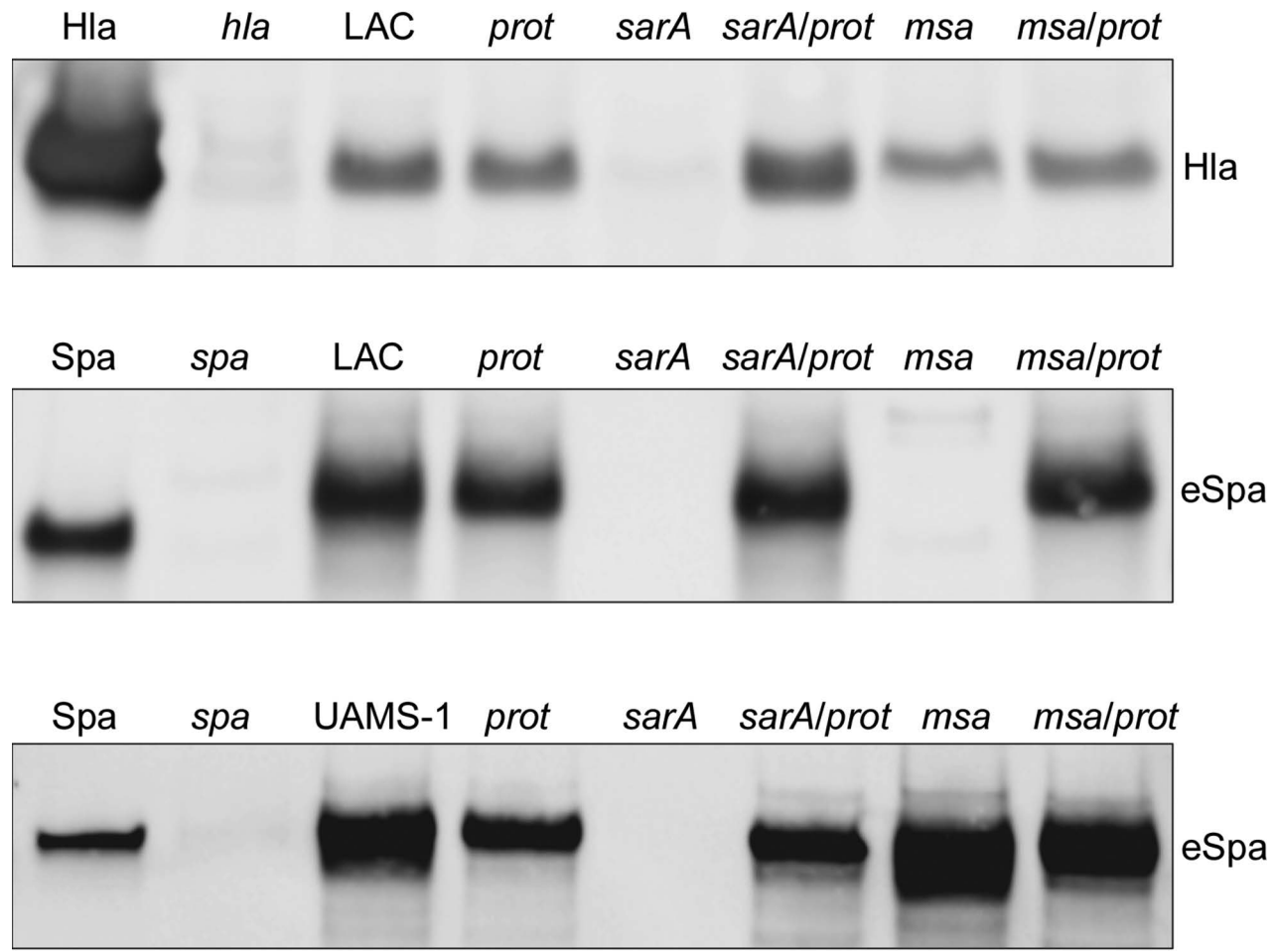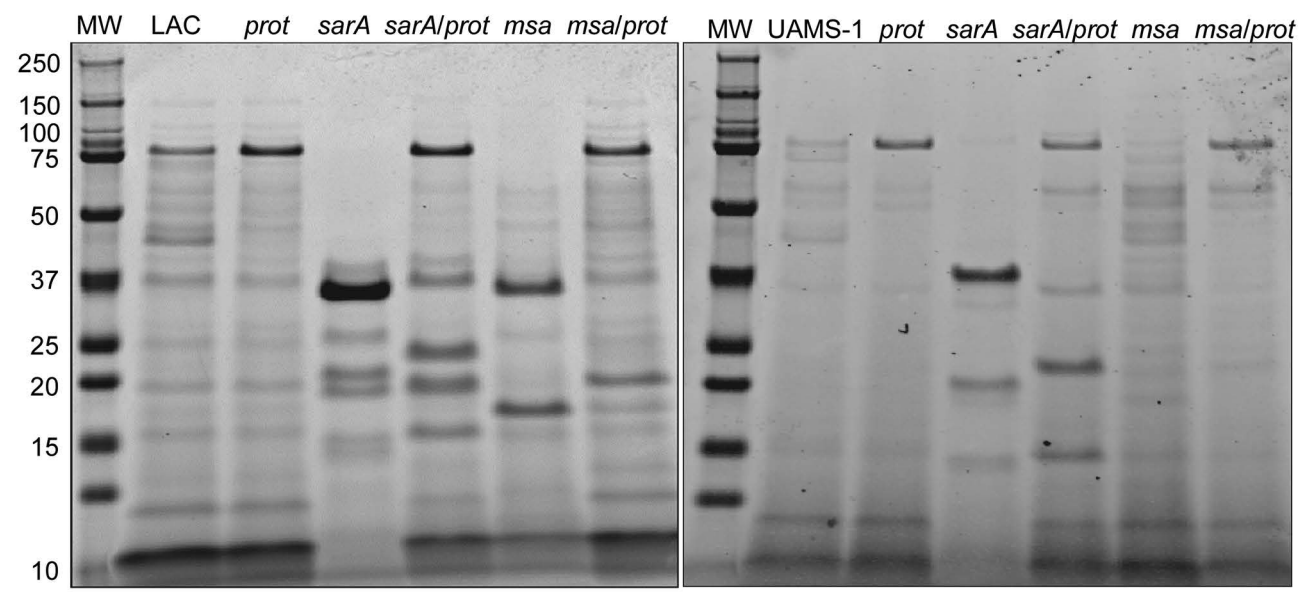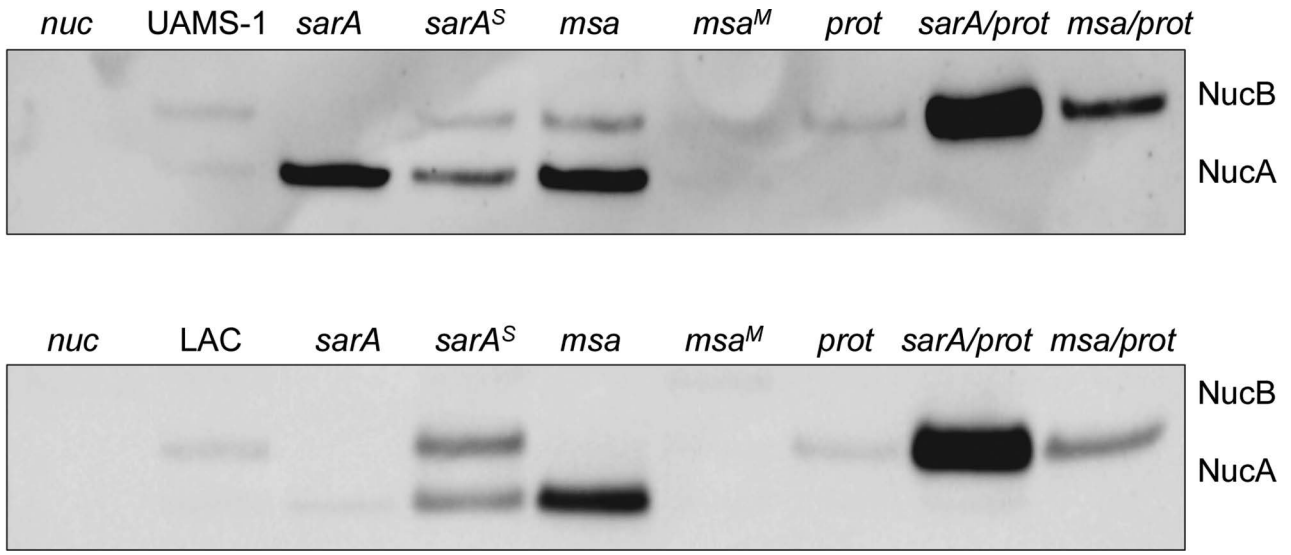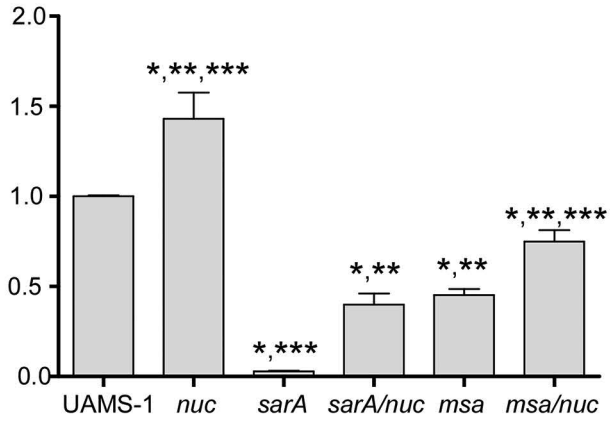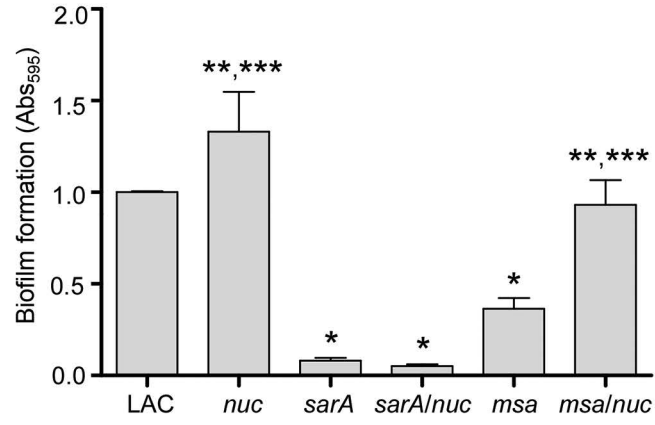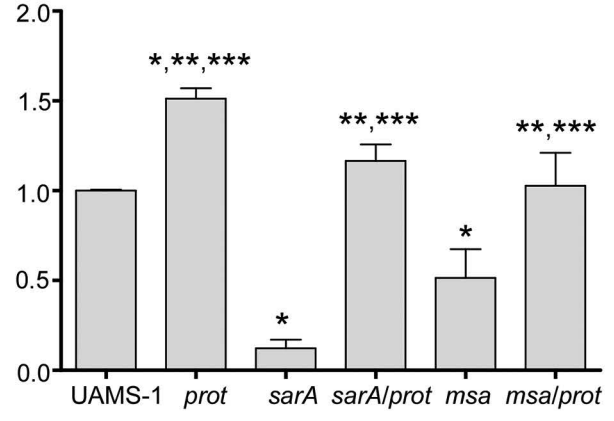
Hla	*hla*	LAC	*prot*	*sarA*	*sarA*/*prot*	*msa*	*msa*/*prot*	
								Hla

Spa	*spa*	LAC	*prot*	*sarA*	*sarA*/*prot*	*msa*	*msa*/*prot*	
								eSpa

Spa	*spa*	UAMS-1	*prot*	*sarA*	*sarA*/*prot*	*msa*	*msa*/*prot*	
								eSpa

| *nuc* | UAMS-1 | *sarA* | *sarA*^{S} | *msa* | *msa*^{M} | *prot* | *sarA/prot* | *msa/prot* |

NucB

NucA

| *nuc* | LAC | *sarA* | *sarA*^{S} | *msa* | *msa*^{M} | *prot* | *sarA/prot* | *msa/prot* |

NucB

NucA

Cortical bone destruction

Reactive bone formation

2018 International Consensus Meeting on Musculoskeletal Infection: Summary from the Biofilm Workgroup and Consensus on Biofilm Related Musculoskeletal Infections

Kordo Saeed,[1] Alex C. McLaren,[2] Edward M. Schwarz (iD),[3] Valentin Antoci,[4] William V. Arnold,[5] Antonia F. Chen,[6] Martin Clauss,[7] Jaime Esteban,[8] Vanya Gant,[9] Edward Hendershot,[10] Noreen Hickok,[11] Carlos A. Higuera,[12] Débora C. Coraça-Huber,[13] Hyonmin Choe,[14] Jessica A. Jennings,[15] Manjari Joshi,[16] William T. Li,[17] Philip C. Noble,[18,19] K. Scott Phillips,[20] Paul S. Pottinger,[21] Camilo Restrepo,[5] Holger Rohde,[22] Thomas P. Schaer,[23] Hao Shen,[24] Mark Smeltzer,[25] Paul Stoodley (iD),[26,27,28] Jason C. J. Webb,[29] Eivind Witsø[30]

[1]Department of Microbiology Hampshire Hospitals NHS Foundation Trust, Winchester and Basingstoke, UK and University of Southampton, School of Medicine, Southampton, UK, [2]Department of Orthopaedic Surgery, University of Arizona, College of Medicine-Phoenix, Phoenix, Arizona, [3]Department of Orthopaedics, University of Rochester, Rochester, New York, [4]Department of Orthopaedics, University Orthopedics Rhode Island, Providence, Rhode Island, [5]Department of Orthopaedics, Rothman Institute at Thomas Jefferson University Hospital, Philadelphia, Pennsylvania, [6]Department of Orthopaedics, Brigham and Women's Hospital, Harvard Medical School, Boston, Massachusetts, [7]Department for Orthopaedics and Trauma Surgery Kantonsspital Baselland, Liestal and University Hospital Basel Department for Orthopaedics and Trauma Surgery, Basel, CH, [8]Department of Clinical Microbiology, IIS-Fundacion Jimenez Diaz, UAM, Av. Reyes Catolicos 2., 28040, -Madrid, Spain, [9]College Hospital, Hospital for Tropical Diseases, National Hospital for Neurology and Neurosurgery at University College London Hospitals, London, UK, [10]Department of Internal Medicine and Infectious Diseases at Duke University Hospital, Durham, North Carolina, [11]Department of Orthopaedic Surgery, Department of Biochemistry & Molecular Biology Thomas Jefferson University, 1015 Walnut St., Philadelphia 19107 Pennsylvania, [12]Levitetz Department of Orthopaedic Surgery, Cleveland Clinic Florida, Weston, Florida, [13]Research Laboratory for Implant Associated Infections (Biofilm Lab) − Experimental Orthopaedics, Department of Orthopaedic Surgery, Medical University of Innsbruck, Innsbruck, Austria, [14]Yokohama City University Orthopaedic Department, Fukuura-3-9, Kanazawa-ku, Yokohama, Japan, [15]Department of Biomedical Engineering, The University of Memphis, 303B Engineering Technology Building, Memphis, Tennessee, [16]Department of Internal Medicine and Infectious Diseases at University of Mryland, School of Medicine, R Adams Cowley Shock Trauma Center Baltimore, Baltimore, Maryland, [17]Sydney Kimmel Medical College at Philadelphia University and Thomas Jefferson University, Philadelphia, Pennsylvania, [18]Institute of Orthopaedic Research and Education, Houston, Texas, [19]Baylor College of Medicine Department of Orthopaedic Surgery, Houston, Texas, [20]Division of Biology, Chemistry, and Materials Science, Office of Science and Engineering Laboratories, Center for Devices and Radiological Health, Office of Medical Products and Tobacco, US Food and Drug Administration, Silver Spring, Maryland, [21]Department of Medicine, Division of Allergy and Infectious Diseases, University of Washington, Seattle, Washington, [22]Institute for Medical Microbiology, Virology and Hygiene, University Medical Centre Hamburg-Eppendorf, Hamburg, Germany, [23]Department of Clinical Studies New Bolton Center, University of Pennsylvania School of Veterinary Medicine, Kennett Square, Pennsylvania, [24]Department of Orthopaedics, Shanghai Jiao Tong University Affiliated Sixth People' s Hospital, Shanghai, P. R. China, [25]Department of Microbiology and Immunology, Department of Orthopaedic Surgery, Center for Microbial Pathogenesis and Host Inflammatory Responses, University of Arkansas for Medical Sciences 4301 W. Markham, Slot 511, Little Rock 72205 Arkansas, [26]Department Microbial Infection and Immunity, College of Medicine, The Ohio State University, Columbus, Ohio, [27]Department Orthopaedics, College of Medicine, The Ohio State University, Columbus, Ohio, [28]Department National Centre for Advanced Tribolo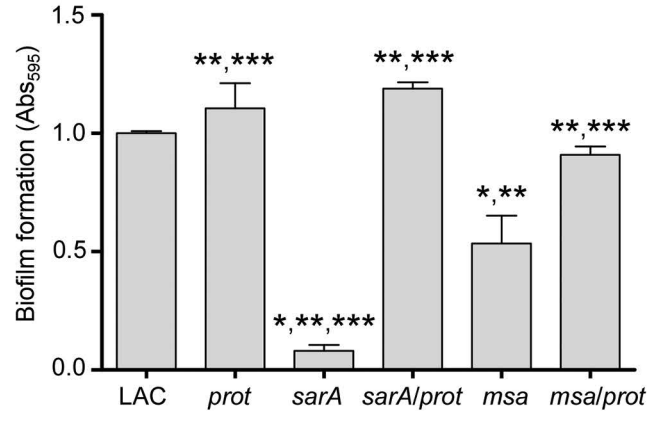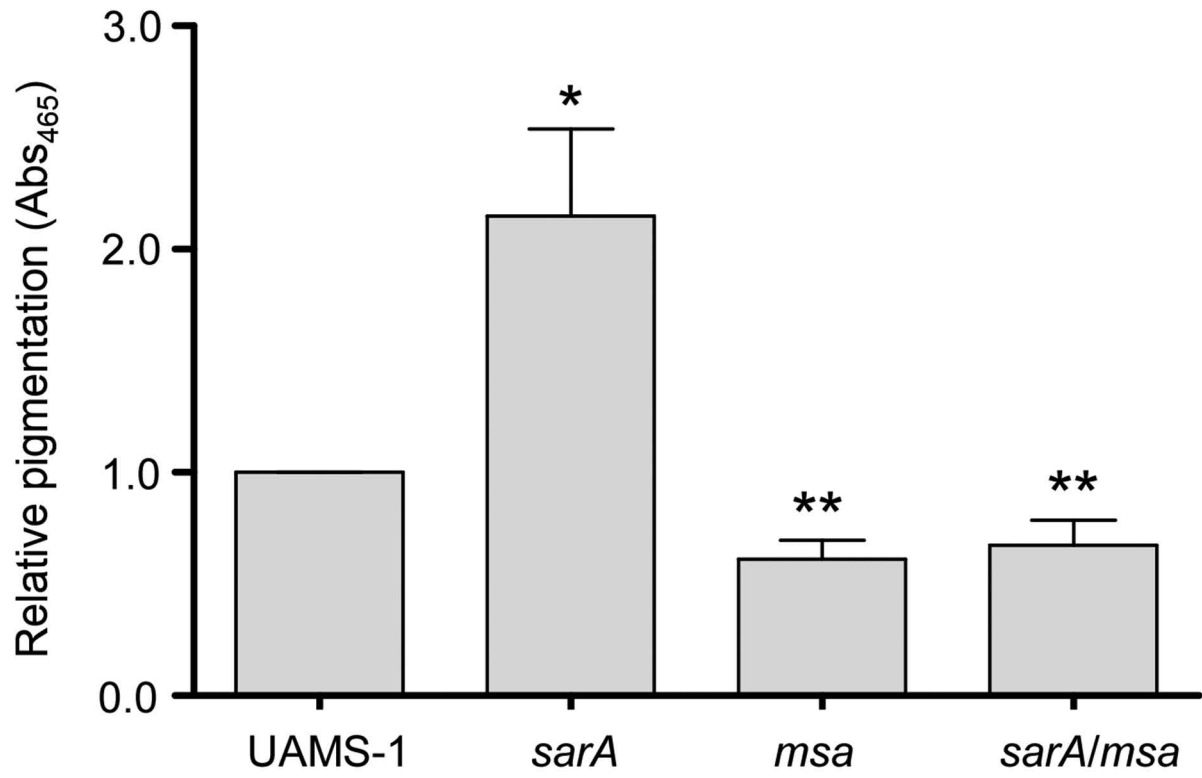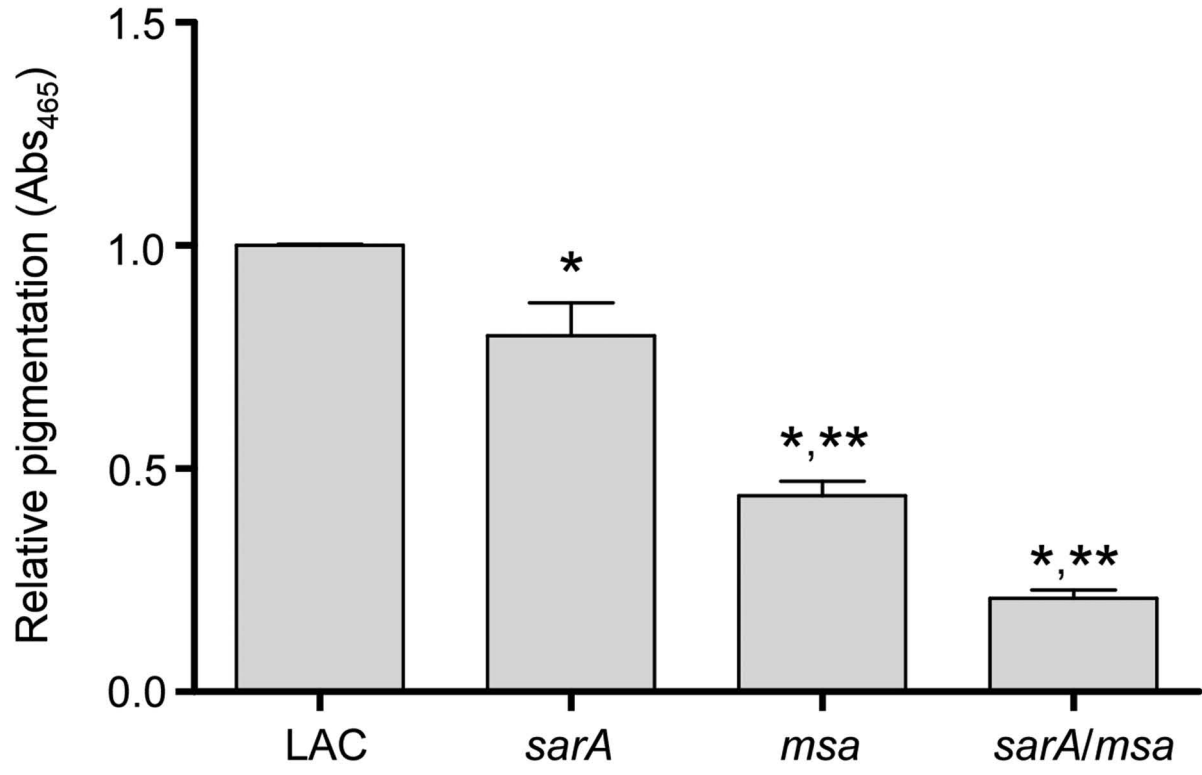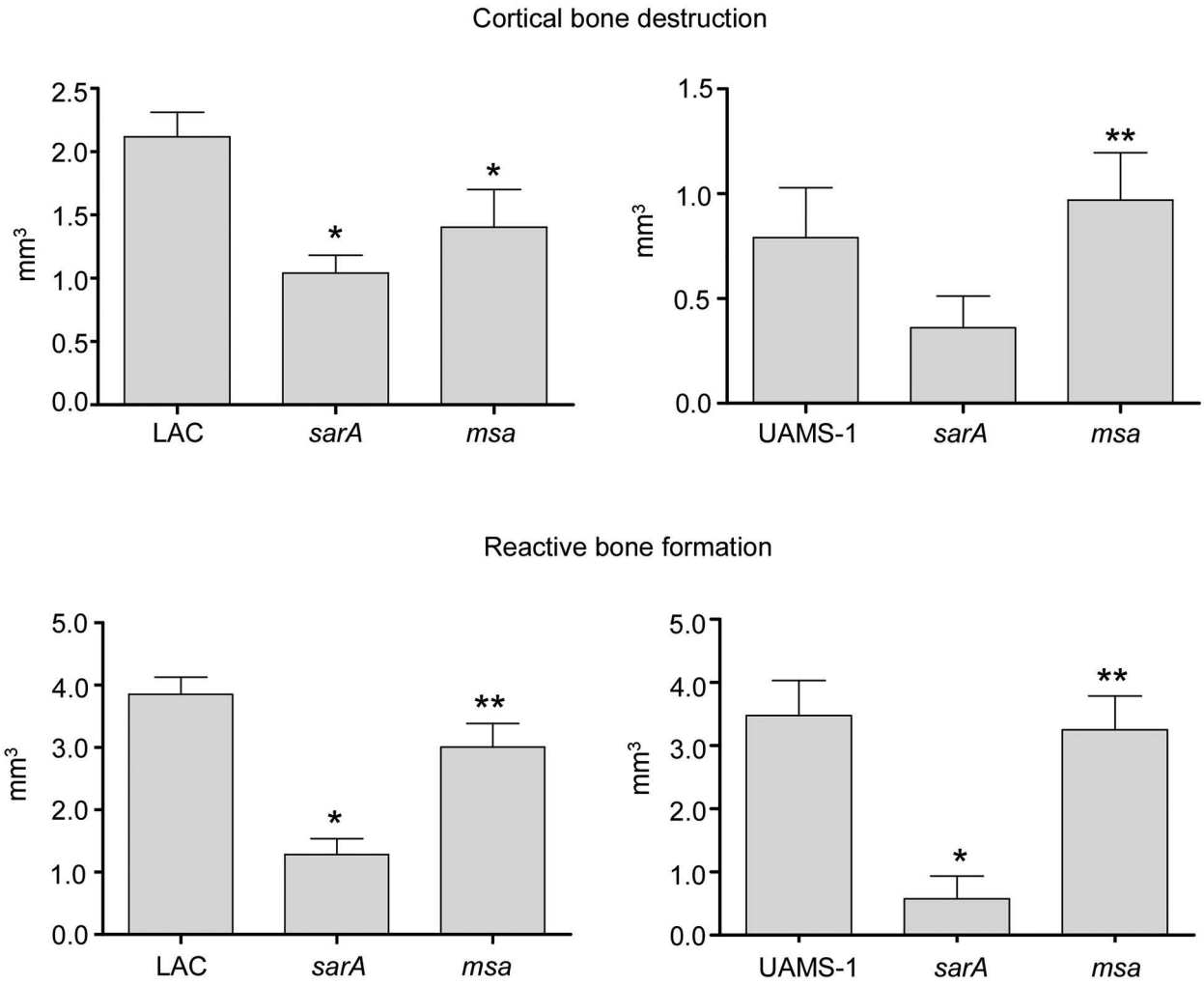gy at Southampton (nCATS), Mechanical Engineering, University of Southampton, Southampton, UK, [29]Department of Orthopaedic Surgery, Avon Orthopaedic Centre, Southmead Hospital, Bristol, UK, [30]Department of Orthopaedic Surgery at St. Olavs Hospital, Trondheim, Norway

ABSTRACT: Biofilm-associated implant-related bone and joint infections are clinically important due to the extensive morbidity, cost of care and socioeconomic burden that they cause. Research in the field of biofilms has expanded in the past two decades, however, there is still an immense knowledge gap related to many clinical challenges of these biofilm-associated infections. This subject was assigned to the Biofilm Workgroup during the second International Consensus Meeting on Musculoskeletal Infection held in Philadelphia USA (ICM 2018) (https://icmphilly.com). The main objective of the Biofilm Workgroup was to prepare a consensus document based on a review of the literature, prepared responses, discussion, and vote on thirteen biofilm related questions. The Workgroup commenced discussing and refining responses prepared before the meeting on day one using Delphi methodology, followed by a tally of responses using an anonymized voting system on the second day of ICM 2018. The Working group derived consensus on information about biofilms deemed relevant to clinical practice, pertaining to: (1) surface modifications to prevent/inhibit biofilm formation; (2) therapies to prevent and treat biofilm infections; (3) polymicrobial biofilms; (4) diagnostics to detect active and dormant biofilm in patients; (5) methods to establish minimal biofilm eradication concentration for biofilm bacteria; and (6) novel anti-infectives that are effective against biofilm bacteria. It was also noted that biomedical research funding agencies and the pharmaceutical industry should recognize these areas as priorities. © 2019 Orthopaedic Research Society. Published by Wiley Periodicals, Inc. J Orthop Res 37:1007–1017, 2019.

Keywords: biofilm; International Consensus Meeting; musculoskeletal infection; periprosthetic joint infection; surgical site infection; osteomyelitis

Around two thirds of all human infections are believed to be biofilm related. Biofilm-associated implant-related bone and joint infections, or biofilm-associated musculoskeletal (MSK) infections, are clinically important due to the extensive morbidity, cost of care, and socioeconomic burden that they cause.[1–3] A biofilm can

be described as a complex and well-structured aggregation of microorganisms, of single or multiple species. Biofilms are found adherent to biotic (host tissue) and abiotic (implant/biomaterial) surfaces, or as floating aggregates, all of which are encased in a self-produced matrix of polymeric substances. Biofilm thickness can vary between a single cell layer to thick, three dimensional communities with columns and channels. Biofilms are tolerant to antimicrobials and evade the host immune system. Biofilm formation is central to the pathogenesis of implant-related infections which develop after microorganisms, bacteria or fungi, attach to the protein conditioned surface. All the materials used in orthopaedic implants are vulnerable to attachment of biofilm forming bacteria. Bacterial attachment is known to occur intraoperatively, post operatively, and on a delayed basis. The propensity for biofilm formation at any of these time points places implants at risk for surgical site infections (SSIs). Following attachment there is a stepwise progression of biofilm formation and maturation leading to an established infection.

Biofilm associated infection is one of the most common causes for failure of orthopaedic implants. Clinically, biofilm-associated infections can exist innocuously with few symptoms or signs.[4] With currently available diagnostic tests, clinical diagnosis can be challenging unless dispersed microorganism are virulent enough to incite a host response. Diagnostically, the sensitivity of conventional microbiologic culture methods can be low, due to the inability of microorganisms to propagate in the sessile phenotype. Failure to isolate and identify the pathogen is not only associated with challenges in antimicrobial management, but also can lead to continuation of the infection and failure following revision surgery, and lead to a falsely low incidence of implant-related infections. Surgical debridement is an important part of treatment. Many times the debridement is intralesional, making it difficult for the surgeon to be certain removal of biofilm is complete and biofilm fragments remaining in the surgical site have the potential to propagate the infection.[5–8]

Although research in the field of biofilms has expanded in the past two decades, there is still an immense knowledge gap related to many clinical aspects of biofilm-associated infections. Given this, and the great clinical and financial impact of biofilm infections, this subject was assigned to the Biofilm Workgroup during the second International Consensus Meeting on Musculoskeletal Infection held in Philadelphia USA, July 25–27, 2018 (ICM 2018) (https://icmphilly.com).

METHODOLOGY

The main objective of ICM 2018 was to bring together experts in MSK infections from around the world to assimilate the best available data on management of patients afflicted with implant-related, bone and joint infections (MSK Infections), including SSI and Periprosthetic Joint Infections (PJI), to ultimately derive a consensus document (https://icmphilly.com). The first step, led by ICM 2018 co-chairs, Drs. Javad Parvizi and Thorsten Gehrke, was to identify and recruit 869 MSK infection experts from 92 countries. These experts agreed to serve as delegates tasked to identify the controversies and challenges related to prevention, diagnosis, and treatment of MSK infection, then seek consensus on those issues using Delphi methodology,[9] which have emerged as a critical tool by which thought leaders debate all existing knowledge to derive "general agreement" in response to clinical care driven questions. The complete details for the Delphi methods and timelines of the 13 specific steps used to complete the 2018 ICM have been published.[10] All of the consensus questions, voting responses and additional information on the 2018 ICM are available online (https://icmphilly.com), or on the iOS and Android App (ICMPHILLY). Only delegates with an established expertise in the field of MSK infection were invited. These distinguished delegates generated 652 questions addressing clinical issues related to MSK infection. These questions were grouped into 18 clinical and basic science areas, each addressed by separate workgroups, including a workgroup to address issues related to biofilms. Over 24 months, each question was assigned to two or more delegates to prepare responses. Response preparation consisted of a systematic literature review, data summary and an independent narrative response written from the perspective and experience of each authoring delegate. These responses were reviewed by a facilitator and combined into a single document. The compiled response was then edited by both authors to an agreed response to be posted to the ICM web site for review and comment by all 869 delegates. The authoring delegates then refined their responses based on the comments in preparation for discussion and voting at the in-person meeting that was held on July 25th–27th 2018, in Philadelphia, USA. The controversial questions and responses were discussed and further edited on the initial day of the meeting. The delegates who attended the meeting in person then voted to: (1) agree; (2) disagree; or (3) abstain, on each response during the latter 2 days of the meeting, following Delphi methodology[9] and the voting results were rated as: A) Simple majority (50.1–59%); No Consensus; b) Majority (60–65%); Weak Consensus; c) Super Majority (66–99%); Strong Consensus; and d) Unanimous (100%): Unanimous Consensus.

Among the 18 work groups there was one made up of the 28 authors of this consensus document dedicated to biofilms. This group consisted of biofilm experts from backgrounds including both basic and clinical science in microbiology, immunology, biomedical engineering, infectious diseases, and orthopaedic surgery. The biofilm workgroup was tasked with discussion, response editing and voting on the thirteen biofilm related questions that were deemed to be relevant to clinical practice. While the majority of the responses to the ICM questions were focused with the intent to provide clinical recommendation for prevention, diagnosis or treatment, the biofilm responses were more basic science in nature, given as informative narratives without clinical recommendations.

The Workgroup emphasizes that consensus was reached without compulsion, undue influential power or expressiveness, inability to comprehend another course of action, or impatience with the process of debate. Discussion was carried out in a moderated open forum were everyone had

opportunity to study the wording of the questions and responses, review the available evidence and voice their opinion before voting occurred. Below is a summary of the 13 biofilm related questions, responses and/or recommendations with HTML links to a downloadable PDFs for each question, response, consensus, and post-meeting rationale.

RESULTS

The Biofilm Workgroup's response to the 13 questions is summarized in Table 1, which covers biofilm microbiology, life cycle, structure, quorum sensing, susceptibility to host immune response and antimicrobials, and novel therapy technologies. All of the questions and responses were considered with an eye to identifying opportunities for clinical intervention, either now or in the future. The vast majority of the data were basic science in nature with minimal low-level clinical outcome data in isolated areas, making responses to the questions narrative opinions about the current state of knowledge. These narrative responses are felt to be foundational to clinical judgement for management of MSK infections rather than clinical recommendations. We provide an interpretive discussion of the responses. The strength of evidence assigned to each response is based on the collective judgement of the Workgroup about the scientific validity of the data because reports on basic scientific data cannot be categorized by the Level of Evidence methodology used for clinical data. High level clinical outcomes data were not available to address any of the 13 questions. Thus, the audience is encouraged to read the rationale for each question in the ICM 2018 document (https://icmphilly.com) to gain a deeper understanding of the available data.

Question one addresses the life cycle of Biofilms, and **Question four** addresses the timeline of biofilm maturation. These are relevant because diagnosis and treatment options vary by the presence and maturity of biofilms. With biofilm maturity comes the inability to identify bacteria within biofilms using conventional culture and susceptibility testing, and these mature biofilms are resilient to treatment. The life cycle of biofilm is a complex continuum progressing through four stages: (1) attachment; (2) accumulation; (3) maturation; and (4) dispersal, over a time period that ranges from minutes to hours in vitro, and days to weeks or longer in vivo.[11] Biofilms can mature before they present diagnosable findings, because it is the host response to bacteria outside of biofilms that leads to clinical symptoms, physical findings, and positive diagnostic tests. This limits the opportunity to intervene before the biofilm is established. Currently, there is no clinical research available to determine whether the timescale in the development of biofilm formation differs markedly between bacterial species. In vitro experiments and in vivo animal studies find that progression of biofilms is mediated by the interplay of a number of microbial, host, and environmental factors. These factors can be different across microbial species and even across strains within species. The timeline for biofilm formation may not correlate with the onset of infection symptoms; therefore the concept of acute or chronic biofilm-associated MSK infection is likely to be less pertinent for management decisions than previously thought.

Questions two, Question five and Question ten address surface properties that favor attachment and progression to established biofilm. The available data are mostly basic science in nature from in vitro experiments and in vivo animal studies, with limited clinical data on iodine surface modification. There is strong consensus that bacterial attachment can occur on essentially all prosthetic and injured or immune compromised biological surfaces, including surfaces of antimicrobial loaded bone cement (ALBC) spacers utilized to locally deliver antimicrobials when treating MSK infection patients during two-stage treatment plans.[12,13] ALBC surfaces, which are physically favorable for bacterial attachment, can support the growth of either the original pathogen(s), or a secondary pathogen(s) not present in the initial infection. As the antimicrobial load in ALBC is released, the surrounding antimicrobial levels fall below the minimal inhibitory concentration (MIC), and thus the surfaces become susceptible to microbial colonization. Additionally, antimicrobial levels can remain sub-therapeutic for years, which increases the risk for the emergence of microorganisms that are resistant to the incorporated antimicrobial(s), although this has not been realized in clinical practice. The physicochemical properties of materials/implants that are known to affect the time required and robustness of the established biofilms include surface chemistry, surface charge, hydrophilicity/hydrophobicity, micro/nano-topography, and porosity.[14–17] Biofilm formation is affected by surface properties and bacterial attachment to abiotic surfaces is an inherent capability of MSK pathogens. In vitro experiments and in vivo animal models have found that modification of implant surface can decrease bacterial adherence, and thus decrease biofilm formation leading investigators to seek physico-chemical surface modifications and coatings to inhibiting bacterial adhesion to theoretically decrease the risk of infection without limiting osseointegration.[18] The ideal implant surface modification should have a long duration of anti-infective effect, mechanical stability, and host biocompatibility.[19–21] An innovative technology using iodine to produce porous anodic oxide implant surfaces with the antiseptic properties of iodine was studied in a prospective uncontrolled cohort study for both prophylaxis in high risk patients, and for treatment in confirmed MSK infection cases.[22] Confirmatory reports on subsets of these patients with hip replacement implants or fixator pins reported no hip implant infections and decreased pin tract infections respectively.[23,24]

Nano-particulate silver is an example of a surface modification that offers short term protection with

Table 1. Biofilm Related Questions, Responses or Recommendations as Well as Level of Agreement by the Working Group (for Supporting Information: https://www.ors.org/icm-2018-biofilm-workgroup/)

Questions	Response or recommendation	Level of Evidence	Delegate Vote
QUESTION 1: What is the life cycle of biofilm and the mechanism of its maturation?	A biofilm may be defined as a microbe-derived sessile community characterized by organisms that are attached to a substratum, interface, or each other, are embedded in a matrix of extracellular polymeric substance, and exhibit an altered phenotype with respect to growth, gene expression, and protein production. The biofilm infection life cycle generally follows the steps of attachment (interaction between bacteria and the implant), accumulation (interactions between bacterial cells), maturation (formation of a viable 3D structure), and dispersion/detachment (release from the biofilm). The life cycle of biofilm is variable depending on the organism involved. There are characteristics in the life cycle of biofilm formation. These include, attachment, proliferation/accumulation/maturation, and dispersal. Biofilm can either be found as adherent to a surface or as floating aggregates.	Strong (this is a scientific review)	Agree: 100%, Disagree: 0%, Abstain: 0% (Unanimous, Strongest Consensus)
QUESTION 2: What surface properties favor biofilm formation?	The attachment of bacteria to implant and biological surfaces is a complex process, starting with the initial conditioning film. Roughness, hydrophobicity/hydrophilicity, porosity, pore topology, and other surface conditions are the key factors for microbial adhesion. Because of the huge variety of these factors, most of the studies directed at bacterial attachment to the implant surface were limited to specific surface conditions since it is difficult to examine the plethora of parameters concomitantly. There are variable conclusions among the available basic science and animal studies relevant to this topic, many of which will be described in greater detail below. Bacteria can form biofilm on almost all prosthetic surfaces and biological surfaces. To date, this consensus group knows of no surface that is inimicable to the growth of biofilm in vivo.	Strong	Agree: 100%, Disagree: 0%, Abstain: 0% (Unanimous, Strongest Consensus)
QUESTION 3: Is the biofilm on orthopaedic implant surface permeable to neutrophils and macrophages in vivo? Are these innate immune cells	A mature bacterial biofilm has limited permeability to neutrophils and macrophages. Those that get through are clinically ineffective at	Strong	Agree: 100%, Disagree: 0%, Abstain: 0% (Unanimous, Strongest Consensus)

Table 1.   (*Continued*)

Questions	Response or recommendation	Level of Evidence	Delegate Vote
(meaning any macrophages or neutrophils) capable of engulfing and killing bacteria?	eradicating biofilm bacteria. While neutrophils and macrophages are capable of engulfing and killing planktonic bacteria, they are not innately capable of effectively engulfing and killing sessile bacteria in biofilm.		
QUESTION 4: Does the timescale of biofilm formation differ between bacterial species? If so, what is the timescale for common causative organisms?	Currently, there is no clinical research available to answer whether the timescale in the development of biofilm formation differs between bacterial species. In vitro studies show high variability in biofilm formation based on bacterial strains and conditions. Animal studies have demonstrated rapid (minutes to hours) biofilm formation. The group notes that the timeline of biofilm formation may not correlate with the onset of infection symptoms.	Strong	Agree: 100%, Disagree: 0%, Abstain: 0% (Unanimous, Strongest Consensus)
QUESTION 5: Do bacteria form biofilm on the surface of cement spacer in a similar fashion to a metallic implant?	Yes. While the vast majority of studies have been in vitro, there is clinical evidence that majority of bacteria are able to form biofilm on the surface of cement spacer.	Strong	Agree: 100%, Disagree: 0%, Abstain: 0% (Unanimous, Strongest Consensus)
QUESTION 6: Does *Mycobacterium tuberculosis* form a biofilm on implants?	Few data from experimental in vitro and in vivo studies and a limited number of case reports indicate that *M. tuberculosis* has a slow, albeit significant, ability to form biofilm on metal surfaces. The group suggests that management of *M. tuberculosis* implant-related infections should be treated using the same principles as that of other implant-related infections.	Strong	Agree: 100%, Disagree: 0%, Abstain: 0% (Unanimous, Strongest Consensus)
QUESTION 7: What is the role of the microbial synergy in polymicrobial infections?	In polymicrobial infections, a complex environment may be formed in which microbiological interactions exist between microorganisms. Scientific evidence exists to show that combinations of bacterial species may exist whereby these can protect each other from antibiotic action via the exchange of virulence and antibiotic resistance genes, and this may be evident in adverse outcomes for polymicrobial orthopaedic implant-related infections. It is also probable that polymicrobial infections may be more likely in patients with poor immunity and tissue healing.	Strong	Agree: 100%, Disagree: 0%, Abstain: 0% (Unanimous, Strongest Consensus)
QUESTION 8: Is the mapping of biofilm to a particular component or anatomical location an important consideration in	At present, mapping of biofilms is only possible in the laboratory, not in the clinical setting. Therefore, it is of	Consensus	Agree: 100%, Disagree: 0%, Abstain: 0% (Unanimous,

Table 1.   (*Continued*)

Questions	Response or recommendation	Level of Evidence	Delegate Vote
management of implant related infections?	unknown clinical importance in relation to management of implant-related infections.		Strongest Consensus)
QUESTION 9: Is there evidence that interference with bacterial communication by blocking quorum sensing molecules can minimize biofilm formation in vivo?	In vivo animal studies have demonstrated that interference with quorum sensing signals/molecules in some infections leads to decreased biofilm formation. There are contradictory results in *Staphylococcus* species. However, there are no clinical studies demonstrating this phenomenon.	Limited	Agree: 100%, Disagree: 0%, Abstain: 0% (Unanimous, Strongest Consensus)
QUESTION 10: Can a biomaterial surface be modified to dispel bacterial adherence and biofilms? What are the potential concerns in modifying implant surfaces to combat biofilms?	The purpose of the surface modification is to decrease perioperative bacterial adherence and thus prevent biofilm formation. This has been shown in in vitro studies and in vivo animal models. There have been numerous strategies devised to alter surfaces. Such modified surfaces may interfere with the expected osseointegration, mechanical stability, and long-term implant survivability. The duration of long-term anti-infective effects are unknown. To date, no positive in vitro effect has been translated into a clinical setting.	Consensus	Agree: 100%, Disagree: 0%, Abstain: 0% (Unanimous, Strongest Consensus)
QUESTION 11: What is the relevance of Minimum Inhibitory Concentration (MIC) of infecting organisms in biofilm-mediated chronic infection?	The use of Minimum Inhibitory Concentration (MIC) is limited to (1) defining antibiotics that the microorganism is susceptible to in its planktonic state but cannot be used to guide treatment of biofilm-based bacteria, and (2) selecting long-term suppressive antibiotic regimens where eradication of infection is not anticipated. Alternative measures of antibiotic efficacy specifically in the context of biofilm-associated infection should be developed and validated.	Strong	Agree: 100%, Disagree: 0%, Abstain: 0% (Unanimous, Strongest Consensus)
QUESTION 12: What is the Minimum Biofilm Eradication Concentration (MBEC) of anti-infective agents?	The minimum biofilm eradication concentration (MBEC) of antimicrobial agents is a measure of in vitro antibiotic susceptibility of biofilm producing infective organisms. It is dependent on the surface, medium and the exposure period to an antimicrobial agent. There are no standardized measurement parameters for MBEC. MBEC is currently a research laboratory value and lacks clinical availability. In the group's opinion, there is value in developing	Consensus	Agree: 100%, Disagree: 0%, Abstain: 0% (Unanimous, Strongest Consensus)

Table 1. *(Continued)*

Questions	Response or recommendation	Level of Evidence	Delegate Vote
QUESTION 13: Do bacteriophages have a role in treating multidrug-resistant PJI?	a clinically-validated MBEC assay. Unknown. Although some preclinical and clinical studies have demonstrated a good safety profile as well as promising therapeutic effects using bacteriophages for treating bone and joint infections, further clinical research using bacteriophage therapy in patients with multidrug-resistant PJI is required. There are known obstacles to bacteriophage therapy, including the fact that bacteriophages are neutralized in serum and relevant pathogens contain CRISPR/cas9 immunity against bacteriophage. Phages are usually bacterial strain specific; thus, a cocktail of different bacteriophage lineages may be necessary to effectively treat biofilm-mediated infections.	Consensus	Agree: 100%, Disagree: 0%, Abstain: 0% (Unanimous, Strongest Consensus)

some limited local antimicrobial activity in the fluid or tissue adjacent to the surface. However clinical data on silver surface modifications of urinary, vascular, and peritoneal catheters, vascular grafts and heart valves, have not reported on biofilm formation, and these technologies have not been applied to orthopaedic devices.[25] To date, no surface modification found to have a positive in vitro effect has been translated into the clinical setting. Clinical studies are required to determine the long-term impact and outcomes of modified surface properties on biofilm formation in human patients.

Question three addresses biofilm susceptibility to host phagocytosis. While neutrophils and macrophages (10–20 μm) have the ability to access the surface and enter the channels of a mature biofilm (100 μm),[26] they are not able to access biofilm encased microorganisms.[12,13,27–38] When a fragment of biofilm is small enough, phagocytes can engulf it, but they are not able to destroy the bacteria.[39–42] Phagocytized sessile bacteria can persist in peri-implant tissue in vitro, and in the tissues of patients with intravenous catheters colonized by a variety of bacteria.[43,44] *Staphylococcus aureus* has recently been shown to invade the osteocytic-canalicular network of cortical bone and to reside within osteoblasts where accessibility to phagocytes is limited.[45,46] However, after bacteria are dispersed from biofilms they progressively transform into planktonic phenotypes that are more susceptible to antimicrobials, and have surface properties that are

detectable by phagocytes, and are subject to phagocytic killing.

Question six addresses the biofilm forming capabilities *of Mycobacterium tuberculosis.*

While there are bacteria that do not appear to form biofilms, essentially all bacteria that cause implant-related infections form biofilms including *Mycobacteriaceae*. The work group only addressed the data related to *Mycobacterium tuberculosis,* not the faster growing non-tuberculous mycobacteria (NTMB). Thus, the consensus statements for infections related to *M. tuberculosis* cannot be extrapolated to infections related to NTMB. In vitro experiments find that *M. tuberculosis* can form biofilm on metal surfaces; albeit less than on Polymethylmethacrylate (PMMA), and less than is formed by *Staphylococci spp*. Based on in vivo studies and clinical case reports biofilms in TB infections may contribute to casseous necrosis.[47–49] Although no data from clinical trials exist to address this question, the Workgroup felt that the published scientific data are strong enough to warrant consensus opinion on the clinical implications for management of implant-related infections caused by *M. tuberculosis*. Accordingly, we recommend that the fundamental principles for implant-related infections caused by other biofilm forming bacteria should also be followed for *M. tuberculosis*. One of the delegates who was not present for the discussion and voting points out that eradication of implant related infections, due to "susceptible" *M. tuberculosis*, is possible with

chemotherapy alone,[50] and that depending on the anatomic or functional deficiencies, surgical intervention can be performed at a later time point (e.g., weeks to months after initiating anti-TB treatment). This success may be attributed to weak biofilm formation by *M. tuberculosis* and/or, to anti-biofilm properties of the anti-TB agents. The decision of when or if to proceed with surgical debridement for biofilm associated implant related TB infections may best be made in collaboration with an infectious disease specialist experienced in management of extremity TB infections, taking into consideration each patient's response to chemotherapy.

Question seven assesses the role of microbial synergy, which means that different species (e.g., aerobic and anaerobic microbes) collaborate to cause disease that neither pathogen could achieve alone. Patients with polymicrobial biofilm-associated MSK infections are more challenging to treat due to the need for broad spectrum antimicrobial coverage. The reason could be multifactorial, including microbial synergy.[4,51,52] These microbial interactions include cross feeding, quorum sensing, exchange of virulence genes, and exchange of antimicrobial resistance genes, making infection eradication more challenging in clinical practice.

Question eight asks a clinical question about the importance of mapping the location of the biofilm within a patient for management of biofilm-associated MSK infections. Because biofilm eradication requires physical removal, the extent and location of the biofilm is technically important. However there was strong consensus that there are no clinical methods available to actually identify biofilm before or during surgical debridement. While advanced imaging has been used to spatially locate areas of active infection with good resolution, neither ^{99m}Tc WBC SPECT-CT with concordant ^{99m}Tc sulphur colloid marrow map,[53,54] nor PET-CT, specifically identify biofilm. Targeted imaging methods which utilize binding of imaging agents to bacteria also do not distinguish between planktonic and sessile bacteria, and it is unknown if these techniques identify dormant cells such as persister cells.[55] Optical imaging using fluorescence (fluorescein, indocyanine green, and IRDye-800CW) has the potential for identifying microbes on or near a surface. While optical imaging techniques are possible in surgical wounds, none have emerged from the research setting for clinical use.[55] Optical dyes (DMMB 1,9-dimethyl methylene blue) can be used to stain the biofilm matrix, but this has yet to gain acceptance for clinical use. There is a major capability gap for these technologies between research and clinical use, which prevents mapping biofilms to specific anatomic sites or a particular implant component/location in clinical practice.

Question nine evaluates in vivo data on blocking quorum sensing to minimize biofilm formation. While the majority of the data are in vitro, there are some in vivo animal studies that have found that interference with quorum sensing signals/molecules can lead to decreased biofilm formation.[56] The workgroup is not aware of any anti-quorum sensing strategies that are available for clinical use, and confirmed that there are no clinical studies investigating the effectiveness of this strategy.

Question 11 and Question 12 address antimicrobial susceptibility of microorganisms in both biofilm-associated and non-biofilm-associated states. The Workgroup identified the need to emphasize the difference in antimicrobial susceptibility between microorganisms in their planktonic form, and the same microorganisms in their biofilm-associated sessile form, noting that biofilm associated phenotypes are hundreds to thousands of times less susceptible to antimicrobials than their free floating planktonic counterparts. This critically important observation is fundamental to the understanding that the MIC used to quantify antimicrobial susceptibility for non-biofilm associated microorganisms has no role in determining the antimicrobial susceptibility of microorganisms in biofilms. There are established validated methodologies for determining MICs, but not for determination of susceptibility of biofilm-associated bacteria.[57–59] Determining antimicrobial susceptibility of bacteria within biofilm is not easy. Clinicians need an as yet clinically unavailable test that measures antimicrobial efficacy such as minimum biofilm eradication concentration (MBEC), minimum biofilm bactericidal concentration (MBBC), or minimum biofilm inhibitory concentration (MBIC). Because host defenses have limited ability to kill persister cells within biofilm, a measure of total eradication of the bacteria in the biofilm (MBEC) is favored over methods that measure inhibition of bacterial replication (MBIC), but do not kill the persisters. It was noted that the MBEC assays used in research are not standardized, and that MBEC values for each individual bacteria/antimicrobial pair are dependent on the surface that the biofilm is attached to and the duration the biofilm is exposed to the antimicrobial. Clinically-validated assays of antimicrobial susceptibility (MBEC) are needed to provide guidance for local antimicrobial therapy in biofilm-associated orthopaedic infections. During its early accumulation phase, a growing biofilm has less resistance to antimicrobial therapy than a fully mature biofilm with microorganisms that are quiescent metabolically and not replicating. This relative preservation of antimicrobial susceptibility during the early phase of biofilm formation has led to failed efforts to treat early phase orthopaedic infections without surgical intervention.[60]

Finally, **question 13** sought data on the role of bacteriophages in treatment of multidrug-resistant PJI. There are several encouraging strategies emerging as potential therapeutic modalities against biofilms, including immunotherapy, nanoparticles with antibacterial effects and antimicrobial peptides along

with bacteriophage therapy. The Workgroup discussed the role of bacteriophages in treatment of biofilm-associated implant infections. While this concept is over a century old, currently there is insufficient clinical experience to recommend its use. Moreover, the Workgroup identified several obstacles that have the potential to challenge the scientific premise of phage therapy for treating MSK infections including: (1) phages are neutralized in human serum, although this may depend on the route of the phage therapy and requires more evaluation of clinical efficacy;[61] (2) phages are strain specific leading to the need for a cocktail of phages to cover all possible bacteria in the biofilm; and (3) CRISPR Cas9 immunity engenders most bacterial pathogens evolutionarily resistance to phages.[62] While phage therapy costs around $2,000–20,000 USD, and can require more than one round of treatment, this cost is in line with or less than other biologic pharmaceuticals, and is less than surgical debridement. In vivo animal studies are required to identify parameters for clinical trials.

DISCUSSION

The ICM 2018 engaged 869 international experts using the Delphi method to reach consensus on 652 issues related to management of patients with MSK infections, which was the largest orthopaedic consensus meeting in history. However, despite its major strengths, size, scope, and inclusiveness, it is recognized that the Delphi method has some inherent weaknesses. First, and greatest among these weaknesses, is the need to follow the process. While the entire ICM 2018 included a large number of individuals that addressed an expansive docket of questions, which could be at risk for distraction and fatigue among the delegates, the Biofilm Workgroup was a functional size (28) that addressed 13 questions. All those present actively and respectfully participated in the discussion, while two facilitators effectively ensured that all voices were heard and unhampered by more dominant participants, resulting in a comprehensive vetting of each question. However, the ICM design did not allow for anonymous discussion, which could have impeded free expression by some if it was in a less collegial environment. Second, in scientific areas that are advancing rapidly such as biofilm microbiology, a degree of scientific uncertainty and unknowns can be expected. In the case of the 13 biofilm questions it was possible to find common ground based on strong scientific data. Third, inherent to the Delphi method, participants considering questions outside their area of expertise could reach an incorrect consensus with a high level of confidence based on lack of knowledge. The participants in the Biofilm Workgroup included the world leaders in all areas of biofilm science that were covered by the 13 questions posed to them. Thus, it is unlikely there was consensus reached based on lack of knowledge. And finally, the Delphi method is best for addressing single scalar topics. When complex interdependent areas of knowledge such as medicine and biology are considered, the possibility exists that a consensus is impossible, even when some established knowledge exists, or that conflicting consensuses are arrived at by different groups considering similar questions. The Biofilm Workgroup was very precise in refining the wording of the questions and responses to avoid these pitfalls.

As knowledge about biofilms expands and related strategies enter clinical practice the Workgroup expects new questions will arise, and the responses to the current questions will advance justifying clinical recommendations in the future. We anticipate another ICM in the future to update the consensuses from ICM 2018.

CONCLUSION

It is anticipated that the data, rationale and response for each question, while not a specific clinical recommendation, will provide caregivers a higher level of understanding of the pathophysiology they are treating, which can lead to better clinical judgement in the absence of high level clinical outcomes data. Studies dedicated to advance our understanding of biofilms and their role in human implant-related infections are urgently required for better diagnosis and eradication strategies. Consensus was reached on currently available data on biofilms deemed relevant to clinical practice and pertained to: (1) surface modifications that prevent/inhibit biofilm formation; (2) therapies to prevent and treat biofilm infections; (3) polymicrobial biofilms; (4) diagnostics to detect active and dormant biofilm in patients; (5) methods to determine antimicrobial susceptibility of biofilm associated bacteria; and (6) novel anti-infectives that are effective against biofilm associated bacteria. It is also noted that biomedical research funding agencies and the pharmaceutical industry should recognize these areas as priorities.

DECLARATIONS

For pre-, meeting rationales, please refer to https://icmphilly.com/document/icm-2018-biofilm-document/.

The mention of commercial products, their sources, or their use in connection with material reported herein is not to be construed as either an actual or implied endorsement of such products by the Department of Health and Human Services. The findings and conclusions in this communication have not been formally disseminated by the U.S. Food and Drug Administration and should not be construed to represent any Agency determination or policy.

REFERENCES

1. Kapadia BH, Berg RA, Daley JA, et al. 2016. Periprosthetic joint infection. Lancet 387:386–394.
2. Vastag B. 2004. Knee replacement underused, says panel. JAMA 291:413.
3. Lamagni T. 2014. Epidemiology and burden of prosthetic joint infections. J Antimicrob Chemother 69:i5–i10.
4. Khoury AE, Lam K, Ellis B, et al. Prevention and control of bacterial infections associated with medical devices. ASAIO J. 38:M174–M178.
5. Cramton SE, Gerke C, Schnell NF, et al. 1999. The intercellular adhesion (ica) locus is present in *Staphylococcus aureus* and is required for biofilm formation. Infect Immun 67:5427–5433.
6. Rice KC, Mann EE, Endres JL, et al. 2007. The cidA murein hydrolase regulator contributes to DNA release and biofilm development in *Staphylococcus aureus*. Proc Natl Acad Sci 104:8113–8118.
7. Ciofu O, Rojo-Molinero E, Macià MD, et al. 2017. Antibiotic treatment of biofilm infections. APMIS 125:304–319.
8. O'Neill E, Pozzi C, Houston P, et al. 2008. A novel Staphylococcus aureus biofilm phenotype mediated by the fibronectin-binding proteins, FnBPA and FnBPB. J Bacteriol 190:3835–3850.
9. Cats-Baril W, Gehrke T, Ba KH, et al. [date unknown]. International consensus on periprosthetic joint infection: description of the consensus process. [cited2018 Aug 13] Available from: https://static1.squarespace.com/static/58124b89e58c62bc0893a0aa/t/5824df3b46c3c4041b44ce96/1478811451513/Consensus+Process.pdf
10. Parvizi J, Gehrke T, Mont MA, et al. 2019. Introduction: proceedings of international consensus on orthopedic infections. J Arthroplasty 34:S1–S2.
11. Nishitani K, Sutipornpalangkul W, de Mesy Bentley KL, et al. 2015. Quantifying the natural history of biofilm formation in vivo during the establishment of chronic implant-associated *Staphylococcus aureus* osteomyelitis in mice to identify critical pathogen and host factors. J Orthop Res 33:1311–1319.
12. Stoodley P, Ehrlich GD, Sedghizadeh PP, et al. 2011. Orthopaedic biofilm infections. Curr Orthop Pract 22:558–563.
13. Bertazzoni Minelli E, Della Bora T, Benini A. 2011. Different microbial biofilm formation on polymethylmethacrylate (PMMA) bone cement loaded with gentamicin and vancomycin. Anaerobe 17:380–383.
14. Koseki H, Yonekura A, Shida T, et al. 2014. Early staphylococcal biofilm formation on solid orthopaedic implant materials: in vitro study. PLoS ONE 9:e107588.
15. Gbejuade HO, Lovering AM, Webb JC. 2015. The role of microbial biofilms in prosthetic joint infections. Acta Orthop. 86:147–158.
16. Rochford ETJ, Richards RG, Moriarty TF. 2012. Influence of material on the development of device-associated infections. Clin Microbiol Infect Off Publ Eur Soc Clin Microbiol Infect Dis 18:1162–1167.
17. Otto M. 2013. Staphylococcal infections: mechanisms of biofilm maturation and detachment as critical determinants of pathogenicity. Annu Rev Med 64:175–188.
18. Antoci V, Adams CS, Parvizi J, et al. 2007. Covalently attached vancomycin provides a nanoscale antibacterial surface. Clin Orthop Relat Res 461:81–87.
19. Helmus MN, Gibbons DF, Cebon D. 2008. Biocompatibility: meeting a key functional requirement of next-generation medical devices. Toxicol. Pathol. 36:70–80.
20. Bernthal NM, Stavrakis AI, Billi F, et al. 2010. A mouse model of post-arthroplasty *Staphylococcus aureus* joint infection to evaluate in vivo the efficacy of antimicrobial implant coatings. PLoS ONE 5:e12580.
21. Secinti KD, Özalp H, Attar A, et al. 2011. Nanoparticle silver ion coatings inhibit biofilm formation on titanium implants. J Clin Neurosci Off J Neurosurg Soc Australas 18:391–395.
22. Tsuchiya H, Shirai T, Nishida H, et al. 2012. Innovative antimicrobial coating of titanium implants with iodine. J Orthop Sci Off J Japanese Orthop Assoc 17:595–604.
23. Kabata T, Maeda T, Kajino Y, et al. 2015. Iodine-supported hip implants: short term clinical results. Biomed Res. Int. 2015:368124.
24. Shirai T, Watanabe K, Matsubara H, et al. 2014. Prevention of pin tract infection with iodine-supported titanium pins. J Orthop Sci Off J Japanese Orthop Assoc 19:598–602.
25. Darouiche RO. [date unknown]. Anti-infective efficacy of silver-coated medical prostheses. [cited2018 Sep 24] Available from: https://pdfs.semanticscholar.org/a54c/d7fbadef2e8323b42f43970f79165aed4be1.pdf
26. Wilking JN, Zaburdaev V, De Volder M, et al. 2013. Liquid transport facilitated by channels in *Bacillus* subtilis biofilms. Proc Natl Acad Sci 110:848–852.
27. Takeoka K, Ichimiya T, Yamasaki T, et al. 1998. The in vitro effect of macrolides on the interaction of human polymorphonuclear leukocytes with *Pseudomonas aeruginosa* in biofilm. Chemotherapy 44:190–197.
28. Johnson CJ, Cabezas-Olcoz J, Kernien JF, et al. 2016. The extracellular matrix of candida albicans biofilms impairs formation of neutrophil extracellular traps. PLoS Pathog. 12:e1005884.
29. Johnson CJ, Kernien JF, Hoyer AR, et al. 2017. Mechanisms involved in the triggering of neutrophil extracellular traps (NETs) by Candida glabrata during planktonic and biofilm growth. Sci Rep 7:13065.
30. Boelens JJ, Dankert J, Murk JL, et al. 2000. Biomaterial-associated persistence of *Staphylococcus* epidermidis in pericatheter macrophages. J Infect Dis 181:1337–1349.
31. Hänsch GM, Brenner-Weiss G, Prior B, et al. 2008. The extracellular polymer substance of *Pseudomonas aeruginosa*: too slippery for neutrophils to migrate on? Int J Artif Organs 31:796–803.
32. Hänsch GM, Prior B, Brenner-Weiss G, et al. 2014. The Pseudomonas quinolone signal (PQS) stimulates chemotaxis of polymorphonuclear neutrophils. J Appl Biomater Funct Mater 12:21–26.
33. Ma F, Yi L, Yu N, et al. 2017. *Streptococcus suis* serotype 2 biofilms inhibit the formation of neutrophil extracellular traps. Front Cell Infect Microbiol 7:86.
34. Maurer S, Fouchard P, Meyle E, et al. 2015. Activation of neutrophils by the extracellular polymeric substance of S. epidermidis biofilms is mediated by the bacterial heat shock protein groel. J Biotechnol Biomater 5:176–183.

35. Zimmerli W, Lew PD, Cohen HJ, et al. 1984. Comparative superoxide-generating system of granulocytes from blood and peritoneal exudates. Infect Immun 46:625–630.

36. Hirschfeld J. 2014. Dynamic interactions of neutrophils and biofilms. J Oral Microbiol 6:26102.

37. Jesaitis AJ, Franklin MJ, Berglund D, et al. 2003. Compromised host defense on *Pseudomonas aeruginosa* biofilms: characterization of neutrophil and biofilm interactions. J Immunol (Baltimore, Md. 1950) 171:4329–4339.

38. Parks QM, Young RL, Poch KR, et al. 2009. Neutrophil enhancement of *Pseudomonas aeruginosa* biofilm development: human F-actin and DNA as targets for therapy. J Med Microbiol 58:492–502.

39. Hanke ML, Heim CE, Angle A, et al. 2013. Targeting macrophage activation for the prevention and treatment of *Staphylococcus aureus* biofilm infections. J Immunol (Baltimore, Md. 1950) 190:2159–2168.

40. Spiliopoulou AI, Krevvata MI, Kolonitsiou F, et al. 2012. An extracellular Staphylococcus epidermidis polysaccharide: relation to Polysaccharide Intercellular Adhesin and its implication in phagocytosis. BMC Microbiol 12:76.

41. Thurlow LR, Hanke ML, Fritz T, et al. 2011. *Staphylococcus aureus* biofilms prevent macrophage phagocytosis and attenuate inflammation in vivo. J Immunol (Baltimore, Md. 1950) 186:6585–6596.

42. Scherr TD, Hanke ML, Huang O, et al. 2015. *Staphylococcus aureus* biofilms induce macrophage dysfunction through leukocidin AB and alpha-Toxin. MBio 6:pii:e01021–15. https://doi.org/10.1128/mBio.01021-15

43. Broekhuizen CAN, Schultz MJ, van der Wal AC, et al. 2008. Tissue around catheters is a niche for bacteria associated with medical device infection. Crit Care Med 36:2395–2402.

44. Broekhuizen CAN, Sta M, Vandenbroucke-Grauls CMJE, et al. 2010. Microscopic detection of viable *Staphylococcus epidermidis* in peri-implant tissue in experimental biomaterial-associated infection, identified by bromodeoxyuridine incorporation. Infect Immun 78:954–962.

45. de Mesy Bentley KL, Trombetta R, Nishitani K, et al. 2017. Evidence of staphylococcus aureus deformation, proliferation, and migration in canaliculi of live cortical bone in murine models of osteomyelitis. J Bone Miner Res 32:985–990.

46. de Mesy Bentley KL, MacDonald A, Schwarz EM, et al. 2018. Chronic osteomyelitis with *Staphylococcus aureus* deformation in submicron canaliculi of osteocytes. JBJS Case Connect 8:e8.

47. Esteban J, Garća-Coca M. 2017. Mycobacterium biofilms. Front Microbiol 8:2651.

48. Ojha AK, Baughn AD, Sambandan D, et al. 2008. Growth of Mycobacterium tuberculosis biofilms containing free mycolic acids and harbouring drug-tolerant bacteria. Mol Microbiol 69:164–174.

49. Basaraba RJ, Ojha AK. 2017. Mycobacterial biofilms: revisiting tuberculosis bacilli in extracellular necrotizing lesions. Microbiol Spectr 5. https://doi.org/10.1128/microbiolspec. TBTB2-0024-2016

50. Veloci S, Mencarini J, Lagi F, et al. 2018. Tubercular prosthetic joint infection: two case reports and literature review. Infection 46:55–68.

51. Rotstein OD, Pruett TL, Simmons RL. 1985. Mechanisms of microbial synergy in polymicrobial surgical infections. Rev Infect Dis 7:151–170.

52. Murray JL, Connell JL, Stacy A, et al. 2014. Mechanisms of synergy in polymicrobial infections. J Microbiol 52:188–199.

53. Gemmel F, Van den Wyngaert H, Love C, et al. 2012. Prosthetic joint infections: radionuclide state-of-the-art imaging. Eur J Nucl Med Mol Imaging 39:892–909.

54. La Fontaine J, Bhavan K, Lam K, et al. 2016. Comparison between Tc-99m WBC SPECT/CT and MRI for the diagnosis of biopsy-proven diabetic foot osteomyelitis. wounds a compend. Clin Res Pract 28:271–278.

55. Heuker M, Gomes A, van Dijl JM, et al. 2016. Preclinical studies and prospective clinical applications for bacteria-targeted imaging: the future is bright. Clin Transl Imaging 4:253–264.

56. Reuter K, Steinbach A, Helms V. 2016. Interfering with bacterial quorum sensing. Perspect Medicin Chem 8:1–15.

57. Macià MD, Rojo-Molinero E, Oliver A. 2014. Antimicrobial susceptibility testing in biofilm-growing bacteria. Clin Microbiol Infect Off Publ Eur Soc Clin Microbiol Infect Dis 20:981–990.

58. Høiby N, Bjarnsholt T, Givskov M, et al. 2010. Antibiotic resistance of bacterial biofilms. Int J Antimicrob Agents 35:322–332.

59. Høiby N, Bjarnsholt T, Moser C, et al. 2015. ESCMID guideline for the diagnosis and treatment of biofilm infections 2014. Clin Microbiol Infect Off Publ Eur Soc Clin Microbiol Infect Dis 21:S1–25.

60. Barberán J, Aguilar L, Carroquino G, et al. 2006. Conservative treatment of staphylococcal prosthetic joint infections in elderly patients. Am J Med 119:993.e7-10.

61. Łusiak-Szelachowska M, Zaczek M, Weber-Dąbrowska B, et al. 2014. Phage neutralization by sera of patients receiving phage therapy. Viral Immunol. 27:295–304.

62. Chew WL. 2018. Immunity to CRISPR cas9 and cas12a therapeutics. Wiley Interdiscip Rev Syst Biol Med 10:e1408.

SUPPORTING INFORMATION

Additional supporting information may be found online in the Supporting Information section at the end of the article.
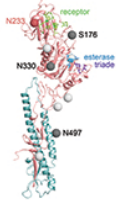
Impact of *Staphylococcus aureus* regulatory mutations that modulate biofilm formation in the USA300 strain LAC on virulence in a murine bacteremia model

Joseph S. Rom, Danielle N. Atwood, Karen E. Beenken, Daniel G. Meeker, Allister J. Loughran, Horace J. Spencer, Tamara L. Lantz & Mark S. Smeltzer

Taylor & Francis
Taylor & Francis Group

RESEARCH PAPER

Impact of *Staphylococcus aureus* regulatory mutations that modulate biofilm formation in the USA300 strain LAC on virulence in a murine bacteremia model

Joseph S. Rom[a,‡], Danielle N. Atwood[a,‡], Karen E. Beenken[a], Daniel G. Meeker[a], Allister J. Loughran[a,†], Horace J. Spencer[b], Tamara L. Lantz[a], and Mark S. Smeltzer[a,c,d]

[a]Department of Microbiology and Immunology, University of Arkansas for Medical Sciences, Little Rock, AR, USA; [b]Department of Biostatistics, University of Arkansas for Medical Sciences, Little Rock, AR, USA; [c]Department of Orthopaedic Surgery, University of Arkansas for Medical Sciences, Little Rock, AR, USA; [d]Department of Pathology, University of Arkansas for Medical Sciences, Little Rock, AR, USA

ABSTRACT

Staphylococcus aureus causes acute and chronic forms of infection, the latter often associated with formation of a biofilm. It has previously been demonstrated that mutation of *atl, codY, rot, sarA*, and *sigB* limits biofilm formation in the USA300 strain LAC while mutation of *agr, fur*, and *mgrA* has the opposite effect. Here we used a murine sepsis model to assess the impact of these same loci in acute infection. Mutation of *agr, atl*, and *fur* had no impact on virulence, while mutation of *mgrA* and *rot* increased virulence. In contrast, mutation of *codY, sarA*, and *sigB* significantly attenuated virulence. Mutation of *sigB* resulted in reduced accumulation of AgrA and SarA, while mutation of *sarA* resulted in reduced accumulation of AgrA, but this cannot account for the reduced virulence of *sarA* or *sigB* mutants because the isogenic *agr* mutant was not attenuated. Indeed, as assessed by accumulation of alpha toxin and protein A, all of the mutants we examined exhibited unique phenotypes by comparison to an *agr* mutant and to each other. Attenuation of the *sarA, sigB* and *codY* mutants was correlated with increased production of extracellular proteases and global changes in extracellular protein profiles. These results suggest that the inability to repress the production of extracellular proteases plays a key role in attenuating the virulence of *S. aureus* in acute as well as chronic, biofilm-associated infections, thus opening up the possibility that strategies aimed at the de-repression of protease production could be used to broad therapeutic advantage. They also suggest that the impact of *codY, sarA*, and *sigB* on protease production occurs via an *agr*-independent mechanism.

Introduction

The production of *Staphylococcus aureus* virulence factors is modulated by a complex and highly interactive regulatory circuit.[1] This affords the bacterium tremendous flexibility with respect to its ability to respond to changing conditions within the host including the influence of an ongoing host immune response.[2-4] This flexibility is reflected in the ability of *S. aureus* to cause a diverse array of infections. In general, these can be characterized as acute infections, the clinical characteristics of which are often defined by toxin production, and chronic infections, the clinical characteristics of which are often associated with formation of a biofilm.[5] To some extent a general theme of the overall *S. aureus* reg-

ulatory circuitry is to modulate the production of specific virulence factors that contribute to these alternative forms of infection.[6] A primary example is the accessory gene regulator (*agr*), expression of which limits biofilm formation but at the same time promotes toxin production.[7,8]

The treatment of all forms of *S. aureus* infection is complicated by the persistent emergence of antibiotic resistant strains, which accounts for its inclusion among the ESKAPE pathogens.[9] The treatment of chronic biofilm-associated infections is further complicated by the presence of the biofilm itself, which confers a therapeutically-relevant level of intrinsic resistance to conventional antibiotics and host defenses.[10] This has created an

CONTACT Dr. Mark S. Smeltzer ✉ smeltzermarks@uams.edu 📧 Department of Microbiology and Immunology, Mail Slot 511, University of Arkansas for Medical Sciences, 4301 W. Markham, Little Rock, AR 72205, USA.
†Current address: Department of Infectious Diseases, St. Jude Children's Research Hospital, Memphis, TN, USA.
‡These authors contributed equally to this work.
ⓘ Supplemental data for this article can be accessed on the publisher's website.

urgent need for new antibiotics that are both effective against the most problematic antibiotic-resistant strains and retain a therapeutically-relevant level of efficacy in the context of a biofilm. New antibiotics have been and continue to be developed,[11] but given the remarkable intrinsic resistance conferred by the presence of a biofilm, accomplishing both of these goals has proven to be a formidable task.[12]

This has led to the suggestion that strategies targeting *S. aureus* regulatory circuits and/or specific virulence factors produced under the control of these circuits could be used to therapeutic benefit either alone or in combination with conventional antibiotics.[13,14] Our approach has been to investigate the regulatory basis for biofilm formation itself, the goal being to identify those regulatory loci that offer the greatest opportunity for therapeutic intervention. These efforts have led us to focus on the staphylococcal accessory regulator (*sarA*), mutation of which limits biofilm formation to a greater extent than mutation of any other regulatory locus we have examined.[15] Moreover, this limitation can be correlated with increased antibiotic susceptibility in biofilm-associated infections caused by diverse strains of *S. aureus* including methicillin-resistant strains.[16] This suggests that inhibitors of *sarA* expression and/or function could be used to therapeutic advantage in the context of biofilm-associated *S. aureus* infections.

However, biofilms are highly dynamic structures in which changes in gene expression promote the development, maturation, and ultimately the dissemination of bacterial cells from the biofilm, at which point they can enter the systemic circulation and cause infection at secondary sites.[17,18] Thus, inhibition of *sarA* as a means of limiting biofilm formation could have the adverse consequence of promoting acute, systemic infection. Conversely, inhibitors of *agr* expression and/or function may be of therapeutic benefit in the context of acute infection, but could also have the adverse consequence of promoting chronic, biofilm-associated infection. Indeed, *agr*-defective strains are often isolated from patients suffering from diverse forms of infection, perhaps owing at least in part to the advantage gained by the intrinsic antibiotic resistance afforded to the bacterium in the context of a biofilm.[19] Moreover, one report that examined the clinical history of 814 patients with *S. aureus* sepsis found that *agr* dysfunction was associated with a statistically significant increase in mortality.[20]

Such results emphasize the need to consider the contribution of individual regulatory loci in diverse forms of *S. aureus* infection. To this end, we also examined the role of *sarA* in acute models of *S. aureus* infection, and the results confirmed that *sarA* mutants are attenuated in murine models of bacteremia and acute, post-traumatic

osteomyelitis.[21-23] This suggests that *sarA* may be a viable therapeutic target in diverse forms of *S. aureus* infection. However, many other regulatory loci have also been shown to impact various forms of infection.[1] Defining the relative impact of these loci in diverse forms of *S. aureus* infection is difficult because most reports focused on individual regulatory loci in the context of a single form of *S. aureus* infection. This precludes the ability to determine which of these loci offer the greatest therapeutic promise in diverse forms of *S. aureus* infection. We have begun to address this by making direct comparisons between regulatory loci in the context of biofilm-associated infection,[15,16] but we have not done so in the context of acute infection. Thus, in this report we extended previous experiments focusing on regulatory loci that impact biofilm-associated infection to directly assess the relative impact of these same regulatory loci on virulence in a murine bacteremia model of acute *S. aureus* infection.

Results

Owing to its current prominence as a cause of *S. aureus* infection,[24-26] the experiments we report were done with a derivative of the USA300 strain LAC cured of its resident erythromycin-resistance plasmid.[23] We initially focused on isogenic derivatives of this strain with mutations in *codY, fur, mgrA, sarA*, and *sigB*. These regulatory loci were chosen to allow direct comparisons with the results observed in previous biofilm studies in which mutation of these same loci was shown to either enhance (*fur, mgrA*) or limit (*codY, sarA* and *sigB*) biofilm formation.[7,15,16] We also included a *rot* mutant based on a recent report concluding that mutation of *rot* limits biofilm formation in LAC.[27] Strains were introduced into NIH-Swiss mice by tail vein injection of 5×10^7 colony-forming units (cfu) as previously described.[23] Over the 7 day period of this experiment, this resulted in the death of 60% of mice infected with the LAC parent strain (Fig. 1). The mutants evaluated in this experiment were found to fall into one of three groups, with mutation of *fur* having no statistically significant effect on virulence, mutation of *codY, sarA*, and *sigB* significantly attenuating virulence, and mutation of *mgrA* and *rot* resulting in a significant increase in virulence relative to LAC (Fig. 1). These results were consistent with our studies examining the relative capacity of these mutants to escape the bloodstream and colonize soft tissues. Specifically, mutation of *codY, sarA*, and *sigB* attenuated virulence as assessed based on colony counts in the spleen (Fig. 2A), heart (Fig. 2B), and peripheral blood (Fig. 2C). Results observed in the kidney were less discriminatory in that the only significant difference was that between LAC and its isogenic *sarA* mutant (Fig. 2D).
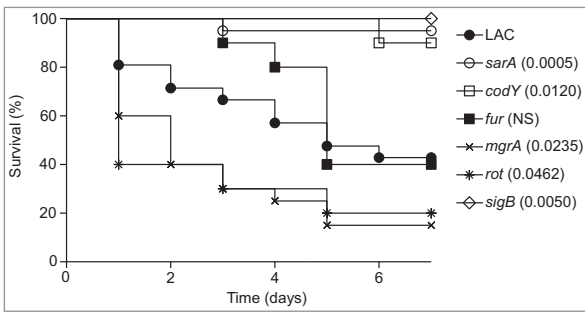
Figure 1. Relative virulence of *S. aureus* regulatory mutants in acute sepsis. Kaplan-Meier survival curves are shown for the USA300 strain LAC and the indicated isogenic mutants. Numbers in parenthesis indicate p values for each mutant by comparison to the results observed with LAC. NS = not significant.

To investigate the mechanistic basis for the virulence phenotypes we observed, we performed western blots of whole cell lysates using antibodies targeting AgrA and SarA as previously described.[23] Mutation of *sarA* and *sigB* resulted in a significant decrease in the accumulation of AgrA (Fig. 3A), which is the response regulator of the two component quorum-sensing system encoded by *agr*.[28] Additionally, mutation of *sigB* resulted in a significant decrease in the accumulation of SarA (Fig. 3B). This suggests that the decreased virulence observed with the *sarA* and *sigB* mutants may be at least partially attributable to the impact of these mutations on expression of *agr*. However, comparison of *agr, sarA*, and *sigB* mutants revealed that all three had distinct phenotypes as defined

by the relative accumulation of alpha toxin and protein A (Spa), which are prototype virulence factors known to be inversely regulated by *agr*.[28] Specifically, as assessed by western blot of conditioned medium from each strain, and as expected based on previous reports,[28] accumulation of Spa was increased in the LAC *agr* mutant while accumulation of alpha toxin was decreased (Fig. 3C and D). In contrast, accumulation of both Spa and alpha toxin was decreased in the *sarA* mutant, while accumulation of Spa was decreased, and accumulation of alpha toxin increased, in the *sigB* mutant (Fig. 3C and D).

Additionally, if the attenuation of *sarA* and *sigB* mutants is defined by the impact of these loci on expression of *agr*, then it would also be anticipated that an isogenic *agr* mutant would be attenuated to a comparable degree by comparison to *sarA* and *sigB* mutants. To examine this issue, we used our murine bacteremia model to compare LAC with its isogenic *agr* mutant. Interestingly, we found that mutation of *agr* had little impact on virulence (Fig. 4). These results were surprising given that mutation of *agr* in LAC as well as other *S. aureus* strains has been shown to limit virulence in animal models of *S. aureus* infection.[29-32] However, most of these models focused on some form of localized infection, primarily of the skin, and such models do not necessarily mimic the systemic infection modeled here. Indeed, Cameron *et al.* recently examined a number of clinical isolates of *S. aureus* and concluded that *agr* expression was not essential for
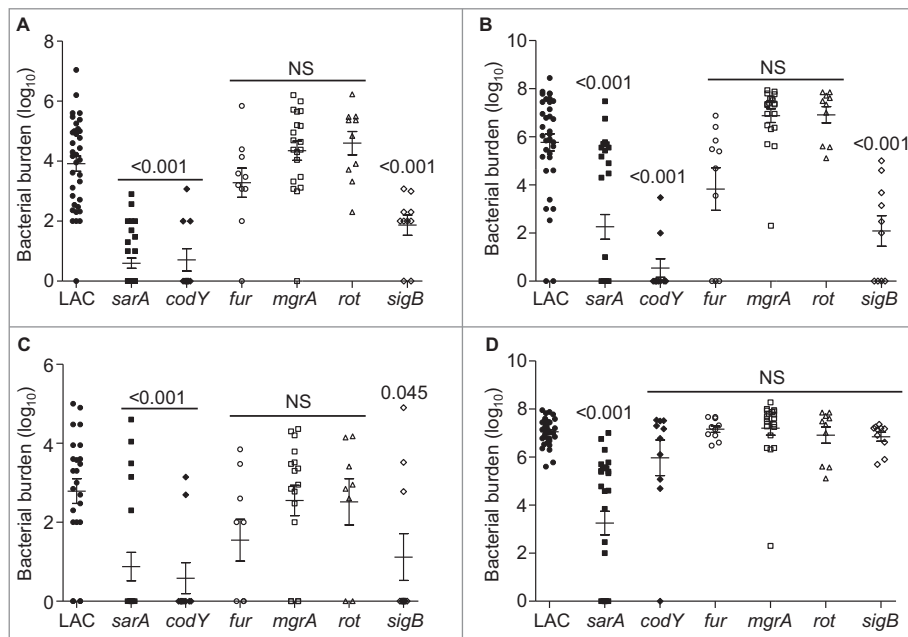
Figure 2. Relative virulence of *S. aureus* regulatory mutants as assessed by colonization. The number of colony-forming units (cfu) in the (A) spleen, (B) heart, (C) peripheral blood, and (D) kidney are shown by scatter plot. Numbers above each plot indicate p values for each mutant by comparison to the results observed with LAC. NS = not significant. Bars represent the mean ± SEM of log₁₀ transformed values.

Figure 3. Relative accumulation of AgrA, SarA, eSpa, and alpha toxin in *S. aureus* regulatory mutants as assessed by immunoblot analysis. Representative western blots of cell lysates (A and B) or conditioned medium (C and D) prepared from LAC and the indicated isogenic mutants were analyzed by western blots using (A) anti-AgrA antibody, (B) anti-SarA antibody, (C) anti-Spa antibody, or (D) anti-alpha toxin antibody. Graphs indicate cumulative densitometric values obtained from all biological and experimental replicates. Asterisks indicate statistical significance ($p \leq 0.05$) by comparison to values obtained with the LAC parent strain.
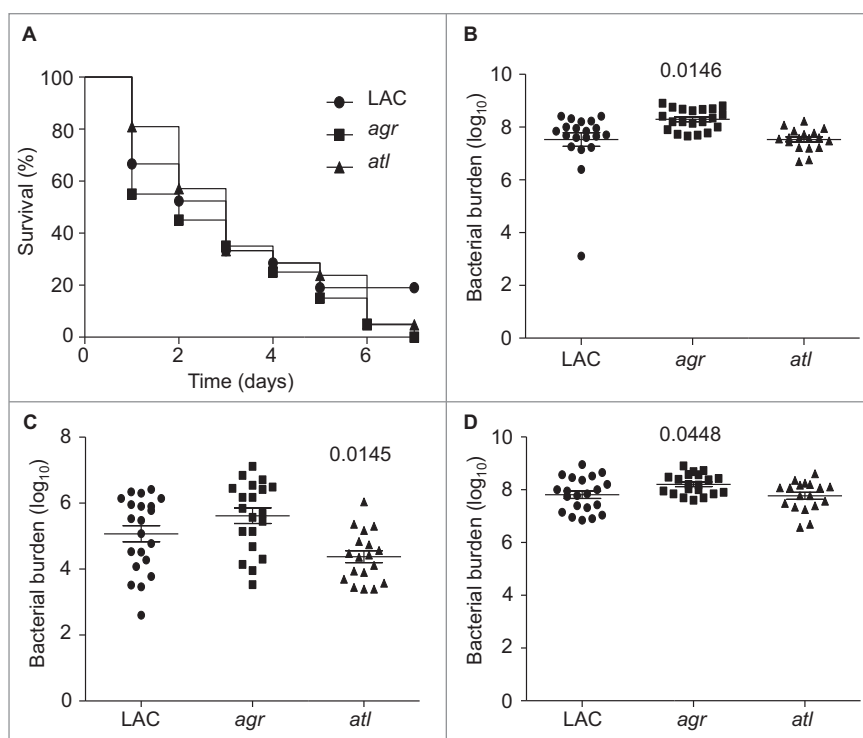
Figure 4. Relative virulence of *S. aureus agr* and *atl* mutants in acute sepsis. (A) Kaplan-Meier survival curves are shown for LAC and the indicated isogenic mutants. Number of cfu observed in homogenates prepared from (B) heart, (C) spleen, and (D) kidney. The number above each scatter plot cluster indicates the p value for each mutant found to significantly different by comparison to LAC. Bars represent the mean $\pm$ SEM of $\log_{10}$ transformed values.

virulence in a murine bacteremia model.[33] However, the more important point in the context of this report is that this finding, together with the alpha toxin and Spa results discussed above, effectively rules out the possibility that the attenuation observed with the LAC *sarA* and *sigB* mutants is a function of their impact on expression of *agr*.

While the focus of the experiments we report was on regulatory loci, we also examined the impact of mutating *atl* in this experiment based on the observation that mutation of *atl* has been shown by several laboratories, including our own, to limit biofilm formation.[15,34,35] This experiment was complicated by the fact that a characteristic phenotype of *atl* mutants grown *in vitro* is the formation of large aggregates.[36] To address this, we first carried out studies in which the apparent number of colony-forming units (cfu) was assessed before and after sonication. The number of detectable cfu increased in all strains after sonication, and in the case of four mutants (*atl, sarA, fur,* and *rot*) the number as assessed before sonication was significantly lower than the number

observed with the LAC parent strain (Fig. 5A). However, with the exception of the *atl* mutant, all of the differences we observed were well within an order of magnitude ($2.6 \times 10^9 - 8.9 \times 10^9$). In contrast, statistical analysis confirmed that the number of cfu as assessed before sonication was significantly higher in every strain we examined by comparison to the *atl* mutant (Fig. 5A). These experiments also confirmed that there was no difference between any of the strains we examined, including the *atl* mutant, after sonication.

Based on these results, *in vivo* analysis of the *atl* mutant was done using an inoculum prepared after sonication. As with *agr*, mutation of *atl* was also found to have no significant impact on overall virulence (Fig. 4). Mutation of *atl* also had no impact on the accumulation of AgrA (Fig. 3A) or SarA (Fig. 3B). Although most studies focusing on the role of *atl* in *S. aureus* pathogenesis have focused on biofilm formation, the results we observed with the *atl* mutant in our bacteremia model are consistent with those of Takahashi *et al.*, who found that mutation of
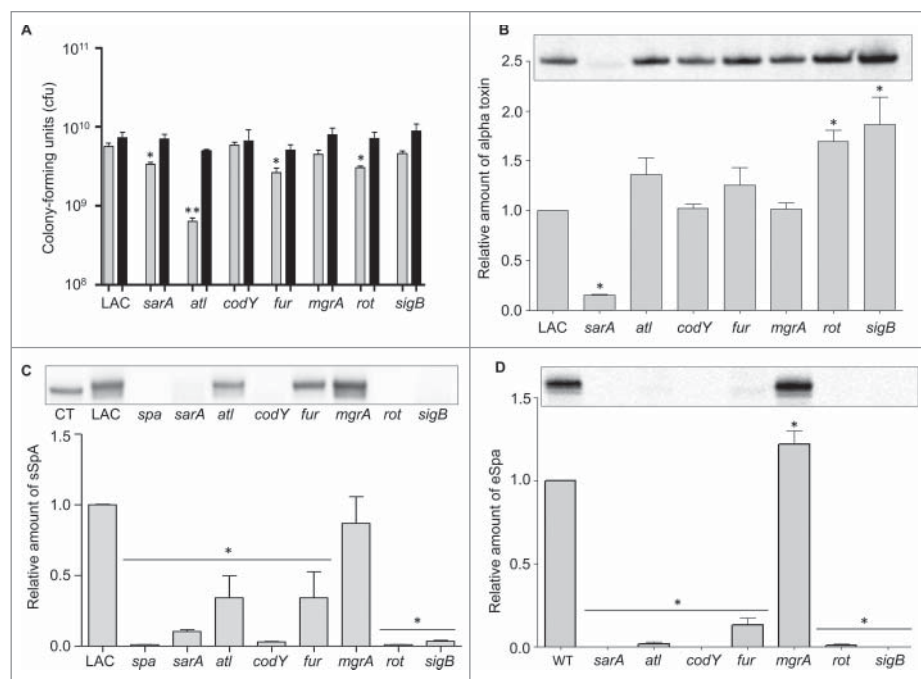
Figure 5. Analysis of mutant aggregative phenotypes and their respective production of alpha toxin and Spa. (A) Bars indicate the number of cfu observed before (grey) and after sonication (black). Single asterisk indicates statistical significance prior to sonication by comparison to LAC. Double asterisk indicates statistical significance of the *atl* mutant by comparison to all other strains prior to sonication. No significant differences were observed after sonication. (B) Representative western blot of conditioned medium from LAC and the indicated isogenic mutants using anti-alpha toxin antibody (top). Graph indicates cumulative densitometric values obtained from all biological and experimental replicates (bottom). (C) Representative western blot of surface protein preparations from LAC and the indicated isogenic mutants using anti-Spa antibody (top). CT = purified Spa control. Graph indicates cumulative densitometric values obtained from all biological and experimental replicates (bottom). (D) Representative western blot of conditioned medium from LAC and the indicated isogenic mutants using anti-Spa antibody (top). Graph indicates cumulative densitometric values obtained from all biological and experimental replicates (bottom). Asterisks in each graph indicate statistical significance ($p \leq 0.05$) by comparison to values obtained with the LAC parent strain.

atl had no impact on virulence in a murine model of intraperitoneal infection.[36]

In contrast to *sarA* and *sigB*, mutation of *fur* and *mgrA* resulted in a modest (<2-fold) but statistically significant increase in the accumulation of AgrA (Fig. 3A). However, this was not reflected in the alpha toxin phenotype of these mutants in that neither produced alpha toxin at significantly greater levels than the isogenic LAC parent strain (Fig. 5B). In contrast, mutation of *rot* and *sigB* resulted in a significant increase in the accumulation of alpha toxin, while mutation of *sarA* had the opposite effect. Indeed, alpha toxin was essentially absent in conditioned medium from LAC *agr* and *sarA* mutants (Fig. 3D). The possibility that the decrease in alpha toxin observed in the *sarA* mutant is at least partially attributable to the impact of mutating *sarA* on *agr* cannot be completely discounted, but previous studies from our laboratory have demonstrated that the accumulation of alpha toxin can be restored to wild-type levels in a *sarA* mutant by eliminating the production of extracellular proteases.[37,38] The relative abundance of alpha toxin in conditioned media was correlated with virulence in *rot* and *sarA* mutants, with both being increased in a *rot* mutant and both being decreased in a *sarA* mutant, but this was not the case with the *sigB* mutant in that the accumulation of alpha toxin was increased (Fig. 5B) while overall virulence was decreased (Fig. 1).

We also assessed the impact of each mutation on the accumulation of protein A (Spa). Because *S. aureus* naturally produces Spa in both extracellular and surface-associated forms, these experiments were done by western blot of both cell extracts enriched for surface-associated proteins (sSpa) and extracellular Spa (eSpa).[39,40] With the exception of the *mgrA* mutant, the amount of both sSpa (Fig. 5C) and eSpa (Fig. 5D) was reduced relative to LAC. In contrast, accumulation of Spa was increased in a LAC *mgrA* mutant, particularly when assessed in its extracellular form (Fig. 5D). These results are consistent with a previous study demonstrating by RNA-seq that the

amount of *spa* transcripts was dramatically increased in a LAC *mgrA* mutant.[41]

In western blots done with surface protein-enriched cell extracts, sSpa was essentially absent in *codY, rot, sarA*, and *sigB* mutants, and present in significantly reduced amounts *atl* and *fur* mutants (Fig. 5C). When assessed using conditioned medium, eSpa was essentially absent in every strain except LAC and its *agr* (Fig. 3C) and *mgrA* mutant (Fig. 5D). To the extent that Spa in both of these forms contributes to the virulence of *S. aureus* by promoting immune evasion, its virtual absence could contribute to the reduced virulence of the *codY, sarA* and *sigB* mutants.[42] Conversely, its increased abundance could contribute to the increased virulence of a LAC *mgrA* mutant. However, it is difficult to envision how reduced accumulation of Spa would contribute to increased virulence of a LAC *rot* mutant.

As noted above, we focused on alpha toxin and Spa because they are prototype virulence factors in the context of the pathogenic versatility of *S. aureus* and are differentially regulated by *agr* relative to each other.[6,43] A number of the loci we examined are also known to impact expression and/or function of *agr*. Although it was not true of the *sarA* or *sigB* mutants, it might therefore be anticipated that mutation of other regulatory loci would result in alpha toxin and Spa phenotypes comparable to those observed in the *agr* mutant (e.g. increased production of Spa and decreased production of alpha toxin). However, all of the mutants we examined exhibited unique alpha toxin and Spa phenotypes relative to the *agr* mutant and relative to each other (Table 1). This provides support for the hypothesis that the virulence changes we observed are largely *agr*-independent. It also emphasizes the overall complexity of *S. aureus* regulatory circuits and suggests that additional virulence factors that remain to be identified are involved in defining the virulence phenotypes of each of these mutants. Additional studies will be required to identify these virulence factors, but one clear correlation

Table 1. Summary of phenotypes. Table summarizes whether the accumulation of AgrA, SarA, alpha (α) toxin, Spa, and virulence was increased, decreased, or unchanged (NC) in each of the indicated LAC regulatory mutants. A dash (-) indicates the indicated protein was absent. Accumulation of SarA in an *agr* mutant was not tested (NT).

Mutation	AgrA	SarA	α toxin	Spa	Virulence
agr	—	NT	Down	Up	NC
atl	NC	NC	NC	Down	NC
codY	NC	NC	NC	Down	Down
fur	Up	NC	NC	Down	NC
mgrA	Up	NC	NC	Up	Up
rot	NC	NC	Up	Down	Up
sarA	Down	—	Down	Down	Down
sigB	Down	Down	Up	Down	Down

we did observe, and one that could potentially be exploited to help identify such virulence factors, was that attenuation of the *sarA*, *codY*, and *sigB* mutants was in all cases correlated with the increased production of extracellular proteases and an altered exoprotein profile (Fig. 6). Mutation of *rot* was also previously shown to result in an increase in protease production to an extent that could be correlated with a reduced capacity to form a biofilm, but in our comparisons we did not observe a significant increase in the accumulation of extracellular proteases in the *rot* mutant (Fig. 6).[27] This is consistent with the observation that, unlike *codY*, *sarA* and *sigB* mutants, the

LAC *rot* mutant exhibited increased rather than decreased virulence (Fig. 1).

Interestingly, mutation of *sarA* and *sigB* resulted in a comparable increase in the overall production of extracellular proteases (Fig. 6) but had opposite effects on the accumulation of alpha toxin (Fig. 3D). One possible explanation that we are currently exploring is that, while *sarA* and *sigB* repress the overall production of extracellular proteases, they do not repress the production of the specific protease(s) that degrade alpha toxin to the same degree. The alternative is that mutation of *sigB* has a much greater impact on the production of alpha toxin than mutation of *sarA*, thus resulting in a net increase in the accumulation of alpha toxin in a LAC *sigB* mutant despite its increased production of extracellular proteases.

Finally, we did not include complementation studies in our *in vivo* experiments for two reasons. The first is the number of mice this would have required would have been very large given the number of mutants we examined, particularly since all of our *in vivo* experiments were repeated at least twice. The second is that such studies are sometimes inconclusive owing to plasmid instability *in vivo*. However, we did confirm that all mutations that had a significant impact on Spa and/or alpha toxin phenotypes could be complemented under *in vitro* conditions (Fig. S1).

Discussion

The continuing increase in antibiotic resistance has led to the suggestion that strategies targeting *S. aureus* virulence factors and/or the regulatory circuits that control the production of these virulence factors could be therapeutically beneficial.[13,44-50] The two *S. aureus* regulatory loci that have been explored to the greatest extent as therapeutic targets are *agr* and *sarA*.[51-53] These loci interact with each other, with SarA being required for full expression of *agr*.[54] Although we did not assess this at the level of gene expression, we did confirm that AgrA is present in reduced amounts in a LAC *sarA* mutant. However, it is also clear that *sarA* and *agr* serve independent regulatory functions. This is evident in the observation that mutation of *agr* enhances biofilm formation while mutation of *sarA* has the opposite effect.[7,50,55-57] Thus, the therapeutic focus on these loci has generally been targeted toward different forms of infection, with *agr* being proposed as a target for acute, toxin-mediated diseases and *sarA* as a target for chronic, biofilm-associated infections.[51,52,58]

Our results confirm that mutation of *sarA* limits the virulence of LAC in a murine sepsis model to a

Figure 6. Protease activity in LAC regulatory mutants. Top: Total protease production in LAC and the indicated regulatory mutants was assessed using a commercially available FITC-casein cleavage hydrolysis assay. Results are reported as mean fluorescence values ± the standard error of the mean. Asterisks indicate statistically significant differences (p ≤ 0.05) between the indicated mutants relative to the results observed with LAC. As indicated above the graph, individual comparisons also confirmed that the amount of total protease activity observed in the *sarA* mutant was increased to a statistically significant extent by comparison to the results observed with both the *sigB* and *codY* mutants and that total protease activity in the *sigB* mutant was increased to a statistically significant extent by comparison to those observed with the *codY* mutant. Bottom: Extracellular protein profiles for LAC and each regulatory mutant were assessed by SDS-PAGE. MW = molecular weight markers, with the molecular weight in kilodaltons (kDa) of representative markers shown to the left.

significant degree relative to the isogenic parent strain, but also demonstrate that mutation of *codY* and *sigB* attenuate virulence in this clinical context to a comparable degree. Mutation of these same three loci also limited the ability of LAC to form a biofilm which suggests that these loci are all viable therapeutic targets in the context of both acute and chronic forms of *S. aureus* infection.[15] This is particularly true since mutation of all of these loci could be correlated with enhanced susceptibility to daptomycin *in vivo* in a murine catheter model.[16] However, when assessed using ceftaroline, only mutation of *sarA* and *sigB* had a significant effect. This suggests that *sarA* or *sigB* would be preferable therapeutic targets by comparison to *codY*.

Further support for this hypothesis comes from the observation that, while mutation of *codY* has been shown to limit biofilm formation in LAC and other strains of the USA300 clonal lineage, it has also been shown to enhance biofilm formation in UAMS-1 and the clinical isolate SA564.[15,59, 60] Interestingly, mutation of *codY* in these latter strains was also correlated with increased expression of *agr*,[59] which would be expected to decrease rather than increase biofilm formation.[7,50,55,57] At present, the mechanistic basis for these strain-dependent biofilm phenotypes is not fully understood, but it has been suggested that it may be related to the relative contribution of the polysaccharide intercellular adhesion (PIA) to biofilm formation in different strains of *S. aureus*.[15,59, 60]

There are also conflicting reports regarding the role of *codY* in defining the virulence of *S. aureus* in acute infections. For instance, our results are consistent with a report demonstrating that mutation of *codY* in LAC limited virulence in a neutropenic murine model of pulmonary infection,[61] but they are in contrast to a report demonstrating that a *codY* mutant generated in the USA300 strain 923 exhibited increased virulence in murine models of skin infection and necrotizing pneumonia.[62] These disparate results may simply reflect the use of different animal models and the importance of the microenvironment *in vivo*, or perhaps differences between strains of *S. aureus*. However, the more important point in the context of this report is that, when viewed collectively, such conflicting reports in the context of both biofilm-associated and acute infection further diminish enthusiasm for *codY* as a therapeutic target. They also emphasize the need to extend the studies we report here to include evaluation of these same loci in alternative animal models and additional strains of *S. aureus*.

Similarly, while mutation of *sigB* in LAC did have a significant impact on daptomycin susceptibility in the context of an established biofilm, it did not have a significant impact *in vivo* in the methicillin-sensitive, USA200 strain UAMS-1.[16] This would suggest that, in the context of coverage for diverse clinical isolates of *S. aureus, sarA* would be the preferable target even by comparison to *sigB*. Moreover, much as with *codY*, there are conflicting reports regarding the phenotypic impact of mutating *sigB*. For example, Bischoff *et al.* concluded that mutation of *sigB* results in decreased levels of *sarA* expression.[63] In contrast, Cheung *et al.* concluded that mutation of *sigB* in the 8325-4 strain RN6390 results in increased production of SarA.[64] These authors also concluded that this accounts for the increased production of alpha toxin in a *sigB* mutant. We did not include studies assessing gene expression in the context of *sarA*, but we did find that the accumulation of SarA is reduced in a LAC *sigB* mutant. This suggests that mutation of *sigB* and *sarA* in LAC would result in similar phenotypes, and in fact we found that this was generally the case.

However, one notable exception to this is that mutation of *sarA* essentially abolished the accumulation of alpha toxin while mutation of *sigB* had the opposite effect. Despite the fact that both mutants were attenuated in our sepsis model, this provides further support for the hypothesis that *sarA* would be the preferred therapeutic target by comparison to *sigB*, particularly when combined with the observation that mutation of *sarA* limits biofilm formation to a greater extent than mutation of *sigB*.[15] At the same time, it has been reported that *sigB* is required for intracellular persistence and development of small colony variants (SCV), both of which are considered key elements in the development of chronic *S. aureus* infections, and that this is not the case with *sarA*.[65,66] Thus, the possibility that *sigB* would be the preferred target in the context of chronic infections cannot be ruled out without additional experimentation that includes direct comparisons between these loci in an appropriate animal model.

From a mechanistic point of view, the increased accumulation of alpha toxin in a LAC *sigB* mutant is consistent with a report concluding that mutation of *sigB* results in increased levels of *agr* expression.[63] To the extent that *rsbU* is required for maximum *sigB* activity, this is also consistent with the observation that repair of the *rsbU* defect in the 8325-4 strain RN6390 resulted in increased *sigB* activity and reduced expression of *agr*.[67] Repair of the *rsbU* defect in RN6390 also resulted in decreased hemolytic activity, increased production of Spa, and an increased capacity to form a biofilm,[68] all of which are consistent with decreased levels of *agr* expression. Additionally, to the extent that mutation of *sigB* would be expected to result in the opposite phenotypes, they are also consistent with the observation that a LAC *sigB* mutant exhibited increased accumulation of alpha toxin, decreased production of Spa, and a decreased

capacity to form a biofilm as was observed both here and in our previous reports.[15,16] However, none of these phenotypes are consistent with the observation that mutation of *sigB* in LAC was correlated with decreased accumulation of AgrA.

One possible explanation for this apparent disparity is related to the experimental methodologies employed. Specifically, previous reports focused on *agr* at a transcriptional level, generally with a specific focus on RNAIII, while we focused on the accumulation of AgrA. Indeed, the mechanistic basis by which *sigB* impacts *agr* is unclear,[27] and it is possible that mutation of *sigB* impacts the production of RNAIII differently than it does production of AgrA. An alternative possibility is that the increased production of extracellular proteases in the LAC *sigB* mutant results in increased degradation of AgrA, which would not be apparent in assays focusing on transcription. Indeed, we previously demonstrated that the accumulation of AgrA is limited in a *sarA* mutant owing to protease-mediated degradation.[38] Although it remains to be determined whether this is also the case in a *sigB* mutant, the studies we report confirm that protease activity is increased in a LAC *sigB* mutant to a degree that approaches that observed in an isogenic *sarA* mutant.

Irrespective of the mechanism(s) involved, none of these results can explain the attenuation of a LAC *sigB* mutant despite the increased accumulation of alpha toxin. At the same time, while repair of *rsbU* in RN6390 was previously reported to result in reduced expression of *agr*, it was also correlated with what the authors described as a "surprising increase in mouse lethality" as assessed using a bacteremia model.[68] To the extent that repair of *rsbU* results in increased expression of *sigB*, this is consistent with the observation that mutation of *sigB* resulted in reduced lethality in the studies we report. The fact that mutation of *sigB* limited the accumulation of AgrA suggests that this attenuation could be at least partially *agr*-dependent, although as noted above this seems unlikely given that the isogenic *agr* mutant was not attenuated in our model. This was surprising in light of the many reports demonstrating that *agr* mutants are attenuated in animal models of infection.[31,69-71] However, most of these other reports focused on models other than bacteremia, and it has been shown that serum apolipoprotein B, including that from mice, binds and effectively inactivates the quorum-sensing pheromone of the *agr* system.[72] Additionally, serum lipoproteins have been shown to inactivate phenol soluble modulins (PSMs), which have been shown in turn to be a primary determinant of the virulence of community-associated, methicillin-resistant *S. aureus* strains like LAC.[22,26,73,74] Thus, one possible explanation for the fact that mutation

of *sigB* limited virulence in a murine bacteremia model while mutation of *agr* did not is that the functionality of *agr* and/or PSMs is decreased owing to the presence of serum lipoproteins. Such a scenario would also suggest that the attenuation we observed in a LAC *sigB* is independent of its impact on *agr* expression.

Mutation of *rot* was previously reported to result in increased virulence and increased production of both alpha toxin and extracellular proteases.[75] We also observed increased virulence and increased accumulation of alpha toxin. However, we did not observe a significant increase in the production of extracellular proteases in our LAC *rot* mutant. This suggests that the increased virulence we observed with a *rot* mutant is likely due to changes in the production of important virulence factors relative to the rate of their protease-mediated degradation. This is consistent with the observation that *rot* was originally identified as a repressor of *S. aureus* toxin production.[75] This was subsequently shown to involve an interaction between the *agr*-encoded RNAIII and *rot* mRNA that limits translation of the latter.[76,77] Thus, it would be anticipated that mutation of *agr* and mutation of *rot* would have opposite effects on virulence. This is consistent with the observation that mutation of *rot* enhanced the virulence of LAC while mutation of *agr* did not.

In contrast, our results demonstrating that mutation of *mgrA* enhances virulence are not consistent with reports demonstrating that mutation of *mgrA* attenuates virulence in murine models of sepsis and septic arthritis as well as rabbit models of sepsis and endocarditis.[41,78] We have no explanation for this disparity, but would note that these collective studies were also done using different strains of *S. aureus*. Indeed, none of the *mgrA* mutants employed in these earlier virulence studies were generated in LAC. Rather, they were generated in the commonly-studied *S. aureus* strain Newman, which has a recognized mutation in the *saeRS* regulatory system,[68] or in MW2 and 502A.[41] Even aside from recognized regulatory defects like those present in Newman, different strains of *S. aureus* exhibit a great deal of genetic and phenotypic diversity. In fact, a recent report confirmed that there is as much phenotypic diversity within different clonal lineages of *S. aureus* as there is between these clonal lineages.[79] It is also virtually certain that all strains of *S. aureus* carry mutations,[68] thus making it essentially impossible to define a definitive wild-type strain. Although no specific mutations have been identified in LAC that we are aware of, this is presumably true of USA300 strains. Nevertheless, the clinical predominance of such strains makes them worthy of investigation, and this is the primary reason we chose LAC for our studies. Thus, we believe the possibility that the impact of

mutating *mgrA* on virulence in acute infection is strain-dependent diminishes enthusiasm for *mgrA* as a therapeutic target, particularly when viewed in light of the fact that mutation of *mgrA* enhances biofilm formation.[15,41]

While much remains to be explored regarding the virulence phenotypes of the mutants we examined, one common phenotype observed with the attenuated *codY*, *sarA* and *sigB* mutants is that they all produced extracellular proteases at significantly increased levels relative to LAC. However, the impact of mutating these loci was not equivalent. Specifically, protease production was highest in the *sarA* mutant and decreased progressively in the *sigB* and *codY* mutants, respectively. As discussed above, mutation of *sigB* results in increased accumulation of alpha toxin, and to the extent that mutation of *sarA* resulted in a greater increase in protease production than mutation of *sigB*, one possible explanation for the disparate alpha toxin phenotypes we observed in LAC *sigB* and *sarA* mutants may be due to the relative impact of these loci on the production vs. protease-mediated degradation of alpha toxin. Alternatively, our protease assays did not allow us to distinguish between the activity of different proteases, and it is also possible that mutation of *sigB* vs. *sarA* has a differential impact on the production of specific proteases that contribute to the degradation of alpha toxin. Nevertheless, the correlation between the increased production of extracellular proteases and decreased virulence suggests that the inability to repress the production of extracellular proteases may play a key role in attenuating the virulence of *S. aureus* in acute as well as chronic, biofilm-associated infections. The observations that mutation of *sarA* results in a greater increase in protease production than any other mutant we have examined, and that this can be correlated with a reduced capacity to cause both acute and biofilm-associated infections suggests that *sarA* may be the best target by which this observation can be exploited to therapeutic advantage.[21,23]

Materials and methods

Bacterial strains and growth conditions

The strains used in these experiments are summarized in Table S1. With the exception of the *spa* mutant and the complemented *rot* mutant, the methods used to generate and confirm all mutants and the corresponding complemented strains were described in previous reports.[15,34,80-82] The Nebraska Transposon Mutant Library (NTML) was utilized to generate the *spa* mutant by phage transduction from the original JE2 mutant into our strain of LAC. The *rot* complementation strain was constructed similarly by transducing a previously described *rot* complementation

plasmid into the *rot* mutant.[15,83] All strains were maintained at $-80°C$ in a suspension containing tryptic soy broth (TSB) and 25% (v/v) glycerol. For each experiment, strains under study were retrieved from cold storage by plating on tryptic soy agar (TSA) with appropriate antibiotic selection. Antibiotics were incorporated into the culture media as appropriate at the following concentrations: erythromycin, 10 μg ml^{-1}; chloramphenicol 10 μg ml^{-1}; tetracycline, 5 μg ml^{-1}; kanamycin, 50 μg ml^{-1}; and neomycin, 50 μg ml^{-1}; spectinomycin, 1 mg ml^{-1}. Kanamycin and neomycin were always used together to avoid selection of spontaneously resistant strains.

Murine bacteremia model

Bacterial strains were retrieved from cold storage and grown at 37°C to stationary phase (16-17 hrs) in TSB with appropriate antibiotic selection. Cultures were standardized to an OD_{560} of 0.05 in TSB without antibiotics and grown to an OD_{560} of 1.0. Bacterial cells were harvested by centrifugation and separate aliquots were resuspended in an equal volume of sterile phosphate-buffered saline (PBS) containing 10% DMSO and 5% bovine serum albumin (BSA) which were stored at $-80°C$. The number of colony-forming units (cfu) in aliquots prepared from each strain was confirmed by plate count after 20 hrs incubation at 37ºC.

The bacteremia model used in this study was previously described by Zielinska et al. (2012).[23] Briefly, the strains under study were removed from cold storage, washed with PBS, and standardized in PBS to a cell density of 5 $\times$ 10^8 cfu per ml. For each experiment, groups of ten 5–8 week-old female NIH-Swiss mice were infected via tail vein injection with 5 $\times$ 10^7 cfu of LAC or one of its isogenic mutants. Organs and tissues were harvested from any mice found dead or which required compassionate euthanasia; otherwise, tissues were harvested at 7 days post-infection. Organs were removed aseptically and homogenized. Serial dilutions of each homogenate were then plated on TSA without selection, and the number of cfus per organ determined following overnight incubation at 37°C. To rule out the possibility of contaminants skewing the results, replicate samples were also plated on CHROMagar (BBL^{TM}, Cat. # 254102/215081). All experiments were repeated at least twice, with the total number of mice infected with each strain indicated in the scatter plots.

Western blotting

Samples for western blots and the primary and secondary antibodies used were all prepared and used as previously described.[23,38] Western blots included at least two

biological replicates with at least two experimental replicates of each. Densitometric values were obtained with a Bio-Rad ChemiDocMP Imaging System and Image Lab Software (Bio-Rad Laboratories, Inc., Irvine, CA).

Sonication assay

To ensure that the results were not skewed by the impact of any given mutation on cellular clumping, all strains were grown in overnight cultures with appropriate selection and standardized to an OD_{560} of 10.0 in a volume of 5 ml. Serial dilutions of a 100 μl aliquot were performed on ice and plated on TSA without selection. The remaining cultures were kept on ice and sonicated (QSonica S4000, Newtown, CT) for a period of 4 minutes at 6 watts. Serial dilutions were then prepared post-sonication and plated on TSA. The number of cfu before and after sonication was determined by plate count after 20 hrs incubation at 37°C.

Characterization of exoprotein profiles

Exoprotein profiles were examined as described by Zielinksa et al. (2012).[23] Briefly, overnight (16-17 hrs) cultures were standardized to an OD_{560} of 10.0. Conditioned medium from each culture was then harvested by centrifugation and the supernatant filter sterilized. Samples were resolved by SDS-PAGE using 4–12% gradient Novex Bis-Tris Plus gels (Life Technologies, cat. # NW04125BOX). Proteins were visualized by staining with SimplyBlue[TM] SafeStain (Life Technologies, cat. # LC6060) and imaging using Bio-Rad ChemiDocMP Imaging System (Bio-Rad Laboratories, Inc., Irvine, CA).

Total protease activity

Total protease activity was assessed using conditioned media prepared as described above and the Protease Fluorescent Detection Kit (Sigma Chemical Co., cat # PF0100). MFI values for conditioned medium from LAC were set to a value of 100% activity, with the activity observed in each mutant shown relative to this value. All assays included two biological replicates with at least three experimental replicates of each.

Cell lysis procedure

Bacterial cells from overnight cultures standardized as described above were harvested by centrifugation and resuspended in 750 μl of ice-cold TEG buffer (25 mM Tris at a pH of 8 and 25 mM EGTA). Cell suspensions were then transferred to 2 ml RNase/DNase free Fastprep Lysing Matrix B tubes (MP Biomedicals, cat. #

116911050). Cell suspensions were then lysed in a FastPrep®-24 benchtop homogenizer (MP Biomedicals, Solon, OH) for two separate 40 second intervals at a rate of 6.0 m/sec (interrupted by a 5 minute interval in which the homogenates were chilled on ice). After centrifugation at 15,000 X g at 4°C for 10 minutes, supernatants were aliquoted and stored at -20°C until use.

Preparation of samples for analysis of surface-associated Spa (sSpa)

To examine relative amounts of sSpa, samples enriched for surface-associated proteins were prepared as previously described.[23] Here, bacterial cells from overnight cultures standardized as described above were harvested by centrifugation. Cell pellets were then resuspended to a density 1×10^{9} cells per ml. Cells were then washed in distilled water before resuspending in 200 μl of filter-sterilized digestion buffer consisting of 100 μl of 1M Tris-HCl (pH 7.5), 50 μl of 5M NaCl, 675 mg of sucrose, 50 μl of 1M $MgCl_2$, 25 μl of lysostaphin (10 mg/ml), 100 μl mutanolysin (1.25 mg/ml), 5 units of DNase I, 50 μl of 100 mM PMSF, 2.5 μl of 1M benzamidine, 50 μl of 100 mM N_{α}-p-Tosyl-L-arginine methyl ester hydrochloride (TAME), 25 μl leupeptin (1 mg/ml), and 12.5 μl pepstatin (1 mg/ml). Samples were then brought to a final volume of 2.5 ml using distilled water. Cell suspensions were then incubated at 37°C for 4 hours. The lysis reactions were then centrifuged at 6000 X g for 20 minutes at 4°C and the supernatants aliquoted and stored at -80°C until used for western blot.

Ethics statement

All experiments involving animals were reviewed and approved by the Institutional Animal Care and Use Committee of the University of Arkansas for Medical Sciences and performed according to NIH guidelines, the Animal Welfare Act, and US Federal law.

Statistical analysis

To allow for statistical comparison across biological and experimental replicates from all *in vitro* assays, the results obtained for each mutant were averaged across all replicates. This average was then plotted relative to the results observed with LAC after setting the value observed with LAC either to 1.0 (western blots) or 100% (protease assay). Analysis of variance (ANOVA) models were then used to assess the statistical significance of the results observed with each mutant relative to LAC (Bonferroni correction). ANOVA methods were also used to analyze cfu data. Specifically, Dunnett's procedure was

used to compare each mutant mean to the mean of LAC. The cfu data were log_{10}-transformed prior to analysis, and P-values were calculated using permutation methods. P-values less than or equal to 0.05 were considered to be statistically significant. Statistical analyses were performed using the statistical programming language R version 3.3.3 (Vienna, Austria), SAS 9.4 (Cary, NC) and GraphPad Prism 5.0 (La Jolla, CA).

Disclosure of potential conflicts of interest

No potential conflicts of interest were disclosed.

Funding

References

[1] Priest NK, Rudkin JK, Feil EJ, van den Elsen JM, Cheung A, Peacock SJ, Laabei M, Lucks DA, Recker M, Massey RC. From genotype to phenotype: Can systems biology be used to predict *Staphylococcus aureus* virulence? Nature Rev Microbiol. 2012;10:791-97. https://doi.org/10.1038/nrmicro2880

[2] Bröker BM, Mrochen D, Péton V. The T cell response to *Staphylococcus aureus*. Pathogens. 2016;5:31. https://doi.org/10.3390/pathogens5010031

[3] Flannagan RS, Heit B, Heinrichs DE. Antimicrobial mechanisms of macrophages and the immune evasion strategies of *Staphylococcus aureus*. Pathogens. 2015;4:826-68. https://doi.org/10.3390/pathogens4040826. PMID:26633519

[4] Wilde AD, Snyder DJ, Putnam NE, Valentino MD, Hammer ND, Lonergan ZR, Hinger SA, Aysanoa EE, Blanchard C, Dunman PM, et al. Bacterial hypoxic responses revealed as critical determinants of the host-pathogen outcome by TnSeq analysis of *Staphylococcus aureus* invasive infection. PLoS Pathog. 2015;11:e1005341. https://doi.org/10.1371/journal.ppat.1005341. PMID:26684646

[5] Brady RA, Leid JG, Calhoun JH, Costerton JW, Shirtliff ME. Osteomyelitis and the role of biofilms in chronic infection. FEMS Immunol Med Microbiol. 2008;52:13-22. https://doi.org/10.1111/j.1574-695X.2007.00357.x. PMID:18081847

[6] Lowy FD. *Staphylococcus aureus* infections. N Engl J Med. 1998;339:520-32. https://doi.org/10.1056/NEJM199808203390806. PMID:9709046

[7] Beenken KE, Mrak LN, Griffin LM, Zielinska AK, Shaw LN, Rice KC, Horswill AR, Bayles KW, Smeltzer MS. Epistatic relationships between *sarA* and *agr* in *Staphylococcus aureus* biofilm formation. PLoS ONE. 2010;5:e10790.5. https://doi.org/10.1371/journal.pone.0010790

[8] Yarwood JM, Bartels DJ, Volper EM, Greenberg PE. Quorum sensing in *Staphylococcus aureus* biofilms. J Bacteriol. 2004;186:1838-50. https://doi.org/10.1128/JB.186.6.1838-1850.2004. PMID:14996815

[9] Boucher HW, Talbot GH, Bradley JS, Edwards JE, Gilbert D, Rice LB, Scheld M, Spellberg B, Bartlett J. Bad bugs, no drugs: No ESKAPE! An update from the Infectious Diseases Society of America. Clin Infect Dis. 2009;48:11-12. https://doi.org/10.1086/595011

[10] Lewis K. Multidrug tolerance of biofilms and persister cells. Curr Top Microbiol Immunol. 2008;322:107-31. PMID:18453274

[11] Fernandes P, Martens E. Antibiotics in late clinical development. Biochem Pharmacol. 2017;133:152-63. https://doi.org/10.1016/j.bcp.2016.09.025. PMID:27687641

[12] Meeker DG, Beenken KE, Mills WB, Loughran AJ, Spencer HJ, Lynn WB, Smeltzer MS. Evaluation of antibiotics active against methicillin-resistant *Staphylococcus aureus* based on activity in an established biofilm. Antimicrob Agents Chemother. 2016;60:5688-94. https://doi.org/10.1128/AAC.01251-16. PMID:27401574

[13] Maura D, Ballok AE, Rahme LG. Considerations and caveats in anti-virulence drug development. Curr Opin Microbiol. 2016;33:41-46. https://doi.org/10.1016/j.mib.2016.06.001. PMID:27318551

[14] Conlon BP, Nakayasu ES, Fleck LE, LaFleur MD, Isabella VM, Coleman K, Leonard SN, Smith RD, Adkins JN, Lewis K. Activated ClpP kills persisters and eradicates a chronic biofilm infection. Nature. 2013;503:365-70. https://doi.org/10.1038/nature12790. PMID:24226776

[15] Atwood DN, Loughran AJ, Courtney AP, Anthony AC, Meeker DG, Spencer HJ, Gupta RK, Lee CY, Beenken KE, Smeltzer MS. Comparative impact of diverse regulatory loci on *Staphylococcus aureus* biofilm formation. MicrobiologyOpen. 2015;4:436-51. https://doi.org/10.1002/mbo3.250. PMID:25810138

[16] Atwood DN, Beenken KE, Lantz TL, Meeker DG, Lynn WB, Mills WB, Spencer HJ, Smeltzer MS. Regulatory mutations impacting antibiotic susceptibility in an established *Staphylococcus aureus* biofilm. Antimicrob Agents Chemother. 2016;60:1826-29. https://doi.org/10.1128/AAC.02750-15. PMID:26824954

[17] Boles BR, Horswill AR. Staphylococcal biofilm disassembly. Trends Microbiol. 2011;19:449-55. https://doi.org/10.1016/j.tim.2011.06.004. PMID:21784640

[18] Moormeier DE, Bayles KW. *Staphylococcus aureus* biofilm: A complex developmental organism. Mol Microbiol. 2017;104:365-76. https://doi.org/10.1111/mmi.13634. PMID:28142193

[19] Painter KL, Krishna A, Wigneshweraraj S, Edwards AM. What role does the quorum-sensing accessory gene regulator system play during *Staphylococcus aureus* bacteremia? Trends Microbiol. 2014;22:676-85. https://doi.org/10.1016/j.tim.2014.09.002. PMID:25300477

[20] Schweizer ML, Furuno JP, Sakoulas G, Johnson JK, Harris AD, Shardell MD, McGregor JC, Thom KA, Perencevich EN. Increased mortality with accessory gene regulator (*agr*) dysfunction in *Staphylococcus aureus* among bacteremic patients. Antimicrob Agents Chemother. 2011;55:1082-87. https://doi.org/10.1128/AAC.00918-10. PMID:21173172

[21] Loughran AJ, Atwood DN, Anthony AC, Harik NS, Spencer HJ, Beenken KE, Smeltzer MS. Impact of individual extracellular proteases on *Staphylococcus aureus* biofilm formation in diverse clinical isolates and their

isogenic *sarA* mutants. MicrobiologyOpen. 2014;3:897-909. https://doi.org/10.1002/mbo3.214. PMID:25257373

[22] Loughran AJ, Gaddy D, Beenken KE, Meeker DG, Morello R, Zhao H, Byrum SD, Tackett AJ, Cassat JE, Smeltzer MS. Impact of *sarA* and phenol-soluble modulins on the pathogenesis of osteomyelitis in diverse clinical isolates of *Staphylococcus aureus*. Infect Immun. 2016;84:2586-94. https://doi.org/10.1128/IAI.00152-16. PMID:27354444

[23] Zielinska AK, Beenken KE, Mrak LN, Spencer HJ, Post GR, Skinner RA, Tackett AJ, Horswill AR, Smeltzer MS. *sarA*-mediated repression of protease production plays a key role in the pathogenesis of *Staphylococcus aureus* USA300 isolates. Mol Microbiol. 2012;86:1183-96. https://doi.org/10.1111/mmi.12048. PMID:23075270

[24] Mediavilla JR, Chen L, Mathema B, Kreiswirth BN. Global epidemiology of community-associated methicillin resistant *Staphylococcus aureus* (CA-MRSA). Curr Opin Microbiol. 2012;15:588-95. https://doi.org/10.1016/j.mib.2012.08.003. PMID:23044073

[25] Nimmo GR. USA300 abroad: Global spread of a virulent strain of community-associated methicillin-resistant *Staphylococcus aureus*. Clin Microbiol Infect. 2012;18:725-34. https://doi.org/10.1111/j.1469-0691.2012.03822.x. PMID:22448902

[26] Otto M. Basis of virulence in community-associated methicillin-resistant *Staphylococcus aureus*. Ann Rev Microbiol. 2010;64:143-62. https://doi.org/10.1146/annurev.micro.112408.134309

[27] Mootz JM, Benson MA, Heim CE, Crosby HA, Kavanaugh JS, Dunman PM, Kielian T, Torres VJ, Horswill AR. Rot is a key regulator *of Staphylococcus aureus* biofilm formation. Mol Microbiol. 2015;96:388-404. https://doi.org/10.1111/mmi.12943. PMID:25612137

[28] Novick RP, Geisinger E. Quorum sensing in staphylococci. Annu Rev Genet. 2008;42:541-64. https://doi.org/10.1146/annurev.genet.42.110807.091640. PMID:18713030

[29] Abdelnour A, Arvidson S, Bremell T, Rydén C, Tarkowski A. The accessory gene regulator (*agr*) controls *Staphylococcus aureus* virulence in a murine arthritis model. Infect Immun. 1993;61:3879-85. PMID:8359909

[30] Cheung GYC, Wang R, Khan BA, Sturdevant DE, Otto M. Role of the accessory gene regulator *agr* in community-associated methicillin-resistant *Staphylococcus aureus* pathogenesis. Infect Immun. 2011;79:1927-35. https://doi.org/10.1128/IAI.00046-11. PMID:21402769

[31] Gillaspy AF, Hickmon SG, Skinner RA, Thomas JR, Nelson CL, Smeltzer MS. Role of the accessory gene regulator (*agr*) in pathogenesis of staphylococcal osteomyelitis. Infect Immun. 1995;63:3373-80. PMID:7642265

[32] Montgomery CP, Boyle-Vavra S, Daum RS. Importance of the global regulators *agr* and *saeRS* in the pathogenesis of CA-MRSA USA300 infection. PLoS ONE. 2010;5:e15177. https://doi.org/10.1371/journal.pone.0015177. PMID:21151999

[33] Cameron DR, Lin YH, Trouillet-Assant S, Tafani V, Kostoulias X, Mouhtouris E, Skinner N, Visvanathan K, Baines SL, Howden B, et al. Vancomycin-intermediate *Staphylococcus aureus* isolates are attenuated for virulence when compared to susceptible progenitors. Clin Microbiol Infect. 2017;pii: S1198-743X(17)30199-4. https://doi.org/10.1016/j.cmi.2017.03.027. PMID:28396035

[34] Bose JL, Lehman MK, Fey PD, Bayles KW. Contribution of the *Staphylococcus aureus* Atl AM and GL murein hydrolase activities in cell division, autolysis, and biofilm formation. PLoS ONE. 2012;7:e42244. https://doi.org/10.1371/journal.pone.0042244. PMID:22860095

[35] Houston P, Rowe SE, Pozzi C, Waters EM, O'Gara JP. Essential role for the major autolysin in the fibronectin-binding protein-mediated *Staphylococcus aureus* biofilm phenotype. Infect Immun. 2011;79:1153-65. https://doi.org/10.1128/IAI.00364-10. PMID:21189325

[36] Takahashi J, Komatsuzawa H, Yamada S, Nishida T, Labischinski H, Fujiwara T, Ohara M, Yamagishi J, Sugai M. Molecular characterization of an *atl* null mutant of *Staphylococcus aureus*. Microbiol Immunol. 2002;46:601-12. https://doi.org/10.1111/j.1348-0421.2002.tb02741.x. PMID:12437027

[37] Zielinska AK, Beenken KE, Joo H-S, Mrak LN, Griffin LM, Luong TT, Lee CY, Otto M, Shaw LN, Smeltzer MS. Defining the strain-dependent impact of the staphylococcal accessory regulator (*sarA*) on the alpha-toxin phenotype of *Staphylococcus aureus*. J Bacteriol. 2011;193:2948-58. https://doi.org/10.1128/JB.01517-10. PMID:21478342

[38] Beenken KE, Mrak LN, Zielinska AK, Atwood DN, Loughran AJ, Griffin LM, Matthews KA, Anthony AM, Spencer HJ, Post GR, et al. Impact of the functional status of *saeRS* on *in vivo* phenotypes of *Staphylococcus aureus* *sarA* mutants. Mol Microbiol. 2014;92:1299-312. https://doi.org/10.1111/mmi.12629. PMID:24779437

[39] Movitz J. Formation of extracellular protein A by *Staphylococcus aureus*. Eur J Biochem. 1976;68:291-99. https://doi.org/10.1111/j.1432-1033.1976.tb10788.x. PMID:964266

[40] O'Hallorana DP, Wynneb K, Geoghegana JA. Protein A Is released into the *Staphylococcus aureus* culture supernatant with an unprocessed sorting signal. Infect Immun. 2015;83:1598-609. https://doi.org/10.1128/IAI.03122-14. PMID:25644005

[41] Crosby HA, Schlievert PM, Merriman JA, King JM, Salgado-Pabón W, Horswill AR. The *Staphylococcus aureus* global regulator MgrA modulates clumping and virulence by controlling surface protein expression. PLoS Pathog. 2016;12:e1005604. https://doi.org/10.1371/journal.ppat.1005604. PMID:27144398

[42] Foster TJ. Immune evasion by staphylococci. Nature Rev Microbiol. 2005;3:948-58. https://doi.org/10.1038/nrmicro1289

[43] Li S, Arvidson S, Möllby R. Variation in the *agr*-dependent expression of alpha-toxin and protein A among clinical isolates of *Staphylococcus aureus* from patients with septicaemia. FEMS Microbiol Lett. 1997;152:155-61. https://doi.org/10.1016/S0378-1097(97)00195-X. PMID:9228782

[44] Moellering RC. MRSA: The first half century. J Antimicrob Chemother. 2012;67:4-11. https://doi.org/10.1093/jac/dkr437. PMID:22010206

[45] Hiramatsu K, Hanaki H, Ino T, Yabuta K, Oguri T, Tenover FC. Methicillin-resistant *Staphylococcus aureus* clinical strain with reduced vancomycin susceptibility. J Antimicrob Chemother. 1997;40:135-36. https://doi.org/10.1093/jac/40.1.135. PMID:9249217

[46] Sievert DM, Boulton ML, Stoltman G, Johnson D, Stobierski MG, Downes FP, Somsel PA, Rudrik JT, Brown W, Hafeez W, et al. Staphylococcus aureus resistant to

vancomycin — United States. Atlanta (GA): CDC MMWR; 2002.

[47] Kumar K, Chopra S. New drugs for methicillin-resistant *Staphylococcus aureus*: An update. J Antimicrob Chemother. 2013;68:1465-70. https://doi.org/10.1093/jac/dkt045. PMID:23429643

[48] Rodvold KA, McConeghy KW. Methicillin-resistant *Staphylococcus aureus* therapy: Past, present, and future. Clin Infect Dis. 2014;58:S20-S27. https://doi.org/10.1093/cid/cit614. PMID:24343828

[49] Jansen KU, Girgenti DQ, Scully IL, Anderson AS. Vaccine review: "*Staphyloccocus aureus* vaccines: Problems and prospects." Vaccine. 2013;31:2723-30. https://doi.org/10.1016/j.vaccine.2013.04.002. PMID:23624095

[50] Boles BR, Horswill AR. *agr*-mediated dispersal of *Staphylococcus aureus* biofilms. PLoS Pathog. 2008;4:e1000052. https://doi.org/10.1371/journal.ppat.1000052. PMID:18437240

[51] Arya R, Ravikumar R, Santhosh RS, Princy SA. SarA based novel therapeutic candidate against *Staphylococcus aureus* associated with vascular graft infections. Front Microbiol. 2015;6:416. https://doi.org/10.3389/fmicb.2015.00416. PMID:26074884

[52] Gray B, Hall P, Gresham H. Targeting *agr*- and *agr*-like quorum sensing systems for development of common therapeutics to treat multiple gram-positive bacterial infections. Sensors. 2013;13:5130-66. https://doi.org/10.3390/s130405130. PMID:23598501

[53] Muhs A, Lyles JT, Parlet CP, Nelson K, Kavanaugh JS, Horswill AR, Quave CL. Virulence inhibitors from Brazilian Peppertree block quorum sensing and abate dermonecrosis in skin infection models. Sci Rep. 2017;7:42275. https://doi.org/10.1038/srep42275. PMID:28186134

[54] Chien Y, Cheung AL. Molecular interactions between two global regulators, *sar* and *agr*, in *Staphylococcus aureus*. J Biol Chem. 1998;273:2645-52. https://doi.org/10.1074/jbc.273.5.2645. PMID:9446568

[55] Beenken KE, Blevins JS, Smeltzer MS. Mutation of *sarA* in *Staphylococcus aureus* limits biofilm formation. Infect Immun. 2003;71:4206-11. https://doi.org/10.1128/IAI.71.7.4206-4211.2003. PMID:12819120

[56] Valle J, Toledo-Arana A, Berasain C, Ghigo J-M, Amorena B, Penadés JR, Lasa I. SarA and not σ^B is essential for biofilm development by *Staphylococcus aureus*. Mol Microbiol. 2003;48:1075-87. https://doi.org/10.1046/j.1365-2958.2003.03493.x. PMID:12753197

[57] Vuong C, Saenz HL, Götz F, Otto M. Impact of the *agr* quorum-sensing system on adherence to polystyrene in *Staphylococcus aureus*. J Infect Dis. 2000;182:1688-93. https://doi.org/10.1086/317606. PMID:11069241

[58] Balamurugan P, Hema M, Kaur G, Sridharan V, Prabu PC, Sumana MN, Princy SA. Development of a biofilm inhibitor molecule against multidrug resistant *Staphylococcus aureus* associated with gestational urinary tract infections. Front Microbiol. 2015;6:832. https://doi.org/10.3389/fmicb.2015.00832. PMID:26322037

[59] Majerczyk CD, Sadykov MR, Luong TT, Lee C, Somerville GA, Sonenshein AL. *Staphylococcus aureus* CodY negatively regulates virulence gene expression. J Bacteriol. 2008;190:2257-65. https://doi.org/10.1128/JB.01545-07. PMID:18156263

[60] Tu Quoc PH, Genevaux P, Pajunen M, Savilahti H, Georgopoulos C, Schrenzel J, Kelley WL. Isolation and characterization of biofilm formation-defective mutants of *Staphylococcus aureus*. Infect Immun. 2007;75:1079-88. https://doi.org/10.1128/IAI.01143-06. PMID:17158901

[61] Ibberson CB, Jones CL, Singh S, Wise MC, Hart ME, Zurawski DV, Horswill AR. *Staphylococcus aureus* hyaluronidase is a CodY-regulated virulence factor. Infect Immun. 2014;82:4253-64. https://doi.org/10.1128/IAI.01710-14. PMID:25069977

[62] Montgomery CP, Boyle-Vavra S, Roux A, Ebine K, Sonenshein AL, Daum RS. CodY deletion enhances *in vivo* virulence of community-associated methicillin-resistant *Staphylococcus aureus* clone USA300. Infect Immun. 2012;80:2382-89. https://doi.org/10.1128/IAI.06172-11. PMID:22526672

[63] Bischoff M, Entenza JM, Giachino P. Influence of a functional *sigB* operon on the global regulators *sar* and *agr* in *Staphylococcus aureus*. J Bacteriol. 2001;183:5171-79. https://doi.org/10.1128/JB.183.17.5171-5179.2001. PMID:11489871

[64] Cheung AL, Chien Y, Bayer AS. Hyperproduction of alpha-hemolysin in a *sigB* mutant is associated with elevated SarA expression in *Staphylococcus aureus*. Infect Immun. 1999;67:1331-37. PMID:10024579

[65] Mitchell G, Fugère A, Gaudreau KP, Brouillette E, Frost EH, Cantin AM, Malouin F. SigB Is a dominant regulator of virulence in *Staphylococcus aureus* small-colony variants. PLoS ONE. 2013;8:e65018. https://doi.org/10.1371/journal.pone.0065018. PMID:23705029

[66] Tuchscherr L, Bischoff M, Lattar SM, Noto Llana M, Pförtner H, Niemann S, Geraci J, Van de Vyver H, Fraunholz MJ, Cheung AL, et al. Sigma factor SigB is crucial to mediate *Staphylococcus aureus* adaptation during chronic infections. PLoS Pathog. 2015;11: e1004870. https://doi.org/10.1371/journal.ppat.1004870. PMID:25923704

[67] Shaw LN, Aish J, Davenport JE, Brown MC, Lithgow JK, Simmonite K, Crossley H, Travis J, Potempa J, Foster SJ. Investigations into σ^B-modulated regulatory pathways governing extracellular virulence determinant production in *Staphylococcus aureus*. J Bacteriol. 2006;188:6070-80. https://doi.org/10.1128/JB.00551-06. PMID:16923874

[68] Herbert S, Ziebandt A-K, Ohlsen K, Schäfer T, Hecker M, Albrecht D, Novick R, Götz F. Repair of global regulators in *Staphylococcus aureus* 8325 and comparative analysis with other clinical isolates. Infect Immun. 2010;78:2877-89. https://doi.org/10.1128/IAI.00088-10. PMID:20212089

[69] Cheung AL, Eberhardt KJ, Chung E, Yeaman MR, Sullam PM, Ramos M, Bayer AS. Diminished virulence of a *sar⁻*/*agr⁻* mutant of *Staphylococcus aureus* in the rabbit model of endocarditis. J Clin Invest. 1994;94:1815-22. https://doi.org/10.1172/JCI117530. PMID:7962526

[70] Heyer G, Saba S, Adamo R, Rush W, Soong G, Cheung A, Prince A. *Staphylococcus aureus agr* and *sarA* functions are required for invasive infection but not inflammatory responses in the lung. Infect Immun. 2002;70:127-33. https://doi.org/10.1128/IAI.70.1.127-133.2002. PMID:11748173

[71] Smeltzer MS, Hart ME, Iandolo JJ. Phenotypic characterization of *xpr*, a global regulator of extracellular virulence factors in *Staphylococcus aureus*. Infect Immun. 1993;61:919-25. PMID:8432612

[72] Peterson MM, Mack JL, Hall PR, Alsup AA, Alexander SM, Sully EK, Sawires YS, Cheung AL, Otto M, Gresham HD. Apolipoprotein B is an innate barrier against invasive *Staphylococcus aureus* infection. Cell Host Microbe. 2008;4:555-66. https://doi.org/10.1016/j.chom.2008.10.001. PMID:19064256

[73] Surewaard BGJ, Nijland R, Spaan AN, Kruijtzer JAW, de Haas CJC, van Strijp JAG. Inactivation of staphylococcal phenol soluble modulins by serum lipoprotein particles. PLoS Pathog. 2012;8:e1002606. https://doi.org/10.1371/journal.ppat.1002606. PMID:22457627

[74] Cassat JE, Hammer ND, Campbell JP, Benson MA, Perrien DS, Mrak LN, Smeltzer MS, Torres VJ, Skaar EP. A secreted bacterial protease tailors the *Staphylococcus aureus* virulence repertoire to modulate bone remodeling during osteomyelitis. Cell Host Microbe. 2013;13:759-72. https://doi.org/10.1016/j.chom.2013.05.003. PMID:23768499

[75] McNamara PJ, Milligan-Monroe KC, Khalili S, Proctor RA. Identification, cloning, and initial characterization of *rot*, a locus encoding a regulator of virulence factor expression in *Staphylococcus aureus*. J Bacteriol. 2000;182:3197-203. https://doi.org/10.1128/JB.182.11.3197-3203.2000. PMID:10809700

[76] Boisset S, Geissmann T, Huntzinger E, Fechter P, Bendridi N, Possedko M, Chevalier C, Helfer AC, Benito Y, Jacquier A, et al. *Staphylococcus aureus* RNAIII coordinately represses the synthesis of virulence factors and the transcription regulator Rot by an antisense mechanism. Genes Dev. 2007;21:1353-66. https://doi.org/10.1101/gad.423507. PMID:17545468

[77] Geisinger E, Adhikari RP, Jin R, Ross HF, Novick RP. Inhibition of *rot* translation by RNAIII, a key feature of *agr* function. Mol Microbiol. 2006;61:1038-48. https://doi.org/10.1111/j.1365-2958.2006.05292.x. PMID:16879652

[78] Jonsson IM, Lindholm C, Luong TT, Lee CY, Tarkowski A. *mgrA* regulates staphylococcal virulence important for induction and progression of septic arthritis and sepsis. Microbes Infect. 2008;10:1229-35. https://doi.org/10.1016/j.micinf.2008.07.026. PMID:18692591

[79] King JM, Kulhankova K, Stach CS, Vu BG, Salgado-Pabón W. Phenotypes and virulence among *Staphylococcus aureus* USA100, USA200, USA300, USA400, and USA600 clonal lineages. mSphere. 2016;1:e00071-16. https://doi.org/10.1128/mSphere.00071-16. PMID:27303750

[80] Blevins JS, Gillaspy AF, Rechtin TM, Hurlburt BK, Smeltzer MS. The staphylococcal accessory regulator (*sar*) represses transcription of the *Staphylococcus aureus* collagen adhesin gene (*cna*) in an *agr*-independent manner. Mol Microbiol. 1999;33:317-26. https://doi.org/10.1046/j.1365-2958.1999.01475.x. PMID:10411748

[81] Torres VJ, Attia AS, Mason WJ, Hood MI, Corbin BD, Beasley FC, Anderson KL, Stauff DL, McDonald WH, Zimmerman LJ, et al. *Staphylococcus aureus fur* regulates the expression of virulence factors that contribute to the pathogenesis of pneumonia. Infect Immun. 2010;78:1618-28. https://doi.org/10.1128/IAI.01423-09. PMID:20100857

[82] Luong TT, Sau K, Roux C, Sau S, Dunman PM, Lee CY. *Staphylococcus aureus* ClpC divergently regulates capsule via *sae* and *codY* in strain Newman but activates capsule via *codY* in strain UAMS-1 and in strain Newman with repaired *saeS*. J Bacteriol. 2011;193:686-94. https://doi.org/10.1128/JB.00987-10. PMID:21131496

[83] Benson MA, Lilo S, Nygaard T, Voyich JM, Torres VJ. Rot and SaeRS cooperate to activate expression of the staphylococcal superantigen-like exoproteins. J Bacteriol. 2012;194:4355-65. https://doi.org/10.1128/JB.00706-12. PMID:22685286

Impact of *sarA* and Phenol-Soluble Modulins on the Pathogenesis of Osteomyelitis in Diverse Clinical Isolates of *Staphylococcus aureus*

Allister J. Loughran,[a] Dana Gaddy,[b*] Karen E. Beenken,[a] Daniel G. Meeker,[a] Roy Morello,[b] Haibo Zhao,[c] Stephanie D. Byrum,[d] Alan J. Tackett,[d] James E. Cassat,[e] Mark S. Smeltzer[a,f]

Department of Microbiology and Immunology,[a] Department of Physiology and Biophysics,[b] Department of Internal Medicine,[c] Department of Biochemistry,[d] and Department of Orthopaedic Surgery,[f] University of Arkansas for Medical Sciences, Little Rock, Arkansas, USA; Department of Pediatrics and Pathology, Microbiology, and Immunology, Vanderbilt University Medical Center, Nashville, Tennessee, USA[e]

We used a murine model of acute, posttraumatic osteomyelitis to evaluate the virulence of two divergent *Staphylococcus aureus* clinical isolates (the USA300 strain LAC and the USA200 strain UAMS-1) and their isogenic *sarA* mutants. The results confirmed that both strains caused comparable degrees of osteolysis and reactive new bone formation in the acute phase of osteomyelitis. Conditioned medium (CM) from stationary-phase cultures of both strains was cytotoxic to cells of established cell lines (MC3TC-E1 and RAW 264.7 cells), primary murine calvarial osteoblasts, and bone marrow-derived osteoclasts. Both the cytotoxicity of CM and the reactive changes in bone were significantly reduced in the isogenic *sarA* mutants. These results confirm that *sarA* is required for the production and/or accumulation of extracellular virulence factors that limit osteoblast and osteoclast viability and that thereby promote bone destruction and reactive bone formation during the acute phase of *S. aureus* osteomyelitis. Proteomic analysis confirmed the reduced accumulation of multiple extracellular proteins in the LAC and UAMS-1 *sarA* mutants. Included among these were the alpha class of phenol-soluble modulins (PSMs), which were previously implicated as important determinants of osteoblast cytotoxicity and bone destruction and repair processes in osteomyelitis. Mutation of the corresponding operon reduced the cytotoxicity of CM from both UAMS-1 and LAC cultures for osteoblasts and osteoclasts. It also significantly reduced both reactive bone formation and cortical bone destruction by CM from LAC cultures. However, this was not true for CM from cultures of a UAMS-1 *psm*$_\alpha$ mutant, thereby suggesting the involvement of additional virulence factors in such strains that remain to be identified.

Staphylococcus aureus is a highly versatile pathogen capable of causing a remarkable array of human infections. One of the most devastating of these is osteomyelitis, which is extremely difficult to eradicate without extensive and often repetitive surgical debridement (1). Indeed, it has been suggested that, as with cancer, "remission" is a more appropriate term than "cure" in the context of osteomyelitis (2). Several factors contribute to this therapeutic recalcitrance, including the inability to diagnose the infection before it has progressed to a chronic stage in which the local vasculature is compromised, the formation of a bacterial biofilm that limits the efficacy of both conventional antibiotics and host defenses, the emergence of phenotypic variants within the biofilm (persister cells and small-colony variants) that exhibit metabolic traits that limit their antibiotic susceptibility, and the ability of the pathogens involved, including *S. aureus*, to invade and replicate within host cells, including osteoblasts (3–9). Collectively, these factors dictate that the clinical problem of osteomyelitis extends far beyond acquired resistance and the increasingly limited availability of effective antibiotics.

Our laboratories have placed a major emphasis on overcoming this problem by exploring alternative means for early diagnosis (3, 10), developing improved methods for localized antibiotic delivery for the prevention and treatment of infection (11–14), and identifying the bacterial factors that contribute to the prominence of *S. aureus* as an orthopedic pathogen. With respect to the last area of exploration, our studies have led us to place a primary emphasis on the staphylococcal accessory regulator (*sarA*), mutation of which limits biofilm formation to a greater degree than mutation of any other regulatory locus that we have examined (11, 15). The negative impact of mutated *sarA* on biofilm formation is

also apparent in all *S. aureus* strains that we have examined, other than those with recognized regulatory defects (16, 17). Moreover, even in those cases in which a mutation enhanced biofilm formation, concomitant mutation of *sarA* reversed this effect (12, 15–17). We also confirmed that the limited ability of *sarA* mutants to form a biofilm can be correlated with increased susceptibility to diverse functional classes of antibiotics *in vivo* (18, 19). Additionally, mutation of *sarA* limits the ability of *S. aureus* to persist in the bloodstream and cause secondary infections, including hematogenous osteomyelitis (20, 21).

Taken together, these results suggest that *sarA* is a viable and perhaps preferred regulatory target in the context of biofilm-associated infections, including osteomyelitis. However, this conclusion must be interpreted with caution. For instance, under *in*

vitro conditions, the relative impact of *sarA* versus that of the *saePQRS* (*saeRS*) regulatory locus on biofilm formation was recently shown to be dependent on the medium used to carry out the biofilm assay (22). Moreover, mutation of *saeRS* in the USA300 strain LAC was shown to limit virulence in a murine model of posttraumatic osteomyelitis owing to the increased production of the extracellular protease aureolysin, which results in the decreased accumulation of phenol-soluble modulins (PSMs) that would otherwise promote cytotoxicity for osteoblasts and bone destruction (23). A recent report also demonstrated that, under the hypoxic conditions encountered in bone, particularly as the infection progresses to a point that compromises the local blood supply, the *srrAB* regulatory locus plays a key role in *S. aureus* survival (24). Such results emphasize the complexity of the disease process in osteomyelitis and the fact that biofilm formation *per se* is not the only relevant consideration.

In this respect, it is important to note that the impact of mutating *sarA* has not been evaluated in the context of bone infection. It has been demonstrated that, at least under *in vitro* conditions, mutation of *sarA* results in a much greater increase in protease production than mutation of *saeRS* (12, 17) and that this can be correlated with the reduced accumulation of multiple virulence factors, including PSMs (20). Thus, it would be anticipated that mutation of *sarA* would also have a significant impact in this clinical context, but this has not been experimentally determined. Additionally, studies examining the role of different regulatory loci in a newly developed murine model of posttraumatic osteomyelitis have been limited to date to the USA300 strain LAC, which produces PSMs at high levels by comparison to many other strains of *S. aureus* (25–27). In this report, we address these issues by using the same murine model to assess the relative virulence of two genetically and phenotypically divergent strains of *S. aureus* and their isogenic *sarA* and *psm* mutants.

MATERIALS AND METHODS

Bacterial strains and growth conditions. The *S. aureus* strains utilized in this study included a plasmid-cured, erythromycin-sensitive derivative of methicillin-resistant *S. aureus* (MRSA) USA300 strain LAC (28), USA200 methicillin-sensitive *S. aureus* osteomyelitis isolate UAMS-1 (29), and derivatives of each carrying mutations in *sarA* or the operon encoding the alpha class of PSMs (αPSMs). Mutants were generated by phage φ11-mediated transduction from mutants already on hand (19, 20, 23). Mutations in *sarA* and the *psm*$_α$ operon were genetically complemented using pSARA and pTX$_{Δα}$ as previously described (16, 27). Strains were maintained at −80°C in tryptic soy broth (TSB) containing 25% (vol/vol) glycerol. For analysis, strains were cultured from cold storage by plating on tryptic soy agar (TSA) with selection with the appropriate antibiotic. The following antibiotics were used at the indicated concentrations: chloramphenicol (Cm), 10 μg ml^{-1}; erythromycin (Erm), 10 μg ml^{-1}; kanamycin (Kan), 50 μg ml^{-1}; neomycin (Neo), 50 μg/ml; and tetracycline (Tet), 5 μg ml^{-1}.

Preparation of conditioned medium. Stationary-phase cultures were standardized to an optical density at 560 nm of 8.0. Cells were harvested by centrifugation, and the supernatants were filter sterilized. The culture medium was combined 1:1 with the appropriate cell culture medium containing 10% fetal bovine serum (FBS) and added to cell monolayers for cytotoxicity assays.

Cultivation of primary murine calvarial osteoblasts. Murine primary calvarial osteoblasts were obtained from 3- to 5-day-old C57BL/6 mouse pups according to standard procedures (30), modified as follows: whole calvariae were dissected (the periosteum and endosteum were scraped off with a scalpel) and sequentially digested for 20 min at 37°C in

alpha minimal essential medium (alpha-MEM) containing 0.1 mg/ml collagenase P (Roche), 0.04% trypsin-EDTA, and penicillin-streptomycin (166 U/ml and 166 μg/ml, respectively). The first 2 fractions of cells were discarded. Calvariae were further diced with sterile surgical scissors and digested in 1 ml of alpha-MEM with a double amount of collagenase and trypsin-EDTA for 1 h at 37°C with vigorous shaking every 15 to 20 min. Then, 3.75 ml of alpha-MEM containing 15% FBS and penicillin-streptomycin was added. After 24 h, the osteoblasts were washed with sterile phosphate-buffered saline (PBS) and expanded alpha-MEM containing 10% FBS, 2 mM glutamine, and penicillin and streptomycin (100 μg/ml and 100 μg/ml, respectively) for 2 to 4 days before passaging. Only early-passage osteoblasts grown in culture medium supplemented with 100 μg/ml of ascorbic acid were used for cytotoxicity assays.

Cytotoxicity assay. Cytotoxicity assays with primary osteoblasts and established cell lines were done using the methods described above. MC3T3-E1 and RAW 264.7 cells were obtained from the American Type Culture Collection (ATCC) and propagated according to ATCC recommendations. Cells were grown at 37°C in 5% CO$_2$ with the replacement of medium every 2 or 3 days. For cytotoxicity assays, cells were seeded into black clear-bottom 96-well tissue culture-grade plates at a density of 10,000 cells per well for MC3T3-E1 cells, 50,000 cells per well for RAW 264.7 cells, or 10,000 cells per well for calvarial osteoblasts. After 24 h, the growth medium was removed and replaced with medium containing a 1:1 ratio of cell culture complete growth medium and *S. aureus* conditioned medium. The monolayers were incubated for an additional 24 h prior to removal of the medium and assessment of cell viability using calcein-AM to stain live cells (Thermo Fisher Scientific) according to the manufacturer's specifications. An Omega FLUOstar microplate reader (BMG Labtech) was used to determine the fluorescent intensity at 517 nm. The results of the microtiter plate assays were confirmed through fluorescence microscopy.

Cultivation and TRAP staining of primary osteoclasts. Whole bone marrow was extracted from the tibia and femurs of one or two 8- to 10-week-old mice. Red blood cells were lysed in buffer (150 mM NH$_4$Cl, 10 mM KNCO$_3$, 0.1 mM EDTA, pH 7.4) for 5 min at room temperature. Bone marrow cells (5 × 10^6) were plated in a 100-mm petri dish and cultured in alpha-10 medium (alpha-MEM, 10% heat-inactivated FBS, and PSG [100 U/liter penicillin, 0.1 mg/liter streptomycin, and 2 mM L-glutamine]) containing 1/10 volume of conditioned medium (CM) supernatant from CMG 14-12 cells containing recombinant macrophage colony-stimulating factor (M-CSF) at 1 μg/ml for 4 to 5 days. Preosteoclasts and osteoclasts were generated by culturing bone marrow macrophages (BMMs) at a density of 160 BMMs/mm^2 in 1/100 vol of CMG 14-12 culture supernatant and 100 ng/ml of recombinant RANKL. To determine cell viability, tartrate-resistant acid phosphatase (TRAP) staining was used to count the viable cells. BMMs were cultured on a 48-well tissue culture plate in alpha-10 medium with M-CSF and RANKL for 4 to 5 days. After medium replacement, the cells were treated with *S. aureus* culture supernatants diluted 1:1 in complete growth medium. The cells were then fixed with 4% paraformaldehyde–PBS and TRAP stained with NaK tartrate and naphthol AS-BI phosphoric acid (Sigma-Aldrich).

Murine model of acute posttraumatic osteomyelitis. The murine model of acute posttraumatic osteomyelitis model was performed as previously described (23). Briefly, surgery was performed on the right hind limb of 8- to 10-week-old female C57BL/6 mice. Prior to surgery, the mice received 0.1 mg/kg of body weight buprenorphine via subcutaneous injection. Anesthesia was then maintained using isoflurane. The femur was exposed by blunt dissection, and a 1-mm unicortical bone defect was created at the lateral midshaft of the femur with a 21-gauge Precision Glide needle (Becton Dickinson). A bacterial inoculum of 1 × 10^5 CFU in 2 μl was delivered into the intramedullary canal. The muscle fasciae and skin were then closed with sutures, and the mice were allowed to recover from anesthesia. Infection was allowed to

proceed for 14 days, at which time the mice were euthanized and the right femur was removed and subjected to micro-computed tomography (micro-CT) analysis. All experiments involving animals were reviewed and approved by the Institutional Animal Care and Use Committee of the University of Arkansas for Medical Sciences and were performed according to NIH guidelines, the Animal Welfare Act, and U.S. federal law.

Micro-computed tomography. The analysis of cortical bone destruction and new bone formation was performed using micro-CT imaging with a Skyscan 1174 micro-CT (Bruker), and scans were analyzed using the manufacturer's analytical software. Briefly, axial images of each femur were acquired at a resolution of 6.7 μm at 50 kV and 800 μA through a 0.25-mm aluminum filter. Bones were visualized using a scout scan and then scanned in three sections as an oversize scan to image the entire femoral length. The volume of cortical bone was isolated in a semiautomated process per the manufacturer's instruction. Briefly, cortical bone was isolated from soft tissue and the background by global thresholding (low threshold, 89; high threshold, 255). The processes of opening, closing, dilation, erosion, and despeckling were configured using the bones from sham-treated controls to separate the new bone from the existing cortical bone, and a task list was created to apply the same process and values to all bones in the data set. After processing of the bones using the task list, the volume of interest (VOI) was corrected by drawing inclusive or exclusive contours on the periosteal surface. Cortical bone destruction analysis consisted of 600 slices centered on the initial surgical bone defect. Destruction was determined by subtraction of the volume of infected bones from the average bone volume from sham-treated controls. Reactive new bone formation was assessed by first isolating the region of interest (ROI) that contained only the original cortical bone (as described above). After cortical bone isolation the new bone volume was determined by subtraction of the original bone volume from the total bone volume. All calculations were performed on the basis of direct voxel counts.

Proteomic analysis. Assessment of the secreted proteome of both *S. aureus* parent strains and their isogenic *sarA* mutants was performed in triplicate as previously described (20). Briefly, the lanes of SDS-polyacrylamide gels were divided into 20 slices and subjected to in-gel trypsin digestion. The gel slices were destained in 50% methanol, 100 mM ammonium bicarbonate, followed by reduction in 10 mM Tris(2-carboxyethyl)phosphine and alkylation in 50 mM iodoacetamide. The gel slices were then dehydrated in acetonitrile, followed by addition of 100 ng of sequencing-grade porcine trypsin (Promega, Madison, WI) in 100 mM ammonium bicarbonate and incubation at 37°C for 12 to 16 h. The peptide products were then acidified in 0.1% formic acid (Fluka, Milwaukee, WI). Tryptic peptides were analyzed by high-resolution tandem mass spectrometry (MS/MS) with a Thermo LTQ Orbitrap Velos mass spectrometer coupled to a Waters nanoAcquity liquid chromatography (LC) system. The proteins were identified from the MS/MS spectra by searching the UniprotKB USA300 (LAC) or MRSA252 (UAMS-1) database for the organism *Staphylococcus aureus* (2,607 entries) using the Mascot search engine (Matrix Science, Boston, MA).

Statistical analysis. The results of both *in vitro* and *in vivo* experiments were tested for statistical significance using the Student *t* test. Comparisons were made between the two parent strains or between each parent strain and its appropriate isogenic mutant. *P* values of ≤0.05 were considered statistically significant.

RESULTS AND DISCUSSION

A primary focus of our laboratories has been on developing alternative strategies that can be used to overcome the therapeutic recalcitrance of orthopedic infections, including osteomyelitis. Despite the current prominence of hypervirulent isolates of the USA300 clonal lineage (25), it is imperative that the genetic and phenotypic diversity of different *S. aureus* strains be taken into account in this regard. Based on this, we chose to focus on the USA300 methicillin-resistant strain LAC and the USA200 methicillin-sensitive isolate UAMS-1, which have been shown to be dis-
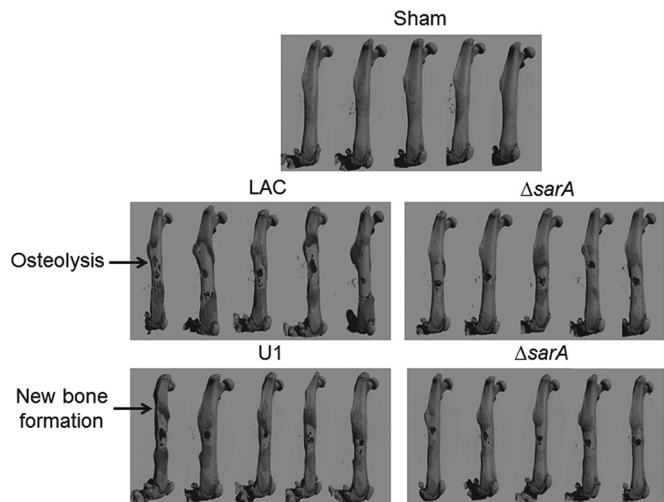

FIG 1 Bone destruction and reactive bone formation in osteomyelitis as a function of *sarA*. C57BL/6 mice (*n* = 5) were infected with LAC, UAMS-1 (U1), or their isogenic *sarA* mutants (Δ*sarA*). Femurs were harvested at 14 days after inoculation and subjected to micro-CT imaging analysis. Anteroposterior views of infected femurs are shown for comparison. Sham, results for mice subjected to the surgical procedure and injected with sterile PBS.

tinct with respect to both gene content and overall transcriptional patterns by comparison to each other (29, 31). Of note is the fact that LAC and many other USA300 isolates express the accessory gene regulator (*agr*) at higher levels than strains like UAMS-1 and, consequently, produce extracellular toxins, including phenol-soluble modulins (PSMs), at higher levels (25, 27). At the same time, UAMS-1 (ATCC 49230) has a proven clinical provenance in the specific context of osteomyelitis, having been isolated directly from the bone of a patient during surgical debridement (32).

Thus, we used equivalent numbers (10^5 CFU) of LAC, UAMS-1, and their isogenic *sarA* mutants to infect mice via direct inoculation into the medullary canal via a unicortical defect (23). Femurs were harvested at 14 days postinfection and subjected to micro-CT analysis to assess cortical bone destruction and reactive new bone (callus) formation. Quantitative analysis was based on reconstructive evaluation of a series of images spanning from the prominence of the lessor trochanter to the distal femoral growth plate. This analysis confirmed that infection with either strain caused osteolysis at and around the site of inoculation and reactive new bone (callus) formation both proximally and distally to this site (Fig. 1). The prevalence of both of these phenotypes was elevated in mice infected with LAC by comparison to those infected with UAMS-1, although these differences were not statistically significant (Fig. 2).

In LAC, mutation of *sarA* limited both osteolysis and reactive new bone formation to a significant degree by comparison to those in the isogenic parent strain (Fig. 2). In UAMS-1, the impact of mutating *sarA* was statistically significant only in the context of reactive bone formation, with cortical bone destruction being reduced, but not to a significant degree. However, these results must be interpreted with caution, in that the surgical procedure itself involves the destruction of cortical bone to gain access to the intramedullary canal, thus complicating the analysis by comparison to that involving new bone formation.
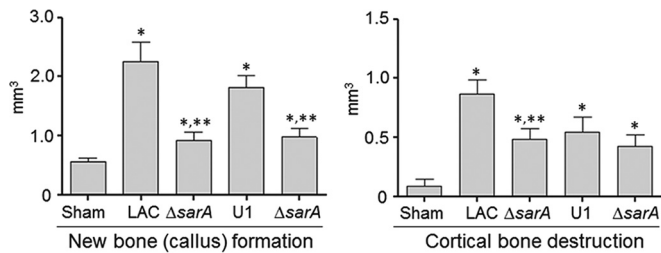
FIG 2 Quantitative analysis of micro-CT imaging. Images were analyzed for reactive new bone (callus) formation and cortical bone destruction in mice infected with LAC, UAMS-1 (U1), or their isogenic *sarA* mutants (Δ*sarA*). Sham, results of the same analysis with mice subjected to the surgical procedure and injected with sterile PBS. *, statistical significance compared to the results of sham treatment; **, statistical significance compared to the results for the isogenic parent strain.

Nevertheless, these results suggest that the virulence factor(s) produced by *S. aureus* that contributes to bone remodeling in osteomyelitis is likely produced in larger amounts by LAC than UAMS-1 and that mutation of *sarA* limits the production and/or accumulation of these virulence factors in both strains. Thus, while mutation of *sarA* has been shown to limit biofilm formation both *in vitro* and *in vivo* to a degree that can be correlated with increased antibiotic susceptibility (15, 18, 19, 33) and to limit virulence in a murine model of bacteremia that can be correlated with a reduced capacity to cause hematogenous osteomyelitis (20, 21), this is the first demonstration that it also limits virulence in a relevant model of posttraumatic bone infection and, perhaps more importantly, that it does so in diverse clinical isolates.

Bone is a highly dynamic physiological environment in which constant remodeling occurs in response to biomechanical stresses and hormonal influences (34, 35). This remodeling process is mediated by osteoblasts and osteoclasts, with the first being responsible for new bone formation (ossification) and the second being responsible for bone resorption prior to osteoblast-mediated ossification. Osteocytes are terminally differentiated osteoblasts that become embedded within lacunae in the mineralized bone matrix; they extend long cytoplasmic processes through apertures of the lacunae that form a dense canalicular network inside the bone. They are the most abundant cell type in the adult skeleton and form an interconnected network that can coordinate the activity of osteoblasts and osteoclasts to facilitate bone repair and ultimately maintain its structural integrity (34, 35). Thus, disruption in the balance of osteoblast versus osteoclast function has the potential to compromise this integrity. For instance, bone destruction could result from increased osteoclast function or decreased osteoblast function. Conversely, new bone (callus) formation in the form of woven bone could result from increased osteoblast function or decreased osteoclast function.

To investigate whether osteoblasts and osteoclasts are directly affected by the secreted products of *S. aureus*, we evaluated the extent to which conditioned medium (CM) from cultures of LAC, UAMS-1, and their isogenic *sarA* mutants impact osteoblast and osteoclast viability. We chose to focus on CM based on a previous report demonstrating that the increased production of extracellular proteases in a LAC *saeRS* mutant limits the accumulation of important extracellular virulence factors that contribute to the bone destruction and repair process (23) and our studies demon-

strating that mutation of *sarA* results in a greater increase in protease production than mutation of *saeRS* (12, 17). We initially focused on the preosteoblast cell line MC3T3-E1 because these cells have characteristics similar to those of primary calvarial osteoblasts and are derived from C57BL/6 mice, which is the same mouse strain used for our *in vivo* experiments. Similarly, we used the RAW 264.7 macrophage cell line as a surrogate for osteoclasts because they exhibit characteristics similar to those of bone marrow macrophages, the precursors of primary osteoclasts, but as an established cell line offered the advantage of ready accessibility and ease of manipulation.

CM from LAC (Fig. 3) and UAMS-1 (Fig. 4) cultures was cytotoxic for both MC3T3-E1 and RAW 264.7 cells, and in both strains, mutation of *sarA* limited this cytotoxicity. This was also true when the experiments were repeated using primary calvarial osteoblasts (Fig. 5) and when the results were assessed on the basis of the number of TRAP-positive multinucleated, primary bone marrow-derived osteoclasts (Fig. 6). When the results were assessed using primary osteoclasts, CM from LAC cultures appeared to be more cytotoxic for primary bone marrow-derived macrophages, although the difference did not reach statistical significance. The changes observed with each parent strain and its isogenic *sarA* mutants were consistent when both established cell lines and primary cells were used, and this finding is important, given that cell lines are much easier to maintain and more amenable to use in experiments. More importantly, these results are also consistent with the hypothesis that there is a cause-and-effect relationship between osteoblast and osteoclast cytotoxicity and bone destruction and repair processes in acute, posttraumatic osteomyelitis.

Given the cytotoxicity of CM from both LAC and UAMS-1 cultures for osteoblasts and osteoclasts and the impact of both strains on bone destruction and repair processes, we examined the exoprotein profiles of each strain and their isogenic *sarA* mutants by in-gel tryptic digestion followed by GeLC-MS/MS. These studies revealed global differences between both LAC and UAMS-1 and their isogenic *sarA* mutants (see Table S1 in the supplemental material). A draft genome sequence of UAMS-1 has been published (36), but a fully annotated protein database is not yet available. Thus, on the basis of our studies demonstrating that they are closely related strains (31), identification of UAMS-1 proteins was based on comparisons to MRSA252 proteins. However, it should be noted that while these two strains are closely related, they are not identical. For instance, the MRSA252 genome, like that of LAC, does not encode the toxic shock syndrome toxin 1 (TSST-1) gene (*tst*), which is present in UAMS-1 (31).

Nevertheless, several particularly notable differences between LAC and UAMS-1 were identified (Table 1). For instance, the analyses confirmed that, unlike LAC, UAMS-1 does not produce LukD/LukE, the Panton-Valentine leucocidin (PVL), or alpha toxin, all of which are potentially important virulence factors in the phenotypes that we observed. However, LukD was present in increased amounts in a LAC *sarA* mutant relative to the amounts in its parent strain, while LukE was detected at very low levels in both strains (Table 1). Similarly, PVL was also present in increased amounts in a LAC *sarA* mutant relative to the amounts in its isogenic parent strain. This suggests that LukD/LukE or PVL is unlikely to contribute to the attenuation of a LAC *sarA* mutant. In contrast, alpha toxin was present in dramatically reduced amounts in a LAC *sarA* mutant (at ~11% of the amount in the isogenic parent strain). This suggests that alpha toxin could con-
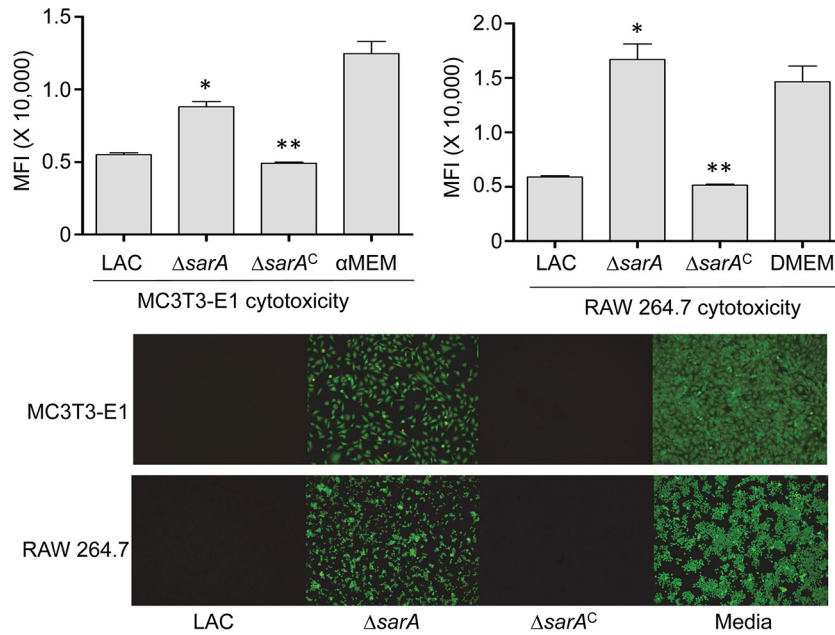
FIG 3 Cytotoxicity of LAC assessed using established cell lines. MC3T3-E1 or RAW 264.7 cells were exposed to CM from cultures of LAC, its *sarA* mutant (Δ*sarA*), and its complemented *sarA* mutant (Δ*sarA*^C). Viability was assessed after 24 h using Invitrogen Live calcein-AM staining (top) or fluorescence microscopy (bottom). The results of calcein-AM staining are reported as the average mean fluorescence intensity (MFI) ± standard deviation. *, statistical significance compared to the results observed with the isogenic parent strain; **, statistical significance compared to the results observed with the isogenic *sarA* mutant. DMEM, Dulbecco modified Eagle medium.

tribute to both the enhanced virulence of LAC relative to that of UAMS-1 and the reduced virulence of a LAC *sarA* mutant (24). However, given its absence in UAMS-1, alpha toxin clearly does not contribute to the cytotoxicity or bone remodeling that we observed with this strain.

In general, these proteomics studies also confirmed the findings of our previous experiments (26) demonstrating that PSMs, specifically, the alpha class of PSMs (αPSMs), are present in increased levels in LAC relative to UAMS-1 and at reduced levels in both LAC and UAMS-1 *sarA* mutants relative to the levels in the
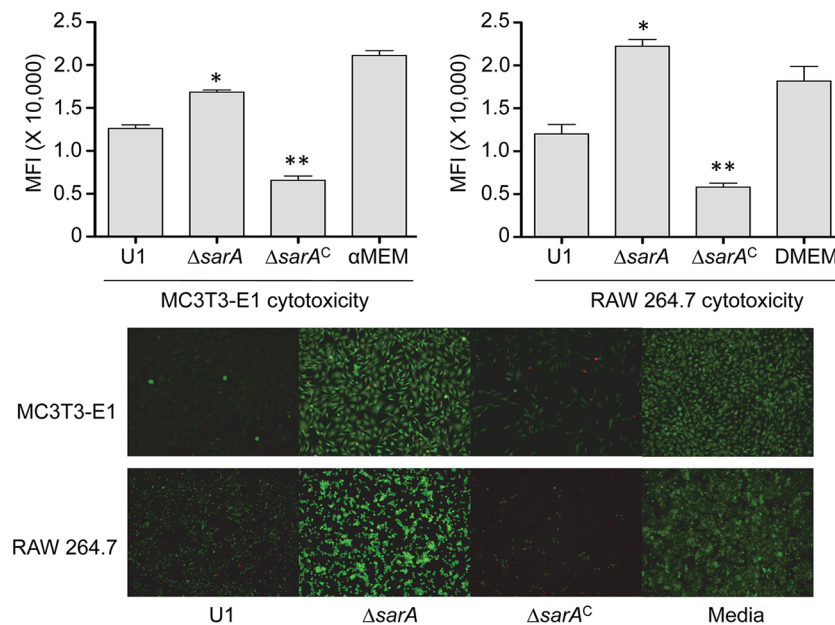

FIG 4 Cytotoxicity of UAMS-1 assessed using established cell lines. MC3T3-E1 or RAW 264.7 cells were exposed to CM from cultures of UAMS-1 (U1), its *sarA* mutant (Δ*sarA*), and its complemented sarA mutant (Δ*sarA*^C). Viability was assessed after 24 h using Invitrogen Live calcein-AM staining (top) or fluorescence microscopy (bottom). The results of calcein-AM staining are reported as the average mean fluorescence intensity (MFI) ± standard deviation. *, statistical significance compared to the results observed with the isogenic parent strain; **, statistical significance compared to the results observed with the isogenic *sarA* mutant.
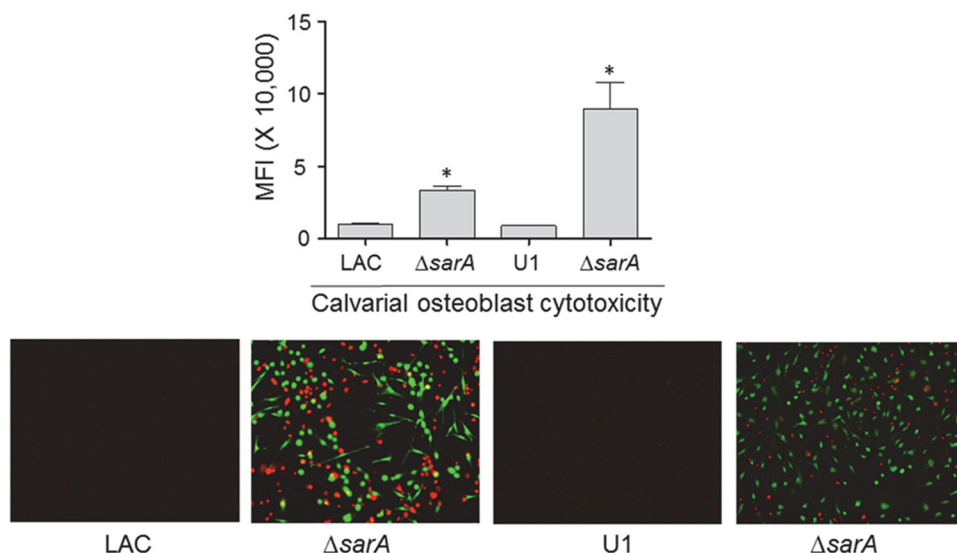
FIG 5 Cytotoxicity of conditioned medium for primary osteoblasts. Primary osteoblast cells were exposed to conditioned CM from cultures of the indicated strains, and viability was assessed after 24 h using Invitrogen Live calcein-AM staining (top) or fluorescence microscopy (bottom). The results of calcein-AM staining are reported as the average mean fluorescence intensity (MFI) ± standard deviation. *, statistical significance compared to the results observed with the isogenic parent strain.

isogenic parent strains (Fig. 7 and Table 1). In fact, in UAMS-1 the amounts of α2PSM and α3PSM were below the limit of detection of the assay. Nevertheless, the differences observed between UAMS-1 and its *sarA* mutant did reach statistical significance with respect to α1PSM and α4PSM, and statistically significant differences were observed between LAC and its *sarA* mutant with respect to all αPSMs (Fig. 7 and Table 1). These results are consistent with the results of our previous experiments, in which PSM levels were measured directly by high-pressure liquid chromatography (26). Moreover, previous studies employing a mutagenesis approach in LAC implicated αPSMs as key factors contributing to osteoblast cytotoxicity and bone remodeling in the same murine model that we employed in the experiments whose results are reported here (23).
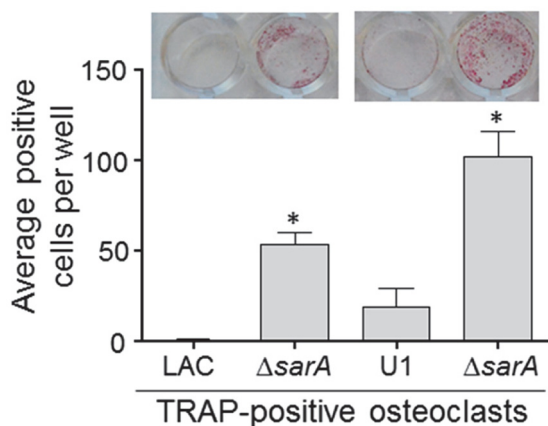
Based on this, we examined the extent to which these peptides contribute to the phenotypes that we observed in each parent strain. In both LAC and UAMS-1, mutation of the operon encoding αPSMs resulted in a significant decrease in cytotoxicity for both MC3T3-E1 cells and RAW 264.7 cells (Fig. 8). This effect appeared to be greater for LAC than for UAMS-1, particularly when it was assessed using MC3T3-E1 cells. The cytotoxicity of both LAC and UAMS-1 αPSM mutants was also significantly reduced when it was assessed using primary osteoblasts and osteoclasts, and when it was assessed using calvarial osteoblasts, the impact of eliminating αPSM production was significantly greater for LAC than for UAMS-1 (Fig. 9). This is consistent with the observation that LAC produces PSMs at higher levels than UAMS-1 (26). Nevertheless, these results demonstrate that PSMs play an important role in mediating osteoblast and osteoclast cytotoxicity even in a strain like UAMS-1 that produces PSMs at relatively low levels, and they suggest that the reduced accu-

FIG 6 Cytotoxicity of conditioned medium for primary osteoclasts. Primary bone marrow-derived murine osteoclasts were exposed to CM from cultures of the indicated strains. After 12 h, viability was assessed by TRAP staining, with the graph representing the results of quantitative analysis of all replicates. (Inset) TRAP-positive multinucleated cells. *, statistical significance compared to the results observed with the isogenic parent strain.

TABLE 1 Relative production of select proteins in LAC, UAMS-1, and their isogenic *sarA* mutants

Protein	Avg no. of spectral counts[a]			
	LAC	LAC *sarA* mutant	UAMS-1	UAMS-1 *sarA* mutant
Alpha toxin	1,019	117	0	0
PVL (LukF)	324	2,292	0	0
PVL (LukS)	229	1,458	0	0
LukD	104	576	0	0
LukE	23	3	0	0
α1PSM	102	15	56	13
α2PSM	32	0	0	0
α3PSM	12	0	0	0
α4PSM	112	5	64	14
Delta toxin	159	40	317	83
Spa	903	1	1,379	29

[a] Results reflect the average number of spectral counts from triplicate samples as assessed by GeLC-MS/MS.
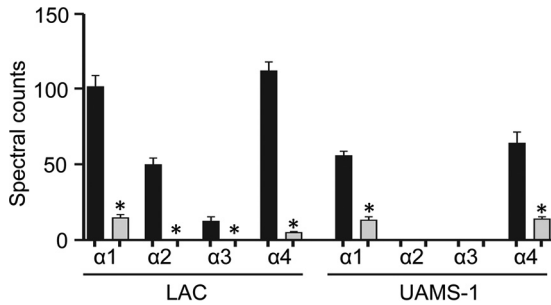
FIG 7 αPSM levels assessed by GeLC-MS/MS. Black bars, amounts of the indicated PSMs produced by LAC or UAMS-1; gray bars, amounts of the indicated PSMs produced by the isogenic *sarA* mutants. *, statistically significant difference for the indicated peptide compared to the amount of the same peptide observed in the isogenic parent strain.

mulation of αPSMs may be a primary factor contributing to the reduced virulence of both LAC and UAMS-1 *sarA* mutants in our model.

To address this, we used our murine osteomyelitis model to compare each parent strain and its αPSM mutants. The results confirmed that eliminating the production of αPSMs in LAC significantly reduced both the reactive new bone formation and the cortical bone destruction observed in this model (Fig. 10). In contrast, neither of these parameters was significantly reduced in the UAMS-1 αPSM mutant in comparison to that in the isogenic parent strain. Thus, while these results suggest that PSMs play some role in the pathogenesis of acute, posttraumatic osteomyelitis even in strains like UAMS-1, they likely play a much more predominant role in defining USA300 strains like LAC. It is important to note in this regard that while the results observed with *sarA* mutants *in vitro* in the context of cytotoxicity (Fig. 3 to 6) were consistent with those observed *in vivo* in the overall context of bone remodeling (Fig. 2), this was not the
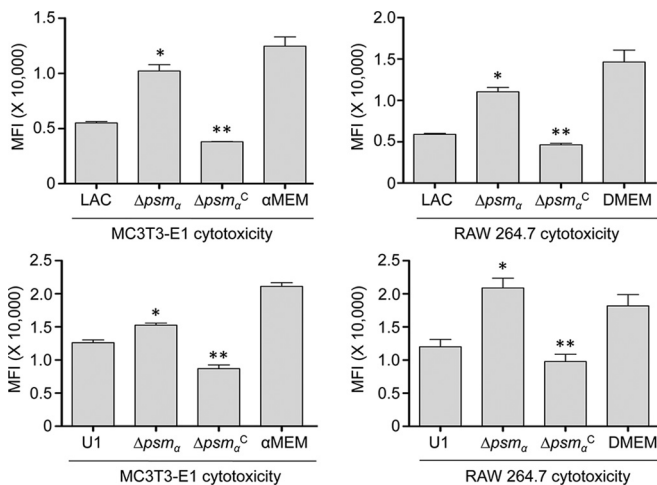

FIG 8 Cytotoxicity in established cell lines as a function of PSM production. MC3T3-E1 or RAW 264.7 cells were exposed to CM from cultures of LAC, UAMS-1 (U1), their isogenic α*psm* mutants (Δ*psm*α), and complemented *psm* mutants (Δ*psm*α^C). Viability was assessed after 24 h using Invitrogen Live calcein-AM staining. Results of calcein-AM staining are reported as the average mean fluorescence intensity (MFI) ± standard deviation. *, statistical significance compared to the results observed with the isogenic parent strain; **, statistical significance compared to the results observed with the isogenic *psm* mutant.
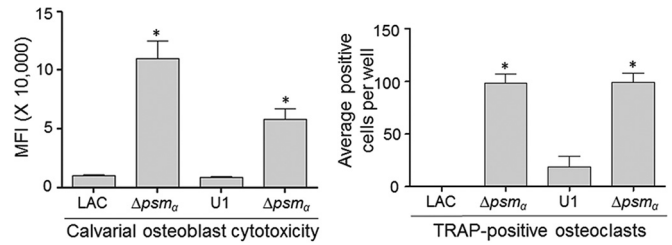

FIG 9 Impact of PSMs on cytotoxicity for primary osteoblasts and osteoclasts. Primary osteoblast cells were exposed to CM from cultures of the indicated strains. Viability was assessed after 24 h using Invitrogen Live calcein-AM staining. (Left) The results of calcein-AM staining are reported as the average mean fluorescence intensity (MFI) ± standard deviation. (Right) Primary bone marrow-derived murine osteoclasts were exposed to CM from cultures of the indicated strains. After 12 h, viability was assessed by TRAP staining, with the graph representing the results of quantitative analysis of all replicates. *, statistical significance compared to the results observed with the isogenic parent strain in both cell types.

case with a UAMS-1 αPSM mutant (Fig. 8 to 10). This may be due to the fact that PSMs can be inactivated when bound by host lipoproteins (37), an effect that would presumably be more evident in a strain like UAMS-1 that produces PSMs at relatively low levels.

The mechanistic basis for the role of PSMs in the pathogenesis of osteomyelitis also remains undetermined, but they are known to act as intracellular toxins that lyse osteoblasts, and this is particularly true for PSMs from hypervirulent strains of *S. aureus*, like LAC (5). PSMs have also been shown to induce the production of interleukin-8 (27), which in turn can promote osteoclast differentiation and activity (38). Taken together, these would presumably have the effect of increasing bone destruction by decreasing osteoblast activity while increasing osteoclast activity. It is difficult to envision how either would promote reactive bone formation, but it is noteworthy that this occurred at distinct sites distal to the inoculation site (Fig. 1). Together, these factors suggest the possibility that reactive bone formation is a downstream effect arising from the recruitment of osteoclasts to the site of infection and/or the systemic inflammatory response.

Finally, while our results demonstrate an important role for PSMs in the pathogenesis of osteomyelitis in LAC, they also suggest that other virulence factors play an important role in defining both the virulence of UAMS-1 and the attenuation of its isogenic *sarA* mutant. For instance, the fact that CM from a UAMS-1 αPSM mutant culture exhibited more cytotoxicity for primary osteoblasts than CM from a LAC αPSM mutant culture (Fig. 9) suggests that UAMS-1 produces a potentially relevant cytolytic factor that either is not produced by LAC or is produced in reduced amounts relative to the amounts in which it is produced by UAMS-1. Additionally, the fact that a UAMS-1 *sarA* mutant was less cytotoxic than a LAC *sarA* mutant (Fig. 3 to 6) suggests that the abundance of the relevant factor(s) is decreased in a UAMS-1 *sarA* mutant.

One possibility is this regard are superantigens like TSST-1 and those encoded within the enterotoxin gene cluster (*egc*), which are produced by UAMS-1 but not LAC (39). However, while we did not detect TSST-1 in our proteomics analysis for the reasons discussed above, mutation of *sarA* has been shown to result in an increase in the production of TSST-1, albeit under *in vitro* conditions (40). One other possibility that does meet these criteria is protein A (Spa), which is present in both cell-associated and ex-
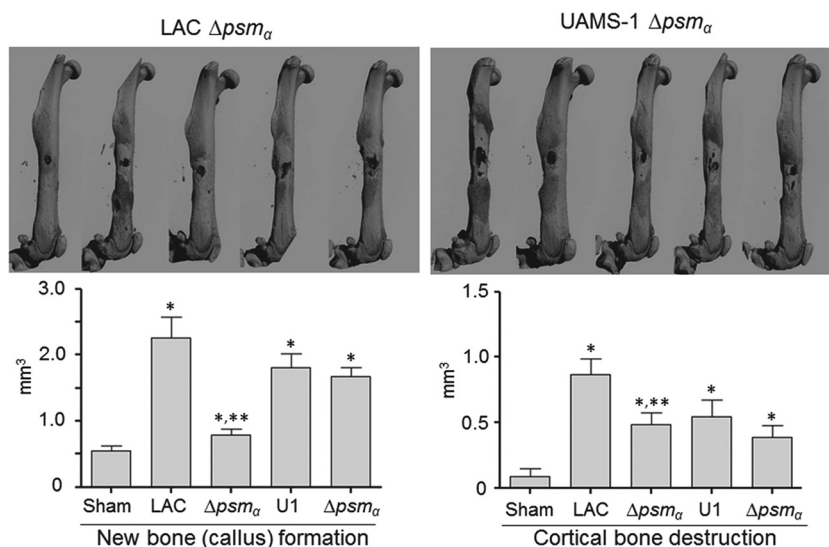
FIG 10 Impact of PSMs assessed by micro-CT. Images were analyzed for reactive new bone (callus) formation and cortical bone destruction in mice infected with LAC, UAMS-1 (U1), or their isogenic α*psm* (Δ*psm*α) mutants. Sham refers to the results of the same analysis with mice subjected to the surgical procedure and injected with sterile PBS. *, statistical significance compared to the results observed with the sham treatment; **, statistical significance compared to the results observed with the isogenic parent strain.

tracellular forms (41, 42) and was previously shown to bind to preosteoblastic cells via tumor necrosis factor alpha receptor 1, resulting in apoptosis and, ultimately, bone loss (43). Thus, protein A was present in increased amounts in UAMS-1 relative to the amounts in LAC (Spa in Table 1) and could have contributed to the virulence of UAMS-1, and elimination of PSM production in UAMS-1 had comparatively little impact in this model. The fact that the accumulation of Spa was reduced in a UAMS-1 *sarA* mutant could also account for why mutation of *sarA* had a comparable impact in both strains. At the same time, the generated *sarA* mutants of both strains still caused bone destruction and new bone formation to a degree that exceeded that observed with the sham-treated controls (Fig. 2). This is potentially important because it implicates virulence factors whose abundance is not impacted by mutation of *sarA* at the level of either their production or their accumulation.

ACKNOWLEDGMENTS

REFERENCES

1. **Lew DP, Waldvogel FA.** 2004. Osteomyelitis. Lancet **364:**369–379. http://dx.doi.org/10.1016/S0140-6736(04)16727-5.

2. **Rao N, Ziran BH, Lipsky BA.** 2011. Treating osteomyelitis: antibiotics and surgery. Plast Reconstr Surg **127**(Suppl 1):177S–187S. http://dx.doi.org/10.1097/PRS.0b013e3182001f0f.

3. **Brown TL, Spencer HJ, Beenken KE, Alpe TL, Bartel TB, Bellamy W, Gruenwald JM, Skinner RA, McLaren SG, Smeltzer MS.** 2012. Evaluation of dynamic [18F]-FDG-PET imaging for the detection of acute post-surgical bone infection. PLoS One **7:**e41863. http://dx.doi.org/10.1371/journal.pone.0041863.

4. **Flannagan RS, Heit B, Heinrichs DE.** 2015. Antimicrobial mechanisms of macrophages and the immune evasion strategies of *Staphylococcus aureus*. Pathogens **4:**826–868. http://dx.doi.org/10.3390/pathogens4040826.

5. **Rasigade JP, Trouillet-Assant S, Ferry T, Diep BA, Sapin A, Lhoste Y, Ranfaing J, Badiou C, Benito Y, Bes M, Couzon F, Tigaud S, Lina G, Etienne J, Vandenesch F, Laurent F.** 2013. PSMs of hypervirulent *Staphylococcus aureus* act as intracellular toxins that kill infected osteoblasts. PLoS One **8:**e63176. http://dx.doi.org/10.1371/journal.pone.0063176.

6. **Flannagan RS, Heit B, Heinrichs DE.** 2016. Intracellular replication of *Staphylococcus aureus* in mature phagolysosomes in macrophages precedes host cell death, and bacterial escape and dissemination. Cell Microbiol **18:**514–535. http://dx.doi.org/10.1111/cmi.12527.

7. **Scherr TD, Hanke ML, Huang O, James DB, Horswill AR, Bayles KW, Fey PD, Torres VJ, Kielian T.** 2015. *Staphylococcus aureus* biofilms induce macrophage dysfunction through leukocidin AB and alpha-toxin. mBio **6:**e01021-15. http://dx.doi.org/10.1128/mBio.01021-15.

8. **Cassat JE, Skaar EP.** 2013. Recent advances in experimental models of osteomyelitis. Expert Rev Anti Infect Ther **11:**1263–1265. http://dx.doi.org/10.1586/14787210.2013.858600.

9. **Hammer ND, Cassat JE, Noto MJ, Lojek LJ, Chadha AD, Schmitz JE, Creech CB, Skaar EP.** 2014. Inter- and intraspecies metabolite exchange promotes virulence of antibiotic-resistant *Staphylococcus aureus*. Cell Host Microbe **16:**531–537. http://dx.doi.org/10.1016/j.chom.2014.09.002.

10. **Jones-Jackson L, Walker R, Purnell G, McLaren SG, Skinner RA, Thomas JR, Suva LJ, Anaissie E, Miceli M, Nelson CL, Ferris EJ, Smeltzer MS.** 2005. Early detection of bone infection and differentiation from post-surgical inflammation using 2-deoxy-2-[18F]-fluoro-D-glucose positron emission tomography (FDG-PET) in an animal model. J Orthop Res **23:**1484–1489.

11. **Beenken KE, Spencer H, Griffin LM, Smeltzer MS.** 2012. Impact of extracellular nuclease production on the biofilm phenotype of *Staphylococcus aureus* under in vitro and in vivo conditions. Infect Immun **80:**1634–1638. http://dx.doi.org/10.1128/IAI.06134-11.

12. **Beenken KE, Mrak LN, Zielinska AK, Atwood DN, Loughran AJ, Griffin LM, Matthews KA, Anthony AM, Spencer HJ, Post GR, Lee CY, Smeltzer MS.** 2014. Impact of the functional status of *saeRS* on *in vivo*

phenotypes of *Staphylococcus aureus sarA* mutants. Mol Microbiol 92: 1299–1312. http://dx.doi.org/10.1111/mmi.12629.

13. **Jennings JA, Carpenter DP, Troxel KS, Beenken KE, Smeltzer MS, Courtney HS, Haggard WO.** 2015. Novel antibiotic-loaded point-of-care implant coating inhibits biofilm. Clin Orthop Relat Res 473:2270–2282. http://dx.doi.org/10.1007/s11999-014-4130-8.

14. **Parker AC, Beenken KE, Jennings JA, Hittle L, Shirtliff ME, Bumgardner JD, Smeltzer MS, Haggard WO.** 2015. Characterization of local delivery with amphotericin B and vancomycin from modified chitosan sponges and functional biofilm prevention evaluation. J Orthop Res 33: 439–447. http://dx.doi.org/10.1002/jor.22760.

15. **Atwood DN, Loughran AJ, Courtney AP, Anthony AC, Meeker DG, Spencer HJ, Gupta RK, Lee CY, Beenken KE, Smeltzer MS.** 2015. Comparative impact of diverse regulatory loci on *Staphylococcus aureus* biofilm formation. Microbiologyopen 4:436–451. http://dx.doi.org/10.1002/mbo3.250.

16. **Beenken KE, Mrak LN, Griffin LM, Zielinska AK, Shaw LN, Rice KC, Horswill AR, Bayles KW, Smeltzer MS.** 2010. Epistatic relationships between *sarA* and *agr* in *Staphylococcus aureus* biofilm formation. PLoS One 5:e10790. http://dx.doi.org/10.1371/journal.pone.0010790.

17. **Mrak LN, Zielinska AK, Beenken KE, Mrak IN, Atwood DN, Griffin LM, Lee CY, Smeltzer MS.** 2012. *saeRS* and *sarA* act synergistically to repress protease production and promote biofilm formation in *Staphylococcus aureus*. PLoS One 7:e38453. http://dx.doi.org/10.1371/journal.pone.0038453.

18. **Weiss EC, Spencer HJ, Daily SJ, Weiss BD, Smeltzer MS.** 2009. Impact of *sarA* on antibiotic susceptibility of *Staphylococcus aureus* in a catheter-associated *in vitro* model of biofilm formation. Antimicrob Agents Chemother 53:2475–2482. http://dx.doi.org/10.1128/AAC.01432-08.

19. **Weiss EC, Zielinska A, Beenken KE, Spencer HJ, Daily SJ, Smeltzer MS.** 2009. Impact of *sarA* on daptomycin susceptibility of *Staphylococcus aureus* biofilms *in vivo*. Antimicrob Agents Chemother 53:4096–4102. http://dx.doi.org/10.1128/AAC.00484-09.

20. **Zielinska AK, Beenken KE, Mrak LN, Spencer HJ, Post GR, Skinner RA, Tackett AJ, Horswill AR, Smeltzer MS.** 2012. *sarA*-mediated repression of protease production plays a key role in the pathogenesis of *Staphylococcus aureus* USA300 isolates. Mol Microbiol 86:1183–1196. http://dx.doi.org/10.1111/mmi.12048.

21. **Loughran AJ, Atwood DN, Anthony AC, Harik NS, Spencer HJ, Beenken KE, Smeltzer MS.** 2014. Impact of individual extracellular proteases on *Staphylococcus aureus* biofilm formation in diverse clinical isolates and their isogenic *sarA* mutants. Microbiologyopen 3:897–909. http://dx.doi.org/10.1002/mbo3.214.

22. **Zapotoczna M, McCarthy H, Rudkin JK, O'Gara JP, O'Neill E.** 2015. An essential role for coagulase in *Staphylococcus aureus* biofilm development reveals new therapeutic possibilities for device-related infections. J Infect Dis 212:1883–1893. http://dx.doi.org/10.1093/infdis/jiv319.

23. **Cassat JE, Hammer ND, Campbell JP, Benson MA, Perrien DS, Mrak LN, Smeltzer MS, Torres VJ, Skaar EP.** 2013. A secreted bacterial protease tailors the *Staphylococcus aureus* virulence repertoire to modulate bone remodeling during osteomyelitis. Cell Host Microbe 13:759–772. http://dx.doi.org/10.1016/j.chom.2013.05.003.

24. **Wilde AD, Snyder DJ, Putnam NE, Valentino MD, Hammer ND, Lonergan ZR, Hinger SA, Aysanoa EE, Blanchard C, Dunman PM, Wasserman GA, Chen J, Shopsin B, Gilmore MS, Skaar EP, Cassat JE.** 2015. Bacterial hypoxic responses revealed as critical determinants of the host-pathogen outcome by TnSeq analysis of *Staphylococcus aureus* invasive infection. PLoS Pathog 11:e1005341. http://dx.doi.org/10.1371/journal.ppat.1005341.

25. **Li M, Diep BA, Villaruz AE, Braughton KR, Jiang X, DeLeo FR, Chambers HF, Lu Y, Otto M.** 2009. Evolution of virulence in epidemic community-associated methicillin-resistant *Staphylococcus aureus*. Proc Natl Acad Sci U S A 106:5883–5888. http://dx.doi.org/10.1073/pnas.0900743106.

26. **Zielinska AK, Beenken KE, Joo HS, Mrak LN, Griffin LM, Luong TT, Lee CY, Otto M, Shaw LN, Smeltzer MS.** 2011. Defining the strain-dependent impact of the staphylococcal accessory regulator (*sarA*) on the

alpha-toxin phenotype of *Staphylococcus aureus*. J Bacteriol 193:2948–2958. http://dx.doi.org/10.1128/JB.01517-10.

27. **Wang R, Braughton KR, Kretschmer D, Bach TH, Queck SY, Li M, Kennedy AD, Dorward DW, Klebanoff SJ, Peschel A, DeLeo FR, Otto M.** 2007. Identification of novel cytolytic peptides as key virulence determinants for community-associated MRSA. Nat Med 13:1510–1514. http://dx.doi.org/10.1038/nm1656.

28. **Wormann ME, Reichmann NT, Malone CL, Horswill AR, Grundling A.** 2011. Proteolytic cleavage inactivates the *Staphylococcus aureus* lipoteichoic acid synthase. J Bacteriol 193:5279–5291. http://dx.doi.org/10.1128/JB.00369-11.

29. **Cassat J, Dunman PM, Murphy E, Projan SJ, Beenken KE, Palm KJ, Yang SJ, Rice KC, Bayles KW, Smeltzer MS.** 2006. Transcriptional profiling of a *Staphylococcus aureus* clinical isolate and its isogenic *agr* and *sarA* mutants reveals global differences in comparison to the laboratory strain RN6390. Microbiology 152:3075–3090. http://dx.doi.org/10.1099/mic.0.29033-0.

30. **Robey PG, Termine JD.** 1985. Human bone cells *in vitro*. Calcif Tissue Int 37:453–460. http://dx.doi.org/10.1007/BF02557826.

31. **Cassat JE, Dunman PM, McAleese F, Murphy E, Projan SJ, Smeltzer MS.** 2005. Comparative genomics of *Staphylococcus aureus* musculoskeletal isolates. J Bacteriol 187:576–592. http://dx.doi.org/10.1128/JB.187.2.576-592.2005.

32. **Gillaspy AF, Hickmon SG, Skinner RA, Thomas JR, Nelson CL, Smeltzer MS.** 1995. Role of the accessory gene regulator (*agr*) in pathogenesis of staphylococcal osteomyelitis. Infect Immun 63:3373–3380.

33. **Beenken KE, Blevins JS, Smeltzer MS.** 2003. Mutation of *sarA* in *Staphylococcus aureus* limits biofilm formation. Infect Immun 71:4206–4211. http://dx.doi.org/10.1128/IAI.71.7.4206-4211.2003.

34. **Goldring SR.** 2015. The osteocyte: key player in regulating bone turnover. RMD Open 1:e000049. http://dx.doi.org/10.1136/rmdopen-2015-000049.

35. **Goldring SR.** 2015. Inflammatory signaling induced bone loss. Bone 80: 143–149. http://dx.doi.org/10.1016/j.bone.2015.05.024.

36. **Sassi M, Sharma D, Brinsmade SR, Felden B, Augagneur Y.** 2015. Genome sequence of the clinical isolate *Staphylococcus aureus* subsp. *aureus* strain UAMS-1. Genome Announc 3(1):e01584-14. http://dx.doi.org/10.1128/genomeA.01584-14.

37. **Surewaard BG, Nijland R, Spaan AN, Kruijtzer JA, de Haas CJ, van Strijp JA.** 2012. Inactivation of staphylococcal phenol soluble modulins by serum lipoprotein particles. PLoS Pathog 8:e1002606. http://dx.doi.org/10.1371/journal.ppat.1002606.

38. **Bendre MS, Montague DC, Peery T, Akel NS, Gaddy D, Suva LJ.** 2003. Interleukin-8 stimulation of osteoclastogenesis and bone resorption is a mechanism for the increased osteolysis of metastatic bone disease. Bone 33:28–37. http://dx.doi.org/10.1016/S8756-3282(03)00086-3.

39. **King JM, Kulhankova K, Stach CS, Vu BG, Salgado-Pabún W.** 2016. Phenotypes and virulence among Staphylococcus aureus USA100, USA200, USA300, USA400, and USA600 clonal lineages. mSphere 1(3): e00071–16. http://dx.doi.org/10.1128/mSphere.00071-16.

40. **Andrey DO, Jousselin A, Villanueva M, Renzoni A, Monod A, Barras C, Rodriguez N, Kelley WL.** 2015. Impact of the regulators *sigB*, *rot*, *sarA* and *sarS* on toxic shock *tst* promoter and TSST-1 expression in *Staphylococcus aureus*. PLoS One 10:e135579. http://dx.doi.org/10.1371/journal.pone.0135579.

41. **Edwards AM, Bowden MG, Brown EL, Laabei M, Massey RC.** 2012. *Staphylococcus aureus* extracellular adherence protein triggers TNF alpha release, promoting attachment to endothelial cells via protein A. PLoS One 7:e43046. http://dx.doi.org/10.1371/journal.pone.0043046.

42. **O'Halloran DP, Wynne K, Geoghegan JA.** 2015. Protein A is released into the *Staphylococcus aureus* culture supernatant with an unprocessed sorting signal. Infect Immun 83:1598–1609. http://dx.doi.org/10.1128/IAI.03122-14.

43. **Widaa A, Claro T, Foster TJ, O'Brien FJ, Kerrigan SW.** 2012. *Staphylococcus aureus* protein A plays a critical role in mediating bone destruction and bone loss in osteomyelitis. PLoS One 7:e40586. http://dx.doi.org/10.1371/journal.pone.0040586.